

**Purinergic Signalling in Müller Cells in the
Context of Glaucomatous
Neuroinflammation and Neurodegeneration**

Sofia Noor Habib

**Thesis presented for the degree of
Doctor of Medicine (M.D.)**

**School of Medicine
University of East Anglia, Norwich, UK**

April 2023

© This copy of the thesis has been supplied on condition that anyone who consults it is understood to recognise that its copyright rests with the author and that use of any information derived there-from must be in accordance with current UK Copyright Law. In addition, any quotation or extract must include full attribution.

Abstract

Purpose: Glaucoma describes progressive optic neuropathies characterised by retinal ganglion cell (RGC) death with corresponding loss of visual field. Our group demonstrated P2X7 receptor (P2X7R)-mediated RGC death, increase in interleukin-1 β (IL-1 β) and interleukin-10 (IL-10) expression in the human retina. Müller cells may have a role in glaucomatous neuroinflammation and neurodegeneration. The purpose of this research was to: (i) identify the purinergic (P2) receptors; (ii) determine if stimulation of the P2X7R mediates cell-death and (iii) determine if stimulation of the P2X7R mediates IL-1 β and IL-10 cytokine expression in human Müller cells.

Methods: P2 receptor mRNA expression in MIO-M1 cells (immortalised human Müller cell line) and retinal tissue was evaluated using real time quantitative polymerase chain reaction (RT-qPCR). Purinergic (P2) evoked intracellular Ca²⁺ responses were measured using calcium microfluorimetry. Change in cell viability or cell cytotoxicity was determined with MTS and LDH assays respectively. IL-1R1, IL-1 α , IL-1 β and IL-10 mRNA and protein were measured with RT-qPCR and enzyme-linked immunosorbent assay (ELISA) respectively. Inhibitors of IL-1 β downstream signalling pathways were used to investigate IL-1 β induced IL-10 release.

Results: MIO-M1 cells expressed mRNA for P2X4-7, P2Y₁, P2Y₂, P2Y₄, and P2Y₁₂₋₁₄ with enriched expression of P2X7R and P2Y₄R compared to human retinal tissue. Intracellular Ca²⁺ responses provided functional evidence for P2X7R, P2Y₁R, P2Y₁₂R and P2Y₁₄R. Prolonged stimulation of the P2X7R showed no significant change in viability or death of MIO-M1 cells. Stimulation of the P2X7R did not cause an increase in IL-1 α , IL-1 β or IL-10 mRNA expression. IL-1R1 was expressed in MIO-M1 cells. IL-1 β stimulation of IL-1R1 produced a 6.2-fold rise in IL-10 mRNA expression (p=0.03) and 1.37-fold rise in intracellular protein (p<0.0001) at 24 hours.

Conclusions: Evidence demonstrated functioning P2X7R, P2Y₁R, P2Y₁₄R and suggested functioning P2Y₄R, P2Y₁₂R in human Müller cells. Other groups established high concentrations of ATP stimulate P2X7R mediated IL-1 β release from microglial cells. Here it is suggested retinal IL-1 β activates IL-1R1 in Müller cells causing IL-10 protein production. Thereby, high concentrations of ATP in the human retina may cause activation of an IL-1 β -IL-10 axis mediated by the Müller cell. There was no evidence that the P2X7R in the human Müller cell contributed to the proposed IL-1 β -IL-10 axis.

Access Condition and Agreement

Each deposit in UEA Digital Repository is protected by copyright and other intellectual property rights, and duplication or sale of all or part of any of the Data Collections is not permitted, except that material may be duplicated by you for your research use or for educational purposes in electronic or print form. You must obtain permission from the copyright holder, usually the author, for any other use. Exceptions only apply where a deposit may be explicitly provided under a stated licence, such as a Creative Commons licence or Open Government licence.

Electronic or print copies may not be offered, whether for sale or otherwise to anyone, unless explicitly stated under a Creative Commons or Open Government license. Unauthorised reproduction, editing or reformatting for resale purposes is explicitly prohibited (except where approved by the copyright holder themselves) and UEA reserves the right to take immediate 'take down' action on behalf of the copyright and/or rights holder if this Access condition of the UEA Digital Repository is breached. Any material in this database has been supplied on the understanding that it is copyright material and that no quotation from the material may be published without proper acknowledgement.

Table of Contents

Chapter 1: Introduction	23
1.1 Anatomy and Physiology of the Human Eye.....	23
1.1.1 Gross anatomy	23
1.1.2 Anterior chamber angle (ACA) and aqueous humour dynamics	23
1.1.3 Retina	26
1.2 Glaucoma	37
1.2.1 Overview and classification.....	37
1.2.2 Risk factors	38
1.2.3 Diagnosis and monitoring	40
1.2.4 Treatment	42
1.2.5 Pathophysiology.....	47
1.2.5.1 Pathophysiology of glaucoma and purinergic signalling.....	49
1.3 Purinergic Signalling.....	51
1.3.1 Overview	51
1.3.2 Mechanisms of nucleotide release and breakdown.....	52
1.3.3. Purinergic receptors.....	55
1.3.4 Purinergic signalling in the retina	71
1.3.5 Therapeutic potentials of purinergic agents in disease.....	75
1.4 Purinergic signalling and calcium responses.....	76
1.4.1 Overview of calcium homeostasis and signalling	76
1.4.2 Purinergic calcium responses in the Müller cell	77
1.5 Interleukins.....	80
1.5.1 Overview	80
1.5.2 Interleukins and glaucoma	81
1.5.3 IL-1.....	82
1.5.4 IL-10.....	88
1.6 Aims of the thesis.....	90
Chapter 2: Materials and Methods.....	91
2.1 MIO-M1 cells	91

2.1.1 Cell culture	91
2.2 Enzymatic Dissociation of Human Retinal Tissue.....	92
2.3 Agonists and Antagonists	93
2.4 Reverse transcription quantitative polymerase chain reaction (RT-qPCR)	96
2.4.1 RNA extraction	96
2.4.2 First-strand complementary DNA (cDNA) synthesis.....	97
2.4.3 TaqMan RT-qPCR.....	97
2.5 MTS assay	99
2.6 LDH assay	99
2.7 Calcium microfluorimetry	100
2.8 Enzyme-linked immunosorbent assay (ELISA)	101
2.9 Statistical analysis	102
Chapter 3: Purinergic P2-receptors in the Human Müller Cell	104
3.1 Introduction	104
3.2 Results	109
3.2.1 P2 Receptor mRNA expression in MIO-M1 cells.....	109
3.2.2 P2 receptor mRNA expression in MIO-M1 cells relative to human retinal tissue	110
3.2.3 P2 receptor calcium responses in MIO-M1 cells.....	111
3.3 Discussion.....	126
3.3.1 P2X7, P2Y ₁ , P2Y ₄ , P2Y ₁₂ and P2Y ₁₄ are functional receptors on human Müller cells.	126
3.3.2 <i>P2X7R</i> and <i>P2Y4R</i> are enriched in human Müller cells compared with human retina.....	129
3.3.3 ADP is the most potent endogenous P2-receptor agonist at human Müller cells.....	129
3.3.4 ATP activates P2Y ₁ Rs and with higher concentrations also activating P2X7Rs in human Müller cells.	130
3.3.5 ADP activates P2Y ₁ Rs and with higher concentrations also activating P2X12Rs in human Müller cells.....	130
3.3.6 UTP may activate P2Y ₄ Rs in human Müller cells.....	131

3.3.7 Endogenous agonist UDP-glucose and the synthetic agonist MRS 2690 activate the P2Y ₁₄ R in human Müller cells.....	131
3.3.8 The synthetic agonist BzATP induced calcium responses selectively via the P2X7R in human Müller cells.	132

Chapter 4: P2X7R-mediated Interleukin mRNA Expression in Human Müller Cells

.....133

4.1 Introduction	133
4.2 Results	134
4.2.1 MIO-M1 cell viability and cell death in response to purinergic agonist and antagonist exposure.....	134
4.2.2 IL-1 α , IL-1 β , IL-1R1 and IL-10 mRNA expression in MIO-M1 cells.....	135
4.2.3 P2X7R-mediated IL-1 α , IL-1 β , IL-1R1 and IL-10 mRNA expression in MIO-M1 cells	136
4.2.3.1 P2X7R-mediated IL-1 α mRNA expression in MIO-M1 cells	137
4.2.3.2 P2X7R-mediated IL-1 β mRNA expression and protein release in MIO-M1 cells.....	137
4.2.3.3 P2X7R-mediated IL-1R1 mRNA expression in MIO-M1 cells	141
4.2.3.4 P2X7R-mediated IL-10 mRNA expression in MIO-M1 cells.....	142
4.3 Discussion.....	143
4.3.1 Prolonged stimulation of the P2X7R does not cause cell death in human Müller cells.....	143
4.3.2 Stimulation of the P2X7R in human Müller cells does not induce IL-1 α , IL-1 β or IL-10 mRNA expression.....	144
4.3.2 Human Müller cells may be a contributing source of IL-1 β in the retina via pathway(s) independent of the P2X7R	145
4.3.2 Human Müller cells express IL-1R1	147

Chapter 5: IL-1 β -mediated IL-10 mRNA expression and protein release in a human Müller cell model.....148

5.1 Introduction	148
5.2 Results	152
5.2.1 MIO-M1 evoked cell death in response to IL-1 β and IL-1R1 downstream signalling inhibitors	154

5.2.2 IL-1 β induced IL-10 mRNA and protein expression in MIO-M1 cells.....	156
5.2.3 IL-1 β induced IL-10 in MIO-M1 cells treated with IL-1R1 downstream signalling inhibitors	160
5.3 Discussion.....	161
5.3.1 IL-1 β stimulation of human Müller cells induces IL-10 mRNA expression and intracellular protein	161
Chapter 6: Discussion.....	165
6.1 Summary discussion.....	165
6.1.1 P2X7, P2Y ₁ , P2Y ₄ , P2Y ₁₂ and P2Y ₁₄ were identified as functioning receptors in the MIO-M1 cell model of human Müller cells.	165
6.1.2 Stimulation of P2X7R in the MIO-M1 cell model of human Müller cells does not appear to cause cell-death.....	166
6.1.3 Stimulation of the P2X7R in the MIO-M1 cell model of human Müller cells did not cause pro-inflammatory IL-1 β or anti-inflammatory IL-10 cytokine mRNA expression or protein release.	167
6.2 Possibility of an IL-10-IL-1 β axis in the human retina	168
6.3 Limitations.....	171
6.3.1 The MIO-M1 cell line as a research model for studying human Müller cells	171
6.3.1 <i>P2X7R</i> gene polymorphisms and post-transcriptional regulation	173
6.3.2 Purinergic signalling is a promiscuous system.....	175
6.4 Future Work	175
Appendix 1: Isolation of Primary Müller Cells from Porcine Retina	178
Appendix 1.1 Introduction	178
Appendix 1.2 Materials and Methods.....	178
Appendix 1.2.1 Preparation of a Percoll stock solution and Percoll density gradients.....	178
Appendix 1.2.2 Porcine retinal dissection	179
Appendix 1.2.3 Mechanical and enzymatic digestion of retinal tissue	180
Appendix 1.2.4 Loading cell suspension onto Percoll gradient	180
Appendix 1.2.5 Cell counting	181
Appendix 1.2.6 Optical microscopy and immunohistochemistry.....	182

Appendix 1.3 Results	182
Appendix 1.3.1 Cell yield	182
Appendix 1.3.2 Identification of isolated Müller cells with optical microscopy and immunofluorescence	183
Appendix 1.4 Discussion	184
References	186

List of Figures and Tables

Chapter 1

Figure 1.1	Cross-section of the human eye	23
Table 1.1	Relative concentrations of common constituents in blood and aqueous humour	25
Figure 1.2	Aqueous humor flow from the posterior chamber of the eye to the anterior chamber of the eye	26
Figure 1.3	Retinal layers and cell types	28
Figure 1.4	A. In-vitro imaging of RGC axons in an in-tact mouse retina B. Colour photograph of the human optic nerve head	29
Figure 1.5	Retinal Ganglion Cell Types	30
Figure 1.6	Human Müller cell	31
Table 1.2	Homeostatic functions of the Müller cell	32
Figure 1.7	Microglial morphology	34
Figure 1.8	Schematic representation of the inner and outer blood-retinal barriers	36
Figure 1.9	Fundal photographs of optic disc	41
Figure 1.10	Typical visual field abnormalities in glaucoma	41
Figure 1.11	Laser peripheral iridotomy	43
Table 1.3	MIGS techniques and devices	46
Figure 1.12	Molecular structure of nucleotides	51
Figure 1.13	Mechanisms of ATP release	54

Table 1.4	P2Y receptors G-protein transduction mechanisms	57
Figure 1.14	Classification of purinergic receptors	59
Figure 1.15	A. Stereoview of the zebra fish P2X4R in a closed state; B. 'Dolphin' structure of a single P2XR subunit	61
Figure 1.16	The P2X7 receptor	64
Table 1.5	P2X7 receptor cytolytic pore formation capability by cell type	65
Table 1.6	Summary of P2 receptor locations, roles, isoforms and heterodimers	69-70
Figure 1.17	Expression of purinergic receptors in the adult retina	71
Figure 1.18	Immunohistochemistry for P2X7Rs in enzymatically dissociated Müller cells	74
Figure 1.19	Cellular calcium homeostasis	77
Figure 1.20	P2YR mediated Ca ²⁺ release from internal stores	78
Figure 1.21	LGIC channel and BK channel	79
Figure 1.22	ATP and BzATP generated responses in single human Müller cells. A. Intracellular Ca ²⁺ responses elicited by ATP and BzATP in dissociated human Müller cells using fura-2 AM microfluorimetry. B. Evoked currents (x, mV) over time (y, s)	80
Table 1.7	IL-1 family of ligands and receptors	82
Figure 1.23	IL-1 α precursor, propeptide and mature forms	84
Figure 1.24	NLRP3 inflammasome structure and possible mechanisms of IL-1 β release	87

Chapter 2

Figure 2.1	Phase contrast microscopy images of MIO-M1 cells	91
-------------------	--	-----------

Table 2.1	Seeding density of MIO-M1 cells used for experimental assays	92
Table 2.2	Agonists and antagonists used for experimental assays	94-
		95
Figure 2.2	Stages of reverse transcription quantitative polymerase chain reaction	96
Table 2.3	TaqMan probes	98
Figure 2.3	A. Fura-2 AM binding intracellular calcium B. Fura 2 AM excitation	100

Chapter 3

Table 3.1	P2 Receptor Expression in Muller cells in different Species	104
Table 3.2	P2 Receptors agonists and antagonists	108-
		9
Table 3.3	P2 receptor mRNA expression in MIO-M1 cells (n=3)	110
Graph 3.1	Fold change expression of P2 receptors on MIO-M1 cells relative to the human retina (n=3)	111
Graph 3.2	Purinergic agonist induced Ca ²⁺ response in MIO-M1 cells (n=4)	113-
		5
Graph 3.3	Purinergic agonist induced Ca ²⁺ response in MIO-M1 cells pre-incubated with P2X4R antagonists (n=4)	116-
		7
Graph 3.4	Purinergic agonist induced Ca ²⁺ response in MIO-M1 cells pre-incubated P2X7R antagonists (n=4)	118-
		9
Graph 3.5	Purinergic agonist induced Ca ²⁺ response in MIO-M1 cells pre-incubated with MRS 2170 (P2Y ₁ R antagonist; n=4)	120-
		1

Graph 3.6	Purinergic agonist induced Ca ²⁺ response in MIO-M1 cells pre-incubated with AR-C118925XX (P2Y ₂ R antagonist; n=4)	121
Graph 3.7	UTP induced Ca ²⁺ response in MIO-M1 cells pre-incubated with suramin (pan-antagonist; n=4)	122
Graph 3.8	ADP induced Ca ²⁺ response in MIO-M1 cells pre-incubated with PSB 0739 (P2Y ₁₂ R; n=4)	123
Graph 3.9	ADP induced Ca ²⁺ response in MIO-M1 cells pre-incubated with MRS 2211 (P2Y ₁₃ R; n=4)	124
Graph 3.10	Purinergic agonist induced Ca ²⁺ response in MIO-M1 cells pre-incubated with PPTN (P2Y ₁₄ R antagonist; n=4)	125-6

Chapter 4

Figure 4.1	Immunohistochemistry showing P2X7R-mediated RGC loss in the HORC model	134
Graph 4.1	A. Cell viability (n=8) and B. cell death (n=6) of MIO-M1 cells after exposure to BzATP (10μM-3mM) and ATP (100μM-3mM) for 24h.	135
Table 4.1	IL-1α, IL-1β, IL-1R1 and IL-10 mRNA expression in MIO-M1 cells in resting or control conditions (n=4)	136
Table 4.2	ATP and BzATP concentrations subthreshold and suprathreshold for P2X7R activation in MIO-M1 cells	136
Graph 4.2	Fold change in IL-1α mRNA expression in MIO-M1 cells stimulated with P2X7R agonists and antagonists (t=3h; n=4)	137

Graph 4.3	Fold change in IL-1 β mRNA expression in MIO-M1 cells stimulated with P2X7R agonists and antagonists (t=3h; n=4)	139
Graph 4.4	Fold change in IL-1 β protein expression in MIO-M1 cells stimulated with ATP 300 μ M (t=3h, 6h, 12h, 24h, 48h and 72h; n=4)	140
Graph 4.5	Fold change in IL-1 β mRNA expression in MIO-M1 cells stimulated with LPS 0.5 μ g/mL (t=3h, 6h, 12h, 24h, 48h and 72h; n=3)	141
Graph 4.6	Fold change in IL-1R1 mRNA expression in MIO-M1 cells stimulated with P2X7R agonists and antagonists (t=3h; n=4)	142
Graph 4.7	Fold change in IL-10 mRNA expression in MIO-M1 cells stimulated with P2X7R agonists and antagonists (t=3h; n=4)	143

Chapter 5

Figure 5.1	IL-1 β binding to IL-1R1 and IL-1R2 and subsequent downstream signalling	150
Figure 5.2	IL-1R1 downstream signalling antagonists: (A) characteristics and (B) site of action.	153
Graph 5.1	Evoked cell death of MIO-M1 cells after exposure to IL-1 β (1-100ng/mL) for 24h (n=4)	154
Graph 5.2	Evoked cell death of MIO-M1 cells after exposure to IL-1 β 10ng/mL and IL-1R1 downstream signalling antagonists (A) LY294002 10 μ M, (B) bardoxyl methyl 5 μ M and (C) SB203508 2.5 μ M for 24h (n=4)	156
Graph 5.3	IL-10 mRNA expression in MIO-M1 cells in response to IL-1 β 10ng/mL stimulation (t=24h; n=4).	157

Graph 5.4	Extracellular (A-B) and intracellular (C-D) IL-10 protein expression in MIO-M1 cells in response to IL-1 β 10ng/mL stimulation (t=24h and 48h; n=4)	159
Graph 5.5	IL-1 β 10ng/mL mediated IL-10 (A) mRNA and (B) intracellular protein expression in MIO-M1 cells pre-treated with IL-1R1 downstream signalling antagonists (t=24h; n=4)	161
Figure 5.3	IL-1 β induced IL-10 mRNA and protein expression in human Müller cells	164

Chapter 6

Figure 6.1	Proposed IL-10-IL-1 β axis in the human retina	170
Table 6.1	Characteristics of Müller cell lines	173
Table 6.2	Common <i>P2X7R</i> gene polymorphisms and associated changes in receptor function	174

Appendix 1

Appendix table 1.1	Dilution of stock isotonic Percoll to lower densities	179
Appendix figure 1.1	Discontinuous Percoll gradient	179
Appendix figure 1.2	Isopycnic banding of retinal cells at percoll interfaces	181
Appendix figure 1.3	Optical microscopy (A & B) and immunofluorescence (C & D) images of primary porcine Müller cell culture	183

Glossary of Abbreviations

ABC	ATP binding cassette
AC	Adenylyl cyclase
ACA	Anterior chamber angle
ADA	Adenosine deaminase
ADP	Adenosine diphosphate
ADPβS	Adenosine 5'-(β -thio)-diphosphate
AGIS	Advanced Glaucoma Intervention Study
AK	Adenosine kinase
ALT	Argon laser trabeculoplasty
ALPI	Argon laser peripheral iridoplasty
AMP	Adenosine monophosphate
ANOVA	Analysis of variance
AP	Alkaline phosphatases
Ap₄A	Diadenosine tetraphosphate
Ap₅γB	Adenosine pentaphosphate γ -boranophosphate
ASC	Apoptosis-associated speck-like protein containing a CARD
ATP	Adenosine triphosphate
ATPγS	Adenosine 5'-O-(3-thio)triphosphate
A₃P₅P	Adenosine-3'-phosphate-5' -phosphosulfate
BBG	Brilliant blue G
BGI	Baerveldt glaucoma implant
BK	Big-conductance potassium channels
BPTU	1-(2-(2-(tert-butyl)phenoxy)pyridin-3-yl)-3-(4-(trifluoromethoxy)phenyl)urea
BzATP	Benzoyl-benzoyl adenosine 5'-triphosphate
CALMH	Calcium homeostasis modulator channels
CAM	Complementary alternative medicines
cAMP	Cyclic adenosine monophosphate
CCL2	C-C motif chemokine ligand 2
CCT	Central corneal thickness

CD	Cluster of differentiation
cDNA	Complimentary deoxyribonucleic acid
CD73	Ecto-5'-nucleotidase
CITGS	Collaborative Initial Glaucoma Treatment Study
CNS	Central nervous system
CNT	Concentrative nucleoside transporters
CNTGS	Collaborative Normal Tension Glaucoma Study
CORM 2	Carbon monoxide donor 2
CSF	Cerebrospinal fluid
CSIF	Cytokine synthesis inhibitory factor
Ct	Cycle threshold
CTP	Cytidine-5'-triphosphate
Cyclodiode	Trans-scleral diode laser cyclophotocoagulation
CXCL1	C-X-C motif chemokine 1
CXCL10	C-X-C motif chemokine ligand 10
CYC 1	Cytochrome C1
DAG	Diacylglycerol
DAMP	Damage associated molecular pattern
DMEM	Dulbecco's Modified Eagle Medium
DMSO	Dimethyl Sulfoxide
DNA	Deoxyribonucleic acid
dNTP	Deoxyribonucleotide triphosphate
DPBS	Dulbecco's phosphate buffered saline
DS	Directionally sensitive [retinal ganglion cell]
EAGLE	Effectiveness of early lens extraction for the treatment of primary angle-closure glaucoma study
ECP	Endocyclophotocoagulation
EC₅₀	50% effective drug concentration
ELISA	Enzyme-linked immunosorbent assay
EMGT	Early Manifest Glaucoma Trial
ENPPs	Ecto-nucleotide pyrophosphatase/phosphodiesterases

ENT	Equilibrative nucleoside transporters
ENTPDases	Ecto-nucleoside triphosphate diphosphohydrolases
ER	Endoplasmic reticulum
ERK	Extracellular signal-related kinases
ETC	Electron transport chain
FADH2	1,5-dihydro-fad
FBS	Fetal bovine serum
Fura-2 AM	Fura-2-acetoxymethyl
GABA	Gamma-aminobutyric acid
GCL	Ganglion cell layer
GFAP	Glial fibrillary acidic protein
GPCR	G-protein coupled receptors
GS	Glutamine synthetase
GTP	Guanosine-5'-triphosphate
GWAS	Genome-wide association studies
HBSS	Hanks' Balanced Salt Solution
HORC	Human organotypic retinal culture
HRP	Horse-radish peroxidase
IFN-γ	interferon- γ
ILM	Inner limiting membrane
IL-1α	Interleukin-1 alpha
IL-1β	Interleukin-1 beta
IL-(1-40)	Interleukin-(1-40)
IL-1R	Interleukin-1 receptor
IL-1Ra	Interleukin-1 receptor antagonist
IL-1RAcP	Interleukin-1 receptor accessory protein
IL-1R1	Interleukin-1 type 1 receptor
IL-1R2	Interleukin-1 type 2 receptor
IL-1R3	See IL-1RAcP
IL-10R	Interleukin-10 receptor
IL-10Rα	Interleukin-10 receptor 1

IL-10Rβ	Interleukin-10 receptor 2
IL-10R1	See IL-10Ra
IL-10R2	See IL-10Rβ
IL-20RB	Interleukin-20 receptor B
INL	Inner nuclear layer
IOP	Intraocular pressure
IPL	Inner plexiform layer
IP₃	Inositol 1,4,5-triphosphate
IP₃R	Inositol 1,4,5-triphosphate receptor
Ip₅I	Diinosine pentaphosphate
IRAK	IL-1 receptor-associated kinases
Iso-PPADS	Iso-pyridoxalphosphate-6-azophenyl-2',4'-disulfonic acid
JAM-B	Junctional adhesion molecule B
JNK	c-Jun N-terminal kinases
J-RGC	Junctional adhesion molecule B-positive retinal ganglion cell
LC	Lamina cribosa
LCC	L-type Ca ²⁺ channel
LDH	Lactate dehydrogenase
LEDs	Local edge detectors
LGIC	Ligand gated ion channel
LIGHT	Selective laser trabeculoplasty versus eye drops for first-line treatment of ocular hypertension and glaucoma study
LPS	Lipopolysaccharide
L-$\beta\gamma$-meATP	$\beta\gamma$ -methylene-adenosine 5'-triphosphate
MAPK	Mitogen-activated protein kinases
MIGS	Minimally invasive glaucoma surgery
MIO-M1	Moorfield's/Institute of Ophthalmology – Müller 1 cells
miRNA	MicroRNA
mRNA	Messenger RNA
MRI	Magnetic resonance imaging
mtCU	Mitochondrial Ca ²⁺ uniporter

MTS	3-(4,5-dimethylthiazol-2-yl)-5-(3-carboxymethoxyphenyl)-2-(4-sulfophenyl)-2H-tetrazolium
MyD88	Myeloid differentiation primary response gene 88
NAADP	Nicotinic acid adenine dinucleotide phosphate
NAD+	Nicotinamide adenine dinucleotide
NADH	Nicotinamide adenine dinucleotide and hydrogen
NCX	Na ⁺ /Ca ²⁺ exchange transporter
NEK7	NIMA-related kinase 7
NEMO	NF-κB essential modulator
NFL	Nerve fibre layer
NF-κB	Nuclear factor kappa B
NLRP3	Nacht, LRR and PYD domains-containing protein 3
NLS	Nuclear localisation sequence
NMDA	N-methyl D-aspartate
NMDG	N-methyl-d-glucamine
NO	Nitric oxide
NOS-2	Nitric oxide synthase 2
Nrf2	Nuclear factor erythroid 2–related factor 2
NTG	Normal tension glaucoma
o-ATP	Oxidised adenosine triphosphate
OCT	Optical coherence tomography
OFF DS	OFF directionally selective [retinal ganglion cells]
OHT	Ocular hypertension
OHTS	Ocular Hypertension Treatment Study
OLM	Outer limiting membrane
ON	Optic nerve
ONH	Optic nerve head
ONL	Outer nuclear layer
ON DS	ON directionally selective [retinal ganglion cells]
ON-OFF DS	ON-OFF directionally selective [retinal ganglion cells]
OPL	Outer plexiform layer

OS	Outer segment layer
PACG	Primary angle closure glaucoma
PAMP	Pathogen associated molecular patterns
PAPET-ATP	p-aminophenylethylthio-ATP
PBS	Phosphate buffered saline
PCM	Phase contrast microscopy
PDL	Poly-D-Lysine
PEGF	Pigment epithelium derived growth factor
PI	Peripheral iridotomy
PIP₂	Phosphatidylinositol 4,5-bisphosphate
PIT	2,2'-pyridylisatogen tosylate
PI3K	Phosphoinositol-3 kinase
PKA	Protein kinase A
PLC	Phospholipase C
PMCA	Plasma membrane Ca ²⁺ ATPase
POAG	Primary open angle glaucoma
PPADS	pyridoxalphosphate-6-azophenyl-2',4'-disulfonic acid
PPTN	4-[4-(4-Piperidinyl)phenyl]-7-[4-(trifluoromethyl)phenyl]-2-
hydrochloride	naphthalenecarboxylic acid hydrochloride
pTVT	Primary Tube versus Trabeculectomy study
RB2	Reactive blue 2
RCT	Randomised control trial
RGC	Retinal ganglion cell
RNA	Ribonucleic acid
RNFL	Retinal nerve fibre layer
ROCK inhibitors	Rho kinase inhibitors
ROS	Reactive oxygen species
RPE	Retinal pigment epithelium
RT-qPCR	Real time quantitative polymerase chain reaction
RyR	Ryanodine receptor
SbC	Suppressed-by-contrast [retinal ganglion cell]

SEM	Standard error of the mean
SERCA	Smooth endoplasmic reticular Ca ²⁺ ATPase
SIP	Stock isotonic Percoll
SLT	Selective laser trabeculoplasty
SNARE	Soluble N-ethylmaleimide-sensitive factor attachment protein receptor
SNP	Single nucleotide polymorphism
SR	Sarcoplasmic reticulum
TAB1	TGF-β-activated kinase 1 binding protein 1
TAB2	TGF-β-activated kinase 1 binding protein 2
TAK1	TGF-β-activated kinase 1
TCA	Tricarboxylic acid cycle
TGF-β	Transforming growth factor beta
Th1	T helper 1 cytokine
Th2	T helper 2 cytokine
TIR	Toll/interleukin-1 receptor homology
TLPD	Translaminar pressure difference
TLPG	Translaminar pressure gradient
TLR	Toll-like receptor
TLR-4	Toll-like receptor 4
TMB	3,3',5,5'-Tetramethylbenzidine
TNF-α	Tumour necrosis factor alpha
TNP-ATP	2',3'-O-(2,4,6-Trinitrophenyl)-ATP
TOP 1	Topoisomerase
TRAF6	Tumour necrosis factor-associated factor 6
UDP	Uridine 5'-diphosphate
UDPβS	Uridine 5'-O-thiodiphosphate
UKGTS	United Kingdom Glaucoma Treatment Study
Up₄U	Uridine adenosine tetraphosphate
UTP	Uridine 5'-triphosphate
UTPyS	Uridine-5'-(γ-thio)-triphosphate

VEGF	Vascular endothelial growth factor
VGCC	Voltage-gated Ca ²⁺ channel
VNUT	Vesicular nucleotide transporter
YFP	Yellow fluorescent protein
YO-PRO	Yohimbine-proline
α,β-meATP	α,β-methylene ATP
α-RGC	Alpha retinal ganglion cell
β,γ-CF₂ATP	α,β-difluoromethylene-ATP
2-MeSADP	2-Methylthioadenosine diphosphate trisodium
2-MeSAMP	2-Methylthio-AMP triethylammonium
2-MeSATP	2-Methylthioadenosine triphosphate
5'-AMPS	Adenosine 5'-O-thiomonophosphate
5-BDBD	5-(3-bromophenyl)-1,3-dihydro-2H-benzofuro[3,2-e]-1,4-diazepin-2-one
5'-NT	See CD73

Acknowledgements

Completing this MD has been a long and wonderful journey. Alongside my studies there have been some challenges, I would like to acknowledge the individuals whose practical support and kindness have helped me progress even at times I felt unable to.

I have been lucky to study under the auspices of three exceptional supervisors. Dr Julie Sanderson, who uplifted me from having minimal research experience to a standard required to complete a higher degree. Beyond this, she has been a source of endless encouragement enabling me to persevere through hard times. Professor David Broadway, who introduced me to this research opportunity and supported my entry into a profession that has transformed my life. Mr Nuwan Niyadurupola, who I will never forget was the first person to teach me how to use a slit-lamp! Later, inspiring within me a genuine passion to practise in glaucoma.

My time as a researcher was made unforgettable by my wonderful lab partners Dr Matthew Felgate and Dr Noelia Domínguez Falcón. A special thanks to Matt for handling every teratogenic compound whilst I was pregnant or breast-feeding Isaac.

Additionally, I would like to thank Dr Philip Wright for teaching me the introductory research techniques and Dr Leanne Stokes for developing my repertoire.

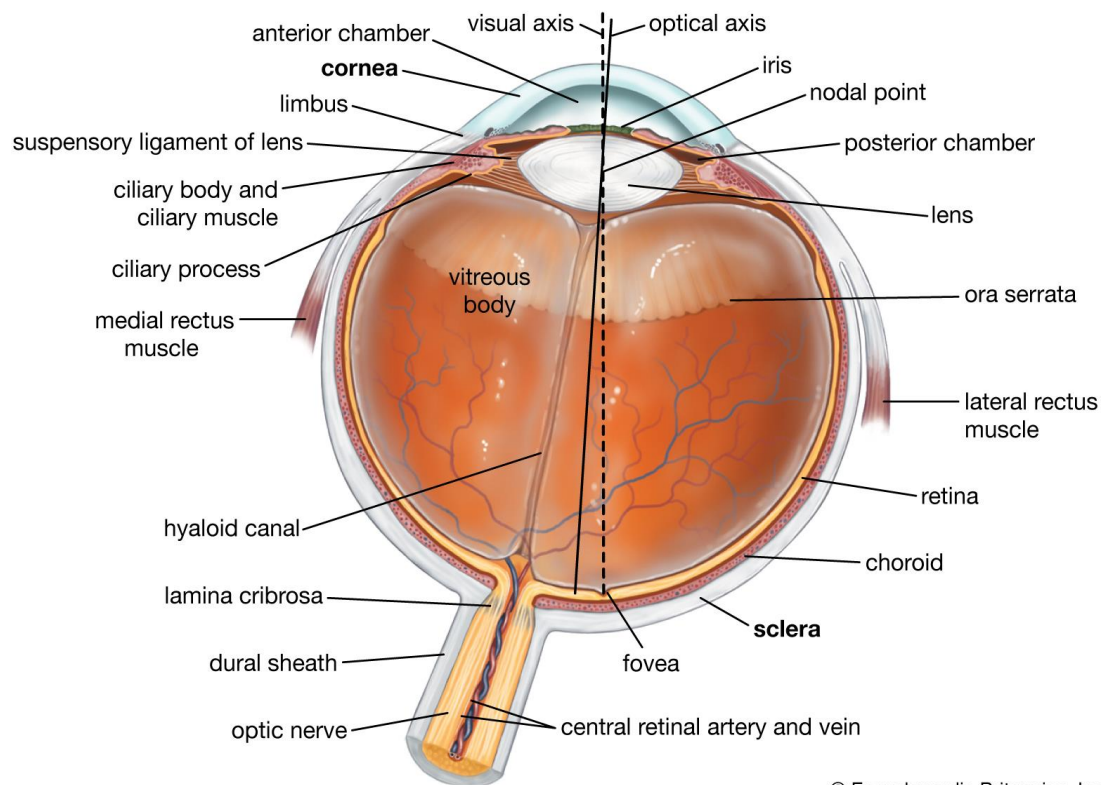
Finally, I would like to thank Isaac – I started this piece of work pregnant with you and look at us now.

Chapter 1: Introduction

1.1 Anatomy and Physiology of the Human Eye

1.1.1 Gross anatomy

The eye is a specialised organ that converts light into electrical energy, which is processed by the brain to produce the sense of sight. The transparent cornea at the front of the eye and the lens within the eye transmit and focus light onto a layer of photosensitive cells in the retina (figure 1.1). Cone and rod photoreceptor cells have differing sensitivities to specific wavelengths of light differentiating and converting the signal into an algorithm of electrical action potentials. Action potentials are transmitted along retinal ganglion cell (RGC) axons which group together to form the optic nerve transmitting information to the brain.



© Encyclopædia Britannica, Inc

Figure 1.1: Cross-section of the human eye (Encyclopædia Britannica, 2021)

1.1.2 Anterior chamber angle (ACA) and aqueous humour dynamics

Aqueous humour fills the two chambers of the eye between the cornea and lens, the anterior and posterior chambers (figure 1.1 and 1.2).

Aqueous is a transparent, colourless fluid derived from blood plasma by active secretion, ultrafiltration and diffusion (Pietrowska *et al.*, 2018). Aqueous is hypertonic compared to plasma, the greatest differences in its constituents are a significantly lower concentration of protein (table 1.1; Hubens *et al.*, 2020; Pietrowska *et al.*, 2018; Chowdhury *et al.*, 2010; Kuchle *et al.*, 1994; Rosenfeld *et al.*, 2015 and Tripathi *et al.*, 1989) and a significantly higher concentration of the antioxidant ascorbic acid (vitamin C; Senthilkumari *et al.*, 2014; Huang *et al.*, 1997 and Taylor *et al.*, 1997). Protein concentration is lower to allow optical clarity (Goel *et al.*, 2010). Ascorbic acid is actively secreted into aqueous against a concentration gradient by sodium-dependent vitamin C transporter 2 (SVCT 2; Tsukaguchi *et al.*, 1999). Ascorbic acid acts as an ultraviolet-filter thereby protecting the structures behind it from ultraviolet-induced DNA damage (Ito *et al.*, 2019; Reddy *et al.*, 1998; Ringwold, 1996; Rose and Bode, 1991). Ascorbic acid protects against UV radiation by properties of absorption, fluorescence quenching and wavelength transformation (Ringwold, 1996). Additionally, it acts as a free-radical scavenger and protects against oxidative damage (Ito *et al.*, 2019; Nemet *et al.*, 2007; Rubowitz *et al.*, 2003 and Reddy *et al.* 1998). Ascorbic acid regulates the synthesis of extracellular matrix molecules collagen and elastin (Yue *et al.*, 1990 and Higginbotham *et al.*, 1988). Low concentrations of ascorbic acid in aqueous humour are associated with cataract (Wei *et al.*, 2016; Canadanovic *et al.*, 2015; Reddy *et al.*, 1998 and Chandra *et al.*, 1986) and may be associated with pseudoexfoliation syndrome (Koliakos *et al.*, 2002) and Lowe's syndrome (Hayasaka *et al.*, 1997).

Constituent	Blood plasma	Aqueous humour
Protien ¹⁻⁶	↑	↓
Ascorbate ^{1,7-9}	↓	↑
Lactate ^{1&10}	↓	↑
Urea ¹	↑	↓
Glucose ¹	↑	↓
Na ⁺ ¹¹	↔	↔

1. Hubens *et al.*, 2020; 2. Pietrowska *et al.*, 2018; 3. Chowdhury *et al.*, 2010; 4. Kuchle *et al.*, 1994; 5. Rosenfeld *et al.*, 2015; 6. Tripathi *et al.*, 1989; 7. Senthikumari *et al.*, 2014; 8. Huang *et al.*, 1997; 9. Taylor *et al.*, 1997; 10. Levin *et al.*, 2011; 11. Goel *et al.*, 2010.

Table 1.1: Relative concentrations of common constituents in blood and aqueous humour

Key: ↑ indicates a relatively higher concentration of constituent; ↓ indicates a relatively lower concentration on constituent; ↔ indicates an equivalent concentration of constituent

Aqueous humour is derived from blood plasma by active secretion, ultrafiltration and diffusion. Aqueous contains similar constituents including: oxygen; carbon dioxide; sugars; proteins (Gaasterland *et al.*, 1979; Dickinson *et al.*, 1968; Kinsey 1953 and 1951); antioxidants (Reiss *et al.*, 1986); immunoglobulins (Allansmith *et al.*, 1973; McClellan *et al.*, 1973) and growth factors (Cousins *et al.*, 1991). Most of the constituents of aqueous are at a lower concentration than blood plasma, except for the antioxidants ascorbic acid and lactate.

Aqueous has two physiologically important roles for the healthy functioning of the eye: (i) it provides nourishment and removes waste from the avascular cornea and lens (ii) the balance between production and drainage maintains the intraocular pressure (IOP) of the eye between 11-24mmHg (Chan *et al.*, 2017), which is necessary to maintain the shape and optical properties of the eye.

Aqueous is secreted by the ciliary body into the posterior chamber. Aqueous flows around the lens and through the pupil into the anterior chamber (figure 1.2). Within the anterior chamber there is convective flow created by a temperature gradient (Heys and Barocas, 2002). Aqueous leaves the eye at the anterior chamber angle (ACA) by passive flow via two pathways: a pressure-dependent conventional pathway, and a pressure-independent non-conventional pathway (figure 1.2; Alm and Nilsson 2009; Bill 2003; Brubaker 2001; Bill and Hellsing, 1965).

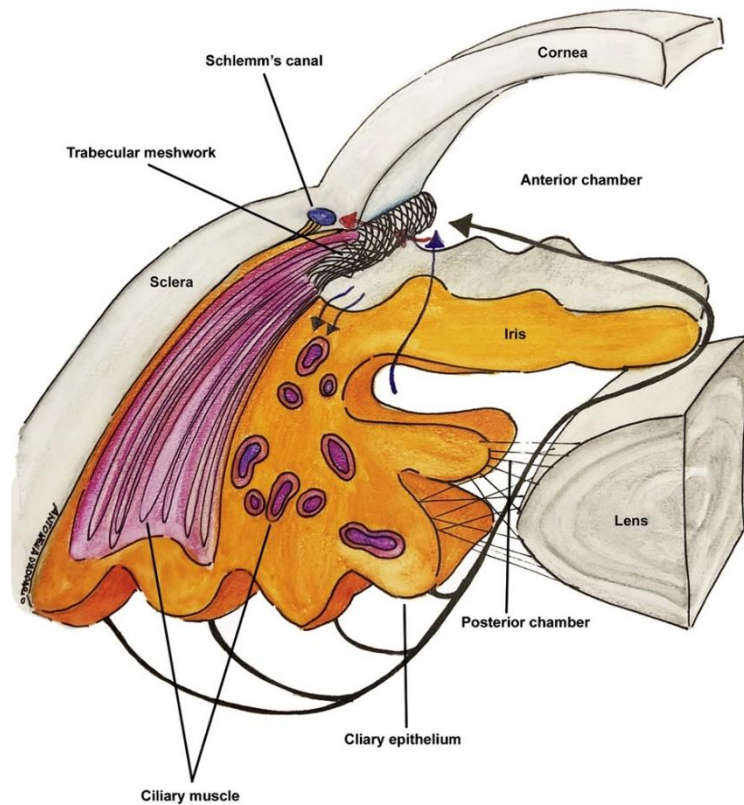


Figure 1.2: Aqueous humor flow from the posterior chamber of the eye to the anterior chamber of the eye (Costagiola *et al.*, 2020)

- | | | | |
|---|---|---|--|
| ← | Conventional pathway aqueous humor outflow | ↖ | Conventional pathway aqueous humor outflow |
| ↗ | Diffusional pathway of aqueous humor inflow | ↙ | Uveoscleral pathway of aqueous humor outflow |

The ciliary body produces aqueous and it flows through the posterior chamber through the pupil and into the anterior chamber. The aqueous drains from the eye via **(i) the conventional pathway (red arrow)**: trabecular meshwork into Schlemm's canal, the collector channels and taken away by the episcleral veins **(ii) the uveoscleral pathway (blue arrow)**: the face of the ciliary body, the ciliary muscle, suprachoroidal space to either veins in the choroid and sclera or through scleral pores to episcleral tissue.

1.1.3 Retina

The retina is the inner layer of the majority of the eyeball. The choroid and sclera overlie it (figure 1.1). The retina is a photosensitive nervous tissue that transmits visual information to the brain for higher processing. At the posterior pole of the retina is the macula lutea which has a depression called the fovea centralis, the site responsible for producing the highest level visual acuity. The optic nerve is nasal to the fovea and transmits visual information from the eye to the brain (Snell and Lemp, 2016).

The retina is made up of ten layers. Several retinal cell types are arranged along or across these ten layers (figure 1.3). Rod and cone photoreceptors are specialised cells responsible for phototransduction, they convert light energy focused onto the retina into electrical energy which can then be transmitted from cell-to-cell. Rods are responsible for vision in dim light producing low resolution grayscale images, whilst cones are responsible for vision in bright light producing high resolution colour images (Snell and Lemp., 2016). The photoreceptor terminals synapse with dendrites of the bipolar cells whose single axon synapses with RGCs and amacrine cells. There are several types of bipolar cell and they connect a rod or cone photoreceptor to different quantities and types of RGC. Horizontal and amacrine cells act to process photoreceptor signals. In this way, a degree of visual processing also occurs at a retinal level (Snell and Lemp., 2016). Retinal ganglion cell axons group together to form the optic nerve leaving the retina to transmit this visual information to the brain. Retinal homeostasis is supported by its neuroglia cells: Müller cells, astrocytes and microglia.

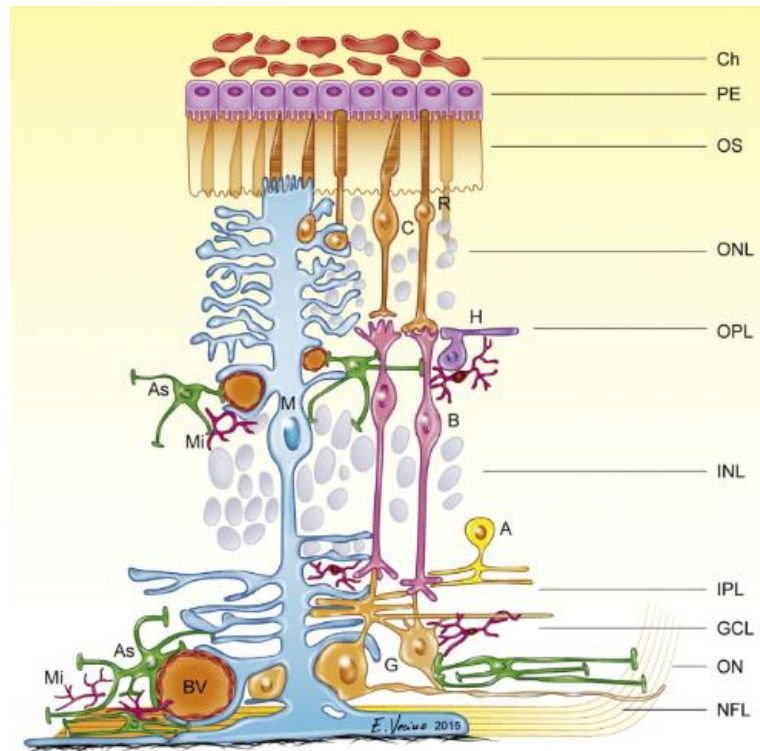


Figure 1.3: Retinal layers and cell types (Vecino *et al.*, 2016).

The retina is made up of ten layers arranged posteriorly (choroid facing, Ch) to anteriorly (vitreous facing, not shown). Posteriorly to anteriorly these layers are: retinal pigment epithelium (PE); photoreceptor outer segment layer (OS); outer limiting membrane (OLM, not shown); outer nuclear layer (ONL); outer plexiform layer (OPL); inner nuclear layer (INL); inner plexiform layer (IPL); ganglion cell layer (GCL); nerve fibre layer (NFL) and inner limiting membrane (ILM, not shown.) Nerve fibres group together to form the optic nerve (ON). Retinal cell types arranged across these layers are: rod cells (R, orange); cone cells (C, orange); horizontal cells (H, purple); bipolar cells (B, pink); amacrine cells (A, yellow); ganglion cells (G, orange), Müller cells (M, blue), astrocytes (As, green) and microglia (Mi, dark pink). Also shown is a retinal blood vessel (Bv).

1.1.3.1 Retinal ganglion cells and the optic nerve head

Retinal ganglion cells are a heterogeneous group of retinal neurons. Visual information is transmitted along RGCs dendrites in the IPL, their cell body in the GCL and their axons traversing across the inner retina forming the NFL (La Morgia *et al.*, 2017). Retinal ganglion cell axons group together and take a right-angled turn through the retina forming the optic nerve head (figure 1.4).

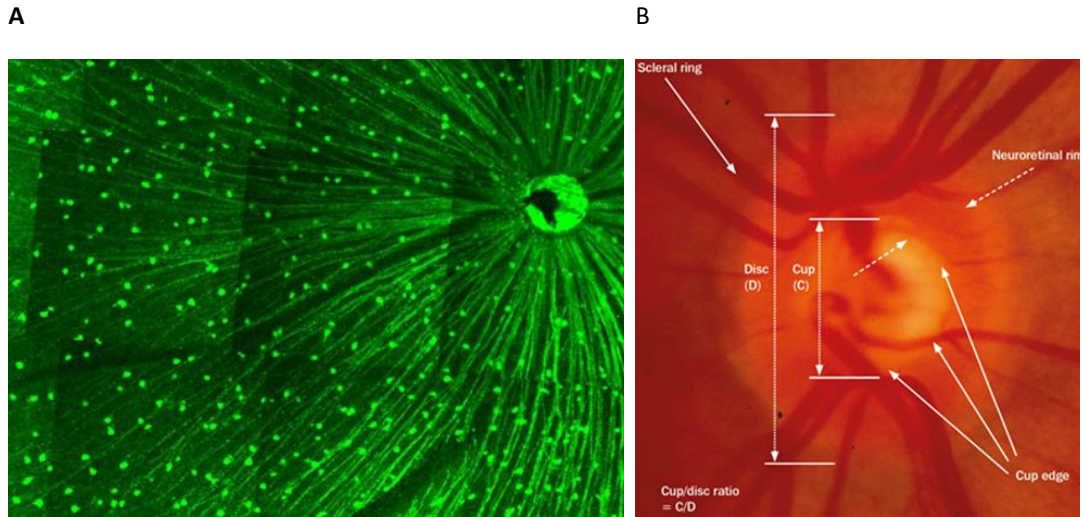


Figure 1.4 (A): In-vitro imaging of RGC axons in an in-tact mouse retina (Norsworthy *et al.*, 2017); **(B):** Colour photograph of the human optic nerve head (Bourne, 2013)

In the first image (A) α RGCs are labelled with YFP, RGC axons traverse the retina in the NFL to the optic nerve head (top right). The second image (B) illustrates the anatomy of the optic nerve head.

Within the eye RGC axons are unmyelinated, after they pierce the lamina cribrosa to leave the eye they become myelinated by oligodendrocyte glial cells in the central nervous system (Snell and Lemp., 2013). Myelinated RGC axons group together to form the optic nerve which transmits visual information to the brain.

Over thirty types of RGC exist and they are classified according to their morphology, gene expression, spacing and physiological properties (figure 1.5; Goetz *et al.*, 2022 and Sanes and Masland, 2015). Not all types of RGCs have been characterised and overlap exists between classification and nomenclature. Early work on rabbits in the 1960's identified a class of ON-OFF directionally selective RGCs (ON-OFF DS), a class of ON directionally selective RGCs (ON DS), a class of OFF directionally sensitive RGCs (OFF DS) and a class of Local Edge Detectors (LEDs). ON-OFF DS RGCs respond to both increases in light intensity or 'ON stimulus' and decreases in light intensity or 'OFF stimulus'. ON DS RGCs and OFF DS RGCs respond only to ON-stimulus or OFF-stimulus respectively. LEDs are compact cells and stimulus exceeding the size of the receptive field (RF) does not cause excitation (Barlow and Levick 1965 and Barlow *et al.*, 1964). RGCs can be further described as transient or sustained. Transient RGCs

respond to low stimulus frequencies, whilst sustained RGCs do not respond to low stimulus frequencies filtering them out (Zhao *et al.*, 2017 and Cleland *et al.*, 1971). Another class, suppressed-by-contrast RGCs (SbC), decrease their steady firing at light onset and offset (Wienbar and Schwartz, 2018; Tien *et al.*, 2015). Studies in the 1980s on cat retina identified a class of alpha RGCs (α RGCs, overlap with the term 'large RGCs'). Alpha RGCs have large somas and branching dendrites and are classified according to their ON or OFF response (Wassel *et al.* 1981). Melanopsin containing RGCs (M1-M4) contain melanopsin and have intrinsic photosensitivity (Sanes and Masland, 2015).

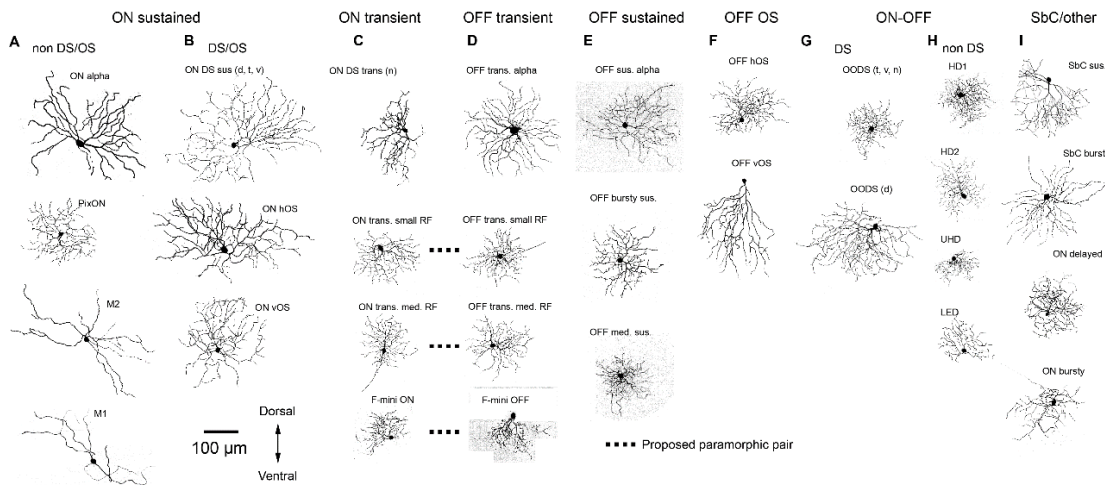


Figure 1.5: Retinal Ganglion Cell Types (Schwartz Lab, 2023)

Mouse RGCs shown en-face or whole-mount views. There is a variation in size, shape and density among RGC types. Abbreviations: DS, directionally selective; OS, orientation sensitivity; M, melanopsin containing; sus, sustained; tr, transient; h, horizontal; v, vertical; RF, receptive field; med, medium; HD, high definition; UHD, ultrahigh definition; LED, local edge detector and SbC, suppressed-by-contrast; (Goetz *et al.*, 2022).

1.1.3.2 Retinal neuroglia

Retinal neuroglia are the homeostatic support cells for the retina. Three types of specialised neuroglia are found in the human retina: Müller cells, astrocytes and microglia.

1.1.3.2.1 Müller cells

In 1851 the anatomist Heinrich Müller described radial fibers in the retina that later became eponymously known as Müller cells. Müller cells are the most predominant glial cell in the human retina, accounting for 4-5% of all retinal cells (Strettoi and Masland, 1995; Jeon *et al.*, 1998). Morphologically they extend vertically traversing all the layers of the retina, placing them in contact with multiple retinal cell types (figure 1.3 and 1.6), this is beneficial for their role in retinal homeostasis. The proximal portion of the Müller cell forms part of the ILM in contact with the vitreous. The cell nucleus lies along the INL. The distal portion forms part of the OLM in contact with photoreceptors. Each cell is positioned intimately with retinal neurons and blood vessels creating an anatomical and functional 'retinal micro-unit' (figure 1.6; Reichenbach *et al.*, 1995).



Figure 1.6: Human Müller cell (Reichenbach *et al.*, 1993).

Müller cells (blue) envelope retinal neurones (green) and contact retinal blood vessel (red).

Müller cells provide multiple homeostatic functions in the healthy retina from providing a scaffold for retinal architecture, metabolic support of retinal neurons and secreting cytokines (table 1.2).

Homeostatic function	Müller cell function
Metabolic support and nutrition of neurons	<ul style="list-style-type: none"> • Delivery of lactate for oxidative metabolism • Glucose metabolism
Ion, pH and water homeostasis	<ul style="list-style-type: none"> • CO₂ buffering • Removal of external potassium ions • Dehydration of inner retina
Protection against oxidative stress	<ul style="list-style-type: none"> • Scavenging free radicals
Contribution to neuronal signalling	<ul style="list-style-type: none"> • Neurotransmitter uptake • Neurotransmitter recycling • Release of neuroactive substances: D-serine, glutamate and adenosine triphosphate (ATP)
Recycling of photopigments	<ul style="list-style-type: none"> • Transport and conversion of bleached photopigments
Regulation of retinal blood flow via release of cytokines with vasoactive properties	<ul style="list-style-type: none"> • Synthesis and release of vascular endothelial growth factor (VEGF), pigment epithelium derived growth factor (PEGF) and transforming growth factor β (TGF-β)
Embryonic retinal development	<ul style="list-style-type: none"> • Provide a scaffold for immature retinal cells allowing histotypic organisation
Act as optical fibres	<ul style="list-style-type: none"> • Contribute to vision by acting as optical fibres to guide light to photoreceptors

Table 1.2: Homeostatic functions of the Müller cell (adapted from Bringmann *et al.*, 2006 including Franze *et al.*, 2007)

Müller cells also have a key role in the pathological retina; they are the first cells to demonstrate changes in retinal stress or disease (Pfeiffer *et al.*, 2016). Müller cells mediate retinal injury and are involved in subsequent retinal remodelling which can be protective or detrimental to retinal function. Müller cells are resilient to damage which allows them to remain available to mediate these events (Silver *et al.*, 1997; Stone *et al.*, 1999). Broadly, in the pathological retina, they produce cytokines such as VEGF and TGF- β (Caspi and Roberge, 1989; Roberge *et al.*, 1991; Drescher and Whittum-Hudson, 1996) as well as phagocytosing cell debris and pathogens (Mano and Puro, 1990; Stolzenburg *et al.*, 1992; Francke *et al.*, 2001). With other retinal glia they cause reactive gliosis. Gliosis describes glial cell activation and later scar formation. Müller cells increase expression of stress marker proteins (e.g. Glial fibrillary acidic protein; GFAP), undergo hypertrophy, proliferate and their nuclei migrate to the apical surface (Bringmann 2009). Initial changes cause alterations in

microvascular and leukocyte migration that are neuroprotective, but later scar formation prevents retinal recovery.

1.1.3.2.2 Astrocytes

Astrocytes are a class of central nervous system (CNS) glial cells. Eleven subtypes are found across the brain, spinal cord and retina. In the retina, astrocytes are predominantly confined to the NFL and accompany blood vessels in the INL (figure 1.5; Vecino *et al.*, 2016). Astrocytes exist in quiescent and reactive states. Homeostatic functions include formation of the blood-retinal barrier (astrocyte endfeet cover and interact with endothelial cells of blood vessels), nourishment of neuronal cells, neurotransmitter turnover, formation of neuronal synapses and signal modulation (Vecino *et al.*, 2016).

Astrocytes are highly plastic cells that alter their morphological and functional properties in response to cytokines produced by other retinal cells or in pathological states. Astrogliosis is a hallmark of neuronal injury whereby astrocytes change in morphology from quiescent to reactive. (Franke and Illes, 2014). Similar to Müller cells previously described, reactive astrocytes initially have neuroprotective functions, but later glial scar formation prevents retinal recovery. Reactive astrocytes alongside other glial cells isolate damaged tissue from surrounding healthy neuronal tissue. Reactive astrocytes also synthesise neurotrophins and pleiotrophins that assist in neuronal recovery (Franke and Illes, 2014 and Pekny *et al.*, 2014). However, they also release several neurotoxic molecules such as nitric oxide (NO) and ultimately contribute to glial scar formation (Franke and Illes, 2014).

1.1.3.2.3 Microglia

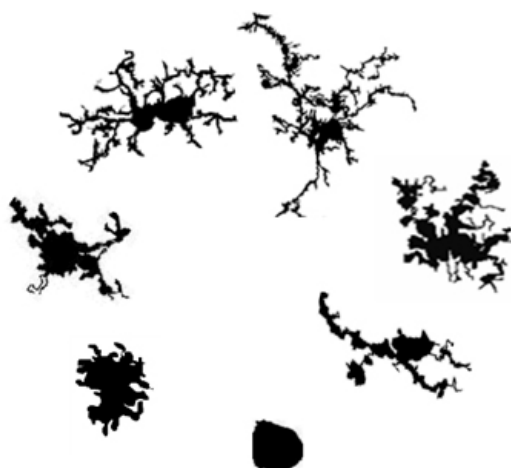


Figure 1.7: Microglial morphology (Karperien *et al.*, 2013).

Ramified microglia have multiple cellular processes and are the dominant morphological form in physiological conditions. Ramified microglia transition during pathological conditions firstly into reactive microglia and later into phagocytic or amoeboid microglia. Reactive microglia have shorter wider processes. Phagocytic microglia lack cellular processes (Beynon and Walker, 2012)

Similar to astrocytes, microglia are also CNS glial cells which exist in quiescent and reactive states (figure 1.7).

In the retina microglia are located in the innermost layers: the NFL, GCL, IPL and INL (Chen *et al.*, 2014; Cuenca *et al.*, 2014; Garcia-Valenzuela *et al.*, 2005; Noailles *et al.*, 2014 and Santiago *et al.*, 2014).

Homeostatic functions include: mediating glial-glial and glial-neuronal interaction (Colton, 2009; Corraliza, 2014; Prinz and Priller, 2014; Ransohoff and Brown, 2012); production of anti-inflammatory cytokines and performing local macrophage functions. In particular, microglial macrophage functions are a crucial role of the innate immune system as the blood-retinal barrier prevents systemic macrophages from entering the retina (Carson *et al.*, 2006).

Microglia are activated by endogenous pro-inflammatory stimuli such as complement or pro-inflammatory cytokines, and exogenous pathogenic stimuli such

as lipopolysaccharide (LPS). Similar to other retinal glial cells, microglia have neuroprotective and neurotoxic effects in the human retina. Neurotoxic effects include release of several neurotoxic molecules such as NO and contribution to glial scar formation (Beynon and Walker, 2012).

1.1.3.3 Blood-retinal barrier (BRB)

The eye is an immune-privileged organ. The constituents of its aqueous humor, vitreous humor and extracellular fluid are regulated and comparatively protected from physiological or pathological variations occurring in the systemic circulation (Lee and Pelis, 2016; Cunha-Vaz *et al.*, 2011). Immune privilege is predominantly afforded by the two blood-ocular barriers: the blood-aqueous barrier in the anterior segment and the blood-retinal barrier in the posterior segment (Lee and Pelis, 2016 and Coca-Prados, 2014).

The BRB was identified by dye experiments, trypan blue was intravenously injected into rabbits staining all organs except the CNS and the retina (Palm, 1947). Similar to the blood-brain barrier, it is a highly selective barrier preventing free-diffusion of substances between the systemic circulation and the retina (Hosoya and Tachikawa, 2012). The BRB regulates the movement of water, ions, protein and cells across the retina efficiently supplying its metabolic requirements (Saunders *et al.*, 2014; Hosoya and Tachikawa, 2012; Cunha-Vaz *et al.*, 2011; 1967 and 1966). Protectively, it restricts the movement of macromolecules and pathogens into the retina. Structurally, it is composed of two distinct barriers: (i) the inner BRB is formed by tight junctions between retinal capillary endothelial cells (Kubo *et al.*, 2018; Díaz-Coránguez *et al.*, 2017) and (ii) the outer BRB is formed by tight junctions between RPE cells (figure 1.8; Kubo *et al.*, 2018; Díaz-Coránguez *et al.*, 2017; Cunha-Vaz *et al.*, 2011). Tight junctions are a family of proteins including occludins, claudins, junctional adhesion molecules and zona occludins (Coca-Prados, 2014). Tight junctions gatekeep paracellular transport, the movement of substances through the intracellular spaces between adjacent cells (Coca-Prados, 2014).

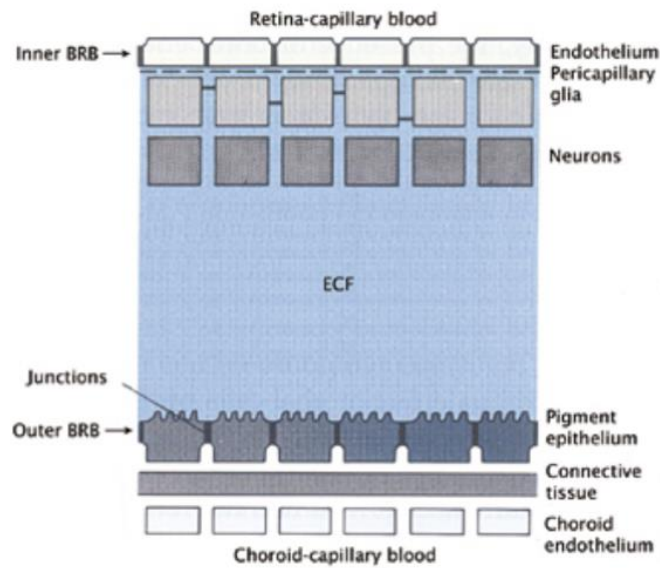


Figure 1.8: Schematic representation of the inner and outer blood-retinal barriers (Cunha-Vaz, 2011).
Abbreviations: BRB, blood-retinal barrier and ECF, extracellular fluid

The BRB is composed of two distinct barriers: (i) the inner BRB is formed by tight junctions between retinal capillary endothelial cells and (ii) the outer BRB is formed by tight junctions between RPE cells.

The inner BRB has a close association of neurones, astrocytes, Müller cell foot projections and pericytes within the retinal capillary endothelium, termed the neuro-vascular unit (Díaz-Coránguez *et al.*, 2017 and Coca-Prados, 2014). Pericytes enwrap capillary endothelial cells promoting endothelial remodelling, maturation and differentiation (Bergers and Song 2005 and Ogawa *et al.* 2002,). Additionally, they promote glial interactions (Genove *et al.* 2010). Pericyte coverage correlates with BRB integrity, with a pericyte to capillary endothelial cell ratio of 1:1 (Díaz-Coránguez *et al.*, 2017). BRB integrity is compromised in several pathological processes including diabetic retinopathy (Frey and Antonetti 2011). Fluorescein angiography can be used to image sites of *leakage in vivo* (Vinores, 1995).

1.2 Glaucoma

1.2.1 Overview and classification

Glaucoma describes a heterogeneous group of progressive optic neuropathies with a characteristic irreversible loss of RGCs causing corresponding visual field defects that may lead to blindness if untreated (Quigley 1999). Glaucoma is a significant contributor to global morbidity as the leading cause of irreversible blindness worldwide (Flaxman *et al.*, 2017). There is a predilection for older populations, it being present in 1% of those over 40 years old and 3% of those over 70 years old in Caucasians (Denniston and Murray, 2018): in the years to come, the prevalence is expected to increase as the population continues to disproportionately shift to an ageing distribution. The pathophysiology of glaucoma is not well-defined and assumed to be multifactorial, research on this is described further in *section 1.2.5*. Currently there is no curative treatment and management focuses on preventing disease progression by reducing IOP, even if this is found to be within the normal range.

Glaucoma represents a final common pathway for a number of conditions. The glaucomas are often classified by aetiology as 'primary' or 'secondary' and by configuration of the anterior chamber angle as 'open' or 'closed'. Primary glaucoma describes glaucomatous optic neuropathy with no associated underlying disease, whilst secondary glaucoma is due to a separate disease process. Aphakic glaucoma is an example of secondary glaucoma, described as a delayed complication of paediatric cataract surgery (Stech *et al.*, 2019; Ekşioğlu *et al.*, 2018; Haargaard *et al.*, 2008; Levin, 2007; Chen *et al.*, 2006; Chen *et al.*, 2004; Magnusson *et al.*, 2000; Taylor *et al.*, 1999; Mills and Robb, 1994; Keech *et al.*, 1989 and Kirsch *et al.*, 1976). The pathophysiology of aphakic glaucoma is not fully understood; aphakia causes complex mechanical and biochemical changes in the anterior segment structures and vitreous (Levin, 2007 and Chen *et al.*, 2006). Many factors are conceivable: (i) co-morbidity of a congenital cataract and an ACA anomaly (Stech *et al.*, 2019 and Kirsch *et al.*, 1976); (ii) iatrogenic trauma or distortion of the immature ACA (Stech *et al.*, 2019 and Kirsch *et al.*, 1976); (iii) iatrogenic synechiae; (iv) vitreous prolapse into the

anterior chamber (Stech *et al.*, 2019 and Chen *et al.*, 2006) and (v) remaining lens epithelial cells proliferating on trabecular meshwork affecting function (Lundvall and Zetterström, 1999). Other examples of secondary glaucomas include those caused by trauma, uveitis, pigment dispersion syndrome, pseudoexfoliation syndrome and iridocorneal endothelial syndrome. Open-angle glaucoma describes glaucomatous optic neuropathy without irido-trabecular meshwork apposition, whilst closed-angle glaucoma is associated with irido-trabecular meshwork apposition that impedes aqueous drainage from the eye. Most cases of glaucoma are acquired, however, rarely glaucoma can present in early life, and this is referred to as congenital glaucoma.

The most common type of glaucoma differs from one region of the world to another: in Europe primary open angle glaucoma (POAG) is the most prevalent form of the disease whilst in Asia primary angle closure glaucoma (PACG) is the most prevalent form of the disease (Denniston and Murray, 2018).

Chronic glaucomas such as PACG, POAG and its subset normal tension glaucoma (NTG) are usually asymptomatic. It is estimated that nearly half of the individuals in populations with chronic glaucoma are unaware of their condition (Topouzis *et al.*, 2007, Mitchell *et al.*, 1996, Dielemans *et al.*, 1994 and Somner *et al.*, 1991). As there is a pre-symptomatic stage and early treatment reduces the risk of sight loss (Maier *et al.*, 2005), free screening is offered in the UK to at risk populations (NHS, 2018 and Health and Medicines Act, 1988) although not population wide (UK NSC, 2019). By contrast, acute angle closure, that can lead to glaucoma occurs less frequently but is highly symptomatic requiring immediate treatment to prevent permanent loss of vision.

1.2.2 Risk factors

Raised IOP is strongly associated with glaucoma. However, the relationship between IOP and glaucoma is not directly causal as there are eyes with low pressure who develop glaucoma (NTG), and eyes with high pressure who may not develop glaucoma (ocular hypertension, OHT). IOP is the only currently proven modifiable

risk factor in the development and progression of glaucoma. Landmark studies have shown that glaucoma onset and progression is slowed by reducing IOP. The Ocular Hypertension Treatment Study (OHTS) showed that reducing the IOP by over 20% and to less than 24mmHg reduced the conversion rate of OHT to POAG (Kass *et al.*, 2010 and 2002). The Collaborative Normal Tension Glaucoma Study (CNTGS) demonstrated that for NTG an IOP reduction by greater than 30% slows the rate of visual field loss (Anderson *et al.*, 2003). Similarly, the Advanced Glaucoma Intervention Study (AGIS) and United Kingdom Glaucoma Treatment Study (UKGTS) demonstrated reducing mean IOP reduced visual field loss (Garway-Heath *et al.*, 2015 and the AGIS Investigators, 2000). The Early Manifest Glaucoma Trial (EMGT) showed that even small reductions in IOP by 1mmHg leads to a 10% reduction in progressive nerve damage (Heijl *et al.*, 2002). However, even with significant reduction in IOP, OHTS, CNTG and EMGT have demonstrated a subset of glaucoma patients who continue to experience disease progression (Anderson *et al.*, 2003; Dance *et al.*, 2004; Bengtsson *et al.*, 2007; Heijl *et al.*, 2009, 2003 and 2002; Hyman *et al.*, 2010; Leske *et al.*, 2007 and 2003; Kass *et al.*, 2002 and Keltner *et al.*, 2006).

Other major risk factors for developing glaucoma include older age, ethnicity, family history of glaucoma and high myopia. Meta-analysis demonstrated the odds ratio for developing POAG was 1.73 for every decade beyond 40 years of age (Tham *et al.*, 2014). Ethnicity is a risk factor, and it has been shown that Afro-Caribbean ethnicities are associated with a greater risk of developing POAG compared with European ethnicities (Tham *et al.*, 2014 and Rudnicka *et al.*, 2006). Family history is a major risk factor, (Green *et al.*, 2007 Le *et al.*, 2003, Wolfs *et al.*, 1998) the lifetime risk of glaucoma increasing from 2.3% to 22% for individuals with a first-degree relative with glaucoma (Wolfs *et al.*,1998). Recent large genome-wide association studies (GWAS) meta-analyses have identified over 100 genetic loci associated with glaucoma (Gharahkhani, *et al.*, 2021; Khawaja *et al.*, 2018; Choquet *et al.*, 2017, Springelkamp *et al.*, 2017 and Hysi *et al.*, 2014) explaining the high degree of heritability. High myopia of >8D has also been demonstrated in several populations to be a risk factor (Qiu *et al.*, 2013; Perera *et al.*, 2010; Xu *et al.*, 2007).

In addition, male gender is associated with a greater risk of developing POAG compared with female gender (Tham *et al.*, 2014; Rudnicka *et al.*, 2006 and Gordon *et al.*, 2002), although female gender is associated with a greater risk of progression (Group CNTGS, 1998).

Landmark trials have revealed additional risk factors for progressive glaucomatous damage, such as disc haemorrhages visible on the optic nerve head (ONH) at diagnosis (figure 1.9) and a history of migraine, in the OHTS and CNTGS respectively (Budenz *et al.*, 2006 and Dance *et al.*, 2004). As with migraine, other factors thought to affect perfusion to the ONH have been implicated such as hypotension (Graham *et al.*, 1995), nocturnal hypotension (Hayreh *et al.*, 1994), history of haemodynamic collapse (Drance *et al.*, 1973) and Raynaud's syndrome or vasospastic disease (Gasser *et al.*, 1990). These vascular and ischaemic risk factors are thought to be more significant in the development of NTG. OHTS identified thin central corneal thickness (CCT) as a risk factor for developing glaucoma: a CCT below 555µm is associated with a three-fold increased risk of developing POAG.

It has been well documented that steroid use can induce glaucoma and previous use causing a rise in IOP 'steroid-response' is a risk factor for going on to develop glaucoma (Razeghinejad and Katz 2012; Kersey and Broadway, 2006).

1.2.3 Diagnosis and monitoring

Diagnosis of glaucoma is made by clinical judgement. Currently there are no specific diagnostic tests. A medical history is taken from the patient to identify any of the glaucoma risk factors outlined above. Clinical examination includes measuring CCT by pachymetry, IOP by tonometry and angle grading by gonioscopy. Examination also assesses for evidence of secondary causes of glaucoma, such as pseudoexfoliation material (pseudoexfoliation glaucoma), pigment (pigment dispersion syndrome) or cataract (phacolytic glaucoma). The optic disc is examined for signs of glaucomatous optic neuropathy (figure 1.9).

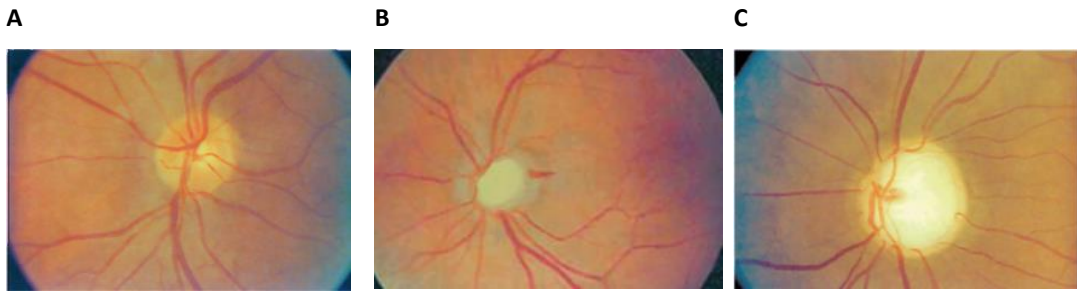


Figure 1.9: Fundal photographs of optic disc (adapted from: Leitman, 2016)

A: Healthy optic disc, the cup: disc ratio is 0.25. B: Optic disc suspicious for glaucoma, the cup: disc ratio is 0.70 and there is a disc haemorrhage. C: Optic disc with advanced glaucoma, the cup: disc ratio is 0.90 and there is nasalisation of blood vessels.

Investigations for the diagnosis and monitoring of glaucoma include perimetry and optical coherence tomography (OCT). Perimetry is the systematic measurement of the visual field. There are several patterns of field loss which are suspicious for glaucoma including horizontal defects, ‘nasal step’, paracentral scotoma and arcuate defects (figure 1.10: EGS, 2017). However, the pattern of field loss should correspond to the individual’s optic disc appearance to be attributable to glaucoma.

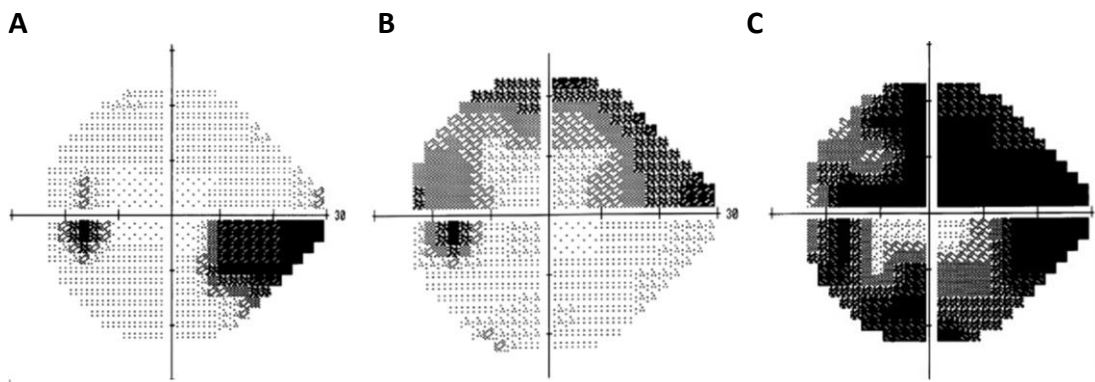


Figure 1.10: Typical visual field abnormalities in glaucoma (adapted from: Yanoff and Duker, 2014).

In the assessment of glaucoma static perimetry is usually used to assess the visual field. During static perimetry testing the position and size of the target are kept constant whilst the brightness is increased until it can be detected by the individual. Several points in the field of vision are tested. Darker areas represent areas of visual loss. Shown above is static perimetry of the left eye showing typical visual field defects in glaucoma: A. nasal step; B. arcuate scotoma and C. tunnel vision as seen in end-stage glaucoma.

Recently, OCT and its newer variants have been used to image the thickness of the retinal nerve fibre layer (RNFL). RGC death in glaucoma causes the RNFL to become

thinner. OCT RNFL has been shown to detect early glaucoma before visual field changes (Larrosa *et al.* 2015, Mwanza *et al.*, 2013, Wu *et al.*, 2012 and Mwanza *et al.*, 2011). It is often used as an adjunct in the diagnosis and monitoring of glaucoma (NICE, 2022).

1.2.4 Treatment

The therapeutic goal is to reduce IOP so there is no further or limited progression of glaucoma (EGS, 2017). IOP can be managed by laser, pharmacologically, surgically or a combination of these.

Selective laser trabeculoplasty (SLT), Argon laser trabeculoplasty (ALT), and trans-scleral diode laser cyclophotocoagulation ('cyclodiode') are IOP reducing lasers used typically in the management of open-angle glaucomas. SLT is preferentially used instead of ALT as it minimises damage to the ACA. The recent selective laser trabeculoplasty versus eye drops for first-line treatment of ocular hypertension and glaucoma (LiGHT) study found that SLT was more clinically and cost-effective as the first line treatment for glaucoma (Gazzard *et al.*, 2019): the National Institute for Health and Care Excellence (NICE) now recommend SLT as a first-line treatment for open-angle glaucomas and ocular hypertension in the UK (NICE, 2017). SLT selectively targets the pigmented cells in the trabecular meshwork, as these exhibit greater absorbance than neighbouring cells thereby mitigating tissue damage (McAlinden, 2014; Latina and Park, 1995). The mechanism by which SLT lowers IOP is unknown (McAlinden, 2014 and Bruen, 2012). Several mechanisms of action have been proposed, whereby SLT produces mechanical, cellular and biochemical changes in the trabecular meshwork (McAlinden, 2014 and Van Buskirk *et al.*, 1984). Initially it was thought mechanical changes such as collagen shrinkage and scarring allowed better outflow of aqueous humour (Bruen *et al.*, 2012; Wise, 1981). Cellular changes including trabecular meshwork cell necrosis (Van Buskirk *et al.*, 1984) and increased phagocytic activity of macrophages in clearing debris were proposed to increase aqueous outflow (Bruen *et al.*, 2012; Blysmá *et al.*, 1988 and Van Buskirk *et al.*, 1984). Biochemically there is a release of pro-inflammatory cytokines interleukin-8 (IL-8), interleukin-1 alpha (IL-1 α), interleukin-1 beta (IL-1 β) and tumour necrosis factor

alpha (TNF- α) which promote matrix metalloproteinase expression implicated in improving aqueous outflow at the juxtacanalicular trabecular meshwork (Lee *et al.*, 2016; Bruen *et al.*, 2012; Cellini *et al.*, 2008 and Bradley *et al.*, 2000). Aqueous permeability is also induced by releasing tight junctions between Schlemm's canal and trabecular meshwork cells (Ansari, 2021 and Alvarado *et al.*, 2010). Cyclodiode laser partially destroys the ciliary body decreasing the production of aqueous humour and subsequently lowering IOP. It is commonly used in refractory glaucoma, traditionally reserved for end-stage management, however recent technique modifications have reduced complications and it has been increasingly used in the seeing-eye (Agrawal *et al.*, 2011).

Peripheral iridotomy (PI) and argon laser peripheral iridoplasty (ALPI) are lasers used typically in the management of angle-closure. PI uses laser to form an 'iridotomy' hole in the peripheral iris (figure 1.11), this permits the flow of aqueous from the posterior chamber to the anterior chamber. ALPI uses laser to burn and shrink the peripheral iris with subsequent changes widening the ACA.

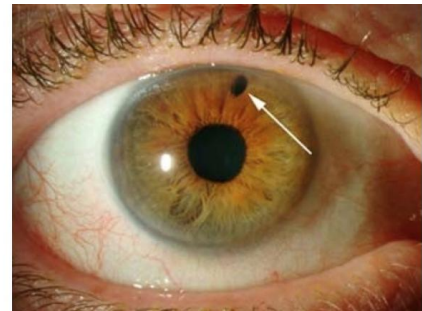


Figure 1.11: Laser peripheral iridotomy (Wajda *et al.*, 2016).

Laser iridotomy is highlighted by the white arrow.

Pharmacological management is used to manage acute IOP rises, OHT and all types of glaucoma. Most commonly it is in the form of topical eye-drops that are self-administrated daily. Initial treatment is usually with a prostaglandin analogue, which is administered once daily and reduces IOP by increasing aqueous outflow in the eye via the uveoscleral outflow pathway. Other classes include carbonic anhydrase inhibitors, beta-blockers and alpha₂-agonists which reduce IOP by decreasing aqueous production. Alpha₂-agonists also increase aqueous outflow through the uveoscleral pathway (Toris *et al.*, 1995). Miotics contract the ciliary muscle, open the trabecular meshwork and dilate Schlemm's canal, these changes increase aqueous outflow via the trabecular route (Kaufman, 2020; EGS, 2017 and Lütjen-Drecoll,

1973). If necessary, topical therapy can be switched or increased until the patient is on maximal therapy using one pharmacological agent from each class of anti-glaucomatous medication. Recent advances include Rho Kinase (ROCK) inhibitors have passed clinical trials in the UK and work by increasing aqueous outflow (Tanna and Johnson., 2018). More recently studies have investigated the role of neuroprotective agents in glaucoma: Citicoline has been shown to enhance retinal function, neural conduction along the visual pathway and increase RNFL thickness (Parisi *et al.*, 2019, Chitu *et al.*, 2019 and Parisi *et al.*, 2015); similarly 17 β -estradiol has shown retinal neuroprotective effects but has significant systemic side-effects (Prokai-Tatrai *et al.*, 2013). Patient compliance with topical therapy is limited by multiple daily dosing, drug and preservative side-effects, no noticeable amelioration of symptoms (Reardon *et al.*, 2011), lack of glaucoma education provided, practical barriers (e.g. location, prescription charges), 'forgetfulness' and correct instillation (Lacey *et al.*, 2009 and Hosoda *et al.*, 1995).

For advanced glaucoma or progressive glaucoma refractory to medical management, there are surgical procedures designed to reduce the IOP of the glaucomatous eye. Trabeculectomy is the gold-standard amongst glaucoma surgery (Coleman, 2005). Trabeculectomy can achieve an IOP below 10mmHg which may be necessary for aggressive glaucoma or NTG. Trabeculectomy is a penetrating eye surgery involving the removal of a full-thickness block of trabecular meshwork beneath a partial thickness scleral flap to allow aqueous to filter out of the eye. Trabeculectomy was initially devised by John Cairns in 1968 (Cairns, 1970; 1969; 1968) who described it as a bypass procedure of making a deep scleral flap with excision of trabecular tissue, allowing an alternative resistance-free pathway for aqueous outflow. The technique was later modified by Peter Watson in 1970 (Watson, 1975) to one similar to that used today. The Collaborative Initial Glaucoma Treatment Study (CIGTS) compared pharmacology versus trabeculectomy as an initial treatment. CIGTS subgroup analysis showed that Caucasian patients with moderate-to-advanced glaucoma at time of diagnosis had better results with initial trabeculectomy management (Musch *et al.*, 2011, 2009 and 2008).

Tube shunts are implantable silicone tubes that drain aqueous humour from the anterior chamber into the subconjunctival space. The most used tubes are the Ahmed glaucoma valve and the Baerveldt glaucoma implant (BGI) (Tseng *et al.*, 2017). Primary Tube versus Trabeculectomy (pTVT) study compared BGI to trabeculectomy in patients with no previous incisional surgery, it revealed greater IOP reduction, lower risk of failure and lower usage of medical therapy for patients with trabeculectomy (Gedde *et al.*, 2020). Trabeculectomy and tube shunt surgery have potential risks of major complications (Khaw *et al.*, 2017) and a three-month period of intense postoperative care (Bar-David and Blumenthal., 2018), so surgical management may not be suitable for some patients.

More recently, there has been the advancement of minimally invasive glaucoma surgery (MIGS). MIGS describes a range of surgical implants (table 1.3) that aim to lower IOP with a less invasive approach than the previously described techniques. They are useful when modest reductions in IOP are required and can be performed as an opportunistic adjunct to cataract surgery (Gazzard, 2016). MIGS procedures share the following characteristics: (i) minimally traumatic (ii) most preserve the conjunctiva (useful if trabeculectomy is required) (iii) high safety profile and (iv) rapid recovery (Gazzard, 2016).

Technique or device	Mechanism of IOP reduction	Conjunctiva sparing	Published RCT studies
Trabectome	Excision or electrocautery of the trabecular meshwork. Aqueous drains into Schlemm's canal.	Yes	No* ^{1,2}
iStent and iStent Inject	Trabecular bypass shunt which creates a permanent opening for aqueous to drain into Schlemm's canal. iStent inject is a second-generation device designed for implantation of two iStents in a single surgical procedure.	Yes	Yes ^{3, 4, 5, 6, 7 & 8}
Hydrus	Trabecular bypass shunt which creates a permanent opening for aqueous to drain into Schlemm's canal.	Yes	Yes ^{5, 9, 10, 11 & 12}
Ab Interno Canaloplasty with iTrack	Dilatation of trabecular meshwork. Aqueous drains into Schlemm's canal.	Yes	No
Endocyclophotocoagulation (ECP)	Targeted ablation of the ciliary processes with diode laser equipped with endoscope. The production of aqueous is decreased.	Yes	No
Microshunt	Shunt which drains aqueous from the anterior chamber into the subtenons or subconjunctival space.	No	Yes ¹³
Xen	Shunt which drains aqueous from the anterior chamber into the subtenons or subconjunctival space.	No	No
Ex-PRESS	Shunt which drains aqueous from the anterior chamber into the subconjunctival space.	No	Yes ^{14, 15, 16, 17, 18, 19 & 20}

1. Ting *et al.*, 2018; 2. Chow *et al.*, 2017; 3. Kozera *et al.*, 2021; 4. Saheb *et al.*, 2021; 5. Ahmed *et al.*, 2020; 6. Fea *et al.*, 2015; 7. Samuelson *et al.*, 2011; 8. Fea, 2010; 9. Laspas *et al.*, 2019; 10. Ahmed *et al.*, 2021; 11. Pfeiffer *et al.*, 2015; 12. Samuelson *et al.*, 2018; 13. Baker *et al.*, 2021; 14. Aihara *et al.*, 2019; 15. Arimura *et al.*, 2018; 16. Gonzalez-Rodriguez *et al.*, 2016; 17. Wagschal *et al.*, 2015; 18. Netland *et al.*, 2014; 19. Dahan *et al.*, 2012 and 20. de Jong LA, 2009.

Table 1.3: MIGS techniques and devices (Updated and adapted from Gazzard., 2016)

*Randomised control trial (RCT) performed but ended early due to difficulty recruiting a sufficient sample size.

Cataract surgery involves ultrasound breakdown of the opaque cataractous lens, aspiration of the fragments and insertion of a new synthetic lens into the lens capsule. It is the most performed surgery in the UK, has a good-safety profile and low rate of risks. In glaucoma it has the additional benefit of reducing IOP: a large systematic review and meta-analysis by Masis *et al.*, in 2017 demonstrated a decrease in IOP by 2.7mmHg in POAG individuals and 6.4mmHg in PAC individuals.

Furthermore, the effectiveness of early lens extraction for the treatment of primary angle-closure glaucoma (EAGLE) study recommends cataract surgery as the primary intervention for patients with angle-closure and IOP greater than 30mmHg or PACG (Azuara-Blanco *et al.*, 2011).

There is currently no well-established evidence to support complementary alternative medicines (CAM) in the management of glaucoma. *Ginkgo biloba* is a herbal supplement that appears to improve ocular perfusion and visual field in patients with glaucoma (Kang and Lin., 2018; Quaranta *et al.*, 2014). *Ginkgo biloba* may be used to supplement conventional management in suitable patients. There is some evidence that the elevation of the head of the bed by thirty degrees lowers IOP (Park *et al.*, 2016 and Yeon *et al.*, 2014). *Marijuana* is known to lower IOP, however its use as a potential therapeutic agent is limited by low response rate, short half-life and side-effects (Bhartiya and Ichhpujani, 2014). Other herbal pharmaceuticals, such as Forskolin 1% (*Coleus forskohlii*; Majeed *et al.*, 2015) and Garcinia 0.5% (*Garcinia kola*; Adefule-Ositelu *et al.*, 2010) have been shown in small studies to reduce IOP

1.2.5 Pathophysiology

There are many proposed contributors to the pathophysiology of glaucoma including biomechanical mechanisms, ischaemia, excitotoxicity and inflammation. Recent studies implicate purinergic signalling in neurodegenerative glaucomatous damage (Reichenbach and Bringmann, 2016; Sanderson *et al.*, 2014; Vhora *et al.*, 2013;

1.2.5.1 Pathophysiology of glaucoma and purinergic signalling

The lamina cribosa (LC) is a sieve-like collagenous structure at the posterior pole of the sclera through which unmyelinated RGC axons pass through as part of their journey from the eye to the brain (Snell and Lemp., 2013). Quigley in the 1980s identified the lamina cribosa (LC) as the main site of RGC axon death in glaucoma (Quigley *et al.*, 1981; Quigley and Addicks, 1980a and 1980b; Quigley and Anderson, 1976) based on optic nerve studies in humans, primates and several other mammals. Early research describes accumulations of organelles in RGC axons only where they traverse the LC, suggesting axoplasmic flow is constricted at the LC (Quigley, 1981;

Quigley and Addicks, 1980a; Quigley and Anderson, 1976; Minckler *et al.*, 1977; Vrabcic, 1976). In addition, these experiments describe a change in LC morphology in glaucomatous eyes: (i) large pore size (Quigley *et al.*, 1981); (ii) localised defects with narrow bundles of connective tissue inferiorly and superiorly (Quigley *et al.*, 1981) and (iii) posterior displacement (Quigley, 1980). Reduced connective tissue support inferiorly and superiorly would lead to a greater vulnerability to axonal damage in these regions. Perhaps explaining the early loss of neuronal tissue inferiorly and superiorly in the ONH of glaucomatous eyes (Quigley and Addicks, 1981). Modern day OCT studies imaging the LC of glaucomatous eyes *in vivo* have demonstrated reduced LC thickness, localised defects and posterior displacement (Andrade *et al.*, 2022).

Biomechanical pathophysiology suggests that the pressure gradient across the LC results in RGC axon death in glaucoma. The term translaminal pressure difference (TLPD) is used to describe the pressure difference between the eye and the cerebrospinal fluid (CSF). The translaminal pressure gradient (TLPG) includes adjustment for the thickness of the LC (Tan *et al.*, 2018): this is important as the pressure difference is used to explain why low-pressure eyes may develop glaucoma (NTG) and some high-pressure eyes may not (OHT). Large retrospective studies have shown a significant increase in TLPD in POAG and NTG eyes (Berdahl *et al.*, 2008a and Berdahl *et al.*, 2008b). Unilateral glaucoma is possibly explained by differences in local CSF pressure for each eye (Killer, 2020).

Ischaemic pathophysiology suggests that ischaemic insult, such as IOP-mediated compression of blood-vessels or vasospasm mediate RGC death in glaucoma. The association between vasospastic conditions, hypotension and haemodynamic collapse with glaucoma have been discussed earlier (section 1.2.2 *Risk factors*). Endothelin-1-mediated vasoconstriction is implicated in these vasospastic conditions, and increased levels of this have been detected in the aqueous and blood of glaucoma patients (Cellini *et al.*, 1997 and Noske *et al.*, 1997). Other links between vascular insufficiency and glaucoma include magnetic resonance imaging (MRI) studies associating glaucoma with pan cerebral ischaemia and infarcts (Stroman *et*

al., 1995 and Ong *et al.*, 1995). The mechanism by which ischaemia results in RGC apoptosis is not fully defined but is linked to secondary damage by inflammatory factors such as tumor necrosis factor alpha (TNF α) and nitric oxide synthase 2 (NOS-2) (Agarwal., 2009).

Glutamate excitotoxicity suggests neurotoxic insult causes RGC death in glaucoma. Glutamate is an amino-acid and a neurotransmitter that acts on several ionotropic and metabotropic receptors in the CNS. It is well-known that prolonged high concentration of glutamate is excitotoxic; this is primarily mediated by ionotropic N-methyl D-aspartate (NMDA) subtype receptors (Choi, 1987). NMDA receptor activation causes an influx of Ca²⁺ and Na⁺ into the neurone and the Ca²⁺ acts as a secondary messenger in signalling cascade leading to cell death (Choi, 1987). Retinal glial cells, particularly Müller cells express glutamate transporters which transports glutamate into the cell; intracellular glutamate is converted to glutamine by glutamine synthetase and glutamine to glutamate by glutamine synthetase. Both high levels of glutamate and impaired glutamate-glutamine cycling have been associated with glaucoma by many groups (Sullivan *et al.*, 2006; Mawrin *et al.*, 2003; Kim *et al.*, 2000; Nakar *et al.*, 2000).

Inflammatory pathophysiology suggests that inflammatory molecules such as interleukins, reactive oxygen species (ROS), NO and tumour necrosis factors mediate RGC death in glaucoma. Aspects of this are discussed further in section 1.5.2 *Interleukins and glaucoma*.

1.2.5.1 Pathophysiology of glaucoma and purinergic signalling

Purinergic signalling describes the action of purine derivatives, particularly ATP and adenosine, acting as neurotransmitters on purinergic receptors (P1_{A1-3}, P2X1-7 and P2Y₁₋₁₄; *figure 1.14: classification of purinergic receptors*). Purinergic signalling is described further in the next section of this thesis 1.3 *purinergic signalling*. ATP binding at P2-receptors and adenosine binding at P1-receptors exert predominantly opposing effects on retinal cells (Ye *et al.*, 2021). ATP is released from all types of retinal neurones: horizontal cells; bipolar cells; amacrine cells and retinal ganglion

cells (1.1.3 *Retina*; Ward *et al.*, 2010). Raised IOP is associated with high concentrations of ATP in the eye, as found in human (Li *et al.*, 2011; Zhang *et al.*, 2007) and rodent (Lu *et al.*, 2017 and 2015) models. High concentrations of ATP activate P2-receptors causing an influx of calcium in neighboring retinal cells: P2X-receptors cause calcium influx through the ion-channel receptor itself or through voltage gated calcium channels (Wurm *et al.*, 2011) and P2Y-receptors cause calcium release from internal stores (Reddish *et al.*, 2017, 1.4.2 *Purinergic calcium responses in the Müller cell*). Of the purinergic receptors, particular research focus has been on the P2X7R which forms a large plasma membrane pore that mediates cytolysis and cell-death (Schmid and Evans, 2019 and Supernatant *et al.*, 1996; 1.3.3.7 *P2X7 receptor*). Several studies show high levels of ATP activate the P2X7R causing RGC death in glaucomatous models (Niyadurupola *et al.*, 2013; Hu *et al.*, 2010; Reigada *et al.*, 2008; Resta *et al.*, 2007; Zhang *et al.*, 2007 and 2005). Benzoyl-benzoyl adenosine 5'-triphosphate (BzATP; P2X7R agonist) causes a dose dependent death of RGCs, brilliant blue G (BBG) and oxidised ATP (P2X7R antagonists) prevent this RGC death (Zhang *et al.*, 2005). Other purinergic receptors are thought to be involved in the pathogenesis of glaucoma. Activation of P1_{A2a}R causes release of pro-inflammatory cytokines associated with RGC death, similarly antagonism of this receptor reduces RGC death in glaucomatous models (Aires *et al.*, 2019; Liu *et al.*, 2016; Madeira *et al.*, 2016 and 2015).

Purinergic receptors also play neuroprotective roles in the pathogenesis of glaucoma (Ye *et al.*, 2021). Activation of the P2Y₆R is thought to lower IOP and P2Y₆R knockout mice develop a high-tension glaucomatous optic neuropathy (Shinozaki *et al.*, 2017). Topical agonists of P2Y₂ and P2Y₆ receptors decrease IOP in rabbit models (Jacobson and Civan, 2016; Ginsburg-Shmuel *et al.*, 2012 and Markovskaya *et al.*, 2008). Adenosine activating P1-receptors generally confers neuroprotection of RGCs, although the contradictory role of P1_{A2a}R is described above. Activation of P1_{A1}R increases aqueous humor outflow and lowers IOP (Lu *et al.*, 2017; Ahmad *et al.*, 2013). Activation of P1_{A3}R inhibits P2X7R-induced RGC death (Boia *et al.*, 2020; Jacobson and Civan, 2016 and Galvao *et al.*, 2015).

1.3 Purinergic Signalling

1.3.1 Overview

Purinergic signalling describes the action of nucleotides and nucleosides as extracellular signalling molecules on purinergic receptors. Purinergic signalling was controversially proposed by Burnstock in 1970, who described the action of ATP as an extracellular signalling molecule. Endogenous nucleotides ATP and uridine 5'-triphosphate (UTP) (figure 1.12) were already known to act as energy carriers, building blocks for nucleic acids and coenzymes (Giuliani *et al.*, 2019). However, it was realised that their molecular structures are also adept for extracellular signalling: small; stable at physiological pH; present in low concentrations extracellularly during 'resting conditions'; stored intracellularly at high concentrations; water soluble and easily catalysed (Giuliani *et al.*, 2019). Purinergic signalling is now established in literature as a ubiquitous part of human physiology and pathology, with critical roles in long-term trophic signalling such as embryogenesis, differentiation and regeneration as well as short-term signalling such as neurotransmission and neuromodulation (Abbracchio & Burnstock, 1998; Burnstock & Verkhratsky, 2010). Endogenous nucleotides and nucleosides stimulate a large family of purine receptors found on nearly all human cells (Ledderose *et al.*, 2016; Burnstock 2012).

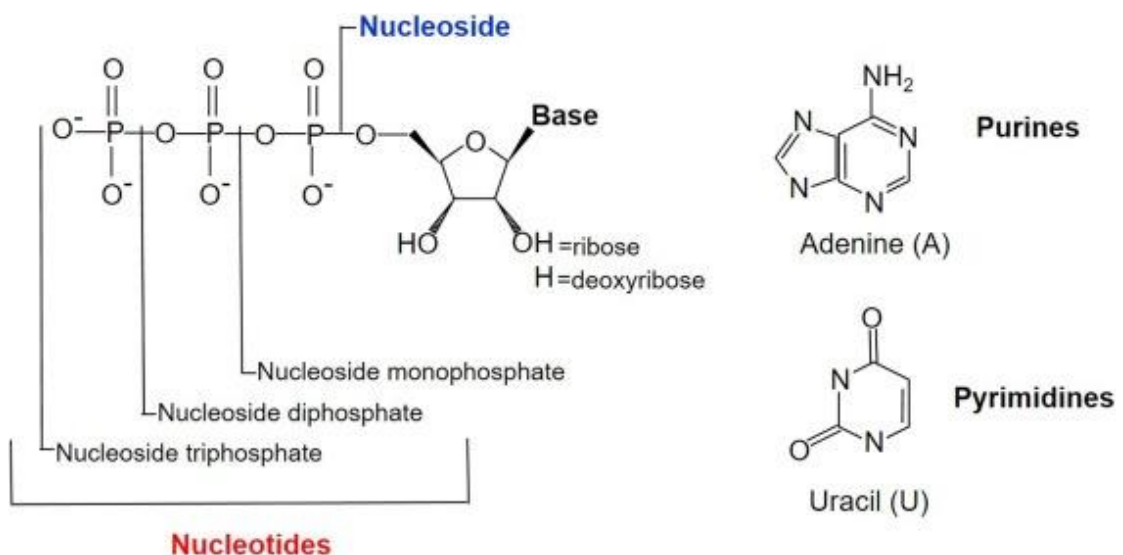


Figure 1.12: Molecular structure of nucleotides (Giuliani *et al.*, 2019)

The molecular structure consists of a purine or pyrimidine base (e.g. adenine or uracil) attached to a pentose sugar (ribose) and three phosphate groups.

1.3.2 Mechanisms of nucleotide release and breakdown

Purinergic signalling involves nucleotide or nucleoside release, receptor activation, nucleotide or nucleoside breakdown or reuptake.

Endogenous nucleotides and nucleosides include ATP and the products of its cleavage adenosine diphosphate (ADP), adenosine monophosphate (AMP) and adenosine, as well as UTP and the products of its cleavage uridine 5'-diphosphate (UDP) and UDP-sugars. Nucleotides are released into the extracellular space by both non-lytic 'specific' mechanisms and cell-damage related 'non-specific' mechanisms. Specific mechanisms of nucleotide release include: cytosolic vesicular exocytosis; microvesicle release and release via channels and transporters (Taruno, 2018). Non-specific nucleotide release is usually induced by cell death or stress, for example during hypoxia, infection or inflammation (Lazarowski, 2012; Lazarowski *et al.*, 2011 and Bodin and Burnstock 2001). Cell plasma membrane disruption causes release of a high concentration of nucleotides due the intracellular/extracellular nucleotide gradient, these high concentrations acts as 'danger' signals (Trautmann, 2009).

ATP is synthesised intracellularly from glucose in a series of metabolic processes: glycolysis, tricarboxylic acid cycle (TCA) and oxidative phosphorylation (Bonora *et al.*, 2012). Glycolysis occurs in the cytoplasm of cells. Glycolysis uses 1 glucose molecule and 2 ATP molecules to produce 4 ATP molecules, 2 nicotinamide adenine dinucleotide and hydrogen (NADH) molecules and 2 pyruvate molecules (Chaudhry *et al.*, 2021). Glycolysis produces a low yield of ATP molecules compared to TCA and oxidative phosphorylation; however it produces pyruvate and NADH for use in TCA and oxidative phosphorylation respectively (Chaudhry *et al.*, 2021). TCA occurs in the mitochondria. Pyruvate is converted by pyruvate dehydrogenase complex to acetyl-CoA and CO₂. Acetyl-CoA enters the TCA cycle to produce 12 ATP molecules (Alabduladhem *et al.*, 2021). Oxidative phosphorylation also occurs in the mitochondria. Oxidative phosphorylation involves a series of oxidation and reduction reactions that involve the transfer electrons from NADH and 1,5-dihydro-fad (FADH₂) to oxygen across several molecules, a process called the electron transport chain (ETC). The ETC produces over 30 ATP molecules (Deshpande and Mohiuddin, 2021).

ATP reaches high millimolar concentrations within the cell, however it has low stability in water and utilised for several cellular processes (Bonora *et al.*, 2012). ATP is co-stored in vesicles with neurotransmitters, suited to its role as an extracellular signalling molecule (Bonora *et al.*, 2012).

ATP is transported into intracellular vesicles by a vesicular nucleotide transporter (VNUT) where it is then stored (Giuliani *et al.*, 2019 and Moriyama *et al.*, 2017). Stimulation of the soluble N-ethylmaleimide-sensitive factor attachment protein receptor (SNARE) causes exocytosis of intracellular vesicles releasing ATP into the extracellular space (Giuliani *et al.*, 2019 and Sudhof and Rothman, 2009). ATP is also released directly from the cytosol by channels and transporters including connexin-43,-37,-36 and -26 (Wang *et al.*, 2013) pannexin-1, ATP binding cassette (ABC) transporters, calcium homeostasis modulator (CALMH) channels and the P2X7R (Giuliani *et al.*, 2019; Taruno, 2018; figure 1.13). In resting conditions connexin and pannexin channels are closed. Connexin channels are opened by increased intracellular calcium concentration, cell membrane depolarisation, ROS and NO (Wang *et al.*, 2017 and Eltzschig *et al.*, 2006). Pannexin channels are opened by increased intracellular calcium, plasma membrane depolarisation (Locovei *et al.*, 2006), activation of P2X7R (Iglesias *et al.*, 2008), redox potential changes (Retamal, 2014) and mechanical stress (Bao *et al.*, 2004). ABC transporters usually facilitate the movement of molecules across the plasma membrane by the hydrolysis of ATP, however some molecules cause ATP release (Abraham *et al.*, 1993). Some voltage-gated CALHM channels allow passage of ATP (Taruno *et al.*, 2013). The P2X7R can form a macropore which also allows passage of ATP (Schmid and Evans, 2019 and Supernatant *et al.*, 1996; 1.3.3.7 P2X7R).

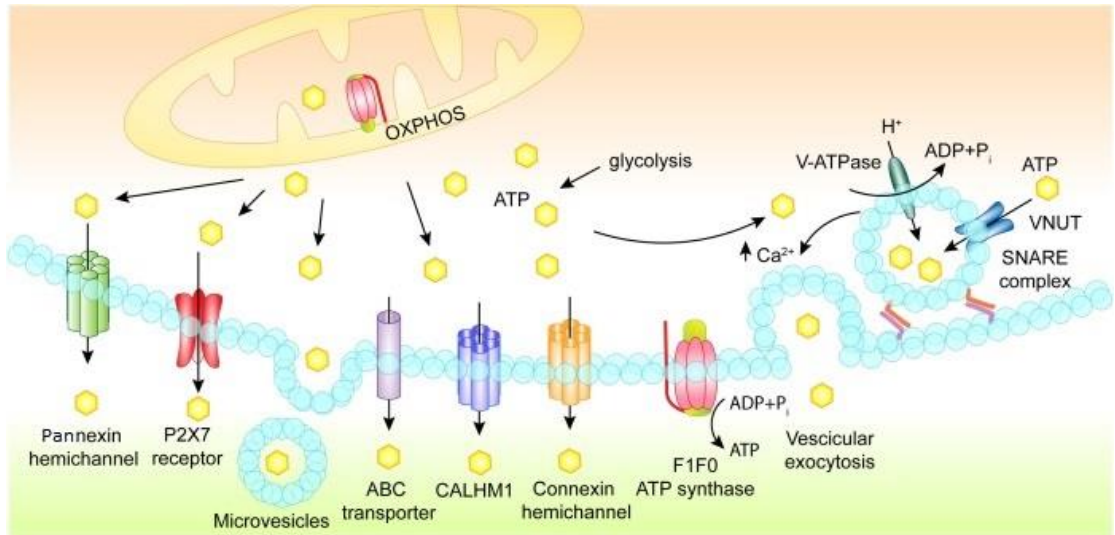


Figure 1.13: Mechanisms of ATP release (Adapted from Giuliani *et al.*, 2019)

Intracellularly ATP is synthesised in the mitochondria by oxidative phosphorylation (OXPHOS) and in the cytoplasm by glycolysis. It can be released extracellularly by SNARE mediated vesicular exocytosis, plasma membrane derived vesicles and membrane channels or transporters.

Adenosine can be released into the extracellular space via exocytosis of intracellular vesicles (Parri, 2013) and passive efflux via equilibrative nucleoside transporters (ENTs; Parri, 2013 and Uckermann *et al.*, 2006). Adenosine can also be produced extracellularly by ecto-nucleotidase enzymes (Newman, 2003; Ribelayga and Mangel, 2005). ENTs and ecto-nucleotidase enzymes are discussed further below.

UTP and UDP are stored intracellularly in vesicles via the VNUT (Anderson and Parkinson, 1997). UTP and UDP are released by the specific and non-specific mechanisms previously discussed for ATP.

Released nucleotides and nucleosides act in an autocrine and paracrine manner allowing cells to respond to local and systemic cues for homeostatic functioning and pathological response (Corriden and Insel, 2010 and Fitz 2007).

Receptor signalling is terminated by removal of the ligand from the extracellular space by either enzymatic conversion or cellular reuptake. P1 receptor signalling is terminated by the conversion of adenosine to inosine or AMP by adenosine deaminase (ADA) and adenosine kinase (AK) respectively. In addition, adenosine can

be removed by cellular reuptake through two families of nucleoside transporters, ENTs and concentrative nucleoside transporters (CNTs; Giuliani *et al.*, 2019).

P2 receptor signalling is terminated by the hydrolysis of nucleotides and nucleosides by a family of ecto-nucleotidase enzymes (Giuliani *et al.*, 2019; Kukulski *et al.*, 2011). Ecto-nucleoside triphosphate diphosphohydrolases (ENTPDases) are a group of enzymes that hydrolyse nucleoside-triphosphates and nucleoside-diphosphates into nucleoside-monophosphates: the enzymes are nucleotide specific, for example the CD39 group converts ATP to AMP and ADP to adenosine (Robson *et al.*, 2006). Ecto-5'-nucleotidase (5'-NT or CD73) converts AMP to adenosine, and with a lower affinity converts UMP to Uracil. Ecto-nucleotide pyrophosphatase/phosphodiesterases (ENPPs) hydrolyse nucleoside-triphosphates, nucleoside-diphosphates and other non-nucleotide groups. Alkaline phosphatases (APs) hydrolyse nucleoside-triphosphates, nucleoside-diphosphates, nucleoside-monophosphates and other non-nucleotide groups (Yegutkin *et al.*, 2008).

Enzymatic hydrolysis of nucleotides not only prevents receptor desensitisation but also allows the degradation products to stimulate other P1 and P2 purinergic receptors resulting in 'cross-talk' (Burnstock *et al.*, 2006).

1.3.3. Purinergic receptors

Purinergic receptors are divided into two subtypes according to ligand-binding. P1 receptors are activated by adenosine. P2 receptors are predominantly activated by ATP and ADP, but also UTP and UDP (Burnstock, 1978). P2 receptors are further subdivided according to receptor morphology into P2X and P2Y. P2X receptors (P2XRs) are ligand gated ion channels (LGIC). Ligand-binding opens the non-selective cation channel allowing rapid influx of Na⁺ and Ca²⁺, efflux of K⁺ through the plasma membrane with subsequent membrane depolarisation. P2Y receptors (P2YR) are G-protein coupled receptors (GPCR). P2YR activation is slower and involves a cascade of secondary intracellular messengers that modulate intracellular Ca²⁺ (Burnstock and Kennedy, 1985). More detail on P2Y GPCRs and intracellular Ca²⁺ are provided in table 1.4 below and 1.4.2 *Purinergic calcium responses in the Müller cell*). During

the 1990s cloning experiments allowed characterisation of purinergic receptors, there are 19 known distinct receptors (figure 1.14). P1 receptors have 4 subtypes: A₁, A_{2A}, A_{2B} and A₃ (Fredholm *et al.*, 2001 and Daly, 1985). P2XRs have 7 subtypes, P2X₁₋₇ (Burnstock, 2014; Abbracchio and Burnstock, 1994; Brake *et al.* 1994 and Valera *et al.* 1994). P2YRs have 8 subtypes, P2Y_{1, 2, 4, 6, 11, 12, 13 and 14} (Burnstock, 2014; Abbracchio and Burnstock, 1994; Lustig *et al.*, 1993 and Webb *et al.*, 1993).

P2Y Receptor	Transduction mechanisms
P2Y ₁	Gαq/Gα11; PLC-β activation, Ca ²⁺ ↑
P2Y ₂	Gαq/Gα11; PLC-β activation, Ca ²⁺ ↑ and possibly Gi/Go (↓cAMP)
P2Y ₄	Gαq/Gα11; PLC-β activation, Ca ²⁺ ↑ and possibly Gi/Go (↓cAMP)
P2Y ₆	Gαq/Gα11; PLC-β activation, Ca ²⁺ ↑
P2Y ₁₁	Gαq/Gα11 and GS; PLC-β activation, Ca ²⁺ ↑ and ↓cAMP
P2Y ₁₂	Gαi; (↓cAMP)
P2Y ₁₃	Gαi/Gαo; (↓cAMP)
P2Y ₁₄	Gαq/Gα11; PLC-β activation, Ca ²⁺ ↑

Table 1.4: P2Y receptors G-protein transduction mechanisms (adapted from Burnstock, 2014)

Activation of GPCRs causes a cascade of secondary intracellular messengers that alter intracellular Ca²⁺ levels (Nash *et al.*, 2001). GPCRs are associated with a group of G-proteins consisting of three subunits α, β and γ. GPCRs are classified into 4 subfamilies according to their α-subunit: (i) Gαi/o; (ii) Gαs; (iii) Gα12/13 and (iv) Gαq (Kamoto *et al.*, 2015). Shown above are each P2YR and the G-protein α-subunit associated, P2YRs mostly couple with Gαq family of proteins (Burnstock, 2014). Important secondary messengers in G-protein signal transduction include phospholipase C (PLC) and cyclic adenosine monophosphate (cAMP). PLC hydrolyses the plasma membrane phospholipid phosphatidylinositol 4,5-bisphosphate (PIP₂) into the secondary messenger Inositol 1,4,5-triphosphate (IP₃) and the by-product diacylglycerol (DAG). IP₃ binds to its receptor IP₃R causing Ca²⁺ release from intracellular stores. cAMP activates protein kinase A (PKA) that in turn phosphorylates intracellular proteins that regulate excitation-contraction coupling through L-type Ca²⁺-channel (LCC), ryanodine receptor (RyR), and myosin binding protein C causing Ca²⁺ release from intracellular stores (Bagur and Hajnoczky, 2017; 1.4.1 Overview of calcium homeostasis and signalling). Gαi/o inhibits cyclic adenosine monophosphate (cAMP) production and voltage-gated Ca²⁺ channels (VGCCs) inhibiting intracellular Ca²⁺ release (Dhyani *et al.*, 2020). Gαs activates adenylyl cyclase (AC) increasing production of cAMP increasing intracellular Ca²⁺ (Dhyani *et al.*, 2020). Gαq activates PLC increasing intracellular Ca²⁺ (Dhyani *et al.*, 2020).

Structurally, G protein-coupled P1 and P2Y receptors have seven transmembrane domains, connected by three extracellular and three intracellular loops. They associate intracellularly with G proteins (table 1.4). LGIC P2X receptors have an extracellular ligand binding loop, two hydrophobic transmembrane domains, intracellular amino-acid (N)-terminals and carboxyl (C)-terminals (Burnstock, 2014 and North, 1996). The subunits form a trimeric cation channel. Three agonist molecules are required to bind and activate a single receptor (Burnstock and Kennedy, 2011; Bean 1990).

P2Y-receptor subtypes exist as homodimeric and/or heterodimeric receptors (Milligan, 2009; Albizu *et al.*, 2010), whilst P2X subtypes exist as homotrimeric and/or heterotrimeric receptors (Surprenant and North 2009). Most P2 subtypes have functionally distinct isoforms produced by alternative splicing (Rangel-Yescas *et al.*, 2012 and Okhubo *et al.*, 2000).

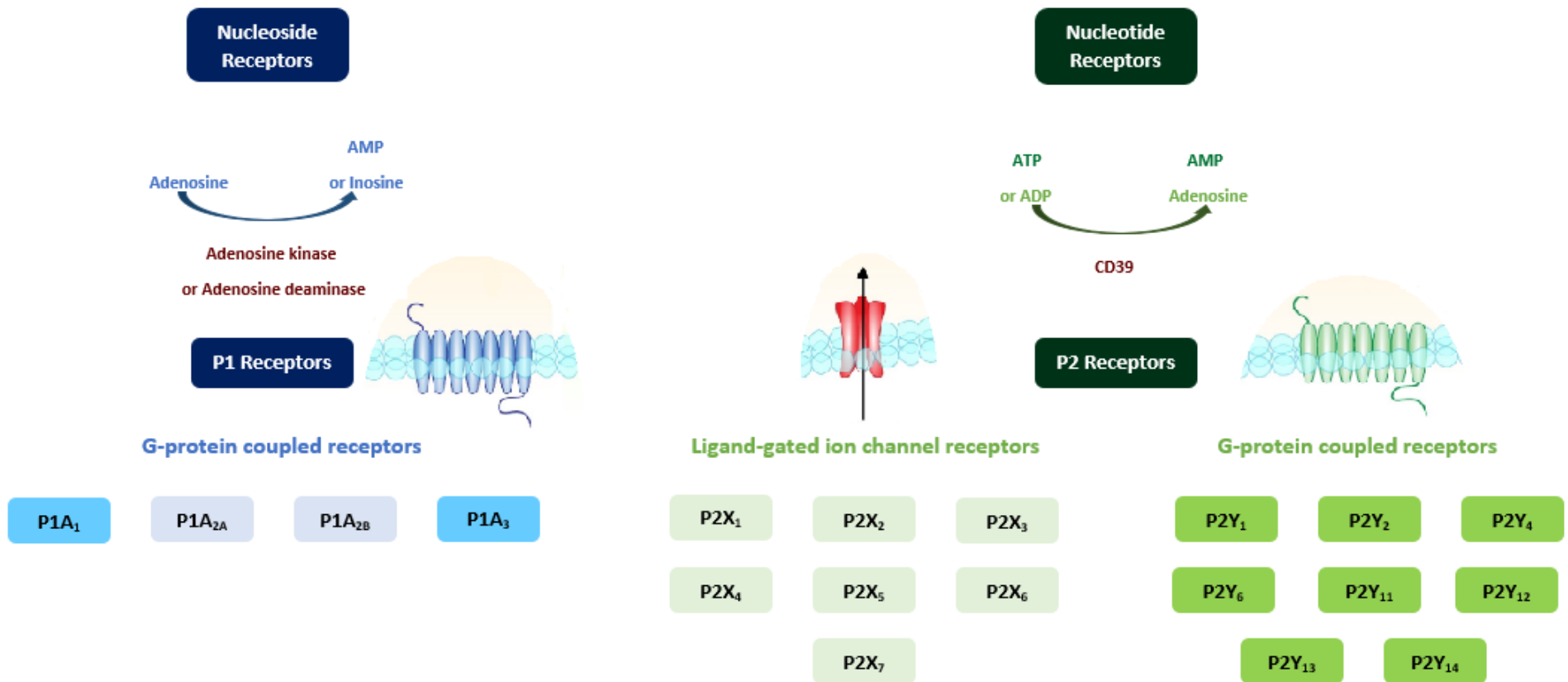


Figure 1.14: Classification of purinergic receptors

P1 (blue) and P2Y receptors (dark green) are G-protein coupled whilst P2X receptors (light green) are ligand gated. Purinergic receptors are stimulated by a variety of nucleotides additional to ATP/ADP including UTP/UDP.

1.3.3.1 P2X1 receptor (P2X1R)

The P2X1R was the first cloned P2XR, isolated from the vas deferens (Valera *et al.*, 1994). Since then it has been identified in smooth muscle, platelets, cerebellum, spinal neurons, immune and glial cells (Burnstock, 2014; Lecut *et al.*, 2009 and Lalo *et al.*, 2008). P2X1R has roles in blood clotting and autoregulation of the kidney (Ralevic and Dunn, 2015).

Pharmacokinetically, P2XRs continually stimulated by ATP display differences in the decline of their excitation current. P2X1R and P2X3R rapidly desensitise. P2X1R desensitises within 1 second and gradually recovers over 5 minutes (Lalo *et al.*, 2010 and North 2002).

P2X1 subunits form a functional P2X1/2, P2X1/4 and P2X1/5 heteromers. Heteromers have their own unique characteristics, for example P2X1/5 has a greater sensitivity to ATP and a biphasic desensitisation phase (Lalo *et al.*, 2008; Haines *et al.*, 1999; Lê *et al.*, 1999 and Torres *et al.*, 1998). Distinct isoforms of the P2X1R have been identified: P2X1a, P2X1del and P2X1b (Rangel-Yescas *et al.*, 2012; Greco *et al.*, 2001 and Ohkubo *et al.*, 2000). Some isoforms are heteromers with P2X1R and display no functionally different properties to the homomeric P2X1R. However, some isoforms are functional as homomers and display different properties to the homomeric P2X1R (Rangel-Yescas *et al.*, 2012).

1.3.3.2 P2X2 receptor (P2X2R)

P2X2Rs are expressed in nervous tissue such as the CNS, retina and autonomic sensory ganglia. P2X2Rs are also expressed in smooth muscle (Burnstock, 2014). Receptor functions are thought to include mediating neurotransmission and sensory transduction (Syed and Kennedy, 2011, Burnstock and Knight, 2004).

P2X2Rs and P2X5Rs minimally desensitise when stimulated by ATP (Schmid and Evans, 2019). They form functional P2X1/2, P2X2/3 and P2X2/6 heteromers (Saul *et al.*, 2013). It is well-established that the P2X2/3R heteromers is highly expressed in the dorsal root ganglia (Jacobson and Müller, 2016).

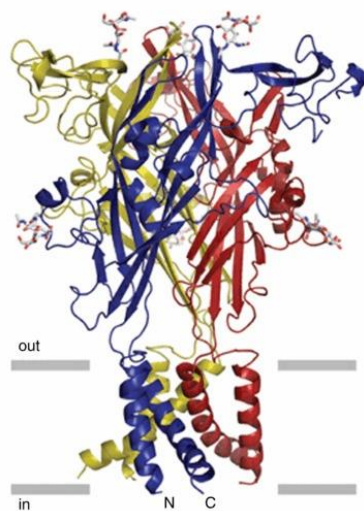
1.3.3.3 P2X3 receptor (P2X3R)

P2X3Rs are also highly expressed in nervous tissue such as the sympathetic nervous system and the nucleus tractus solitarii (Burnstock, 2014). P2X3Rs are expressed in the sensory neurons of the bladder and detect fullness (Kennedy *et al.*, 2007 and Ford *et al.*, 2006). P2X3R and P2X2/3R are expressed on nociceptive fibres, it is likely they play a role in chronic inflammation and neuropathic pain (Kennedy *et al.*, 2003).

1.3.3.4 P2X4 receptor (P2X4R)

P2X4Rs are expressed in the CNS, testes and colon (Burnstock, 2014). The P2X4R was the first P2XR to be structurally determined by Kawate *et al* in 2009 using x-ray crystallography (figure 1.15).

A.



B.

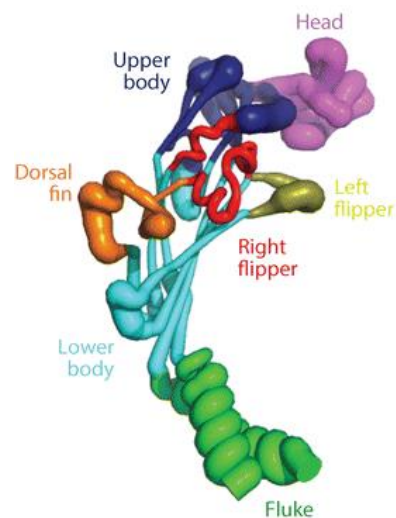


Figure 1.15: A. Stereoview of the zebra fish P2X4R in a closed state (Kawate *et al.*, 2009) B.

'Dolphin' structure of a single P2XR subunit (Schmid and Evans, 2019)

The P2X4R shown is homotrimeric. Each subunit is shown in a different colour, the plasma membrane is shown in grey (A). From this it was determined that each subunit of a P2XR is 'dolphin-like' in structure (B). Since this first P2XR was structurally determined, several other P2XRs from different species in different states of opening have been determined: the transmembrane helices (shown as the 'fluke') are the conformationally variant as they open and close the channel. The beta sheets (shown as 'lower and upper body') are rigid. The extracellular regions (shown as 'head', 'dorsal fin' and 'right flipper') are also conformationally variant due to changes occurring in states of agonist binding (Schmid and Evans, 2019; Hattori and Gouaux, 2012).

The P2X4R displays high calcium permeability (Egan and Khakh, 2004). When stimulated with ATP it displays an intermediate desensitisation profile in comparison to the other P2XRs. Functional heterotrimers include P2X1/4, P2X4/6 and P2X4/7 (Guo *et al.*, 2007).

P2X4R has roles in cardiac contractility (Hu *et al.*, 2002; Yang *et al.*, 2014), regulating surfactant secretion in the lungs (Miklavc *et al.*, 2011) and inflammation (Layhadi *et al.*, 2018; Layhadi & Fountain, 2019; Ulmann *et al.*, 2008; Wareham *et al.*, 2009). Recently, Taspine a natural anti-inflammatory was found to exert its effects via P2X4R in macrophages (Nadzirin *et al.*, 2021).

As mentioned previously, P2X4Rs are highly expressed in the CNS, found in the neurons and glial cells of the brain and spinal cord (Illes *et al.*, 2021). Studies have established an association with P2X4R and neuropathic pain. CNS injury including brain ischaemia, spinal cord injury and trauma increase P2X4R expression in microglial cells. Ulmann *et al.*, found peripheral nerve injury resulted in de novo expression of P2X4Rs in activated microglia in the dorsal horn of the spinal cord (Deng *et al.*, 2018 and Ulmann *et al.*, 2008). P2X4R upregulation in spinal microglia is likely mediated by C-C motif chemokine ligand 21 (CCL21; Biber *et al.*, 2011). Consistent with the association between P2X4R and neuropathic pain, deficient mice lacked mechanical hyperalgesia induced by peripheral nerve injury (Ulmann *et al.*, 2008). The P2X4R is a promising therapeutic target for the management of neuropathic pain, with compounds previously entering animal and clinical trials as part of drug development (Teixeira *et al.*, 2019). Drugs targeting the P2X4R are unlikely to interfere with normal pain sensitivity as the receptor is clustered in activated microglia in the spinal cord where damaged sensory fibres project (Inoue and Tsuda, 2012).

1.3.3.5 P2X5 receptor (P2X5R)

P2X5Rs are widely expressed in the skin, CNS, eye, myocardium, gut, bladder and thymus (Burnstock, 2014). It is highly expressed in differentiating tissue. A non-functional splice variant of the P2X5R is expressed in some human populations (Kotnis *et al.*, 2010).

1.3.3.6 P2X6 receptor (P2X6R)

P2X6Rs are expressed in neuronal tissue (Burnstock, 2014). It is the only P2XR that does not appear to form a functional homomeric receptor, only assembling in a heteromeric form (Burnstock, 2014; Syed and Kennedy 2011).

1.3.3.7 P2X7 receptor (P2X7R)

P2X7Rs exist on multiple cell types but are highly expressed on in glial cells and immunocompetent cells (Burnstock, 2014). It plays an important role in immune responses.

The P2X7R amino-acid sequence is the least closely related to the other P2XRs (North, 2002). It is the most structurally heterogeneous of all purinergic receptors: there is significant interspecies and intraspecies polymorphism as well as multiple splice variants (Xu *et al.*, 2012). This results in variation in receptor mediated responses and complicates understanding of its physiological role. Homomeric assembly is the most common arrangement of P2X7 subunits (Nicke, 2008; figure 1.16).

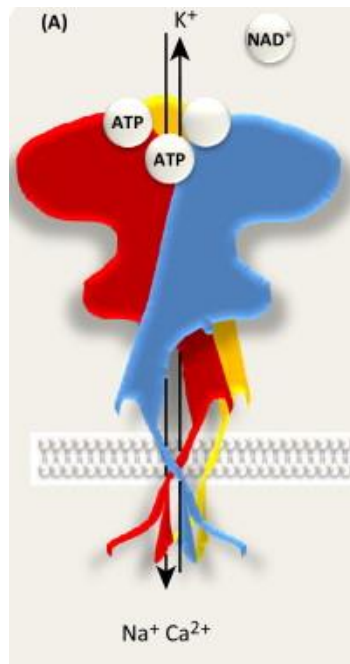


Figure 1.16: The P2X7 receptor (adapted from Sperlagh and Illes., 2014)

The P2X7R is activated at higher ATP concentrations ($EC_{50}=100\mu\text{mol/L}$) than other P2XRs: these agonist concentrations usually occur as part of the inflammatory response (Le Feuvre *et al.*, 2002) and/or at sites of cellular damage therefore P2X7R is often thought of as a 'danger sensor' (Vénéreau *et al.*, 2015 and Ferrari *et al.*, 2006). The receptor is thought to be a major trigger of apoptosis for damaged CNS cells although other processes are likely to be involved (Franke and Illes, 2006 and Volonté *et al.*, 2003).

Early fluorescent dye experiments suggested that prolonged stimulation of the P2X7R with ATP causes the ion channel to dilate into a pore (Browne *et al.*, 2013). Pores allow the passage of large (~900 Da) molecules through the plasma membrane causing cytolytic death. Initially, it was shown that immune cells stimulated with ATP formed large pores in their plasma membrane (Schmid and Evans, 2019 and Supernatant *et al.*, 1996). Activation of P2X2R, P2X4R and P2X7R was shown to cause permeation of large fluorescent YO-PRO and ethidium bromide dyes (Schmid and Evans, 2019; Browne *et al.*, 2013). YO-PRO and ethidium bromide are not able to traverse the in-tact plasma membrane. Subsequent experiments demonstrated prolonged stimulation of P2X7R with ATP progressively increased permeability to the

synthetic large cation N-methyl-d-glucamine (NMDG), suggesting sustained stimulation caused the P2X7R channel to dilate further into a ‘pore’ (Khakh *et al.*, 1999 and Virginio *et al.*, 1999).

P2X7Rs on some cell types were shown to be ‘non-pore forming’ (table 1.5). Some single P2X7R channel conductance studies have shown no change in channel conductance over the time course that pore dilatation was proposed to occur (Riedel *et al.*, 2007). It may be that on some cell types P2X7R is pore-forming whilst on others it is not; this has been attributed to heterogeneity in the C-terminal domain of the P2X7R (Petrou *et al.*, 1997 and Rassendren *et al.*, 1997) or differences in intracellular components required to form pores (Donnelly-Roberts and Jarvis 2007; North, 2002; Pelegrin and Surprenant, 2006).

Cell type	Cytolytic pore formation (Yes/No)
Astrocyte ¹	Y
Lymphocytes ²	N
Thymocyte ³	N
Macrophages ⁴	Y
Macrophage ⁵	Y
Microglial cells ⁶	Y
Müller ⁷	N*

Table 1.5: P2X7 receptor cytolitic pore formation capability by cell type *data equivocal

P2X7R activation initiates intracellular changes, such as: (i) cytoskeletal and mitochondrial alterations (ii) phosphatidylserine translocation (iii) mitochondrial swelling and (iv) membrane blebbing (Liu *et al.*, 2008; Roger *et al.*, 2008). Activation also has a role in cytokine release: in inflammatory cells, the NACHT, LRR, and PYD domains-containing protein 3 (NLRP3) inflammasome triggers caspase-1 mediated interleukin-1 β (IL-1 β) and interleukin-18 (IL-18) maturation and release (Dubyak, 2007; Gudipaty *et al.*, 2003; Sanz and DiVirgilio, 2000). Unpublished data from the Sanderson group has shown P2X7R stimulation in human retinal tissue increases expression and release of both IL-1 β and interleukin-10 (IL-10).

1.3.3.8 P2Y₁ receptor (P2Y₁R)

P2Y₁₋₁₁Rs couple via Gq-proteins (table 1.4) to exert their downstream effects. Agonist binding at P2Y₁R causes homodimerisation and receptor internalisation (Kügelgen, 2019 and Choi *et al.*, 2008). It can form the functional heterodimer P2Y_{1/A1} which displays its own unique characteristics.

The P2Y₁Rs are expressed in CNS neurons and glial cells; it has important roles in mediating neuron-glial calcium signalling (Jacobson *et al.*, 2020 and Shigetomi *et al.*, 2018). Together with P2Y₁₃R and P2X7R it has roles in neuronal cell differentiation, neuroprotection and neurodegeneration (Jacobson *et al.*, 2020 and Miras Portugal *et al.*, 2019). P2Y₁R together with P2Y₂R, P2Y₁₂R and P2Y₁₃R are expressed on nociceptive fibres and exert nociceptive and analgesic effects (Jacobson *et al.*, 2020 and Malin and Molliver, 2010). The P2Y₁R assists P2Y₁₂R with platelet aggregation (Kügelgen, 2019; Liverani *et al.*, 2014 and Cattaneo, 2011). The P2Y₁R also has roles in vasodilation and bone resorption (Jacobson *et al.*, 2020; Burnstock, 2014).

1.3.3.9 P2Y₂ receptor (P2Y₂R)

P2Y₂Rs are expressed in immune cells, epithelial cells, endothelial cells, kidney tubules and osteoblasts (Burnstock, 2014). It has roles in ion transport (Cressman *et al.*, 1999), weight modulation (Merz *et al.*, 2018), cardiac remodeling (Rieg *et al.*, 2011; Cohen *et al.*, 2011), immunomodulation (Relvas *et al.*, 2015; Ayata *et al.*, 2012; Kim *et al.*, 2012 and Müller *et al.*, 2010) and neuroinflammation (de Diego García *et al.*, 2018).

1.3.3.10 P2Y₄ receptor (P2Y₄R)

P2Y₄Rs are expressed in endothelial cells, CNS, intestine, placenta, spleen and thymus (Burnstock 2014; Song *et al.*, 2011; Abbracchio *et al.*, 2006 and von Kügelgen and Wetter, 2000). Similar to P2Y₂Rs they: (i) facilitate the secretion of chloride and water by epithelial cells (Robaye *et al.*, 2003) and (ii) play a beneficial role in recovery after myocardial infarction by down-regulating endothelin-1 (Horckmans *et al.*, 2015).

1.3.3.11 P2Y₆ receptor (P2Y₆R)

P2Y₆R are expressed widely in epithelial cells, placenta, thymus, T-cells, activated microglia, vascular smooth-muscle, CNS, lung, intestine, bone and adipose tissue (Burnstock, 2014; von Kügelgen and Wetter, 2000; Abbracchio *et al.*, 2006). P2Y₆R has roles in vasoconstriction (Malmsjö *et al.*, 2003), bone metabolism (Orriss *et al.*, 2011) and inflammatory responses such as phagocytosis and apoptosis (von Kügelgen, 2019; Quintas *et al.*, 2014; Garcia *et al.*, 2014 and Koizumi *et al.*, 2007).

The P2Y₆R has two functional splice variants producing a protein of 328 and 421 amino-acids each (Maier *et al.*, 1997)

1.3.3.12 P2Y₁₁ receptor (P2Y₁₁R)

The P2Y₁₁R also couples with Gq proteins, but unlike the above P2R activation also causes an increase in adenylyl cyclase.

The P2Y₁₁R is the only GPCR known to form an intergenic splice variant. P2Y₁₁R and the adjacent SSF1 gene splice forms a chimeric protein with no identifiable difference in function (Communi *et al.*, 2001).

P2Y₁₁Rs are expressed in the spleen, intestine, brain and immune cells (Burnstock, 2014). The receptor has roles in immunomodulation (Chadet *et al.*, 2015; Alkayed *et al.*, 2012 and Wilken *et al.*, 2001) and neuropathic pain (Barragán-Iglesias *et al.*, 2014).

1.3.3.13 P2Y₁₂ receptor (P2Y₁₂R)

The P2Y₁₂Rs are less widely expressed, they are mainly in platelets, immune cells and neuronal cells (Burnstock, 2014 and Abbracchio *et al.*, 2006). It is now well-established that P2Y₁₂R stimulation induces platelet aggregation and this receptor is now the target for therapeutic agents (*1.3.5 Therapeutic potentials of purinergic agents in disease*). P2Y₁₂Rs also have roles in vasoconstriction (Wihlborg *et al.*, 2004), renal regulation of urine osmolality (Zhang *et al.*, 2015), immunomodulation (Liverani *et al.*, 2014), bone metabolism (Jorgensen *et al.*, 2012; Su *et al.*, 2012 and Syberg *et al.*, 2012) and neuropathic pain (Bekő *et al.*, 2017; Horváth *et al.*, 2014 and Tozaki-Saitoh

et al., 2008). P2Y₁₂R and P2Y₁₃R in microglia and P2Y₁R in astrocytes cross-communicate to mediate neuroprotective changes in the brain after injury (Shinozaki *et al.*, 2017).

1.3.3.14 P2Y₁₃ receptor (P2Y₁₃R)

P2Y₁₃Rs are expressed in the brain, lymph nodes, bone marrow, erythrocytes and spleen (Burnstock, 2014). It has roles in neuroprotection (see above), mast cell degranulation (Gao *et al.*, 2010) and bone metabolism (Wang *et al.*, 2014 and Orriss *et al.*, 2011).

1.3.3.15 P2Y₁₄ receptor (P2Y₁₄R)

P2Y₁₄Rs are expressed in the brain, thymus, stomach, intestine, spleen, bone marrow and placenta (Burnstock, 2014 and Abbrachio *et al.*, 2006). Activation of the P2Y₁₄R initiates pro-inflammatory roles of immune cells (Sesma *et al.*, 2012 and Gao *et al.*, 2013) and glial cells (Curet and Watters, 2018; Kinoshita *et al.*, 2013). It also has roles in vasoconstriction (Abbas *et al.*, 2018) and glucose metabolism (Meister *et al.*, 2014).

P2 subtype	Cells or tissues identified in	Isoforms and heterodimers	Roles
P2X1R	Smooth muscle; platelets; cerebellum; spinal neurons; immune and glial cells	P2X1R; P2X1aR; P2X1delR; P2X1bR; P2X1/2R; P2X1/4R and P2X1/5R	Blood clotting and Autoregulation of the kidney. ¹
P2X2R	CNS, retina and autonomic sensory ganglia	P2X2R; P2X1/2R; P2X2/3R and P2X2/6R	Mediating neurotransmission and sensory transduction. ^{2&3}
P2X3R	CNS	P2X3R and P2X2/3R	Chronic inflammation; chronic pain and bladder fullness. ⁴
P2X4R	CNS, testes and colon ⁶	P2X1/4R; P2X4/6R and P2X4/7R	Neuropathic pain ⁷⁻⁹ ; cardiac contractility ¹⁰⁻¹¹ ; regulates surfactant secretion in the lung ¹² ; inflammation ¹³⁻¹⁶
P2X5R	Skin, CNS, eye, myocardium, gut, bladder and thymus ⁶	Non-functioning splice variant	
P2X6R	Neuronal tissue ⁶	Only exists as heterodimer	
P2X7R	Multiple cell types but are highly expressed on in glial cells and immunocompetent cells ⁶	Multiple splice variants	Immune responses including cytokine release i.e. IL-1B and IL-18 ¹⁷⁻¹⁹
P2Y1R	CNS neurons and glial cells signalling ^{20 & 21}	P2Y _{1/A1} R	Neuron-glia calcium signalling ^{20,21} , neuronal differentiation; neuroprotection and neurodegeneration ^{20 & 22} ; nociception and analgesia ^{20 & 23} ; platelet aggregation ²⁴⁻²⁶ ; vasodilation and bone resorption. ^{6 & 20}
P2Y2R	Immune cells; epithelial cells; endothelial cells; kidney tubules and osteoblasts ⁶		Ion transport ²⁷ , weight modulation ²⁸ , cardiac remodeling ²⁹⁻³⁰ ; immunomodulation ³¹⁻³⁴ ; neuroinflammation ³⁵
P2Y4R	Endothelial cells; CNS; intestine; placenta; spleen and thymus ^{6, 36-38}		Recovery after myocardial infarction ³⁹ ; chloride and water secretion ⁴⁰
P2Y6R	Epithelial cells; placenta; thymus; T-cells; activated microglia; vascular smooth-muscle; CNS; lung; intestine; bone and adipose tissue ^{6, 36-37}	2 splice variants	Vasoconstriction ⁴¹ , bone metabolism ⁴² , inflammatory responses ⁴³⁻⁴⁶
P2Y11R	Spleen; intestine, brain and immune cells ⁶	P2Y ₁₁ R/SSF1	Immunomodulation ⁴⁷⁻⁴⁹ ; neuropathic pain ⁴⁰
P2Y12R	Platelets; immune cells and neuronal cells ^{6 & 36}		Platelet aggregation; vasoconstriction ⁵¹ ; regulation of urine osmolality ⁵² ; immunomodulation ⁵³ ; bone metabolism ⁵⁴⁻⁵⁶ ; and neuropathic pain ⁵⁷⁻⁵⁹
P2Y13R	Brain; lymph nodes; bone marrow; erythrocytes and spleen ⁶		Neuroprotection; mast cell degranulation ⁶⁰ and bone metabolism ^{42 & 61}

Table 1.6: Summary of P2 receptor locations, roles, isoforms and heterodimers (page 1 of 2)

P2Y₁₄R	Brain; thymus; stomach; intestine; spleen; bone marrow and placenta ⁶ & 36		pro-inflammatory roles of immune ^{60 & 62} and glial cells ^{63 & 64} . Vasoconstriction ⁶⁵ and glucose metabolism ⁶⁶
--------------------------	---	--	--

1. Ralevic and Dunn, 2015; 2. Syed and Kennedy, 2011; 3. Burnstock and Knight, 2004; 4. Kennedy *et al.*, 2007 2003; 5. Guo *et al.*, 2007; 6. Burnstock, 2014; 7. Williams *et al.*, 2019; 8. Biber *et al.*, 2011; 9. Tsuda *et al.*, 2003; 10. Hu *et al.*, 2002; 11. Yang *et al.*, 2014; 12. Miklavc *et al.*, 2011; 13. Layhadi *et al.*, 2018; 14. Layhadi & Fountain, 2019; 15. Ulmann *et al.*, 2008; 16. Wareham *et al.*, 2009; 17. Dubyak, 2007; 18. Gudipaty *et al.*, 2003; 19. Sanz and DiVirgilio, 2002; 20. Jacobson *et al.*, 2020; 21. Shigetomi *et al.*, 2018; 22. Miras Portugal *et al.*, 2019; 23. Malin and Molliver, 2010; 24. Kügelgen, 2019; 25. Liverani *et al.*, 2014 ; 26. Cattaneo, 2011; 27. Cressman *et al.*, 1999; 28. Merz *et al.*, 2018; 29. Rieg *et al.*, 2011; 30. Cohen *et al.*, 2011; 31. Relvas *et al.*, 2015; 32. Ayata *et al.*, 2012; 33. Kim *et al.*, 2012; 34. Müller *et al.*, 2010; 35. de Diego García *et al.*, 2018; 36. Abbracchio *et al.*, 2006; 37. von Kügelgen and Wetter, 2000; 38. Song *et al.*, 2011; 39. Horckmans *et al.*, 2015; 40. Robaye *et al.*, 2003; 41. Malmjö *et al.*, 2003; 42. Orriss *et al.*, 2011; 43. Kügelgen, 2019; 44. Quintas *et al.*, 2014; 45. Garcia *et al.*, 2014; 46. Koizumi *et al.*, 2007; 47. Chadet *et al.*, 2015; 48. Alkayed *et al.*, 2012; 49. Wilken *et al.*, 2001; 50. Barragán-Iglesias *et al.*, 2014; 51. Wihlborg *et al.*, 2004; 52. Zhang *et al.*, 2015; 53. Liverani *et al.*, 2014; 54. Jorgensen *et al.*, 2012; 55. Su *et al.*, 2012; 56. Syberg *et al.*, 2012; 57. Bekő *et al.*, 2017; 58. Horváth *et al.*, 2014; 59. Tozaki-Saitoh *et al.*, 2008; 60. Gao *et al.*, 2010; 61. Wang *et al.*, 2014; 62. Sesma *et al.*, 2012; 63. Curet and Watters, 2018; 64. Kinoshita *et al.*, 2013; 65. Abbas *et al.*, 2018; 66. Meister *et al.*, 2014

Table 1.6: Summary of P2 receptor locations, roles, isoforms and heterodimers (page 2 of 2)

1.3.4 Purinergic signalling in the retina

Nearly all retinal cell types release nucleotides and express multiple purinergic receptors (figure 1.17). Released nucleotides act in an autocrine and paracrine manner allowing cells to respond to both local and systemic cues.

Activation of purinergic receptor(s) is determined by the type of nucleotide released, nucleotide concentration and receptor proximity to the release site(s). The pattern of purinergic receptor activation decides the functional response(s) in the retina (Sanderson *et al.*, 2014). Purinergic signalling in the retina is involved in: cell differentiation and migration during embryogenesis; cell proliferation; cell death; homeostatic and pathological processes (Ventura *et al.*, 2019; Corriden and Insel, 2010 and Fitz 2007).

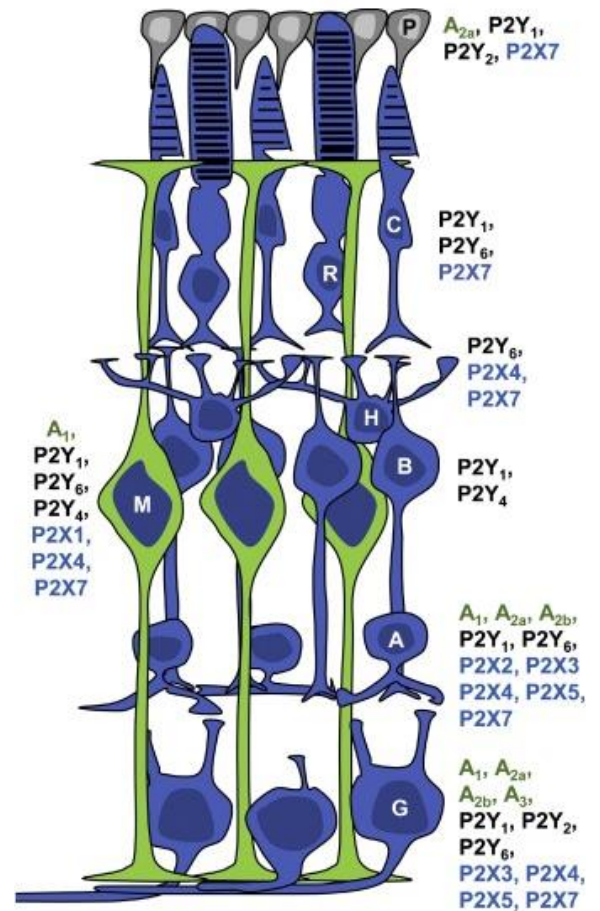


Figure 1.17: Expression of purinergic receptors in the adult retina (Ventura *et al.*, 2019)

P: retinal pigment epithelium cell; R: rod photoreceptor; C: cone photoreceptor; H: horizontal cell; B: bipolar cell; M: Müller cell; A: amacrine cell and G: ganglion cell.

ATP is released by cells via the mechanisms described in section 1.3.2 *Mechanisms of nucleotide release and breakdown*. Retinal neuronal cell types (RGCs, amacrine, bipolar, horizontal and photoreceptors) express VNUT (Moriyama and Hiasa, 2016) supporting their traditional association with a vesicular release of ATP as a neurotransmitter/neuromodulator (Santos *et al.*, 1999). ATP is released through a calcium-dependent vesicular exocytosis (Ho *et al.*, 2015; Santos *et al.*, 1999 and Perez *et al.*, 1986). Neuronal cell types are also capable of channel mediated ATP release: RGCs and horizontal cells employ ATP release via pannexin channels (Xia *et al.*, 2012; Vroman *et al.*, 2014 and Dvorientchikova *et al.*, 2006). By contrast, glial and retinal

pigment epithelium (RPE) cells predominantly release ATP in a calcium independent manner (Newman, 2001; Pearson *et al.*, 2005; Uckermann *et al.*, 2006 and Wurm *et al.*, 2010). Astrocytes, microglial and RPE cells mainly release ATP via hemichannels (Beckel *et al.*, 2014 and Pearson *et al.*, 2005).

RGCs express multiple purinergic receptors (figure 1.17). The P2X7R is the main focus of research on these cells. It is thought to contribute to the pathophysiology of glaucoma via receptor-mediated neurodegeneration of the optic nerve (Kakurai *et al.*, 2013; Niyadurupola *et al.*, 2013 and 2011; Hu *et al.*, 2010; Zhang *et al.*, 2005). Amacrine cells are known to express P2Y₁, P2Y₆, P2X2-5 and P2X7 receptors (Ventura *et al.*, 2019). Amacrine cells postsynaptic to cones express P2X2R whilst cells postsynaptic to rods express P2X3R and P2X7R; this varied receptor profile is thought to contribute to the role of purinergic signalling in modulating visual output (Puthussery and Fletcher 2004, 2006 and 2007). Bipolar cells express P2Y₁R (Ward and Fletcher, 2009) and P2Y₄R over their dendrites and axon terminals (Ward *et al.*, 2008). Horizontal cells express P2Y₆R (Zhang *et al.*, 2012), P2X4R (Kaneda *et al.*, 2004 and Ho *et al.*, 2014) and immunofluorescence experiments have demonstrated high immunoreactivity for the P2X7R (Puthussery and Fletcher, 2004).

Rod and cone cells express P2Y₁, P2Y₆ and P2X7 receptors (Marques Ventura *et al.*, 2019). Stimulation of the P2X7R with BzATP potentiates photoreceptor hyperpolarisation. Additionally, generalised stimulation of P2 receptors with ATP is associated with a rapid loss in photoreceptors (Vessey *et al.*, 2012). Purinergic signalling in these cells is therefore thought to be involved with regulation of photoreceptor function and integrity (Puthussery and Fletcher, 2007 and 2004).

Microglia predominantly express P2Y₆, P2Y₁₂, P2Y₁₃, P2X4 and P2X7 receptors (Calvoli *et al.*, 2019). Levels of P2X7R expression in microglia differ with phenotypic activation states (figure 1.7). Activation is associated with increased cell proliferation and pro-inflammatory changes such as formation of NLRP3 inflammasome, release of chemokines and cytokines (Calvoli *et al.*, 2019). P2X7 and P2X4 receptor stimulation on these cells are associated with pore-formation (see section 1.3.3.7 P2X7 receptor;

Bernier *et al.*, 2012). P2X4R is also associated with pro-inflammatory changes (Gong *et al.*, 2009 and Fujita *et al.*, 2008). The P2Y₆R has a role in microglial phagocytosis (Xu *et al.*, 2016). The P2Y₁₂R is associated with the ramified phenotype of microglial cells and have a role in microglial migration (Lin *et al.*, 2021). The P2Y₁₃R is involved with the release of the pro-inflammatory cytokines IL-1 β , interleukin-6 (IL-6), and TNF- α (Calvoli *et al.*, 2019).

Astrocytes express P1A_{2A}R, P2Y₁R, P2Y₁₂R and P2X7R (Pietrowski *et al.*, 2021). P1A_{2A}R is involved in neurotransmitter recapture, decreasing the uptake of glutamate and increasing the uptake of gamma-aminobutyric acid (GABA; Cristóvão-Ferreira *et al.*, 2013). P2Y₁R mediates Ca²⁺ waves in astrocytes, which is critical for synaptic plasticity and its role in maintaining the blood-retinal-barrier (Bazargani and Attwell, 2016). Astrocytes release ATP causing autocrine stimulation of the P2X7R causing in pro-inflammatory downstream signalling (Albalawi *et al.*, 2017)

RPE cells express multiple purinergic receptors: P1A₁R, P1A₂R (Collison *et al.*, 2005), P2Y₁R, P2Y₂R, P2Y₆R (Tovell *et al.*, 2008) and P2X7R (Sanderson *et al.*, 2014; Guha *et al.*, 2013 and 2014; Liu *et al.*, 2008). Purinergic signalling via A_{2A} and P2X7 have juxtaposing effects on lysosomal pH, lipid oxidation and lipofuscin production (Sanderson *et al.*, 2014; Guha *et al.*, 2013 and 2014; Liu *et al.*, 2008). P2Y₂R has roles in subretinal fluid transport and has been shown to facilitate retinal reattachment in animal models (Maminishkis *et al.*, 2002).

1.3.4.1 Purinergic signalling and Müller cells

Müller cells play important roles in retinal neurone-glial signalling (Newman, 2004), homeostatic functioning and gliotic responses in pathological states (*section 1.1.3.2.1 Müller cells*); purinergic signalling is essential in facilitating these roles (Wurm *et al.*, 2011).

Müller cells predominantly release ATP in response to membrane stretch caused by mechanical and osmotic changes (Newman 2003 and Newman 2001). ATP is also released in response to neurochemical stimuli, for example glutamate acting on

NMDA or AMPA/kainite receptors (Loiola and Ventura, 2011). Specific mechanisms of ATP release include exocytosis and channel-mediated release (Wagner *et al.*, 2017 and Uckermann *et al.*, 2006). Müller cell generated ATP exerts autocrine and paracrine effects. Autocrine actions include the generation of calcium waves and gliosis (Reichenbach and Bringmann, 2016). Paracrine actions include neurone-glia signalling, for example ATP released is converted into adenosine acting on A₁ receptors in RGCs causing them to hyperpolarise (Newman, 2003).

Müller cells express several purinergic receptors; it is currently thought they express more P2YRs than P2XRs. Human Müller cells contain mRNA for P2Y₁R, P2Y₂R, P2Y₄R and P2Y₆R (Fries *et al.*, 2005, Fries *et al.*, 2004 and Pannicke *et al.*, 2001) and Pannicke *et al.* in 2000 provided the first evidence of P2X7R mRNA expression in human Müller cells by single-cell RT-PCR. Immunohistochemistry located clustering of receptors in the cell soma (figure 1.18).

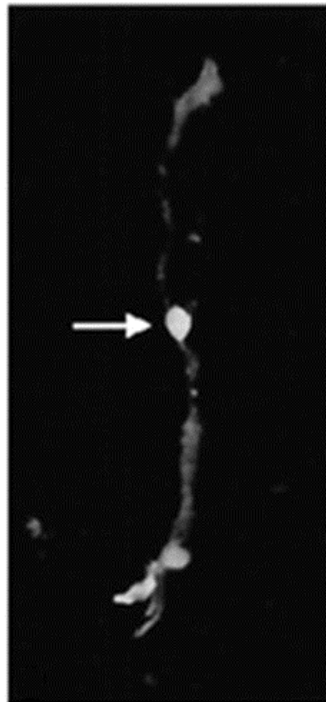


Figure 1.18: Immunohistochemistry for P2X7Rs in enzymatically dissociated Müller cells (Pannicke *et al.*, 2000)

The cell is oriented in the image so the vitreous face is superior and distal processes are inferior. Immunolabelling is with human anti-P2X7 receptor. The image shows immunofluorescence at the cell soma (arrow). Autofluorescence is visible at the distal processes, as determined by a negative control (not shown).

Activation of P2X7Rs in human Müller cells has previously been shown moderate Ca²⁺ influx and no pore formation (Pannicke *et al.*, 2000). It is therefore unlikely that the role of the P2X7R on the Müller cell is to act as a 'suicide trigger' as proposed for other cell types (Ferrari *et al.*, 1997). Müller cell expression of P2X7R increases in certain pathological states, for example proliferative retinopathy (Bringmann *et al.*, 2001).

Previously it was described that P2X7R stimulation in RGCs caused cell-death as seen in glaucoma (*section 1.2.5 Pathophysiology*, Niyadurupola *et al.*, 2013). Müller cells may facilitate P2X7R-mediated RGC death. Increased glutamate stimulating glutamate receptors and high IOP causing mechanical stress causes Müller cells to release ATP (Xue *et al.*, 2016). ATP is released into the IPL where it stimulates P2X7Rs on RGCs causing increased calcium and subsequent apoptosis (Wurm *et al.*, 2008, Resta *et al.*, 2007 and Zhang *et al.*, 2005). Interestingly, released ATP converted to adenosine acts on A₃R in RGCs which has an inhibitory effect on calcium rise and subsequent apoptosis (Zhang *et al.*, 2006). In this way Müller cell purinergic signalling can exert both neurodegenerative and neuroprotective effects (Zhang *et al.*, 2006).

ATP activation of the Müller cell purinome produces a predominant P2Y₁R response with a minimal P2XR response (Wurm *et al.*, 2009). The P2Y₁R in Müller cells plays an essential role in retinal homeostasis. P2Y₁R signalling mediates Müller cell osmotic volume (Grosche *et al.*, 2013; Wurm *et al.*, 2009) allowing them to efficiently transfer ions and fluid from the extracellular space to the vitreous body and blood vessels (Reichenbach and Bringmann, 2013).

1.3.5 Therapeutic potentials of purinergic agents in disease

Recent research on purinergic signalling has focused on the therapeutic potentials of purinergic agonists and antagonists for disease. Established agents include clopidogrel and ticlopidine, P2Y₁₂ antagonists acting on platelet P2Y₁₂Rs to reduce platelet aggregation and thereby preventing cardiovascular events such as stroke

(Sarafoff *et al.*, 2012 and Cattaneo, 2011). Diquafosol is a P2Y₂R agonist used for the treatment of dry eye (Jacobson and Civan, 2016). There are many other purinergic receptor antagonists that are undergoing clinical trials for use in the management of neuropathic pain and inflammation (Huang *et al.*, 2021).

1.4 Purinergic signalling and calcium responses

1.4.1 Overview of calcium homeostasis and signalling

Calcium homeostasis is fundamental to life and therefore responsible cellular mechanisms have been conserved through evolution from prokaryotic to human cells. Virtually all cell functions involve calcium and unregulated calcium increase would result in cell injury or death (Matikainen *et al.*, 2021).

Physiological calcium concentration varies dependent on location. Extracellular calcium is maintained at a concentration 10,000 times higher (10^{-3}M) than intracellular calcium (10^{-7}M) in a resting cell. Within the cell specialised organelles, such as the endoplasmic reticulum (ER), act as intracellular calcium stores. They contain calcium at a concentration of 10^{-4}M . This resting gradient is maintained by specialised proteins: when intracellular calcium concentration is raised the plasma membrane Ca^{2+} transport ATPase (PMCA) and the $\text{Na}^{+}/\text{Ca}^{2+}$ exchanger (NCX) shift calcium out of the cell, whilst the sarcoendoplasmic reticulum Ca^{2+} ATPase (SERCA) and mitochondrial Ca^{2+} uniporter (mtCU) import calcium into the organelles restoring the intracellular concentration (Bagur and Hajnoczky, 2017; figure 1.19).

Certain cell stimuli, such as membrane depolarisation or activation of some receptors, result in an increase of intracellular calcium to 10^{-6}M . Increased intracellular calcium is a result of extracellular calcium influx via plasma membrane Ca^{2+} channels (e.g. LGIC and voltage-gated ion channels) or release from internal stores via inositol 1,4,5-triphosphate receptors (IP₃R) and ryanodine receptors (RyR) (Bagur and Hajnoczky, 2017). In a process known as calcium induced calcium release (CICR; figure 1.19) increased intracellular Ca^{2+} further increases the levels of Ca^{2+} by release from ER/ sarcoplasmic reticulum (SR) stores.

Each cell type has a unique profile of calcium signalling/regulation proteins and agonist specific calcium response to suit its physiological requirements (Berridge *et al.*, 2000).

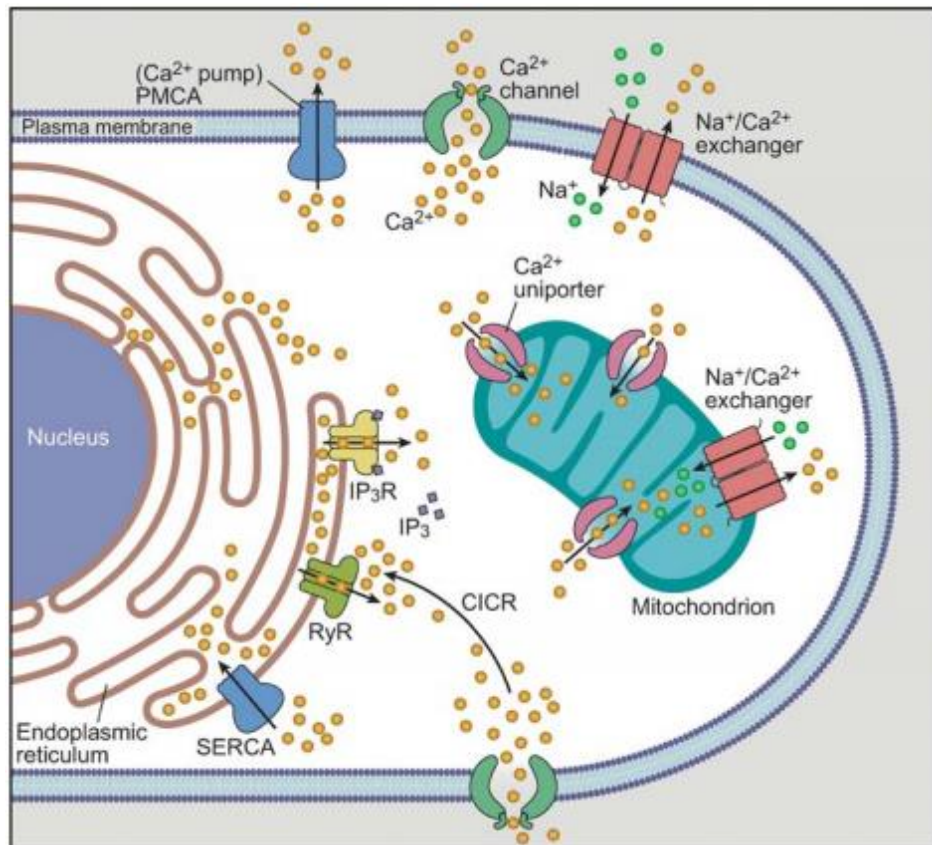


Figure 1.19: Cellular calcium homeostasis (Dong *et al.*, 2006)

Illustration of the main transport proteins involved in the control of intracellular Ca^{2+} concentration. Raised intracellular Ca^{2+} is mitigated by shifting Ca^{2+} out of the cell (PMCA and NCX) and into intracellular organelles (SERCA, mtCU). Conversely, Ca^{2+} channels and release of Ca^{2+} from internal stores (via IP₃R and RyR) increase intracellular Ca^{2+} concentration.

1.4.2 Purinergic calcium responses in the Müller cell

Activation of purinergic receptors on Müller cells induce intracellular Ca^{2+} changes. ATP induced Ca^{2+} rises can be transmitted across retinal tissue in waves forming an important part of glial-glial and glial-neuronal cell signalling (1.3.4.1 Purinergic signalling and Müller cells). Müller cells can signal in this way to modulate local immune, inflammatory, angiogenic and neuroprotective homeostatic functions (Wurm *et al.*, 2011).

P2YR activation results in a signalling cascade which alters intracellular Ca^{2+} levels (Nash *et al.*, 2001). P2YRs are GPCRs associated with a group of G-proteins (table 1.4; Burnstock, 2014). P2YRs can couple with G-proteins that inhibit intracellular Ca^{2+} release (Gai/o subfamily) or signal intracellular Ca^{2+} release from intracellular stores (G α s and G α q subfamily). P2YRs mostly couple with G α q proteins which activate phospholipase C (PLC). PLC hydrolyses the plasma membrane phosphatidylinositol 4,5-bisphosphate (PIP₂) into the secondary messenger IP₃ and the by-product diacylglycerol (DAG). IP₃ binds to its receptor IP₃R on the surface of the ER/SR causing Ca^{2+} release from these internal stores (figure 1.20; Dhyani *et al.*, 2020).

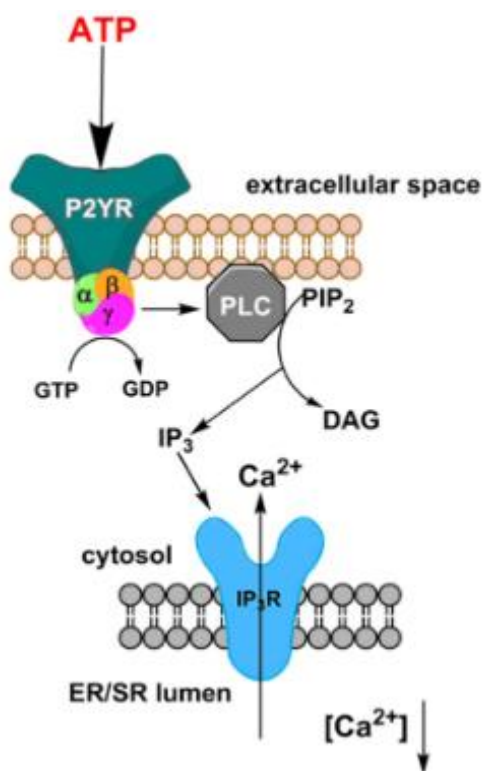


Figure 1.20: P2YR mediated Ca^{2+} release from internal stores (Adapted from Reddish *et al.*, 2017) Nucleotides/nucleosides such as ATP bind to and activate P2YRs on the plasma membrane. P2YRs mostly couple with G α q proteins which activate PLC. PLC hydrolyses the plasma membrane PIP₂ into the secondary messenger IP₃ and the by-product DAG. IP₃ binds to its receptor IP₃R causing calcium release from internal stores.

P2XR activation results in an influx of Ca^{2+} directly through the ion channel (Wurm *et al.*, 2011; figure 1.16). P2 receptor mediated increase in intracellular Ca^{2+} activates big-conductance potassium (BK) channels that cause a K^{+} efflux and

hyperpolarisation. Cell depolarisation caused predominantly by Na^+ and also some Ca^{2+} influx is balanced by hyperpolarisation caused by K^+ efflux through BK channels (figure 1.21). Several groups have utilised intracellular Ca^{2+} imaging to demonstrate functional evidence of P2 receptors on Müller cells.

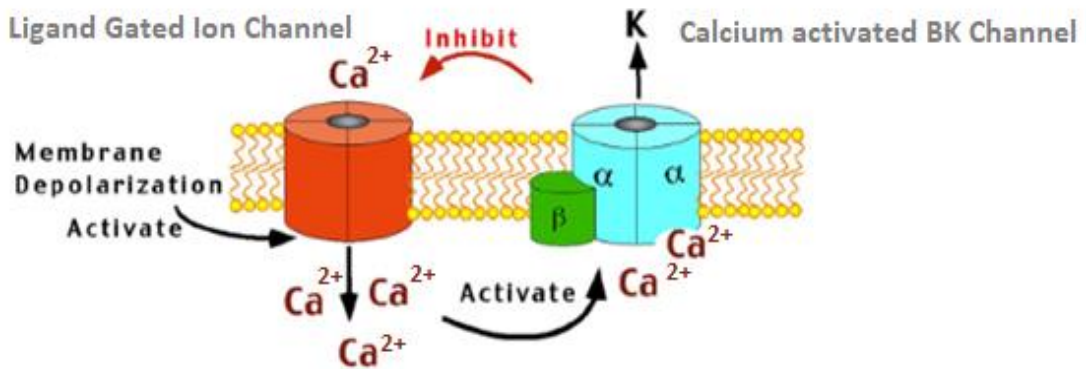


Figure 1.21: LGIC channel and BK channel (Adapted from Wang *et al.*, 2014)

Agonist binding at LGICs, such as the P2X7R, cause Ca^{2+} influx into the cell and membrane depolarisation. Ca^{2+} influx and depolarisation activate BK channels causing a K^+ efflux and membrane repolarisation. BK channels thereby act as a negative feedback mechanism for inward currents across the plasma membrane.

Although mRNA evidence suggests the existence of a wider profile of P1 and P2 receptors, calcium evidence has been demonstrated for P1A₁R, P1A_{2A}R, P1A_{2B}R (Newman, 2005), P2Y₁R, P2Y₂R and P2Y₄R (Weick *et al.*, 2005) and P2X7R (Pannicke *et al.*, 2000) on rat, rabbit and human Müller cells, respectively. It has been postulated that P2Y₁R-activation is predominantly responsible for ATP induced elevations in intracellular Ca^{2+} (Wurm *et al.*, 2009). Activation of P2X7R on human Müller cells has shown moderate Ca^{2+} influx (figure 1.22) and subsequent dye-filling experiments have shown no pore formation (table 6.2; Pannicke *et al.*, 2000). Stimulation of P2X7Rs causes a more sustained response compared to stimulation of P2YRs (figure 1.22). Inward currents through the P2X7R are potentiated by low concentrations of divalent cations in the extracellular fluid (Pannicke *et al.*, 2000).

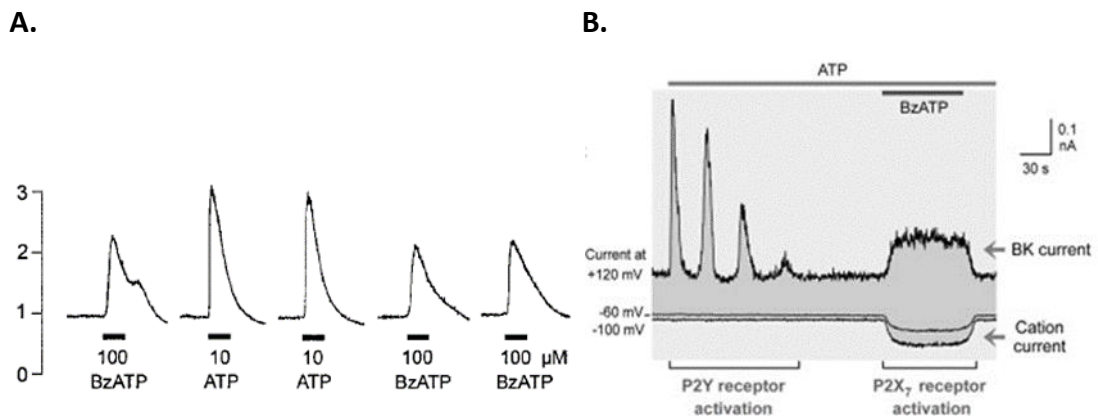


Figure 1.22: ATP and BzATP generated responses in single human Müller cells. A. Intracellular Ca^{2+} responses elicited by ATP and BzATP in dissociated human Müller cells using fura-2-acetoxymethyl (fura-2) AM microfluorimetry. B. Evoked currents (x, mV) over time (y, s) (adapted from Pannicke *et al.*, 2002)

A. ATP evoked fast and transient intracellular calcium rises whilst BzATP showed more sustained responses and occasional double-peaks. Data presented as 340/380 fluorescence ratio measurements using fura-2 AM microfluorimetry. B. ATP (100 μM) and BzATP (50 μM) used to stimulate P2-receptors caused altered currents across a single human Müller cell. Stimulation of P2YRs caused repetitive Ca^{2+} -induced activation of BK channels (left of image and recorded at +120mV). Stimulation of P2X₇Rs caused a cation current through its channel and a sustained Ca^{2+} -induced activation of BK channels (right of image, recorded -60 to -100 and +120mV respectively)

1.5 Interleukins

1.5.1 Overview

Interleukins are cytokines or signalling molecules that are predominantly expressed by leucocytes. Interleukins play essential roles in leucocyte function including modulating physiological immune and pathological inflammatory responses (Vaillant and Qurie, 2021). Physiological roles include differentiation, proliferation, maturation, migration, and adhesion of leucocytes. There are many interleukins assigned interleukin-1 (IL-1) to IL-40, they are broadly classed as pro-inflammatory or anti-inflammatory although this can be more intermingled (Vaillant and Qurie, 2021). Following research is principally focused on IL-1 and IL-10 due to their association with glaucoma described below.

1.5.2 Interleukins and glaucoma

Local inflammatory responses may contribute to the RGC death in glaucoma. Aqueous humor of glaucomatous eyes has increased amounts of interleukins IL-6, IL-8, IL-10, IL-12, IL-36, IL-37 and IL-38 when compared with age-matched controls (Zhang *et al.*, 2019; Freedman and Iserovich, 2013; Chua *et al.*, 2012; Takai *et al.*, 2012 and Kuchtey *et al.*, 2010). Mutations of interleukin-20 receptor-B (IL-20RB) have been identified in a human POAG pedigree, additionally the IL-20 family with its receptors have shown altered levels of expression in a mouse model of glaucoma (Wirtz and Keller, 2016). A polymorphism of the IL-6 gene was associated with changes in the structure of the ONH and RNFL which may relate to increased severity of glaucoma (Wang *et al.*, 2017). Reduced levels of IL-6 and VEGF in the aqueous humour were associated with decreased RGC death in a glaucomatous rat model (Song *et al.*, 2018). Polymorphisms of the IL-10 gene have shown increased susceptibility to glaucoma in the Iranian population (Fakhraie *et al.*, 2020).

Of the interleukins, IL-1 β gene polymorphism, mRNA upregulation and protein release have been shown by several groups to be associated with glaucoma (Niyadurupola *et al.*, 2013 and 2009; Zhang & Chintala, 2004; Lin *et al.*, 2003; Yoneda *et al.*, 2001 and Hangai *et al.*, 1995). The relationship between IL-1 β and glaucoma pathogenesis is unclear with some studies finding a neuroprotective and others a neurodegenerative effect. POAG patients were found by Lin *et al* in 2003 to have a genetic polymorphism of IL-1 β and IL-1 α gene, which increases the levels of IL-1 β secreted. However, since then 4 further studies have found varying results (Markiewicz *et al.*, 2013; Mookherjee *et al.* 2010; How *et al.*, 2007; Wang *et al.*, 2007). Our group has previously shown that stimulation of the P2X7R mediates RGC death in the human organotypic retinal culture (HORC) model (Niyadurupola *et al.*, 2013); there was associated release of IL-1 β and IL-10 (Niyadurupola *et al.*, 2009). IL-1 β mRNA upregulation and protein release have similarly been demonstrated in optic nerve ligation models (Zhang & Chintala, 2004; Hangai *et al.*, 1995). In ischaemic models of glaucoma application of IL-1 β antagonist have mitigated damage, implying a neuroinflammatory role of IL-1 β in glaucoma (Yoneda *et al.*, 2001). Contrary to this,

in NMDA excitatory models of glaucoma application of IL-1 β has provide a neuroprotective effect (Kitaoka *et al.*, 2007).

1.5.3 IL-1

In 1974 research on endogenous factors responsible for mediating fever led to the discovery of a family of cytokine factors eventually named IL-1 (Lomedico *et al.*, 1984). The IL-1 family is primarily associated with roles in innate immunity and inflammation (Dinarello *et al.*, 2018). There are 11 IL-1 cytokines and 10 IL-1 receptors (table 1.7). IL-1 cytokines are divided into 3 subfamilies: (i) IL-1 sub-family; (ii) IL-18 subfamily and (iii) IL-36 subfamily (Dinarello *et al.*, 2018). Thesis research focuses on the IL-1 subfamily isoforms IL-1 α and IL-1 β . IL-1 α and IL-1 β are produced as precursor proteins which are cleaved into mature proteins. IL-1 α and IL-1 β mature protein binds to their interleukin-1 receptor (IL-1R) exerting identical downstream biological responses (Paolo and Shayakhmetov, 2016). IL-1 is a potent inflammatory cytokine: the balance between benefit and toxicity is a narrow margin in humans, as such its synthesis and release are tightly regulated (Dinarello, 1997).

IL-1 family	Specific receptor	Coreceptor	Function
IL-1 α , IL-1 β	IL-1R1	IL-1R3	Pro-inflammatory
IL-1 β	IL-1R2	IL-1R3	Anti-inflammatory
IL-1Ra	IL-1R1	Not applicable	Anti-inflammatory
IL-18	IL-1R5	IL-1R7	Pro-inflammatory
IL-33	IL-1R4	IL-1R3	Pro-inflammatory
IL-36 α , β , γ	IL-1R6	IL-1R3	Anti-inflammatory
IL-36Ra	IL-1R6	IL-1R3	Anti-inflammatory
IL-37	IL-1R5	IL-1R8	Anti-inflammatory
IL-38	IL-1R6	IL-1R9	Anti-inflammatory

Table 1.7: IL-1 family of ligands and receptors (replicated from Dinarello *et al.*, 2018)

1.5.3.1 IL-1 type 1 receptor (IL-1R1) and IL-1 type 2 receptor (IL-1R2)

IL-1 α and IL-1 β bind at IL-1R1 and IL-1R2. IL-1 α and IL-1 β are agonists at the IL-1R1 through which they exert their downstream signalling. IL-1R antagonist (IL-1Ra) is a naturally occurring antagonist at the IL-1R1: it binds to IL-1R1 and inhibits the agonist action of IL-1 α or IL-1 β at their receptor (Yazdi and Ghoreschi, 2016 and Dinarello, 1996). Once IL-1 α or IL-1 β binds to the IL-1R1, another receptor IL-1 receptor accessory protein (IL-1RAcP or IL-1R3) is recruited at the plasma membrane to form a signal transduction complex. The complex recruits myeloid differentiation primary response gene 88 (MyD88) and kinases, it activates nuclear factor kappa B (NF- κ B), c-Jun N-terminal kinases (JNK) and p38 mitogen-activated protein kinases (MAPK) which target gene transcription (figure 5.1; Weber *et al.*, 2010).

IL-1 α or IL-1 β binding at IL-1R2 does not lead to downstream signalling, it is considered a decoy receptor. IL-1 α has greater affinity for the IL-1R1, IL-1 β has greater affinity for IL-1R2 (Dinarello *et al.*, 1996).

1.5.3.2 IL-1 α

IL-1 α is expressed in healthy physiological and inflammatory states in many cell types (Bersudsky *et al.*, 2014). It is highly expressed by epithelial and endothelial cell types (Bersudsky *et al.*, 2014; Garlanda *et al.*, 2013 and Rider *et al.*, 2012).

IL-1A gene is located next to the *IL1B* gene on the long arm of chromosome 2 (Modi *et al.*, 1988). *IL-1A* is translated in a 271 amino acid precursor protein pro-IL-1 α . Pro-IL-1 α contains a nuclear localisation sequence (NLS) in its N-terminal domain. It is cleaved by the protease calpain into a propeptide containing the N-terminal and the mature protein containing the C-terminal (Kobayashi *et al.*, 1990). Both pro-IL-1 α and mature IL-1 α are ligands at the IL-1R1 and produce identical downstream functions (Kim *et al.*, 2013). IL-1 α functions both as a secreted and as a membrane-bound cytokine. Membrane bound is the pro-IL-1 α form (Kurt-Jones *et al.*, 1985, 1986 and

1987). Pro-IL-1 α and mature IL-1 α are released from the cell when the plasma membrane is damaged. Mature IL-1 α can also be released by binding to the Cu²⁺-S100A13 complex (figure 1.23).

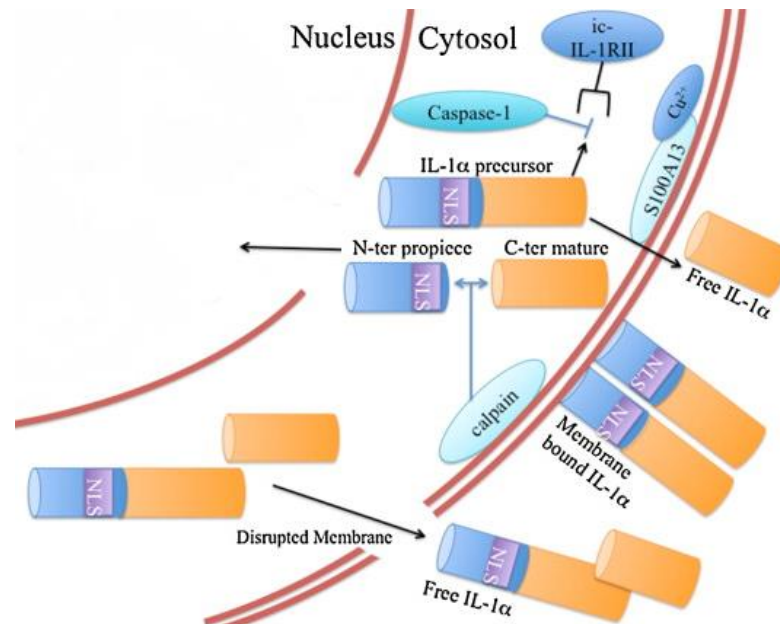


Figure 1.23: IL-1 α precursor, propiece and mature forms (adapted from Rider *et al.*, 2013)

The pro-IL-1 α precursor protein is enzymatically cleaved by the protease calpain into the propiece and the mature protein. Diametrically, the pro-IL-1 α C-terminal can bind to the IL-1R2 which prevents calpain cleavage. The cleaved propiece contains a NLS and this allows translocation into the nucleus. Mature IL-1 α binds to the Cu²⁺-S100A13 complex during pathological states of cell stress which enables its release from the cell. Disruption of the plasma membrane also causes its release. Pro-IL-1 α can also be inserted into the plasma membrane.

IL-1 α is the major cytokine initiating sterile inflammation (Rider *et al.*, 2013). IL-1 α acts as a danger associated molecular pattern (DAMP). IL-1 α is released from damaged or necrotic cells triggering an inflammatory response: meanwhile, apoptotic cells retain IL-1 α within their nucleus and do not initiate an inflammatory response (Lamacchia *et al.*, 2013 and Cohen *et al.*, 2010). Increased levels of this cytokine have been demonstrated in autoimmune conditions such as rheumatoid arthritis (Dinarelli *et al.*, 2012; Chikanza *et al.*, 1995 and Deleuran *et al.*, 1992), psoriasis (Kristensen *et al.*, 1992 and Gomi *et al.*, 1991) and systemic sclerosis (Aden

et al., 2010 and Kawaguchi *et al.*, 1999). Increased IL-1 α is also associated with the neurodegenerative Alzheimer's dementia (Griffin *et al.*, 1995 and Griffin *et al.*, 1989). Both IL-1 α and IL-1 β promote tumour invasiveness, metastasis and chemical-induced carcinogenesis through inflammatory responses they induce (Rider *et al.*, 2013).

IL-1 α and IL-1 β levels are related via the IL-1 α -inflammasome-IL-1 β axis. Necrotic cells activate caspase-1. Caspase-1 cleaves pro-IL-1 β into mature IL-1 β (Ambade and Re, 2009), however it also cleaves IL-1R2. As described earlier (figure 1.23), IL-1R2 inhibits calpain cleavage of pro-IL-1 α therefore its cleavage allows production and secretion of mature IL-1 α . IL-1 α and IL-1 β lack a signal peptide for the classical secretion pathway, in this way caspase-1 play roles in the processing and secretion of both cytokines (Keller *et al.*, 2008). Studies of inflammation in mouse models shows early-on at 24 hours IL-1 α is more highly expressed, whilst later-on at 5 days IL-1 β is more highly expressed (Dinarello *et al.*, 2012).

1.5.3.3 IL-1 β

IL-1 β has homeostatic functions including the regulation of feeding, sleep and temperature (Dinarello, 1996). However, it is predominantly produced in pathological states and it is amongst the most pro-inflammatory agents (Giuliani *et al.*, 2017; Dinarello, 2011 and Gabay *et al.*, 2010). IL-1 β is highly expressed by immunocompetent cells, such as macrophages and mast cells; glial cells, such as microglia and astrocytes and other specialised cell-types, such as keratinocytes and fibroblasts (Ren and Torres, 2009).

IL1B gene is located on the long arm of chromosome 2. *IL-1B* is located alongside an 8 IL-1 family gene cluster (Modi *et al.*, 1988). There are several stages in IL-1 β protein production and release. Pathogen-associated molecular pattern (PAMP) stimulation of toll-like receptors (TLRs) initiate synthesis of the precursor protein pro-IL-1 β (Janeway *et al.*, 2001). Pro-IL-1 β is proteolytically cleaved by the enzyme caspase-1, which removes the N-terminal of the amino-acid resulting in the mature protein.

Caspase-1 requires NLRP3 inflammasome binding before it can exert its enzymatic effects. The inflammasome is an intracellular multi-protein complex that acts as a scaffold for pro-inflammatory caspases. NLRP3 inflammasome is assembled in response to a variety of exogenous PAMPs and DAMPs. High concentrations of ATP act as a DAMP, stimulate the P2X7R and are well associated with NLR3P activation, IL-1 β synthesis and release (1.5.3.3.1 P2X7R and IL-1 β). As mentioned previously, IL-1 β does not contain a leader amino-acid sequence and so is not released from the cell via the endoplasmic reticulum-golgi body secretory pathway (Rubartelli *et al.*, 1990). There are 4 proposed mechanisms for IL-1 β release: (i) lysosomal secretory exocytosis; (ii) microvesicle shedding (iii) exosomal exocytosis and (iv) passive diffusion across a leaky plasma membrane during cell death (Giuliani *et al.*, 2017; figure 1.24).

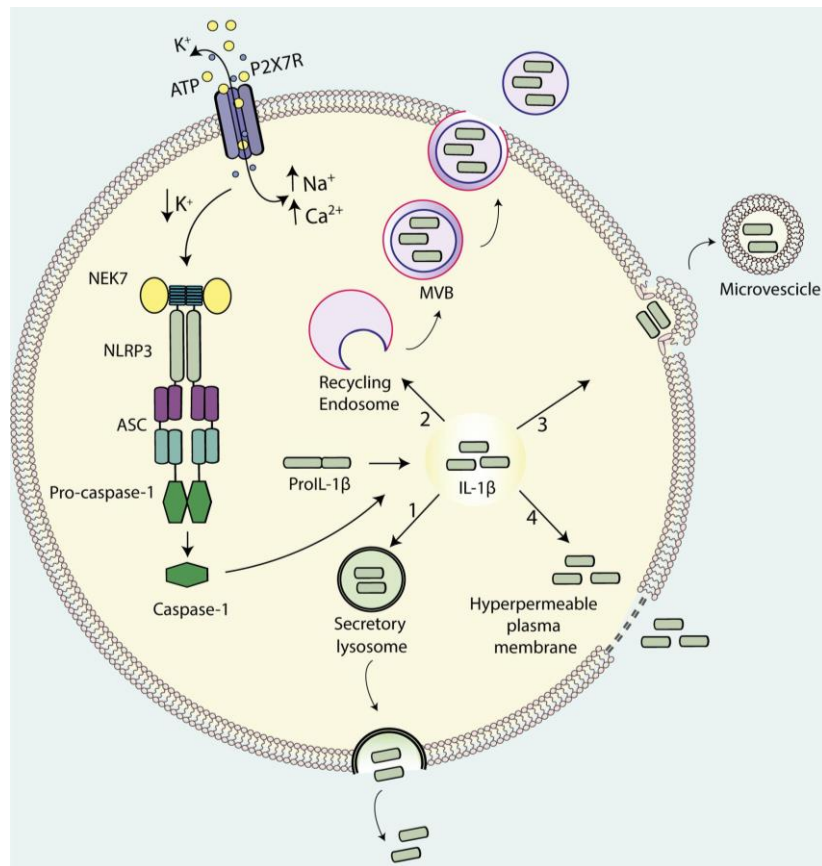


Figure 1.24: NLRP3 inflammasome structure and possible mechanisms of IL-1 β release (Giuliani *et al.*, 2017)

High concentrations of ATP stimulate the P2X7R causing NLRP3 inflammasome assembly. Components of the NLRP3 inflammasome include: NIMA-related kinase 7 (NEK7) binding to NLRP3 protein, engagement with apoptosis-associated speck-like protein containing a CARD (ASC), recruitment of pro-caspase-1 (Yang *et al.*, 2019). Subsequently caspase-1 cleaves pro-IL-1 β forming mature IL-1 β ready for release from the cell. Four mechanisms of release are shown: (i) lysosomal secretory exocytosis; (ii) microvesicle shedding (iii) exosomal exocytosis and (iv) passive diffusion across a leaky plasma membrane during cell death.

Upregulation of IL-1 β is associated with inflammatory and autoimmune conditions, such as rheumatoid arthritis, osteoarthritis, gout and inflammatory bowel disease. It is also associated with neurological conditions such as neuropathic pain and Alzheimer's dementia (Dinarello, 2004, Braddock and Quinn, 2004, Dinarello, 1996 and Ren and Torres, 2009).

1.5.3.3.1 P2X7R and IL-1 β

High concentrations of ATP activating the P2X7R is well recognised as the most important trigger of IL-1 β synthesis and release (Di Virgilio *et al.*, 1998; Pelegrin *et al.*, 2008; Sanz *et al.*, 2009), predominantly because of the role the P2X7R has in NLRP3 inflammasome activation. Supporting this, animal studies show mice lacking P2X7R or NLRP3 are not capable of ATP induced IL-1 β release (Solle *et al.*, 2001; Mariathasan *et al.*, 2004, 2006).

Activation of the NLRP3 inflammasome has two stages: priming and activation. Priming involves inflammatory stimuli, such as Toll-like receptor 4 (TLR-4) agonists, inducing NF- κ B NLRP3 protein and pro-IL-1 β expression. Activation involves PAMPs and DAMPs promoting NLRP3 assembly (Yang *et al.*, 2019). Many PAMPs and DAMPs can activate the NLRP3 inflammasome with the final common pathway of these stimuli hypothesised to be K⁺ efflux (Munoz-Planillo *et al.*, 2013; Murakami *et al.*, 2012). ATP binding at the P2X7R, causes Ca²⁺ influx, membrane depolarisation and activation of BK channels with a K⁺ efflux (described earlier alongside figure 1.21 and figure 1.23): by this mechanism ATP acts via the P2X7R as an efficient NLRP3 activator (Prochnicki *et al.*, 2016). Activation of the P2X7R also causes oxidised mitochondrial DNA release into the cytoplasm, this assists NLRP3 inflammasome activation by direct interaction (Shimada *et al.*, 2012 and Nakahira *et al.*, 2011).

1.5.4 IL-10

IL-10 is a predominantly an anti-inflammatory cytokine. It modulates responses to infection or inflammation so that there is minimal resultant tissue damage. IL-10 was first identified in 1989 as cytokine synthesis inhibitory factor (CSIF) produced by mouse T helper 2 (Th2) cells and noted to inhibit T helper 1 (Th1) cytokine production (Moore *et al.*, 2001). Later research showed that IL-10 suppressed several monocyte/macrophage functions, and that inhibition of Th1 cytokine production was secondary to this (Ding and Shevach, 1992; de Waal Malefyt *et al.*, 1991 and Fiorentino *et al.*, 1991). Its prominent function is to inhibit cytokine synthesis: IL-1 α , IL-1 β , IL-6, IL-10 itself, IL-12, IL-18, granulocyte-macrophage colony-stimulating factor, granulocyte colony-stimulating factor, macrophage colony-stimulating factor,

TNF, leukemia inhibitory factor and platelet-activating factor (Moore *et al.*, 2001 and 1993). IL-10 is highly expressed by immunocompetent cells: monocytes and macrophages; dendritic cells; neutrophils; B-cells and T-cells (Moore *et al.*, 2001 and 1993)

Although IL-10 is considered an anti-inflammatory cytokine, it has also been linked to pro-inflammatory and autoimmune pathology: the best characterised example of this is the association between high IL-10 expression and development of the autoimmune condition Systemic Lupus Erythematosus (Grondal *et al.*, 1999; Rood *et al.*, 1999; Gonzalez-Amaro *et al.*, 1998; Eskdale *et al.*, 1997; Lazarus *et al.*, 1997; Llorente *et al.*, 1997; Llorente *et al.*, 1995). Notably human IL-10 (hIL-10) homologs have been found in Epstein-Barr virus, cytomegalovirus and poxvirus orf (Kotenko *et al.*, 2000; Fleming *et al.*, 1997; Vieira *et al.*, 1991 and Moore *et al.*, 1990).

HIL-10 gene is located on chromosome 1 (Kim *et al.*, 1992). *HIL-10* expression is regulated by the transcription factors Sp1 and Sp3 present in many cell types (Brightbill *et al.*, 2000 and Tone *et al.*, 2000). *HIL-10* encodes a protein made of 178 amino-acids forming an α -helix secondary structure (Viera *et al.*, 1991). X-ray crystallography revealed quaternary assembly as a homodimer, similar in structure to the cytokine interferon- γ (IFN- γ) which notably functions as the primary activator of monocytes/macrophages (Zadnov *et al.*, 1996; Walter and Nagabhushan, 1995 and Zdanov *et al.*, 1995).

IL-10 exerts its downstream effects by binding to the IL-10 receptor (IL-10R). The IL-10R is made of two subunits: IL-10 receptor 1 (IL-10R1 or IL-10R α) and IL-10 receptor 2 (IL-10R2 or IL-10R β). IL-10 binds at the IL-10R1 subunit with high affinity $K_d \sim 35$ -200pM (Liu *et al.*, 1994 and Tan *et al.*, 1993). hIL-10/hIL-10R1 complexes can form multimers with two hIL-10 dimers binding to four IL-10R1 molecules (Josephson *et al.*, 2000). IL-10R employs IL-10R2 as an accessory subunit for signalling, it initiates signal transduction via the jak/stat pathway. The genes for the two subunits are in two different chromosomes: IL-10R1 in chromosome 11 and IL-10R2 in chromosome 21 as part of the interferon receptor gene complex (Lutfalla *et al.*, 1993).

1.6 Aims of the thesis

The purpose of this research is to contribute to the understanding of the role(s) purinergic signalling may have in the pathogenesis of glaucoma. It has been shown that P2X7R stimulation in HORC models is associated with RGC death as seen in glaucoma, as well as release of neuroprotective and neurodegenerative cytokines IL-10 and IL-1 β respectively. The mechanism of RGC death and cell-types involved in cytokine release have yet to be identified. Müller cells are the most abundant glial cell in the human retina. The aims of this thesis research are to firstly identify the functional purinergic receptors in the human Müller cell, then to establish if stimulation of the P2X7R on the Müller cell causes its death and/or IL-10 and IL-1 β mRNA expression and protein release.

Chapter 2: Materials and Methods

2.1 MIO-M1 cells

Moorfield's/Institute of Ophthalmology – Müller 1 cells (MIO-M1; University College London, UK) between passage number 21 and 50 (figure 2.1) were used as an experimental model for human Müller cells throughout this research. MIO-M1 cells are an immortalised human Müller cell line derived from the eye of a 68-year-old donor at 36-hours post-mortem (Limb *et al.*, 2002).

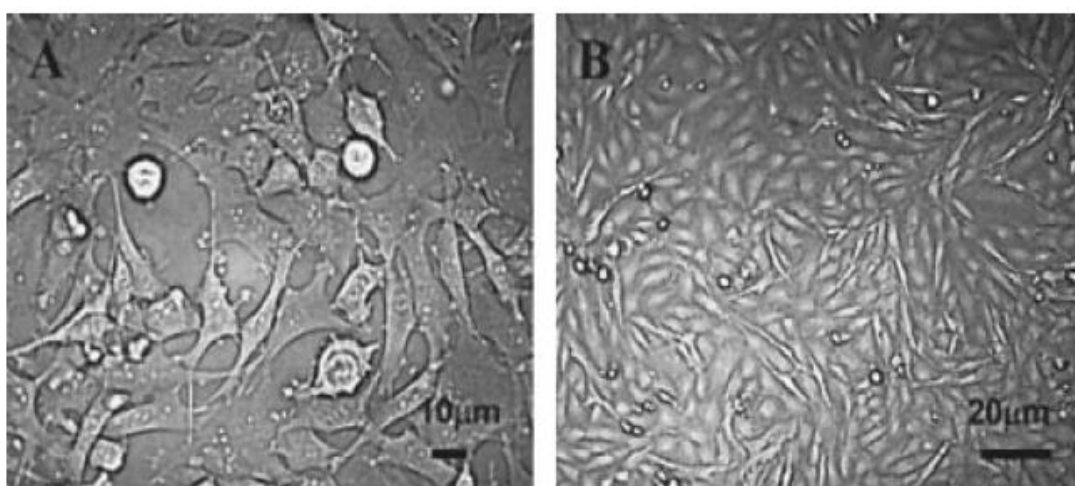


Figure 2.1: Phase contrast microscopy images of MIO-M1 cells (Limb *et al.*, 2002)

The morphological appearance of MIO-M1 cells changes with their confluence. Image A demonstrates a sub-confluent single-cell layer that exhibits long projections and bipolar morphology. Image B demonstrates a confluent single-cell layer exhibiting a 'fibroblast-like' morphology.

2.1.1 Cell culture

MIO-M1 cells were kept in culture in Dulbecco's modified Eagle medium (DMEM) with L-glutamine, pyruvate and 1g/L of glucose (Life technologies, Thermo Fisher Scientific, Paisley, UK) to which heat-inactivated fetal bovine serum (FBS; Life Technologies) was added at a concentration of 10%. Penicillin-Streptomycin (Life Technologies) was added at a concentration of 1% as a bactericide. They were contained in 75cm² culture flasks (Nunc™, Thermo Fisher Scientific, Loughborough, UK) and left to expand in a humidified incubator at 35°C in 95% air, 5% CO₂ until 80-90% confluent.

Once confluent they were passaged. Culture medium was aspirated and cells washed with Dulbecco's phosphate buffered saline (DPBS, Invitrogen, Thermo Fisher Scientific, UK). For cellular detachment 0.05% Trypsin-EDTA (Life technologies) was applied for 5 min whilst incubated, which was then neutralised by the addition of DMEM with FBS. Once transferred to a 15mL universal tube (Nunc™) the cell suspension was centrifuged at 50 x G for 5 min to cause formation of a cell pellet. After removal of the supernatant the cell pellet was re-suspended in culture medium ready for experimental use (table 2.1) and seeding of another 75cm² culture flasks to maintain stock.

Assay	Culture dish	Seeding density	Volume of culture medium (µL)
RT-qPCR	35mm cell culture dishes (Corning)	120, 000 cells per dish	1,500
MTS	96 well plate (Nunc™)	6,000 cells per well	200
LDH	96 well plate (Nunc™)	6,000 cells per well	200
Calcium microfluorimetry	Poly-D-Lysine coated 96 well Plate (Nunc™)	20,000 cells per well	100
ELISA	35mm cell culture dishes (Corning)	120, 000 cells per dish	1,500

Table 2.1: Seeding density of MIO-M1 cells used for experimental assays

2.2 Enzymatic Dissociation of Human Retinal Tissue

Human donor eyes were provided by the East Anglian Eye Bank (Norwich, UK) within 24 hours of post-mortem with consent and ethical approval. Donor eyes were assigned a serial number and any identifiable information regarding the donor was not included in the information provided to the research team. Donor eyes with previous ocular disease(s) were excluded for the purposes of this thesis research. Four eyes, from four individual donors were used. The age range of donors was 57-61 years.

Donor eye retinal tissue was dissected from the remainder of the globe. To gain access to the retina a circumferential ring of sclera was removed at the ora serrata

and the vitreous body removed. The retina was mechanically detached from the underlying RPE and choroid using gentle traction with Calibri straight forceps, the attachment of the retina at the optic nerve was cut using Westcott curved tenotomy scissors. Circumferential 4mm sections of retina were dissected with a trephine (Biomedical Research Instruments, USA) and placed into serum-free DMEM supplemented as described previously in *2.1.1 cell culture*.

Retinal tissue was disassociated into a mixed cell suspension through a series of enzymatic digestion and mechanical steps. Retinal tissue was placed in a 5ml universal tube (Nunc™) and enzymatically digested by incubation with papain (Sigma Aldrich) in a humidified incubator at 35°C for 10 minutes. Mechanical trituration of retinal tissue in papain was performed by repeat pipetting with a P1000 pipette. The cell suspension was centrifuged at 300 x G for 5 min to form a cell pellet. Supernatant was removed and two washing steps were performed by re-suspending the cell pellet in DPBS and centrifuging again. The cell suspension was passed through a 40µm cell strainer (Sigma-Aldrich, Merck, Dorset, UK) ready for experimental use.

2.3 Agonists and Antagonists

A range of non-selective and selective agonists and antagonists were applied to MIO-M1 cells for experimental use throughout this research, these are listed below with their concentration in table 2.2.

Reagent (Manufacturer)	Primary action of reagent	Experimental use	Concentration
ATP (Sigma Aldrich)	Non-selective P2 receptor agonist	Calcium microfluorimetry MTS, LDH and PCR	0.01μM-1mM 100μM to 3mM 300μM and 3mM
ADP (Sigma Aldrich)	P2Y ₁ R, P2Y ₁₂ R and P2Y ₁₃ R agonist	Calcium microfluorimetry	0.01μM-1mM
UTP (Sigma Aldrich)	P2Y ₂ R and P2Y ₄ R agonist	Calcium microfluorimetry	0.01μM-1mM
UDP (Sigma Aldrich)	P2Y ₆ R agonist	Calcium microfluorimetry	0.01μM-1mM
UDP-glucose (Sigma Aldrich)	P2Y ₁₄ R agonist	Calcium microfluorimetry	0.01mM-1mM
MRS 2690 (Tocris Bioscience, Bristol, UK)	Selective P2Y ₁₄ R agonist	Calcium microfluorimetry	0.001-10mM
BzATP (Sigma Aldrich)	P2X ₇ R and P2X ₄ R agonist	Calcium microfluorimetry PCR	10μM-1mM 30μM and 300μM
NF 449 (Tocris Bioscience)	Selective P2X ₁ R antagonist	Calcium microfluorimetry	10μM
PSB 12054 (Tocris Bioscience)	Selective P2X ₄ R antagonist	Calcium microfluorimetry	10μM
5-BDBD (Tocris Bioscience)	Selective P2X ₄ R antagonist	Calcium microfluorimetry	10μM
BX 430 (Tocris Bioscience)	Selective P2X ₄ R antagonist	Calcium microfluorimetry	10μM
AZ10606120 (Tocris Bioscience)	Selective P2X ₇ R antagonist	Calcium microfluorimetry and PCR	10μM
A438079 (Tocris Bioscience)	Selective P2X ₇ R antagonist	Calcium microfluorimetry	10μM

Table 2.2: Agonists and antagonists used for experimental assays (Page 1 of 2)

Reagent (Manufacturer)	Primary action of reagent	Experimental use	Concentration
MRS 2179 (Tocris Bioscience)	Selective P2Y ₁ R antagonist	Calcium microfluorimetry	10μM
AR-C118925XX (Tocris Bioscience)	Selective P2Y ₂ R antagonist	Calcium microfluorimetry	10μM
MRS 2578 (Tocris Bioscience)	Selective P2Y ₆ R antagonist	Calcium microfluorimetry	10μM
PSB 0739 (Tocris Bioscience)	Selective P2Y ₁₂ R antagonist	Calcium microfluorimetry	10μM
MRS 2211 (Tocris Bioscience)	Selective P2Y ₁₃ R antagonist	Calcium microfluorimetry	10μM
PPTN hydrochloride (Tocris Bioscience)	Selective P2Y ₁₄ R antagonist	Calcium microfluorimetry	10μM
Suramin (Sigma Aldrich)	Non-specific pan-antagonist for purinergic receptors	Calcium microfluorimetry	10μM
IL-1β (Abcam, Cambridge, UK)	IL-1R1 agonist	LDH, PCR & IL-10 ELISA	10nM
LY 294002 (Sigma Aldrich)	Selective competitive inhibitor of PI3K	LDH, PCR & IL-10 ELISA	10μM
Bardoxolone methyl (Sigma Aldrich)	Inhibitor of NF-κB	LDH, PCR & IL-10 ELISA	5μM
SB 203580 (Sigma Aldrich)	Selective competitive inhibitor of p38 MAPK	LDH, PCR & IL-10 ELISA	2.5μM

Table 2.2: Agonists and antagonists used for experimental assays (page 2 of 2)

Abbreviations (not defined previously): 5-BDBD: 5-(3-bromophenyl)-1,3-dihydro-2H-benzofuro[3,2-e]-1,4-diazepin-2-one; PPTN hydrochloride: 4-[4-(4-Piperidinyl)phenyl]-7-[4-(trifluoromethyl)phenyl]-2-naphthalenecarboxylic acid hydrochloride

Reagents were in solution with distilled water or dimethylsulfoxide (DMSO). Where DMSO was used as a vehicle this was added to the relevant experimental control group at the same concentration.

2.4 Reverse transcription quantitative polymerase chain reaction (RT-qPCR)

mRNA expression in response to stimulus was evaluated using real time quantitative PCR (figure 2.2).

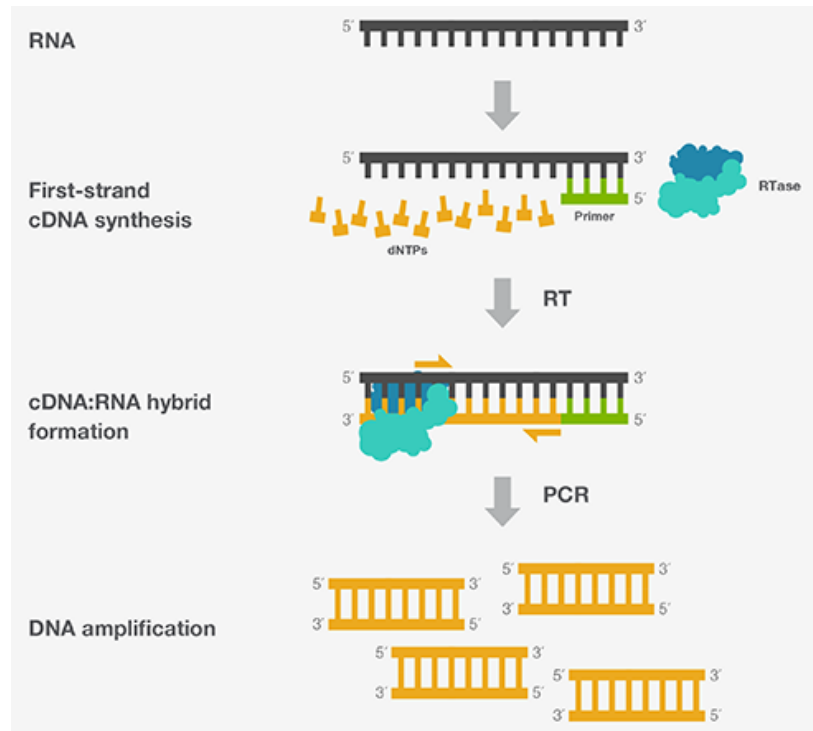


Figure 2.2: Stages of reverse transcription quantitative polymerase chain reaction (ThermoFisher, 2018)

RNA is extracted from cells and then converted to cDNA by reverse transcription. cDNA is amplified by PCR. RT-qPCR allows for analysis of mRNA expressed at low concentrations by cells.

2.4.1 RNA extraction

The ReliaPrep RNA Cell Miniprep System (Promega) was used to extract RNA from treated cells. All materials used were part of the kit unless stated otherwise.

To lyse the cells buffer containing 1-thioglycerol was applied. Cells were then homogenised by vigorous pipetting. Released RNA was then bound to the membrane of the ReliaPrep Minicoloumn through a series of wash and centrifuging steps. DNase was applied directly to the membrane for 15 min at room temperature to digest any DNA contaminant. DNase, protein and cellular contaminants were removed from the membrane by an additional series of wash and centrifuging steps. Finally, 30 μ L of RNase free water was added to the membrane to elute the RNA.

Concentration and purity of RNA was assessed by wavelength absorbance measurements by the NanoDrop spectrophotometer (NanoDrop Technologies, Wilmington, USA). Wavelength ratios 260/280nm and 260/230nm were measured. Ratios >2.0 are indicative of good purity RNA. Ratio <2.0 this threshold indicates protein or phenol contaminants. Only experiments with a sample-set containing good purity RNA were used for PCR.

2.4.2 First-strand complementary DNA (cDNA) synthesis

Single stranded RNA was converted to more stable double-stranded cDNA for storage and use as a template in RT-qPCR.

RNAse free water was added to RNA to ensure a standardised concentration of 10ng/μl for reaction. Random primers (Promega) and deoxyribonucleotide triphosphate (dNTP; Invitrogen) were added to each sample as the necessary components for DNA synthesis. Samples were heated at 65°C for 5 min in the Peltier Thermal Cycler DNA engine (MJ Research, Minnesota, USA). Once chilled, RNAse inhibitor (Promega), dithiothreitol (Invitrogen) and first strand buffer (Invitrogen) were added to prevent degradation of mRNA, break bonds in the secondary structure of RNA to facilitate reverse transcription of cDNA and ensure necessary pH and ions for the reaction. Samples were heated at 25°C for 10 min and 42°C for 2 minutes. Once chilled, the reverse transcriptase enzyme Superscript II (Invitrogen) was added which uses a short primer complementary to the 3' end of the RNA to synthesise first strand cDNA (figure 2.2). Finally, Samples were heated at 42°C for 50 minutes and 70°C for 15 min to produce cDNA.

2.4.3 TaqMan RT-qPCR

RT-qPCR was performed to amplify the cDNA produced in each sample.

RNAse free water was added to cDNA to produce a reaction concentration of 0.5ng/μl. cDNA sample, Mastermix (PCR Biosystems, London, UK), TaqMan probes (table 2.3) and RNAse free water at a reaction mixture volume of 25μL were loaded

on to the Optical 96 reaction plate (Applied Biosystems, Warrington, UK). The PCR reaction was facilitated using Applied Biosystems 7500 Fast Real-Time PCR system (Applied Biosystems) with its programmed cycle of heated stages. Heated stages of 50° C for 2 min, 95° C for 10 min, followed by 40 cycles of 95° C for 15s and 60° C for 60s were used. Higher temperatures denatured double-stranded DNA and cooler temperatures facilitated primer binding to single-stranded DNA resulting in amplification.

Probe	Manufacturer	Part Number	Reporter
Topoisomerase (TOP 1)	Roche Diagnostics, Burgess Hill, UK	CCCTGTACTTCATCGACAAGC	FAM
Cytochrome C1 (CYC 1)	Primer Design, Southampton, UK	HK-DD-hu-300	FAM
P2X1R	ThermoFisher	Hs00175686_m1	FAM
P2X2R*	ThermoFisher	Hs04176268_g1	FAM
P2X3R	ThermoFisher	Hs01125554_m1	FAM
P2X4R	ThermoFisher	Hs00602442_m1	FAM
P2X5R	ThermoFisher	Hs01112471_m1	FAM
P2X6R	ThermoFisher	Hs01003997_m1	FAM
P2X7R	ThermoFisher	Hs00175721_m1	FAM
P2Y1R*	ThermoFisher	Hs00704965_s1	FAM
P2Y2R*	ThermoFisher	Hs04176264_s1	FAM
P2Y4R*	ThermoFisher	Hs00267404_s1	FAM
P2Y6R*	ThermoFisher	Hs00366312_m1	FAM
P2Y11R*	ThermoFisher	Hs01038858_m1	FAM
P2Y12R*	ThermoFisher	Hs01881698_s1	FAM
P2Y13R*	ThermoFisher	Hs03043902_s1	FAM
P2Y14R*	ThermoFisher	Hs01848195_s1	FAM
IL-18	Applied Biosystems, Warrington, UK	Hs00174097_m1	FAM
IL-10	ThermoFisher	Hs00961622_m1	FAM

Table 2.3: TaqMan probes

Probes indicated with an asterisk (*) are within a single exon, they may amplify any contaminating genomic DNA.

Gene of interest amplification was normalised in relation to stably expressed housekeeping genes TOP 1 and CYC 1. Gene of interest mRNA was expressed as fold-

changes relative to control. The delta (Δ) cycle threshold (Ct) method was used to calculate fold-changes in gene expression using the equation below:

$$\Delta Ct1 = Ct (\text{gene of interest, sample}) - Ct (\text{housekeeping gene, sample})$$

$$\Delta Ct2 = Ct (\text{gene of interest, control}) - Ct (\text{housekeeping gene, control})$$

$$\Delta\Delta Ct = \Delta Ct1 (\text{sample}) - \Delta Ct2 (\text{control})$$

$$\text{Normalised target gene expression level} = 2^{-\Delta\Delta Ct}$$

2.5 MTS assay

Cell viability was evaluated using 3-(4,5-dimethylthiazol-2-yl)-5-(3-carboxymethoxyphenyl)-2-(4-sulfophenyl)-2H-tetrazolium (MTS; Promega, Southampton, UK) colorimetric assay: mitochondria of metabolically active cells bioreduce MTS to formazan causing a detectable colour change which can be quantified by wavelength absorbance measurements (Promega, 2018).

Cells were serum starved for 24 hours, then incubated in a range of ATP (100 μ M-3mM) and BzATP (10 μ M-300 μ M) concentrations for a further 24 hours. MTS solution at a 10% concentration was added directly to the culture medium containing cells and incubated for 1 hour at 35°C, 5% CO₂. Absorbance at a wavelength of 490nm was measured using the FLUOstar Omega plate reader (BMG Labtech, Cambridge, UK).

Background readings were adjusted for. Cell viability was expressed as a percentage of the control.

2.6 LDH assay

Cell cytotoxicity was evaluated using lactate dehydrogenase (LDH, Roche, Switzerland) colorimetric assay: dead and lysed cells release LDH which is measured by this chromogenic substrate containing kit for quantification by wavelength absorbance measurements (Roche, 2011).

Cells were serum starved for 24 hours and then incubated in a range of reagents for a further 24 hours: ATP (100 μ M-3mM); BzATP (10 μ M-300 μ M); IL-1 β (1-100nM); LY294002 (10 μ M); Bardoxylone methyl (5 μ M) and SB203508 (2.5 μ M). 100 μ L of culture medium supernatant from each sample was transferred to a 96-well plate (Nunc™) and 100 μ L of the catalyst dye mix was added to this. This was incubated for 15min at 37°C. Absorbance at wavelengths of 490nm and 660nm were measured using the FLUOstar Omega plate reader.

Cell cytotoxicity was calculated by subtracting absorbance readings at 490nm by readings at 660nm. Background readings were adjusted for. Cell cytotoxicity was expressed as a percentage of the control.

2.7 Calcium microfluorimetry

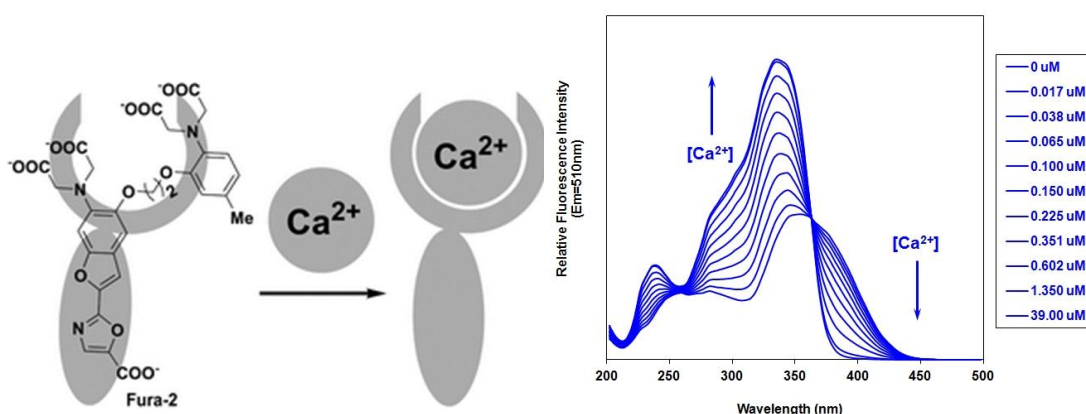


Figure 2.3: A. Fura-2 AM binding intracellular calcium (Yang *et al.*, 2010) and B. Fura 2 AM emission spectra at different concentrations of Ca²⁺ (AAT Bioquest, 2022)

Intracellular calcium responses were measured with the aid of fura-2-acetoxymethyl (fura-2 AM; Hello Bio, Bristol, UK): a dye that binds intracellular calcium (figure 2.3) and can be quantified by wavelength emission measurements.

Fura-2 AM is an esterified form of Fura-2. The addition of the acetoxymethyl group makes the charged molecule neutral, so that it becomes cell-membrane permeable. Once Fura-2 AM enters the cell, esterases remove the acetoxymethyl group and Fura-

2 is trapped within the cell allowing measurement of intracellular calcium (Martinez *et al.*, 2017 and Oakes *et al.*, 1988).

In this assay Fura-2 is excited at wavelengths of 380nm and 340nm. Emission is measured at 510nm and data is expressed as a ratio 340 versus 380nm. Ratiometric measurement reduces effects of uneven dye loading, leakage of dye and unequal thickness of cells (Thermofisher, 2017).

MIO-M1 cells were seeded in a 96-well plate coated with poly-D-lysine (Merck Millipore, Watford, UK) at a density of 20,000 cells per well. Preliminary experiments advised seeding at this higher cell density to produce a reliable calcium response. The cells were left for 1 day to attach. They were loaded with Hanks' Balanced Salt Solution (HBSS) buffer containing fura-2 AM at a concentration of 2 μ M for 1 hour. The dye was removed and a running buffer of physiological saline (containing in mM: NaCl 145.1; HEPES 10.0; D-glucose 13.0; KCl 2.0; CaCl₂ 2.0 and MgCl₂ 1.0, equilibrated to pH 7.3 with 5M NaOH) was applied either in the presence or absence of purinergic antagonists (table 2.2) at a concentration of 10 μ M.

Flexstation 3 (Molecular devices, Wokingham, UK) was used to maintain homeostatic temperature, measure intracellular calcium from 0-300s and apply purinergic agonists (table 2.2) at 30s.

The intracellular calcium response was analysed as total area under the curve and peak response. Background fluorescence was corrected for.

2.8 Enzyme-linked immunosorbent assay (ELISA)

Protein release in response to treatment was evaluated using ELISA (BD Biosciences, USA), a colorimetric assay. All materials were part of the kit unless stated otherwise.

Any protein released is bound to capture antibody and detection antibody. The complex binds horse-radish peroxidase (HRP) which interacts with the chromogenic substrate 3,3',5,5'-Tetramethylbenzidine (TMB) to produce a detectable colour change that can be quantified by wavelength absorbance measurements.

The 96-well ELISA plate (Nunc) was coated with anti-human IL-1 β or anti-human IL-10 capture antibody in coating buffer. The coated plate incubated at 4°C for 12h. The plate was washed 3 times with well wash buffer. The plate was blocked with 200 μ l/well of assay diluent and incubated at room temperature for 1 hour. After another wash stage, a standard curve of 100 μ l/well human IL-1 β or human IL-10 at concentrations of 0.0-250.0pg/mL or 0.0-300.0pg/mL respectively was added to the plate. 100 μ l/well of each sample and a control were added to the plate. The plate was incubated at room temperature for 2h. After another wash stage, 100 μ l/well of detection antibody in assay diluent was added to the plate and it was incubated at room temperature for 1h. After another wash stage, 100 μ l/well of enzyme reagent containing HRP in assay diluent was added to the plate and it was incubated at room temperature for 30 min. After another wash stage, 100 μ l/well of TMB was added to the plate and it was incubated at room temperature for 30 min in the dark. 50 μ L/well of Sulphuric acid at 2M was added to the plate to stop the chromogenic reaction. Absorbance at a wavelength of 450nm was measured using the FLUOstar Omega plate reader. Background readings were adjusted for. Concentration of protein release was expressed relative to the standard curve of known concentrations.

2.9 Statistical analysis

Data was expressed as mean \pm standard error of the mean (SEM). Significance was evaluated using GraphPad Prism 8 software (GraphPad Software, California, USA). When two dependent groups were compared, significance was assessed using Student's T-test. When data of three or more groups were compared, significance was assessed using one-way analysis of variance (ANOVA) or two-way ANOVA in combination with post-hoc testing. One-way ANOVA was used when there was one independent variable, whilst two-way ANOVA was used when there were two

independent variables. One-way ANOVA was used in combination with Dunnett's post-hoc test for comparison against a control group, or Tukey's post hoc test for comparison against all groups. Two-way ANOVA was used in combination with Bonferroni's post-hoc test to correct for type I errors made more likely with multiple comparisons. The null hypothesis was rejected, and the data determined to be statically significant, if the probability (p) value was less than 0.05 ($p < 0.05$).

Chapter 3: Purinergic P2-receptors in the Human Müller Cell

3.1 Introduction

The purpose of this research is to identify the P2 receptor profile in the human Müller cell. Identification of P2 receptors in Müller cells has been partially performed in several species: there is significant interspecies variation so findings cannot be extrapolated across species (table 3.1). Some work has been completed on identifying particularly the P2Y receptors and P2X7R in human Müller cells (*1.3.4.1 Purinergic signalling and Müller cells* and table 3.1), however the full set of P2 receptors have yet to be investigated.

Species	P2 Receptor mRNA	P2 Receptor Calcium Responses	P2 Receptor Imaging
Human	<i>P2Y1R, P2Y2R, P2Y4R, P2Y6R¹ and P2X7R²</i>	<i>P2Y1R, P2Y2R and/or P2Y4R, P2Y6R¹ and P2X7R^{2&3}</i>	<i>P2X7R^{2&3}</i>
Rat	<i>P2Y1R, P2Y2R, P2Y4R, P2Y6R⁴ P2X3R, P2X4R and P2X5R⁵</i>	<i>P2Y1R⁶</i>	<i>P2Y1R and P2Y4R⁶</i>
Mouse			<i>P2Y1R⁷</i>
Guinea Pig		<i>P2Y1R, P2Y2R, and P2Y4R⁸</i>	
Rabbit		<i>P2Y1R^{9&10}, P2Y2R⁹ and/or P2Y4R⁹</i>	

1. Fries *et al.*, 2005; 2. Pannicke *et al.*, 2000; 3. Bringmann *et al.*, 2002; 4. Fries *et al.*, 2004; 5. Jabs *et al.*, 2000; 6. Wurm *et al.*, 2009; 7. Lipp *et al.*, 2009; 8. Weick *et al.*, 2005; 9. Uhlmann *et al.*, 2003; 10. Uckermann *et al.*, 2002

Table 3.1: P2 Receptor Expression in Muller cells in Different Species

As shown in the table above P2 receptor identification in a cell usually involves a combination of demonstrating: (i) gene expression (ii) protein evidence (iii) functionality.

Agonist binding at P2 receptors causes a change in intracellular Ca²⁺ concentration (*1.4.2 Purinergic calcium responses in the Müller cell*) that can be illustrated by calcium microfluorimetry techniques (*2.7 calcium microfluorimetry*). Calcium imaging can be a useful way of demonstrating that a P2 receptor expressed in a cell is functional, although it does not tell us the functions of the receptor in that cell.

Calcium imaging of a specific P2 receptor subtype is derived by using specific receptor agonists or antagonists. These are described briefly below and listed in table 3.2. Early work, described above, on identifying P2 receptors in Müller cells was limited by lack of specific P2 receptor subtype agonists and antagonists available at that time. Additionally, research interest was primarily focused on P2Y₁R, P2Y₂R, P2Y₄R, P2Y₆R and P2X₇R.

ATP, ADP, UTP, UDP and UDP-glucose are endogenous agonists binding at orthosteric sites in P2 receptors. Endogenous agonists usually activate multiple receptor subtypes with differing binding affinities and potencies at each one (1.3.2 *Mechanisms of nucleotide release and breakdown* and table 3.2). ATP is the preferential agonist at all P2X receptors (P2X₁R pEC₅₀ 7.3; P2X₂R pEC₅₀ 5.9; P2X₃R pEC₅₀ 6.5 Jacobson, 2018; P2X₄R pEC₅₀ 7.4 Stokes *et al.*, 2019; P2X₅R pEC₅₀ 6.0; P2X₇R pEC₅₀ 4.0 Jacobson, 2018), P2Y₂R (pEC₅₀ 7.07) and P2Y₁₁R (pEC₅₀ 4.77). ATP also activates P2Y₁R, P2Y₄R and, with less potency, P2Y₆R (Jacobson and Müller, 2016 and Fields and Burnstock, 2006). Notably ATP only activates the P2X₇R at higher concentrations (1.3.3.7 *P2X7 receptor*). ADP is an agonist at P2Y₁R (pEC₅₀ 5.09), P2Y₁₂R (pEC₅₀ 7.22) and P2Y₁₃R (pEC₅₀ 7.94); the P2Y₁R is preferentially activated by ADP over ATP (Jacobson and Müller, 2016 and Burnstock, 2007). UTP is the preferential agonist at P2Y₄R (pEC₅₀ 5.60). UTP is equipotent to ATP at P2Y₂R (pEC₅₀ 8.10), also with a greater potency than ATP it activates the P2Y₆R. UDP is the most potent agonist at the P2Y₆R (pEC₅₀ 6.52) and P2Y₁₄R (Carter *et al.*, 2009). UDP-sugars only activate the P2Y₁₄R (e.g. UDP-glucose pEC₅₀ 6.45; Chambers *et al.*, 2000).

Synthetic agonists are most commonly derivatives of endogenous nucleotides that are modified to alter properties such as stability. Similar to the endogenous ligand they are often non-specific activating multiple P2-receptors. Common ATP derived synthetic agonists include adenosine 5'-O-(3-thio)triphosphate (ATP γ S) and BzATP. ATP γ S is modified with a γ -thiophosphate group substitution increasing its stability (Malmsjö *et al.*, 2003); it is an agonist at several P2-receptors including: P2X₂R, P2X₅R, P2Y₁R, and P2Y₁₁R (Jacobson, 2009 and Waldo and Harden, 2004). BzATP is

modified with additions at the ribose ring, it is partially selective acting at P2X1R, P2X3R, P2X4R (Stokes *et al.*, 2017) and P2X7R. It is commonly used as a selective agonist for the P2X7R as it is ten times more potent than ATP at this receptor, however it has the highest binding affinity for the P2X1R (Syed and Kennedy, 2011 and Zhong *et al.*, 1998). MRS 2690 is an UDP-glucose derivative and like the endogenous ligand a selective agonist at the P2Y₁₄R. Modifications increase potency by seven-fold at the P2Y₁₄R (Ko *et al.*, 2007).

Although there are several endogenous agonists at P2 receptors, there are very few endogenous antagonists (table 3.2). The first synthetic P2 receptor antagonists developed were moderately potent and non-selective: suramin, reactive blue 2 (RB2), pyridoxalphosphate-6-azophenyl-2',4'-disulfonic acid (PPADS) and isopyridoxalphosphate-6-azophenyl-2',4'-disulfonic acid (isoPPADS). Suramin antagonises most P2XR at micromolar concentrations except the P2X7R which requires higher concentrations (Jacobson, 2018). PPADs is a non-competitive pan-antagonist, it is slow to antagonise and reverse. It has low sensitivity for P2X7R and is insensitive at the P2X4R (Jacobson and Müller, 2016). The use of these compounds in the most part has been replaced by selective antagonists.

Most specific P2R antagonists are synthesised to have a nucleotide-structure. Nearly all compete with the endogenous agonist to bind reversibly at the orthosteric site at their target P2 receptor (Jacobson, 2018). P2X1R antagonists are structural derivatives of the pan-antagonist suramin, of these NF 449 has the highest potency (Kassack *et al.*, 2004). The P2X2R antagonist NF770 is similarly a suramin derivative, whilst PSB-1011 is a structural derivative of RB2. Several P2X3R antagonists have been derived from the antibiotic trimethoprim, acting at allosteric binding sites on the receptor (Jacobson and Müller, 2016). Notably the P2X3R has an endogenous antagonist spinorphrin. Spinorphrin is a non-classical opioid that like the P2X3R and P2X1/3R is highly localised in the spinal cord, mitigating the effects of the receptor in neuropathic pain (1.3.3.3 P2X3 receptor; Jung *et al.*, 2007). Common P2X4R

antagonists include: PSB-12054, BX-430 and 5-BDBD. PSB 1204 is the most potent P2X₄R antagonist, it displays 30 to 50-fold selectivity for this receptor over other P2X_R subtypes. PSB 1204 binds at an allosteric site at the P2X₄R. 5-BDBD is a benzodiazepine derivative and BX-430 is a urea-derivative that binds at an allosteric site. 5-BDBD and BX-430 are both moderately potent at the P2X₄R (Jacobson and Müller, 2016). Several P2X₇R antagonists have been developed that bind either at the orthosteric or allosteric site. P2X₇R antagonists binding at the orthosteric site are: (i) ATP derivatives e.g. oATP; (ii) suramin or suramin-derivatives; (iii) tetrazole derivatives e.g. A438079 or (iv) cyanoguanidine derivatives e.g. A740003. Tetrazole and cyanoguanidine derivatives have the highest potency and selectivity for the P2X₇R (Savio *et al.*, 2018). P2X₇R antagonists binding at the allosteric site include: BBG, KN-62 and AZ-10606120. Some of the antagonists acting at the allosteric site at the P2X₇R also act at allosteric sites of other P2X receptors e.g. BBG also antagonises P2X₁R and P2X₄R (Savio *et al.*, 2018).

Selective P2Y₁R antagonists are broadly: (i) nucleotide derivatives e.g. MRS 2179 or (ii) urea derivatives e.g. 1-(2-(2-(tert-butyl)phenoxy)pyridin-3-yl)-3-(4-(trifluoromethoxy)phenyl)urea (BPTU). MRS 2179 competitively binds at the P2Y₁R orthosteric site inducing structural modifications that prevent activation (Baurand and Gachet, 2003). Selective P2Y₂R antagonists are comparatively limited, AR-C1189251XX is a uracil-derivative that binds to the receptor with the greatest affinity (Jacobson and Müller, 2016). There are no selective antagonists for the P2Y₄R. Several UDP-derived synthetic antagonists act at the P2Y₆R, however of these MRS 2578 is the only selective antagonist. P2Y₁₁R antagonists NF 157 and NF 340 are suramin-derivatives. The P2Y₁₂R is the subject of intense research due to its role in platelet aggregation. Many P2Y₁₂R antagonists have been developed due to their therapeutic use as anti-platelet agents (*1.3.5 therapeutic potentials of purinergic agents in disease*). There are four classes of P2Y₁₂R antagonists: β,γ -dihalomethylene bridged 5'-triphosphate mimics (e.g. Cangrelor); uncharged nucleotide like derivatives (e.g. ticagrelor); sulfonated anthraquinone derivatives (e.g. PSB-0739) and uncharged

heterocycles (e.g. AZD 1283). The only selective antagonists at the P2Y₁₃R is MRS 211 and at the P2Y₁₄R is PPTN (Jacobson and Müller, 2016).

P2 Receptor	Agonist(s)	Antagonist(s)
P2X1R	BzATP > βγ-methylene-adenosine 5'-triphosphate (L-βγ-meATP) ≥ α,β-methylene ATP (α,β-meATP) = ATP = 2-Methylthioadenosine triphosphate (2-MeSATP) and p-aminophenylethylthio-ATP (PAPET-ATP)	2',3'-O-(2,4,6-Trinitrophenyl)-ATP (TNP-ATP), Diinosine pentaphosphate (IpsI) , NF023, NF449
P2X2R	ATP ≥ ATPyS ≥ 2-MeSATP >> α,β-meATP, α,β-difluoromethylene-ATP (β,γ-CF2ATP)	Suramin, RB2, NF770, isoPPADS, PSB-1011, NF778, aminoglycosides
P2X3R	BzATP > 2-MeSATP ≥ ATP ≥ α,β-meATP = diadenosine tetraphosphate (Ap₄A), PAPET-ATP	TNP-ATP, isoPPADS, A317491, NF110, RN-1838, spinorphrin, AF353
P2X4R	ATP > α,β-meATP, cytidine triphosphate (CTP), BzATP	PSB 12054, BX 430, TNP-ATP, BBG, paroxetine, 5-BDBD, carbon monoxide donor 2 (CORM 2), phenolphthalein
P2X5R	ATPyS, Ap₄A, guanosine-5'-triphosphate (GTP)	Suramin, PPADS, BBG
P2X6R	Does not function as homomultimer	
P2X7R	BzATP > ATP ≥ 2-MeSATP > α,β-meATP	KN62, KN04, MRS2427, BBG, oxidised ATP (o-ATP), decavanadate, A-804598, RN-6189, AZD-9056, AZ10606120, A740003, A-438079, GSK-1370319
P2Y ₁ R	MRS2365 > 2-Methylthioadenosine diphosphate trisodium (2-MeSADP) = adenosine pentaphosphate γ-boranophosphate (Ap₅γB) >> Adenosine 5'-(β-thio)-diphosphate (ADPβS) > ADP > 2-MeSATP = ATP	MRS2500 > MRS2279 > MRS2179, 2,2'-pyridylisatogen tosylate (PIT), Adenosine-3'-phosphate-5'-phosphosulfate (A3P5P)
P2Y ₂ R	MRS2500 > MRS2279 > MRS2179, PIT	AR-C1189251XX, AR-C126313 > suramin > RB2, PSB-716, MRS2576
P2Y ₄ R	MRS 4062, 2'-azido-dUTP > Uridine-5'-(γ-thio)-triphosphate (UTPyS), UTP ≥ ATP ≥ Ap₄A, uridine adenosine tetraphosphate (Up₄U)	ATP > RB2 > suramin, MRS2577, PPADS
P2Y ₆ R	MRS2693 > uridine 5'-O-thiodiphosphate (UDPβS), PSB-0474 > INS48823, Up₃U >> UDP > UTP >> ATP, α,β-meUDP	MRS2578 > RB2, PPADS, MRS2567, MRS2575

Table 3.2: P2 Receptors Agonists and Antagonists (page 1 of 2)

Common natural (blue) and synthetic (red) agonists and antagonists at the P2 receptors.

P2 Receptor	Agonist(s)	Antagonist(s)
P2Y ₁₁ R	ATPyS > AR-C67085MX > BzATP ≥ ATP, NF546, Nicotinamide adenine dinucleotide (NAD ⁺), nicotinic acid adenine dinucleotide phosphate (NAADP)	NF157 > suramin > RB2, Adenosine 5'-O-thiomonophosphate (5'-AMPS), NF340
P2Y ₁₂ R	2-MeSADP ≥ ADP > ATP, ADPβS	PSB 0739, Ticagrelor, AR-C69931MX > AZD6140, INS50589 > RB2 > 2-Methylthio-AMP triethylammonium (2-MeSAMP), AR-C66096, CT50547, PSB-0413, carba-nucleosides, MRS2395, AR-C67085
P2Y ₁₃ R	ADP = 2-MeSADP > 2-MeSATP, ATP	AR-C69931MX > AR-C67085 > MRS2211, 2-MeSAMP
P2Y ₁₄ R	MRS2690 > UDP > UDP-glucose ≥ UDP-galactose, UDP-glucosamine	PPTN hydrochloride

Table 3.2: P2 Receptors Agonists and Antagonists (page 2 of 2; adapted from: Jacobson and Müller, 2016; Burnstock, 2014; Barrett *et al.*, 2013 and Syed and Kennedy, 2011)

Common natural (blue) and synthetic (red) agonists and antagonists at the P2 receptors.

3.2 Results

3.2.1 P2 Receptor mRNA expression in MIO-M1 cells

To identify P2 receptor gene expression in MIO-M1 cells RT-qPCR to detect mRNA for all the P2 receptor subtypes was performed (2.4 Reverse transcription quantitative polymerase chain reaction).

MIO-M1 cells expressed mRNA for all P2 receptors except P2X1-3R, P2Y6R and P2Y11R (table 39).

P2-receptor	CT value ± SEM
<i>P2X1R</i>	Not detected
<i>P2X2R</i>	Not detected
<i>P2X3R</i>	Not detected
<i>P2X4R</i>	27.1 ± 0.3
<i>P2X5R</i>	34.0 ± 0.2
<i>P2X6R</i>	28.4 ± 0.3
<i>P2X7R</i>	29.1 ± 0.5
<i>P2Y1R</i>	28.6 ± 0.5
<i>P2Y2R</i>	29.7 ± 0.6
<i>P2Y4R</i>	30.6 ± 0.9
<i>P2Y6R</i>	Not detected
<i>P2Y11R</i>	Not detected
<i>P2Y12R</i>	30.3 ± 1.0
<i>P2Y13R</i>	31.4 ± 1.2
<i>P2Y14R</i>	31.3 ± 0.9

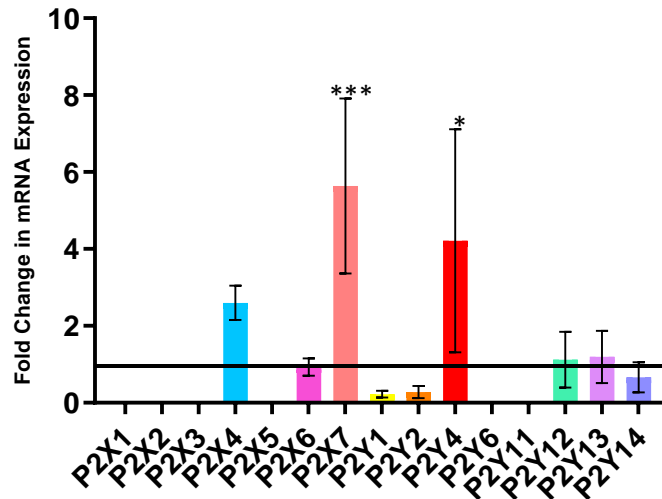
Table 3.3: P2 receptor mRNA expression in MIO-M1 cells (n=3)

RT-qPCR to detect mRNA for all the P2 receptor subtypes in MIO-M1 cells was performed. mRNA was detected for *P2X4-7R*, *P2Y1R*, *P2Y2R*, *P2Y4R* and *P2Y12-14R*. No mRNA was detected for *P2X1-3R*, *P2Y6R* and *P2Y11R*. Data is mean ± SEM.

3.2.2 P2 receptor mRNA expression in MIO-M1 cells relative to primary human retinal tissue

P2 receptor expression varies across human retinal cells (*1.3.4 Purinergic signalling in the retina*). In order to compare the expression of the P2 receptor profile in MIO-M1 cells to human retinal tissue, RT-qPCR to detect mRNA for all P2 receptor subtypes was also performed on homogenised retinal tissue (*2.2 Enzymatic Dissociation of Human Retinal Tissue and 2.4 Reverse transcription quantitative polymerase chain reaction*).

MIO-M1 cells had enriched mRNA expression of *P2X4R*, *P2X7R* and *P2Y4R* relative to human retinal tissue. Enriched expression of *P2X7R* and *P2Y4R* in MIO-M1 cells was statistically significant compared with primary human retinal tissue (graph 3.1).



Graph 3.1: Fold change expression of P2 receptors on MIO-M1 cells relative to primary human retina (n=3)

RT-qPCR to detect mRNA for all the P2 receptor subtypes in MIO-M1 cells and human retinal tissue was performed. Shown is the fold change in Ct value for each P2 receptor subtype in MIO-M1 cells over human retinal tissue. MIO-M1 cells had an enriched expression of *P2X7R* and *P2Y4R* which was statistically significant (*). Data is mean \pm SEM. Statistical analysis with two-way ANOVA Bonferroni's post-hoc.

3.2.3 P2 receptor calcium responses in MIO-M1 cells

MIO-M1 cells were shown to express mRNA for *P2X4-7*, *P2Y1*, *P2Y2*, *P2Y4*, *P2Y12*, *P2Y13* and *P2Y14* receptors (3.2.1 *P2 Receptor mRNA expression in MIO-M1 cells*). Calcium microfluorimetry was performed to determine if these receptors were functional.

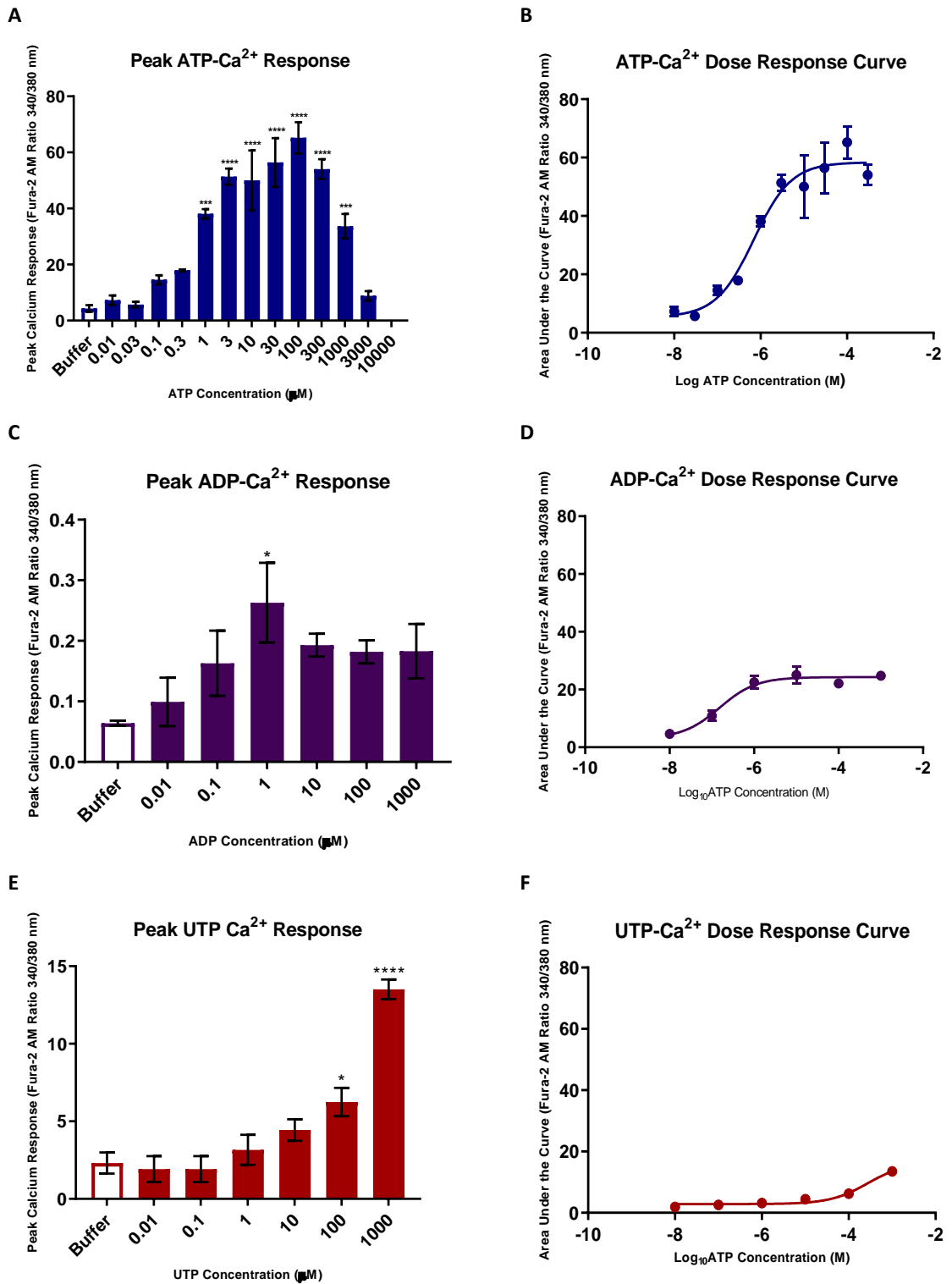
P2 receptors were stimulated with non-specific agonists and receptor-specific agonists to see if a calcium response could be generated. Pan-antagonists and receptor-specific antagonists were used to see if these calcium responses could be inhibited. Utilising agonist and antagonist combinations, functional evidence for individual P2 receptors was obtained.

MIO-M1 cells were pre-treated with selective purinergic antagonists PSB 12054, 5-BDBD, BX 430 (all *P2X4R*), AZ10606120, A740003 (both *P2X7R*), MRS 2179 (*P2Y1R*), AR-C118925XX (*P2Y2R*), PSB 0739 (*P2Y12R*), MRS2211 (*P2Y13R*) and PPTN (*P2Y14R*) at

10 μ M. Pre-treatment with the pan-antagonist suramin was also used to inhibit the P2Y₄R (2.3 *Agonists and Antagonists* and table 3.2).

Purinergic agonists ATP (0.01-10,000 μ M; P2X₄R, P2X₇R, P2Y₂R and P2Y₁₁R), ADP (0.01-1000 μ M; P2Y₁R, P2Y₁₂R and P2Y₁₃R), UTP (0.01-1000 μ M; P2Y₂R and P2Y₄R), UDP (0.01-1000 μ M; P2Y₆R) and UDP-glucose (0.01-1000 μ M; P2Y₁₄R) were applied to MIO-M1 cells and the intracellular calcium response measured. Specific synthetic purinergic agonist BzATP (10-3000 μ M; P2X₄R and P2X₇R) and was used to elicit responses from specific P2 receptors.

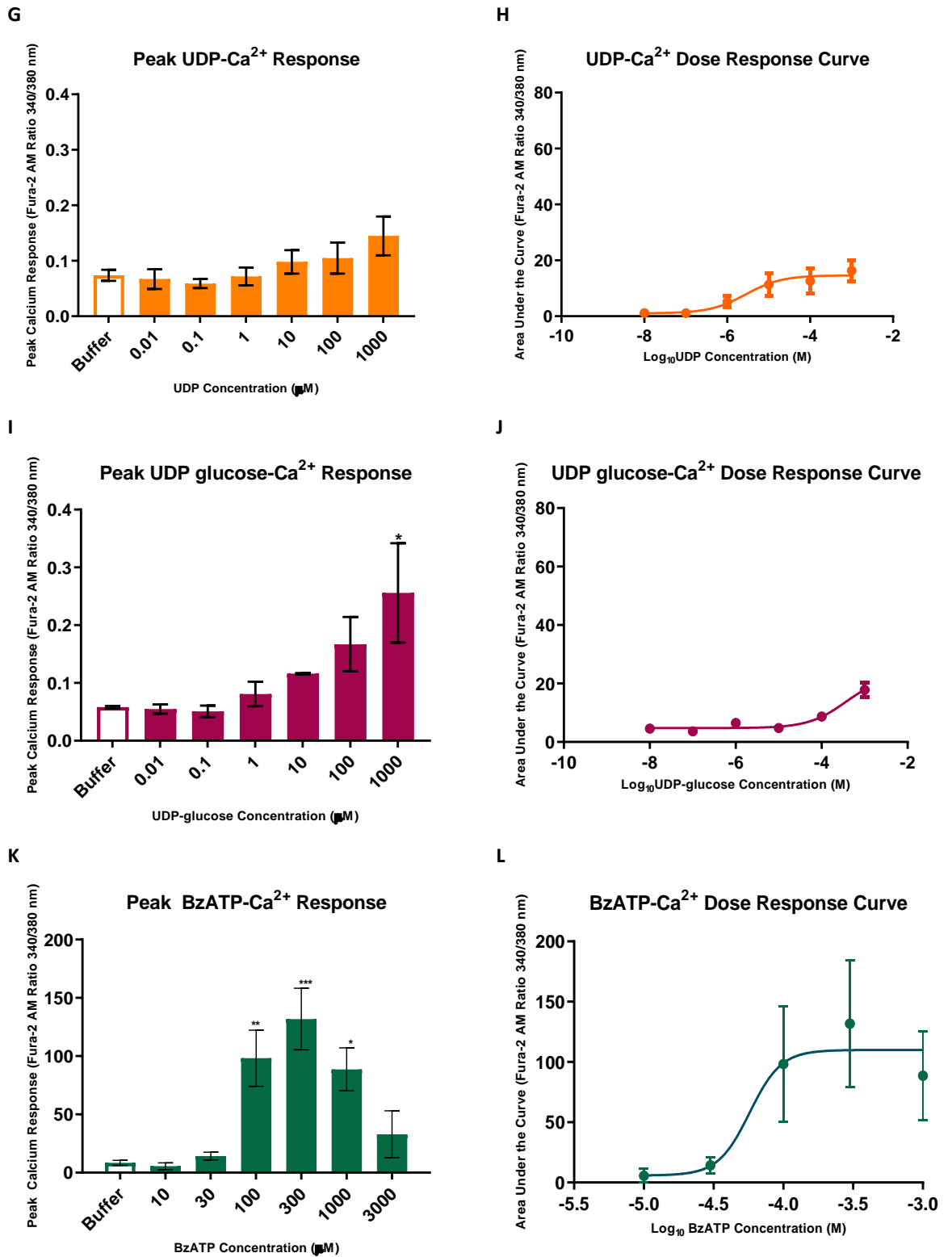
In MIO-M1 cells ATP-Ca²⁺ response was maximal at ATP 100 μ M, with EC₅₀ 0.7 μ M (graph 3.2A & B). ADP induced a maximal response at 1 μ M, with EC₅₀ 0.2 μ M (graph 3.2 B & C); UTP had a maximal response at 1000 μ M, with EC₅₀ 274.7 μ M (graph 3.2 D & E); UDP had a maximal response at 1000 μ M, with EC₅₀ 2.8 μ M (graph 3.2 F & G) and UDP-glucose had a maximal response at 1000 μ M, with EC₅₀ 361.7 μ M (graph 3.2 H & I). Of the natural P2 receptor ligands ADP was the most potent agonist at MIO-M1 cells. Synthetic agonist BzATP induced a maximal response at 300 μ M, with an EC₅₀ 57.3 μ M (graph 3.2 K & L).



KEY:

■ ATP ■ ADP ■ UTP

Graph 3.2: Purinergic agonist induced Ca²⁺ response in MIO-M1 cells (n=4; page 1 of 3)



KEY:

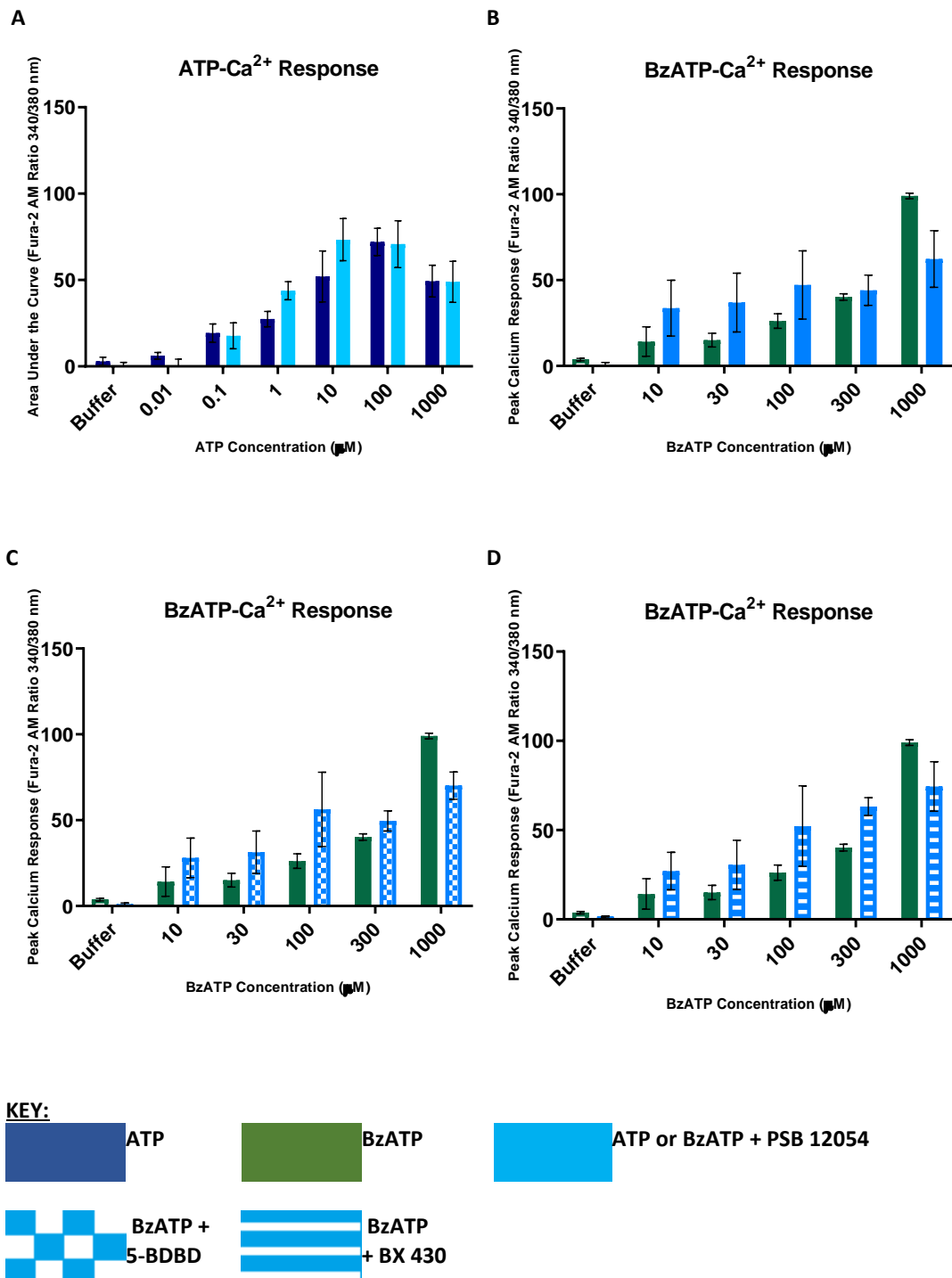
UDP
 UDPG
 BzATP

Graph 3.2: Purinergic agonist induced Ca²⁺ response in MIO-M1 cells (n=4; page 2 of 3)

Graph 3.2: Purinergic agonist induced Ca²⁺ response in MIO-M1 cells (n=4; page 3 of 3)

Endogenous purinergic agonists (ATP 0.01-10,000 μ M, dark blue; ADP 0.01-1000 μ M, dark purple; UTP 0.01-1000 μ M, dark red; UDP 0.01-1000 μ M, brown and UDP-glucose 0.01-1000 μ M, dark pink) and synthetic purinergic agonist (BzATP 10-3000 μ M, dark green) were applied to MIO-M1 cells and the intracellular calcium concentration was measured by calcium microfluorimetry (fura-2 AM ratio 340/380nm). Data is illustrated as: **(A, C, E, G, I and K)** peak calcium response at each purinergic agonist concentration; **(B, D, F, H, J and L)** dose response curve of purinergic agonist concentration (x) and area under the curve calcium response (0-300s; y). There is a dose-dependent relationship with increasing purinergic agonist concentration causing increased intracellular calcium concentration: ATP induces a maximal response at 100 μ M **(A)** and the EC₅₀ 0.7 μ M (95% CI: 0.3-1.4 μ M, **B**); ADP induces a maximal response at 10 μ M **(C)** and the EC₅₀ 0.2 μ M (95% CI: 0.1-0.4 μ M, **D**); UTP induces a maximal response at 1000 μ M **(E)** and the EC₅₀ 274.7 μ M (95% CI: 92.9-812 μ M, **F**); UDP induces a maximal response at 1000 μ M **(G)** and the EC₅₀ 2.8M (95% CI: 0.2-28.1 μ M, **H**); UDP-glucose induces a maximal response at 1000 μ M **(I)** and the EC₅₀ 361.7 μ M (95% CI: 75.3-1736 μ M, **J**) and BzATP induces a maximal response at 300 μ M **(K)** and the EC₅₀ is 57.3 μ M (95% CI: 6.1-538 μ M, **L**). **(A-L)** baseline fluorescence was recorded for 30s prior to purinergic agonist stimulation and then subtracted from the raw data. Data is expressed as mean \pm SEM. **(A, C, E, G, I and K)** statistical significance (P<0.05) calculated by one-way ANOVA and Dunnett's post-hoc (*). **(B, D, F, H, J and L)** statistical analysis with non-linear regression analysis.

The different receptor subtypes were then investigated in more detail. Since there was no expression of *P2X1-3*, the first to be investigated was *P2X4*. ATP and BzATP were used as agonists for the *P2X4R*. ATP induced calcium response in MIO-M1 cells was not inhibited by 10 μ M PSB 12054 (*P2X4R* antagonist; graph 3.3 A). Similarly, BzATP induced calcium response in MIO-M1 cells was not inhibited by 10 μ M PSB 12054, 5BDBD or BX 430 (all *P2X4R* antagonists; graph 3.3 B, C and D respectively).



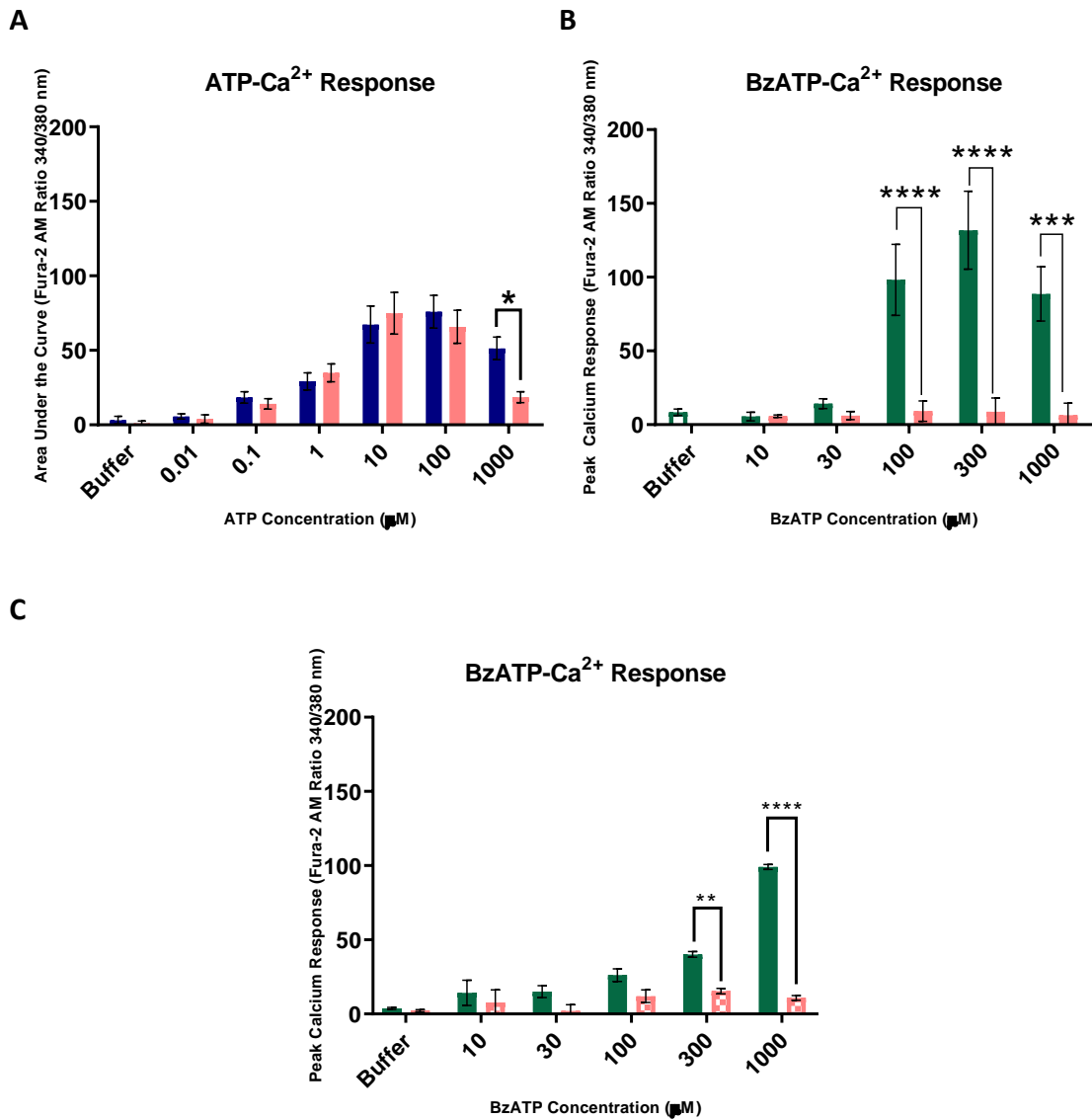
Graph 3.3: Purinergic agonist induced Ca^{2+} response in MIO-M1 cells pre-incubated with P2X4R antagonists (n=4; page 1 of 2)

Purinergic agonists (ATP 0.01-100 μ M, dark blue; BzATP 10-3000 μ M, dark green) were applied to MIO-M1 cells that were either untreated or pre-treated with 10 μ M P2X4R antagonist (PSB 12054, turquoise; 5-BDBD, turquoise check or BX 430, turquoise stripe) and the intracellular calcium concentration was measured by calcium microfluorimetry (fura-2 AM ratio 340/380nm). Data is illustrated as: (A) area under the curve calcium response (0-300s; y) and (B - D) peak calcium response at each purinergic agonist concentration.

Graph 3.3: Purinergic agonist induced Ca²⁺ response in MIO-M1 cells pre-incubated with P2X4R antagonists (n=4; page 2 of 2)

ATP or BzATP induced calcium responses in MIO-M1 cells that were not inhibited by any of the P2X4R antagonists used. Baseline fluorescence was recorded for 30s prior to purinergic agonist stimulation and then subtracted from the raw data. Data is expressed as mean \pm SEM. Statistical significance ($P < 0.05$) calculated by two-way ANOVA Bonferroni's post-hoc (*).

P2X5R and P2X6R calcium microfluorimetry experiments were not performed due to respectively, the lack of a selective antagonist and the receptor not functioning as a homomultimer. The next receptor investigated for functional expression via calcium microfluorimetry imaging was the P2X7R. ATP and BzATP were used as agonists at the P2X7R. Only the highest concentration of ATP (1000 μ M) induced a calcium response that was significantly antagonised by 10 μ M AZ10606120 (P2X7R antagonist; graph 3.4 A). At all concentrations of BzATP (10-1000 μ M) calcium responses were fully antagonised with 10 μ M AZ10606120 and A438079 (P2X7R antagonists; graph 3.4 B and C respectively): this antagonism was insurmountable even at highest BzATP concentrations.



KEY:



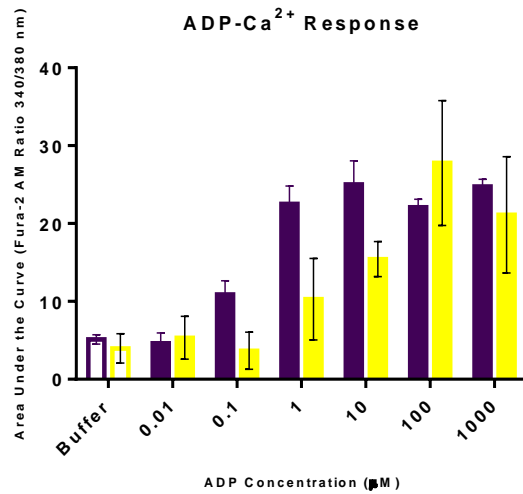
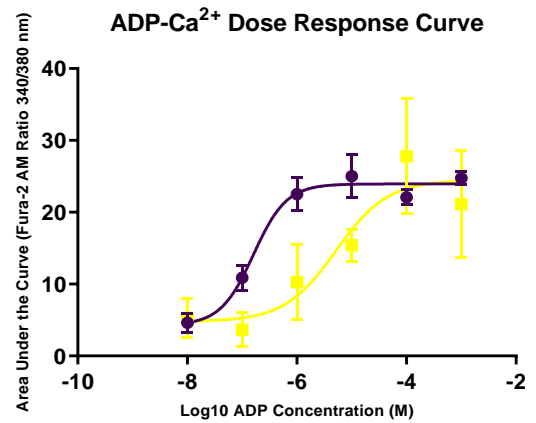
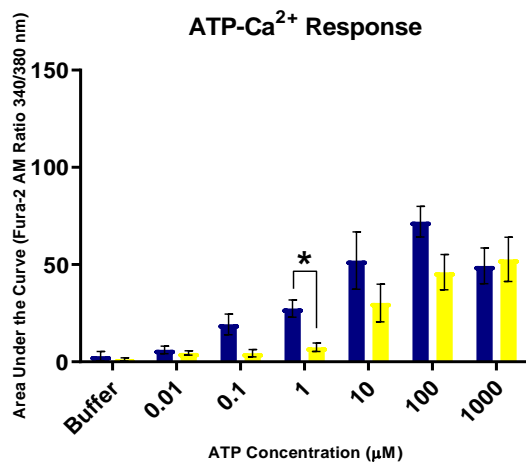
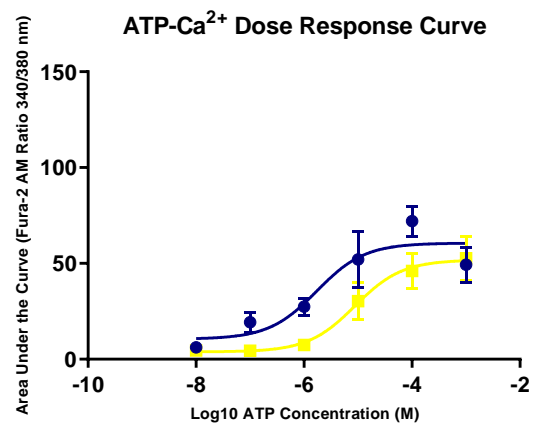
Graph 3.4: Purinergic agonist induced Ca²⁺ response in MIO-M1 cells pre-incubated P2X7R antagonists (n=4, page 1 of 2)

Purinergic agonists (ATP 0.01-1000μM, dark blue; BzATP 10-1000μM, dark green) were applied to MIO-M1 cells that were either untreated or pre-treated with 10μM P2X7R antagonist (AZ10606120, pink or A438079, pink check) and the intracellular calcium concentration was measured by calcium microfluorimetry (fura-2 AM ratio 340/380nm). Data is illustrated as: **(A)** area under the curve calcium response (0-300s; y) and **(B & C)** peak calcium response at each purinergic agonist concentration. **(A)** there was no antagonism of the calcium response with AZ10606120 at lower concentrations of ATP (0.01-100μM), however there was significant antagonism at the highest concentration of ATP (1000μM). **(B & C)** by contrast all concentrations of BzATP were antagonised by AZ10606120 and A438079, but this was only significant for higher concentrations of BzATP (100-1000μM) where there was a greater calcium response.

Graph 3.4: Purinergic agonist induced Ca²⁺ response in MIO-M1 cells pre-incubated P2X7R antagonists (n=4, page 1 of 2)

Baseline fluorescence was recorded for 30s prior to purinergic agonist stimulation and then subtracted from the raw data. Data is expressed as mean \pm SEM. Statistical significance ($P < 0.05$) calculated by two-way ANOVA Bonferroni's post-hoc (*).

ADP and ATP were used as agonists at the P2Y₁R. ADP, the preferential agonist at the P2Y₁R (3.1. *introduction*) was antagonised by 10 μ M MRS 2179 (P2Y₁R antagonist) with a clear shift of the dose response curve to the right (graph 3.5 B). Similarly, ATP was partially antagonised by 10 μ M MRS 2170 with the dose response curve also shifted to the right (graph 3.5 D), antagonism was significant at 1 μ M ATP.

A**B****C****D****KEY:**

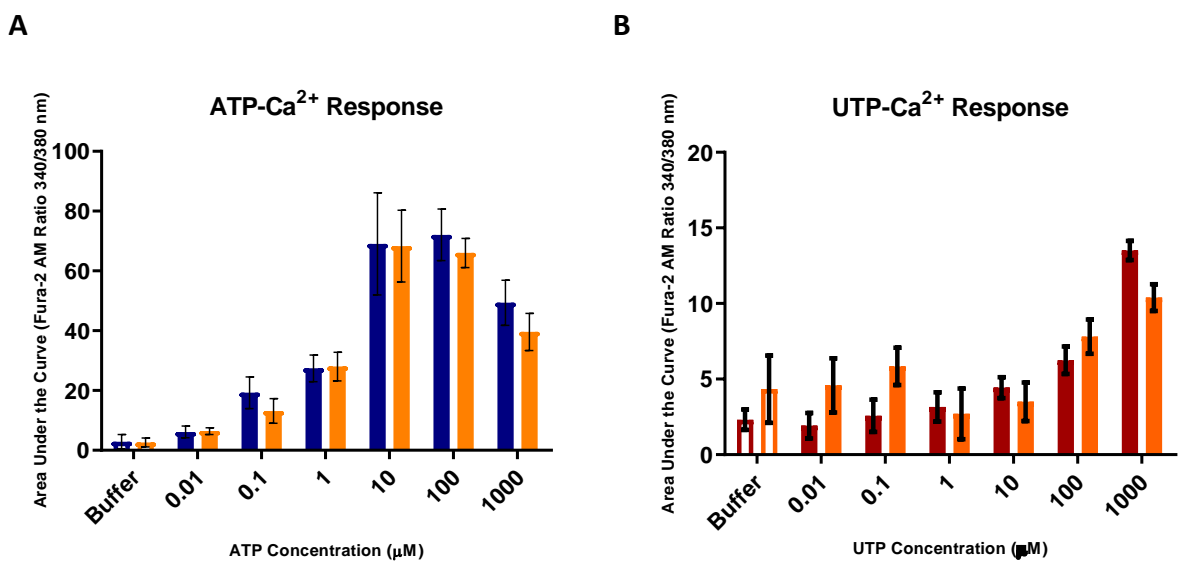
Graph 3.5: Purinergic agonist induced Ca²⁺ response in MIO-M1 cells pre-incubated with MRS 2170 (P2Y₁R antagonist; n=4, page 1 of 2)

Purinergic agonists (ADP 0.01-1000µM, purple; ATP 0.01-1000µM, dark blue) were applied to MIO-M1 cells that were either untreated or pre-treated with 10µM MRS 2179 (P2Y₁R antagonist, yellow) and the intracellular calcium concentration was measured by calcium microfluorimetry (fura-2 AM ratio 340/380nm). Data is illustrated as: (A and C) area under the curve calcium response (0-300s) at each purinergic agonist concentration; (B and D) dose response curve of purinergic agonist concentration (x) and area under the curve calcium response (0-300s; y). (A & B) ADP seemed to be partially antagonised by MRS 2179 with the dose response curve shifting to the right, however this was not statistically significant. (C & D) ATP was partially antagonised by MRS 2170 with the dose response curve shifted to the right, antagonism was significant at 1µM ATP. (A-D)

Graph 3.5: Purinergic agonist induced Ca²⁺ response in MIO-M1 cells pre-incubated with MRS 2170 (P2Y₁R antagonist; n=4, page 2 of 2)

Baseline fluorescence was recorded for 30s prior to purinergic agonist stimulation and then subtracted from the raw data. Data is expressed as mean ± SEM. (A and C) statistical significance (P<0.05) calculated by two-way ANOVA Bonferroni's post-hoc (*). (B and D) statistical analysis with non-linear regression analysis.

ATP and UTP were used as agonists at the P2Y₂R. ATP or UTP induced calcium response in MIO-M1 cells was not inhibited by 10μM AR-C118925XX (P2Y₂R antagonist; graph 3.6 A and B).



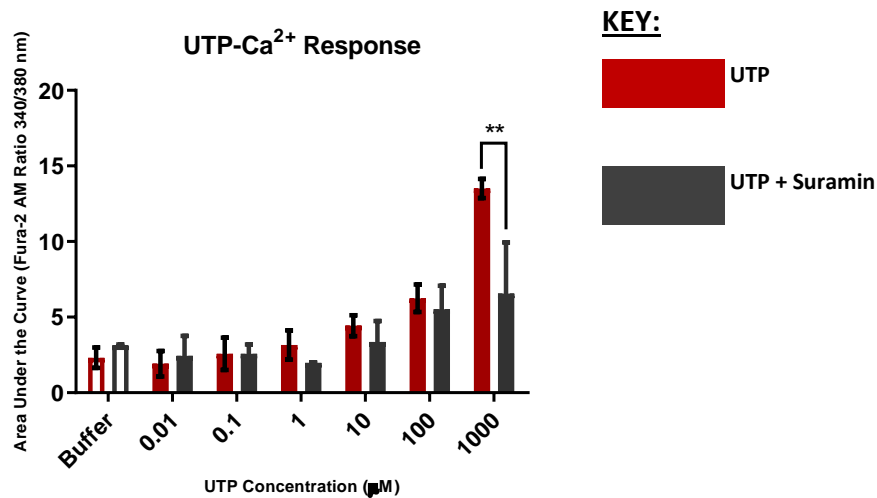
KEY:

■ UTP ■ ATP ■ UTP or ATP + AR-C118925XX

Graph 3.6: Purinergic agonist induced Ca²⁺ response in MIO-M1 cells pre-incubated with AR-C118925XX (P2Y₂R antagonist; n=4)

Purinergic agonists (UTP 0.01-1000μM, dark red; ATP 0.01-1000μM, dark blue) were applied to MIO-M1 cells that were either untreated or pre-treated with 10μM AR-C118925XX (P2Y₂R antagonist; orange) and the intracellular calcium concentration was measured by calcium microfluorimetry (fura-2 AM ratio 340/380nm). Data is illustrated as area under the curve calcium response (0-300s). ATP or UTP induced calcium response in MIO-M1 cells was not inhibited by AR-C118925XX. Baseline fluorescence was recorded for 30s prior to purinergic agonist stimulation and then subtracted from the raw data. Data is expressed as mean ± SEM. Statistical significance (P<0.05) calculated by two-way ANOVA Bonferroni's post-hoc (*).

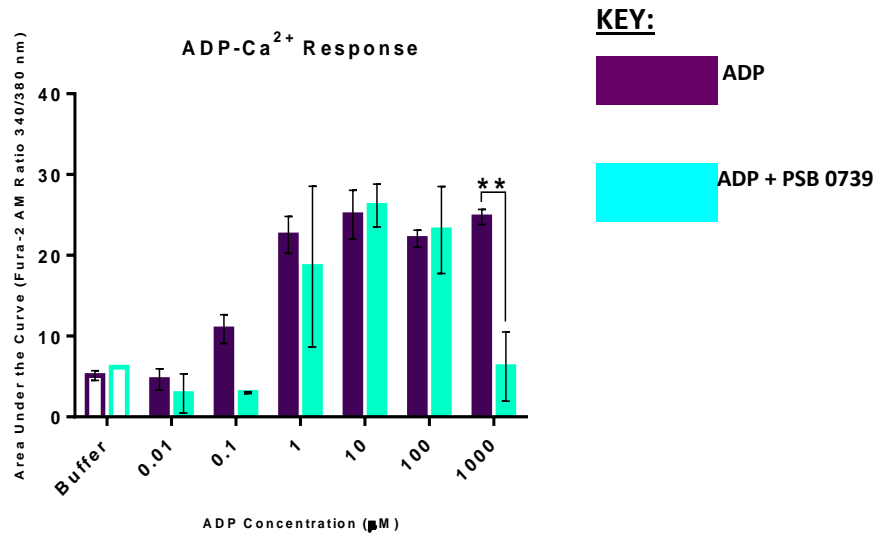
UTP was used as an agonist at the P2Y₄R. UTP 1000μM was significantly antagonised by 10μM Suramin (pan-antagonist; graph 3.7).



Graph 3.7: UTP induced Ca²⁺ response in MIO-M1 cells pre-incubated with suramin (pan-antagonist; n=4)

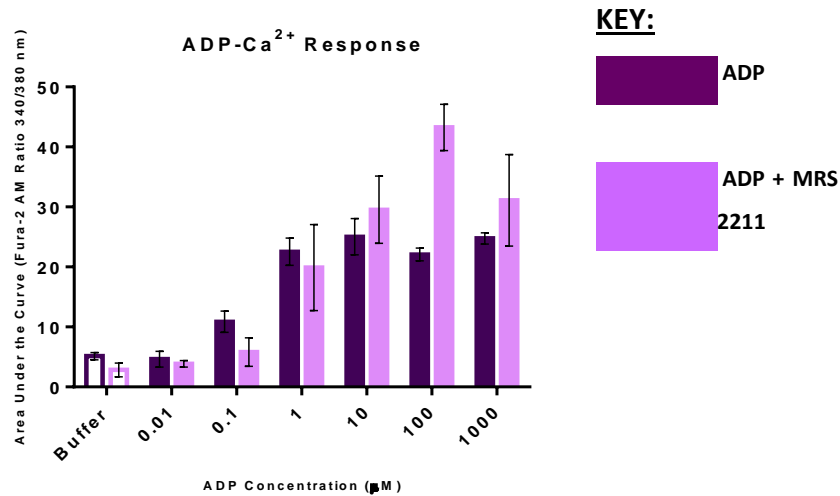
UTP (0.01-1000μM, dark red) was applied to MIO-M1 cells that were either untreated or pre-treated with 10μM suramin (pan-antagonist used as a P2Y₄R antagonist, grey) and the intracellular calcium concentration was measured by calcium microfluorimetry (fura-2 AM ratio 340/380nm). Data is illustrated as area under the curve calcium response (0-300s). UTP 1000μM was significantly antagonised by suramin. Baseline fluorescence was recorded for 30s prior to UTP stimulation and then subtracted from the raw data. Data is expressed as mean ± SEM. Statistical significance (P<0.05) calculated by two-way ANOVA Bonferroni's post-hoc (*).

ADP was used as an agonist at the P2Y₁₂R. ADP 1000μM was significantly inhibited by 10μM PSB 0739 (P2Y₁₂R antagonist; graph 3.8).



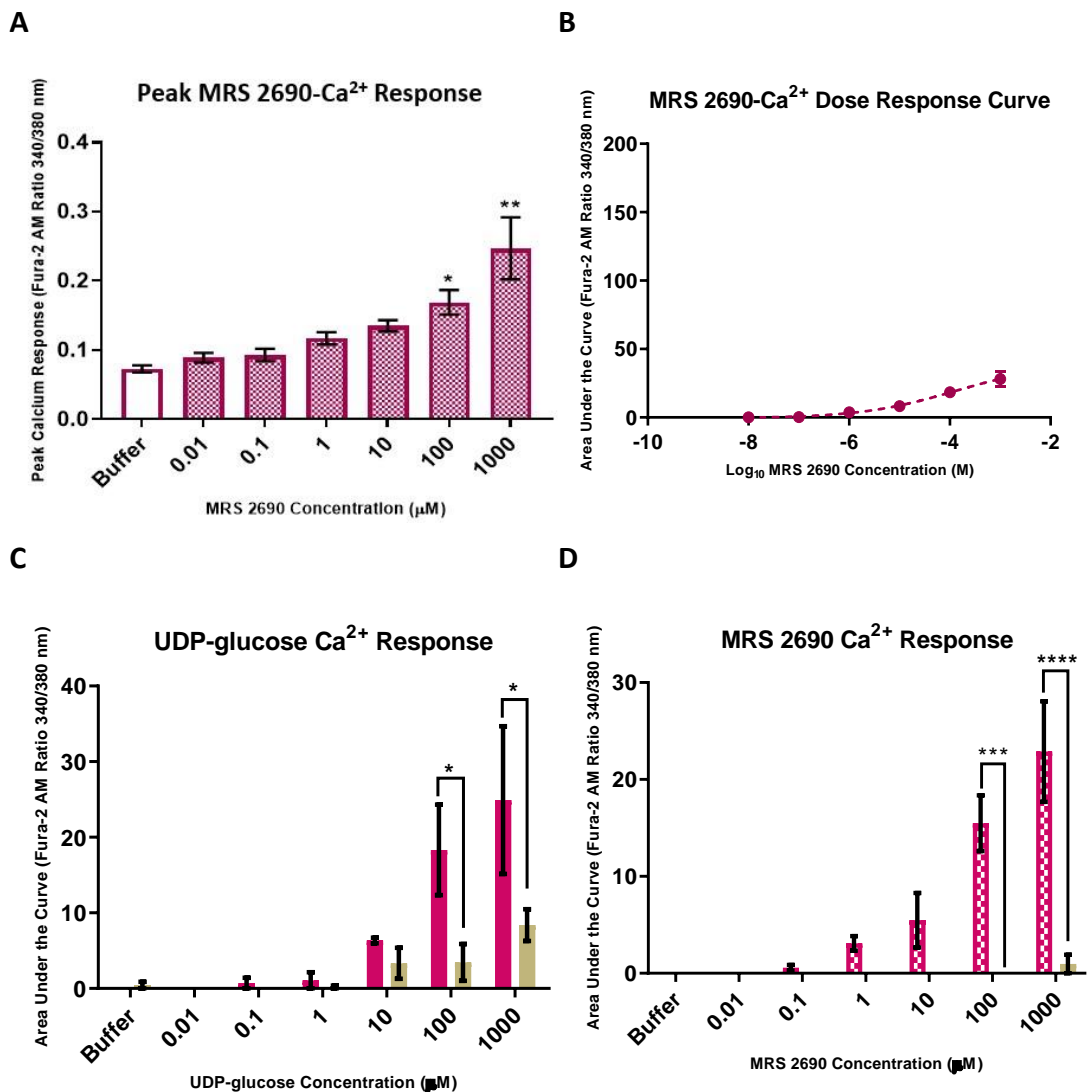
Graph 3.8: ADP induced Ca²⁺ response in MIO-M1 cells pre-incubated with PSB 0739 (P2Y₁₂R; n=4)
 ADP (0.01-1000μM, purple) was applied to MIO-M1 cells that were either untreated or pre-treated with 10μM PSB 0739 (P2Y₁₂R antagonist, turquoise), and the intracellular calcium concentration was measured by calcium microfluorimetry (fura-2 AM ratio 340/380nm). Data is illustrated as area under the curve calcium response (0-300s). ADP 1000μM induced calcium response in MIO-M1 cells was significantly inhibited by PSB 0739. Baseline fluorescence was recorded for 30s prior to ADP stimulation and then subtracted from the raw data. Data is expressed as mean ± SEM. Statistical significance (P<0.05) calculated by two-way ANOVA Bonferroni's post-hoc (*).

ADP was used as an agonist at the P2Y₁₃R. ADP induced calcium response in MIO-M1 cells was not antagonised by 10µM MRS 2211 (P2Y₁₃R antagonist; graph 3.9).

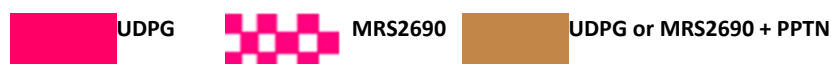


Graph 3.9: ADP induced Ca²⁺ response in MIO-M1 cells pre-incubated with MRS 2211 (P2Y₁₃R; n=4)
 ADP (0.01-1000µM, purple) was applied to MIO-M1 cells that were either untreated or pre-treated with 10µM MRS 2211 (P2Y₁₃R antagonist, lilac) and the intracellular calcium concentration was measured by calcium microfluorimetry (fura-2 AM ratio 340/380nm). Data is illustrated as area under the curve calcium response (0-300s). ADP induced calcium response was not antagonised by MRS 2211. Baseline fluorescence was recorded for 30s prior to ADP stimulation and then subtracted from the raw data. Data is expressed as mean ± SEM. Statistical significance (P<0.05) calculated by two-way ANOVA Bonferroni's post-hoc (*).

Synthetic agonist MRS2690 (0.01-1000 μ M; P2Y₁₄R) was used to elicit a response from P2Y₁₄Rs, there is a dose-dependent relationship with increasing MRS2690 concentration causing increased intracellular calcium concentration. MRS2690 had a maximal response at 1000 μ M, with an EC₅₀ 124 μ M (graph 3.10 A & B). UDP-glucose and MRS 2690 calcium responses were significantly inhibited by PPTN (P2Y₁₄R antagonist; graph 3.10 C & D).



KEY:



Graph 3.10: Purinergic agonist induced Ca²⁺ response in MIO-M1 cells pre-incubated with PPTN (P2Y₁₄R antagonist; n=4, page 1 of 2)

Graph 3.10: Purinergic agonist induced Ca²⁺ response in MIO-M1 cells pre-incubated with PPTN (P2Y₁₄R antagonist; n=4, page 2 of 2)

Purinergic agonists (UDP-glucose 0.01-1000µM, pink; MRS 2690 0.001-10 µM, pink pattern) were applied to MIO-M1 cells that were either untreated or pre-treated with 10µM PPTN (P2Y₁₄R antagonist, brown) and the intracellular calcium concentration was measured by calcium microfluorimetry (fura-2 AM ratio 340/380nm). Data is illustrated as: **(A)** peak calcium response; **(B)** dose response curve and **(C & D)** area under the curve calcium response (90-300s) at each purinergic agonist concentration. MRS 2690 induces a maximal response at 1000µM **(A)** and the EC₅₀ 124µM (95% CI: 0.5-2932µM, **B**). UDP-glucose and MRS 2690 induced calcium responses were significantly inhibited by PPTN. Baseline fluorescence was recorded for 30s prior to purinergic agonist stimulation and then subtracted from the raw data. Data is expressed as mean ± SEM. Statistical significance (P<0.05) calculated by: **(A)** one-way ANOVA and Dunnett's post-hoc (*); **(B)** statistical analysis with non-linear regression analysis and **(C & D)** two-way ANOVA Bonferroni's post-hoc (*)

3.3 Discussion

3.3.1 P2X7, P2Y₁, P2Y₄, P2Y₁₂ and P2Y₁₄ are functional receptors on human Müller cells.

PCR results show mRNA evidence for *P2X4R*, *P2X5R*, *P2X6R*, *P2X7R*, *P2Y1R*, *P2Y2R*, *P2Y4R*, *P2Y12R*, *P2Y13R* and *P2Y14R*. PCR results show no mRNA evidence for *P2X1R*, *P2X2R*, *P2X3R*, *P2Y6R* and *P2Y11R* (table 3.3). There is no published evidence of PCR experiments to detect *PX1-6R* mRNA in any species of Müller cell, so presented here is evidence for the first time that *P2X1-3R* mRNA are not present and *P2X4-6R* mRNA are present in the human Müller cell. Evidence for *P2X7R* and *P2Y1-4R* confirms what has already been detected in human and rat species by other groups (table 3.1; Fries *et al.*, 2005 and 2004 and Pannicke *et al.*, 2000). Conversely, presented research provides contradictory evidence for *P2Y6R* mRNA which is not present in the MIO-M1 model of human Müller cells but previously detected by another group in human and rat Müller cells (Fries *et al.*, 2005 and 2004). It is important to appreciate that this difference may be attributable to: (i) differences in receptor expression in the MIO-M1 cell immortalised cell line model (Carter and Shieh, 2010) (ii) a non-functioning protein produced by a splice variant and (iii) receptor internalisation (Li *et al.*, 2018). There is no published evidence of PCR experiments to detect *P2Y11-14R* mRNA in any species of Müller cell, so presented here is evidence for the first time

that *P2Y11* mRNA is not present and *P2Y12-14R* mRNA are present in the human Müller cell. Comparative to human retinal tissue, levels of *P2X4R*, *P2X7R* and *P2Y4R* mRNA are relatively enriched, *P2X4R* and *P2X7R* significantly so (discussed further in *3.3.2 P2X7R and P2Y4R are enriched in human Müller cells compared with human retina*).

Calcium microfluorimetry showed evidence for functioning *P2X7R* (graph 3.4), *P2Y₁R* (graph 3.5) and *P2Y₁₄R* (graph 3.10). Pannicke *et al.*, in 2000 also performed calcium imaging experiments demonstrating evidence of a functioning *P2X7R* in human Müller cells (figure 1.22). As previously discussed, the *P2X7R* has well determined roles in inflammation, cell-death and the pathophysiology of glaucoma (*1.2.5.1 Pathophysiology of glaucoma and purinergic signalling* and *1.3.3.7 P2X7 receptor*) and the next chapters aim to investigate these in more detail. Calcium imaging demonstrating a functioning *P2Y₁R* in rat (Fries *et al.*, 2004 and Wurm *et al.*, in 2009) and human (Fries *et al.*, 2005) Müller cells have previously been performed by other groups. Previous experiments by these groups have shown that the *P2Y₁R* mediates the bulk of the purinergic calcium response in Müller cells. Evidence presented as part of this thesis corroborates the same, ADP was the most potent endogenous P2-receptor agonist suggesting *P2Y₁R* could be the dominant receptor in these cells (*3.3.3 ADP is the most potent endogenous P2-receptor agonist at human Müller cells*). The ATP evoked calcium response also seemed to act predominantly via *P2Y₁R*. Presented for the first-time is strong evidence for a functioning *P2Y₁₄R* in the human retina (*3.3.7 Endogenous agonist UDP-glucose and the synthetic agonist MRS 2690 activate the P2Y₁₄R in human Müller cells*). Selective *P2Y₁₄R* agonists and antagonists have only recently become available perhaps accounting for the lack of publications on its presence and role in the human retina. The *P2Y₁₄R* modulates leucocyte function causing release of pro-inflammatory cytokines such as IL-8 (Sesma *et al.*, 2012 and Gao *et al.*, 2013).

There was some suggestive evidence for functioning P2Y₄R (graph 3.7) and P2Y₁₂R (graph 3.8). Functional evidence for P2Y₄R was limited due to a lack of commercially available selective agonists or antagonists (discussed further in 3.3.6 *UTP may activate P2Y₄Rs in human Müller cells*). Functional evidence for P2Y₁₂R was not in keeping with what has previously been described for this receptor: ADP activates the P2Y₁₂R at micromolar concentrations (Tozaki-Saitoh *et al.*, 2017) however, as part of this research it was only inhibited by PSB 0739 (P2Y₁₂R antagonist) at millimolar concentrations. It is the first time P2Y₁₂R has been detected in human Müller cells and its role on these cells is yet to be determined. In other retinal glial cells the P2Y₁₂R is involved in immune functions by interacting with leukocytes causing production and release of cytokines (Tozaki-Saitoh *et al.*, 2017 and Cattaneo, 2015).

There was no evidence for functioning P2X₄R (graph 3.3), P2Y₂R (graph 3.6) and P2Y₁₃R (graph 3.9). Despite *P2X₄R* mRNA expression and enrichment on human Müller cells, there was no functional evidence since ATP and BzATP evoked Ca²⁺ responses were not inhibited when tested with three specific P2X₄R antagonists. Similarly, although there was mRNA evidence for *P2Y₂R* the UTP evoked Ca²⁺ response was not inhibited by specific P2Y₂R antagonist suggesting this receptor does not play a prominent role in these cells.

Calcium microfluorimetry experiments were not performed for P2X₅R and P2X₆R. Although there was mRNA evidence for these receptors P2X₅R has no specific agonist or antagonist and therefore could not be distinguished in calcium imaging experiments. P2X₆R does not function as a homomer and also could not be distinguished in calcium imaging experiments.

The above research contributes to our understanding of the functional P2-receptor profile in the human Müller cell, it does not identify where each P2-receptor subtype is localised. In future immunohistochemistry experiments could be performed to

identify this. Additionally, the only functional data that can be inferred is the intracellular Ca^{2+} concentration, however this is sufficient for characterising a functional receptor profile in a cell line.

3.3.2 P2X7R and P2Y4R are enriched in human Müller cells compared with human retina

mRNA expression of *P2X7R* and *P2Y4R* are more highly expressed in Müller cells relative to retinal tissue. Ca^{2+} imaging data previously described indicates that these receptors are functional in Müller cells. P2X7Rs are already known to be more highly expressed in glial cells. P2X7R functions include acting as a 'danger sensor' and IL-1 β maturation and release (1.3.3.7 *P2X7 receptor*): any evidence of these roles of the P2X7R in human Müller cells will be investigated as part of this research.

3.3.3 ADP is the most potent endogenous P2-receptor agonist at human Müller cells.

All the endogenous ligands (ATP, ADP, UTP, UDP and UDP-glucose) induced dose-dependent increases in intracellular calcium in human Müller cells. The rank potency was ADP>ATP>UTP>UDP>UDP-glucose. Adenine agonists (ATP and ADP) produced sigmoid shape dose-response curves, whilst the uracil agonists (UTP, UDP and UDP-glucose) did not reach a maximum response at the concentrations used.

The above research describes purinergic agonist potency in relation to intracellular Ca^{2+} concentration in human Müller cells. Purinergic agonist potency for other downstream effects e.g. interleukin production may not directly correlate with this. Furthermore, *in vivo* endogenous nucleotides are short-lived and are rapidly enzymatically degraded (1.3.2 *Mechanisms of nucleotide release and breakdown*) so that the intracellular Ca^{2+} responses are more promiscuous than those elicited *in vitro*.

3.3.4 ATP activates P2Y₁Rs and with higher concentrations also activating P2X7Rs in human Müller cells.

The above results (graph 3.5) show that some of the ATP-Ca²⁺ response in Müller cells was attributable to activation of P2Y₁Rs (table 3.3 and graph 3.6). There was no evidence P2X1-4 receptors contributed to the ATP-Ca²⁺ response (table 3.3 and graph 3.3). P2X5R and P2X6R contribution to the ATP-Ca²⁺ response could not be assessed, there are no specific P2X5R agonists or antagonists and P2X6R does not form a homomeric receptor. At the highest concentration of ATP (1mM) the P2X7R was activated and contributed to the ATP-Ca²⁺ response (graph 3.4).

Wurm *et al.* in 2009 concluded that the P2Y₁R mediates the bulk of the ATP-Ca²⁺ response in Müller cells and that there is minimal contribution of other P2-receptor subtypes, confirmed as part of this thesis research using MIO-M1 cells. Corroboration of research findings between MIO-M1 cells and primary Müller cells helps validate MIO-M1 cells as a useful tool for researching P2-evoked Ca²⁺ responses. Müller cells exert their homeostatic functions via P2Y₁R, it enables them to: (i) maintain their cell volume and (ii) transfer ions and fluid from the extracellular space to the vitreous body and blood vessels (Reichenbach and Bringmann, 2013).

ATP activated the P2X7R at millimolar concentrations, this is consistent with what has already been published (Donnelly-Roberts *et al.*, 2009; Bianchi *et al.*, 1999 and Surprenant *et al.*, 1996). Endogenously, these represent ATP concentrations found in inflammation; this is consistent with the theory that the P2X7R acts as a danger sensor (Ferrari *et al.*, 2006). The role of the P2X7R in human Müller cells will be investigated later as part of this research.

3.3.5 ADP activates P2Y₁Rs and with higher concentrations also activating P2X12Rs in human Müller cells.

The ADP-Ca²⁺ response in Müller cells was attributable to activation of the P2Y₁R and at millimolar concentrations the P2Y₁₂R. There was no evidence P2Y₁₃Rs contributed to the ADP-Ca²⁺ response (graph 3.9). As mentioned previously this is the first evidence of functional P2Y₁₂Rs in human Müller cells (3.3.1 P2X7, P2Y₁, P2Y₄, P2Y₁₂

and P2Y₁₄ are functional receptors on human Müller cells), however typically micromolar concentrations of ADP activate P2Y₁₂Rs (Tozaki-Saitoh *et al.*, 2017).

3.3.6 UTP may activate P2Y₄Rs in human Müller cells.

It is difficult to decipher how much of the ATP and UTP response is attributable to the P2Y₄R as a selective antagonist for this receptor is not commercially available. There was significant antagonism with suramin (pan-antagonist) which is also antagonist at other P2YRs: P2Y₂R, P2Y₄R and P2Y₁₁R. Selective antagonist AR-C118925XX (P2Y₂R antagonist) did not distinguish any contribution of the P2Y₂R to the UTP-Ca²⁺ response (graph 3.6) and there was no mRNA evidence for the expression of the P2Y₁₁R. It is reasonable to assume that suramin therefore may have antagonised any P2Y₄R contribution to the UTP-Ca²⁺ response. UTP exhibits threshold dose-response curve, this is probably why antagonism was only significant at millimolar concentrations of UTP.

Purinergic signalling is a highly promiscuous system, with agonists activating many P2 receptors either directly or via enzymatic conversion to other nucleotide ligands. Early pan-antagonists also act at several P2 receptors and are likely to have some antagonistic action on other P2 receptors beyond what is reported. Taking these factors into consideration suramin antagonism of the UTP-Ca²⁺ response may not necessarily be due to antagonism of the P2Y₄R.

MRS 49062 is a selective agonist at the P2Y₄R, in future its use could provide confirmatory information on whether this receptor is functional in human Müller cells.

3.3.7 Endogenous agonist UDP-glucose and the synthetic agonist MRS 2690 activate the P2Y₁₄R in human Müller cells.

UDP-glucose and MRS 2690 induced Ca²⁺ responses only via the P2Y₁₄R in human Müller cells (graph 3.10). UDP activates P2Y₆R and P2Y₁₄R. Although UDP-glucose is specific for the P2Y₁₄R, UDP has greater affinity for the P2Y₁₄R than other receptors (table 3.2). UDP was not used in conjunction with PPTN (P2Y₁₄R antagonist) in this

research, so the extent of P2Y₁₄R contribution to the UDP-Ca²⁺ response in human Müller cells could not be determined. However, it is probable that the UDP-Ca²⁺ response is predominantly produced by P2Y₁₄R as there is no expression of P2Y₆R in human Müller cells.

3.3.8 The synthetic agonist BzATP induced calcium responses selectively via the P2X7R in human Müller cells.

BzATP induced Ca²⁺ responses only via the P2X7R in the human Müller cell. BzATP is also an agonist at P2X1R, P2X3R, P2X4R, P2Y₁₁R, also to a lesser degree on P2X2R and P2X6R (table 3.2). BzATP is unlikely to stimulate a Ca²⁺ response via other P2-receptors as the Ca²⁺ response was completely antagonised by P2X7R antagonists. BzATP is a selective P2X7R agonist in human Müller cells.

Pannicke *et al* in 2000 demonstrated functional evidence for the P2X7R on primary human Müller cells, however, this evidence was less definitive as the BzATP induced calcium response was antagonised by the non-selective antagonist suramin. Suramin also antagonises P2X1-3, P2X5, P2Y₁ and P2Y₄₋₁₂ receptors (table 3.2), therefore there was a small possibility that the calcium response was evoked by the P2X5R.

Chapter 4: P2X7R-mediated Interleukin mRNA Expression in Human Müller Cells

4.1 Introduction

The purpose of the research in this chapter was to determine if stimulation of the P2X7R in human Müller cells mediated cell-death and to determine any P2X7R-mediated expression of inflammatory mediators specifically IL-1R1, IL-1 α , IL-1 β and IL-10 in human Müller cells.

P2X7Rs in human Müller cells were initially demonstrated by Pannicke *et al* in 2000 (1.3.4.1 *Purinergic signalling and Müller cells* and figure 1.18). Additionally, as part of this research P2X7R were identified in MIO-M1 cells for the first time (table 3.3 and graph 3.4). Endogenously, high concentrations of ATP activate the P2X7R (Donnelly-Roberts *et al.*, 2009; Bianchi *et al.*, 1999 and Surprenant *et al.*, 1996). Similarly, high concentrations of ATP activate the P2X7Rs in human Müller cells (graph 3.4 and 3.3.4 *ATP activates P2Y₁Rs, with higher concentrations also activating P2X7Rs in human Müller cells*). Activation of the P2X7R is known to cause cytokine release in immunocompetent cells (1.3.3.7 *P2X7 receptor*; He *et al.*, 2017; Nie *et al.*, 2017; Ferrari *et al.*, 2000). The P2X7R acts via NLRP3 inflammasome-caspase-1 complex causing downstream IL-1 β (Giuliani *et al.*, 2017 and Choi *et al.*, 2014), IL-18 (Dinarello, 2007 and Choi *et al.*, 2014) and TNF α (Cieslak *et al.*, 2017) maturation or release. Additionally, this process can initiate pyroptotic inflammatory cell death (Olsen *et al.*, 2016).

Several groups have demonstrated P2X7R-mediated RGC death in the retina (Niyadurupola *et al.*, 2013; Hu *et al.*, 2010; Resta *et al.*, 2007; Zhang *et al.*, 2005). Our research group demonstrated P2X7R-mediated RGC death (figure 4.1; Niyadurupola *et al.*, 2013) was associated with upregulation of cytokines IL-1 β and IL-10 (Niyadurupola *et al.*, 2009) in a human retinal model. IL-1 β is a pro-inflammatory

cytokine (1.5.3.3 *IL-1 β*), whereas IL-10 is an anti-inflammatory cytokine (1.5.4 *IL-10*). IL-1 β exerts an effect via IL-1R1 (1.5.3.1 *Interleukin-1 receptor IL-1R*). Research from our group shows immunolocalisation of IL-1R1 mainly in the NFL and RGC layer, with some immunoreactivity also in the OPL & ONL (Niyadurupola *et al.*, 2009): Müller cells traverse all layers of the human retina and therefore may produce this pattern of immunoreactivity.

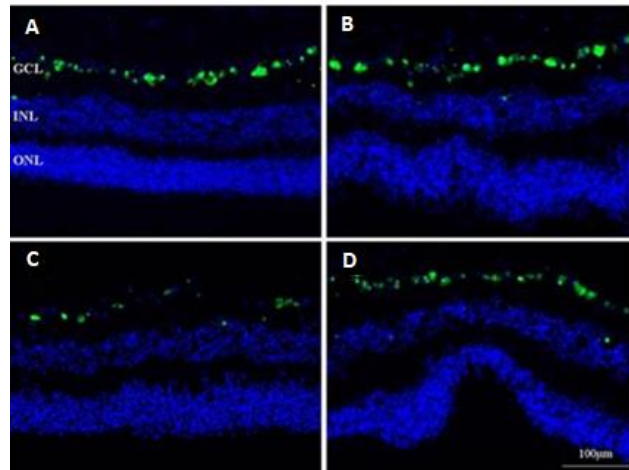


Figure 4.1: Immunohistochemistry showing P2X7R-mediated RGC loss in the HORC model (Niyadurupola *et al.*, 2013)

HORCs were treated in experimental conditions for 24h: (A) control; (B) BBG (1 μ M; P2X7R antagonist) control; (C) BzATP (100 μ M; P2X7R agonist) and (D) BBG and BzATP (1 μ M and 100 μ M respectively). RGCs (green) were immunolabeled with antibody to the RGC marker NeuN. GCL, INL and ONL (all blue) were immunolabeled with the nuclear stain DAPI.

4.2 Results

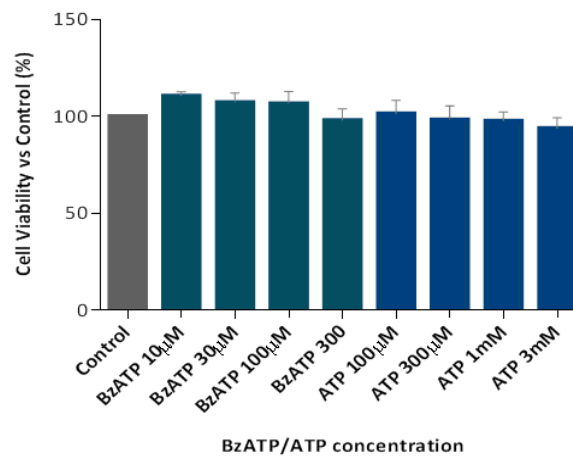
4.2.1 MIO-M1 cell viability and cell death in response to purinergic agonist and antagonist exposure

High concentrations of endogenous purinergic agonists have been shown to cause cell death (1.3.4.1 *Purinergic signalling and Müller cells*). MIO-M1 cell viability and death when stimulated with purinergic agonists was therefore investigated.

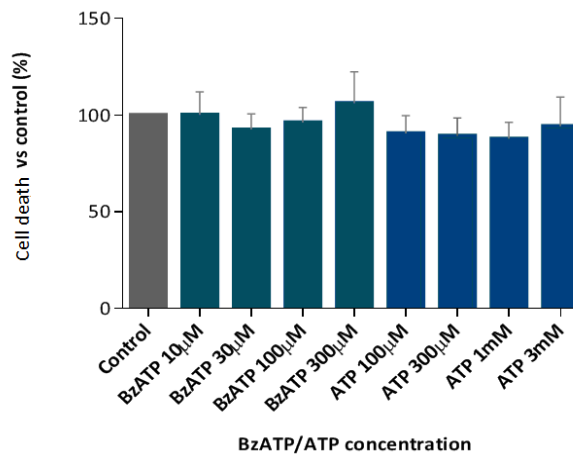
MIO-M1 cells were incubated in a range of ATP (100 μ M-3mM) and BzATP (10 μ M-300 μ M) concentrations for 24 hours. Prolonged stimulation with ATP and BzATP at

all concentrations showed no significant change in MIO-M1 cell viability or death when compared with control (graph 4.1).

A



B



Graph 4.1: A. Cell viability (n=8) and B. cell death (n=6) of MIO-M1 cells after exposure to BzATP (10 μ M-3mM) and ATP (100 μ M-3mM) for 24h.

Cell viability and cell death data were determined by MTS and LDH assays respectively. Data is mean \pm SEM.

4.2.2 IL-1 α , IL-1 β , IL-1R1 and IL-10 mRNA expression in MIO-M1 cells

IL-1 α , IL-1 β , IL-1R1 and IL-10 mRNA expression in MIO-M1 cells under resting conditions was determined (table 4.1) by RT-qPCR (2.4 *Reverse transcription quantitative polymerase chain reaction*). MIO-M1 cells were found to only express mRNA for IL-1R1 at resting conditions. There was no detectable expression of IL-1 α , IL-1 β and IL-10 mRNA at resting conditions.

Gene	Control mean C _t ± SEM
IL-1 α	Not detected
IL-1 β	Not detected
IL-1R1	28.4 ± 0.4
IL-10	Not detected

Table 4.1: IL-1 α , IL-1 β , IL-1R1 and IL-10 mRNA expression in MIO-M1 cells in resting or control conditions (n=4)

The data shown is the mean Ct value ± SEM. A Ct cut-off value of 35 was utilised.

4.2.3 P2X7R-mediated IL-1 α , IL-1 β , IL-1R1 and IL-10 mRNA expression in MIO-M1 cells

ATP (P2 agonist) or BzATP (P2X7R agonist) was applied to MIO-M1 cells that were untreated or pre-treated with 10 μ M AZ10606120 (P2X7R antagonist). ATP and BzATP were used at concentrations subthreshold and suprathreshold for P2X7R activation in MIO-M1 cells (table 4.2). Graph 3.4 demonstrated that ATP >1000 μ M and BzATP >100 μ M activates the P2X7R in MIO-M1 cells: considering this, ATP 300 μ M and BzATP 30 μ M were used as concentrations subthreshold for P2X7R activation and ATP 3000 μ M and BzATP 300 μ M were used as concentrations suprathreshold for P2X7R activation. Graph 4.1 shows that these ATP and BzATP concentrations are not toxic to MIO-M1 cells. Any subsequent changes in IL-1 α , IL-1 β and IL-10 mRNA were determined by RT-qPCR (2.4 Reverse transcription quantitative polymerase chain reaction) at the 3h time-point. Preliminary RT-qPCR time-course (72h) experiments investigating ATP (300 μ M) and BzATP (30 μ M) induced IL-1 β mRNA expression in MIO-M1 cells indicated that BzATP induced a small increase in IL-1 β mRNA expression at the 3h time-point and at no other time-points therefore this timepoint was selected for further experimentation.

	ATP concentration (μ M)	BzATP concentration (μ M)
Subthreshold for P2X7R activation in MIO-M1 cells	300	30
Suprathreshold for P2X7R activation in MIO-M1 cells	3000	300

Table 4.2: ATP and BzATP concentrations subthreshold and suprathreshold for P2X7R activation in MIO-M1 cells.

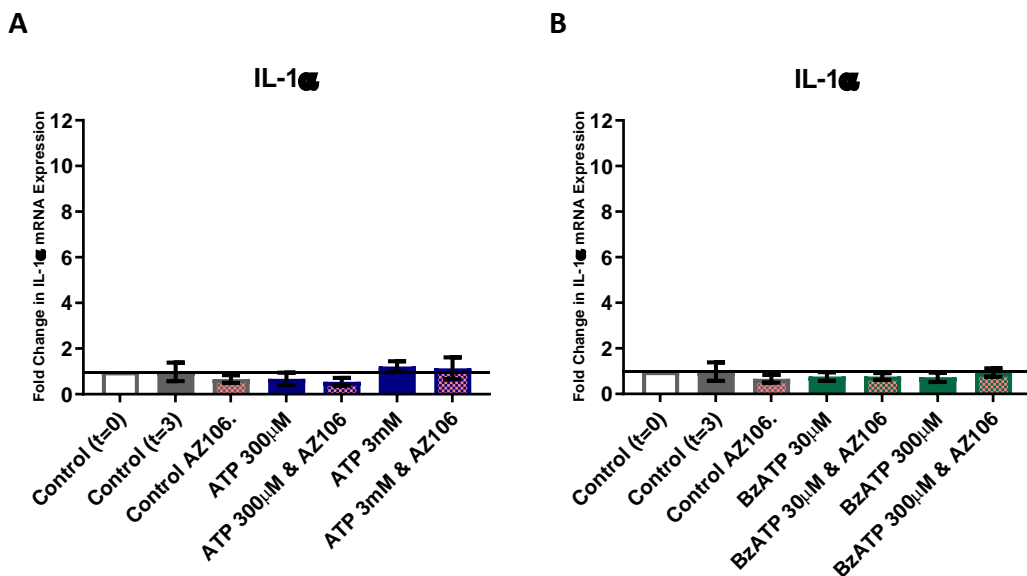
Previous experiments demonstrated that ATP >1000 μ M and BzATP >100 μ M activate the P2X7R in MIO-M1 cells: considering this agonist concentrations subthreshold (ATP 300 μ M and BzATP 30 μ M)

and suprathreshold (ATP 3000 μ M and BzATP 300 μ M) for P2X7R activation in MIO-M1 cells were selected.

4.2.3.1 P2X7R-mediated IL-1 α mRNA expression in MIO-M1 cells

P2X7R-mediated IL-1 α mRNA expression was determined using the experimental conditions described in *section 4.2.3* above.

ATP and BzATP stimulation of MIO-M1 cells did not induce any change in IL-1 α mRNA expression compared with t=0 or t=3 controls (graph 4.2). IL-1 α control (t=0) Ct value was 35.2 \pm 0.4 (n=4; mean \pm S.E.M).



KEY:

■ ATP ■ BzATP ■ AZ10606120

Graph 4.2: Fold change in IL-1 α mRNA expression in MIO-M1 cells stimulated with P2X7R agonists and antagonists (t=3h; n=4)

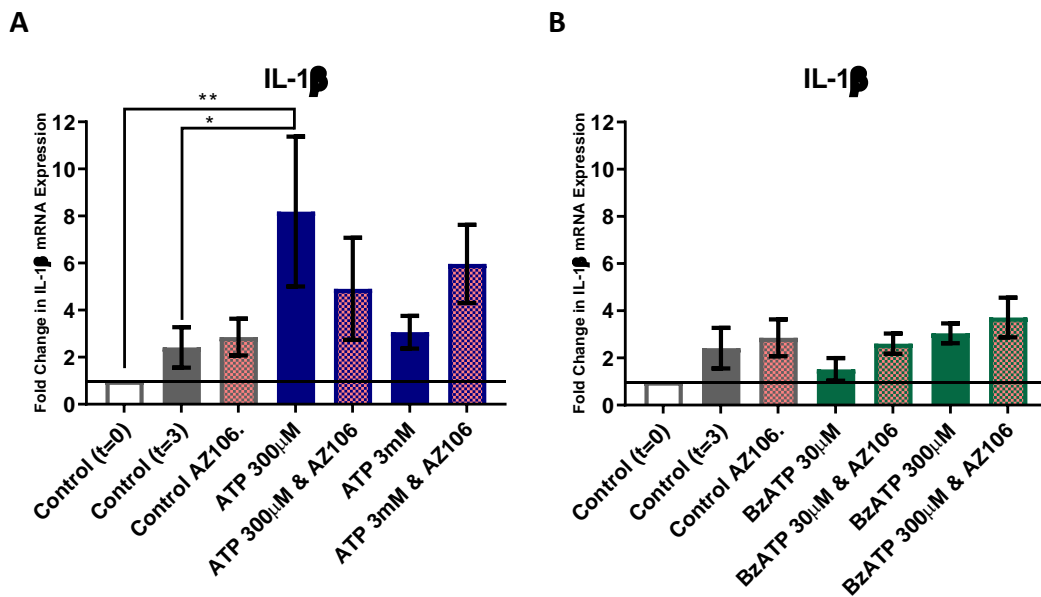
Purinergic agonists (A) ATP (300 μ M and 3000 μ M; blue) and (B) BzATP (30 μ M and 300 μ M; green) were applied to MIO-M1 cells that were either untreated or pre-treated with P2X7R antagonist AZ10606120 (10 μ M; pink). Data is illustrated as a fold-change compared to the t=0 hour control. ATP and BzATP stimulation of MIO-M1 cells did not induce any change in IL-1 α mRNA expression compared with t=0 or t=3 controls. IL-1 α control (t=0) Ct value was 35.2 \pm 0.4. Data is mean \pm SEM, statistical significance (P<0.05) calculated by a one-way ANOVA with Dunnett's post-hoc test (*).

4.2.3.2 P2X7R-mediated IL-1 β mRNA expression and protein release in MIO-M1 cells

P2X7R-mediated IL-1 β mRNA expression and protein release in MIO-M1 cells was investigated by RT-qPCR and ELISA (2.8 *Enzyme-linked immunosorbent assay*)

respectively. The same experimental conditions were used as those described in *section 4.2.3* above. ELISA was performed at 0h, 3h, 6h, 12h, 24h, 48h and 72h time-points.

ATP (300 μ M) stimulation of MIO-M1 cells induced a significant 8.2-fold increase in IL-1 β mRNA expression when compared to t=0 controls (graph 4.3 A). IL-1 β control (t=0) C_t value was 37.4 \pm 0.2 and IL-1 β ATP 300 μ M (t=3) C_t value was 34.4 \pm 0.3 (n=4; mean \pm S.E.M). The increase in IL-1 β expression was not significantly inhibited in MIO-M1 cells treated with AZ10606120 10 μ M. ATP at 3mM did not induce any changes in IL-1 β mRNA expression. BzATP stimulation of MIO-M1 cells did not induce any significant change in IL-1 β mRNA expression compared with t=0 or t=3 controls (graph 4.3 B).



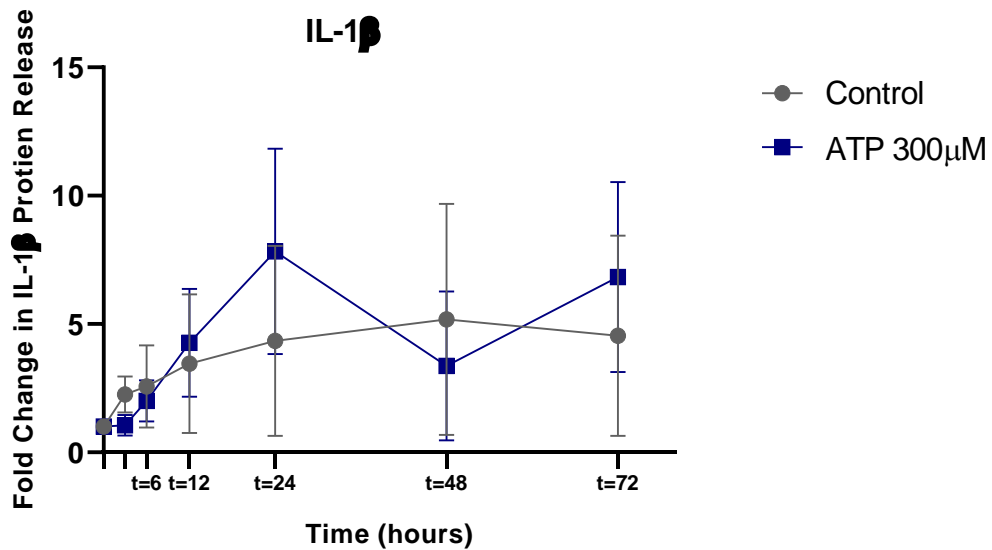
KEY:

ATP
 BzATP
 AZ10606120

Graph 4.3: Fold change in IL-1β mRNA expression in MIO-M1 cells stimulated with P2X7R agonists and antagonists (t=3h; n=4)

Purinergic agonists (A) ATP (300 μM and 3000 μM; blue) and (B) BzATP (30 μM and 300 μM; green) were applied to MIO-M1 cells that were either untreated or treated with P2X7R antagonist AZ10606120 (10 μM; pink). Data is illustrated as a fold-change compared to the t=0 hour control. ATP 300 μM stimulation of MIO-M1 cells induced a significant 8.2-fold increase in IL-1β mRNA expression when compared to t=0 (p=0.0061) controls. IL-1β control (t=0) Ct value was 37.4 ± 0.2 and IL-1β ATP 300 μM Ct value was 34.4 ± 0.3 (n=4; mean ± S.E.M). Data is mean ± SEM, statistical significance (P<0.05) calculated by a one-way ANOVA with Dunnett's post-hoc test (*).

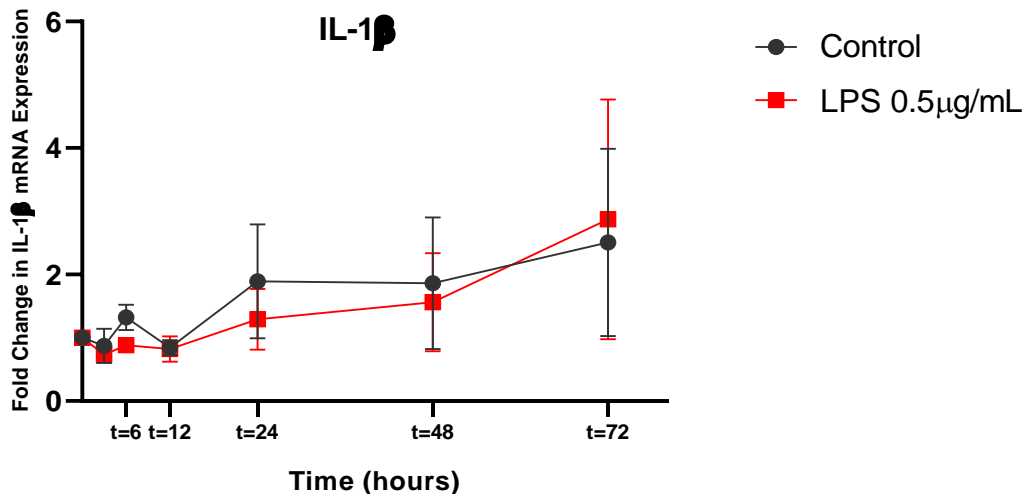
ATP 300 μM induced a significant increase in IL-1β mRNA expression (graph 4.3 A); therefore, ATP 300 μM was applied to MIO-M1 cells and IL-1β protein release was measured over 0-72h. ATP 300 μM stimulation of MIO-M1 cells did not induce any IL-1β protein release at any time-point (3-72h) when compared with t=0 control (graph 4.4).



Graph 4.4: Fold change in IL-1 β protein release in MIO-M1 cells stimulated with ATP 300 μ M (t=3h, 6h, 12h, 24h, 48h and 72h; n=4)

ATP 300 μ M was applied to MIO-M1 cells and any IL-1 β protein release was measured over time. Data is illustrated as a fold-change compared to the t=0 hour control. ATP 300 μ M stimulation of MIO-M1 cells did not induce release of IL-1 β protein. Data is mean \pm SEM, statistical significance ($P < 0.05$) calculated by a one-way ANOVA with Dunnett's post-hoc test (*).

LPS, a bacterial cell wall component, is capable of inducing IL-1 β mRNA and protein expression in several cell-types, ATP has been shown to then cause IL-1 β maturation and release via the P2X7R (Dinarello, 2009). The effect of LPS on IL-1 β expression was therefore investigated, in order to determine whether these pathways were present in MIO-M1 cells. LPS 0.5 μ g/mL was applied to MIO-M1 cells and IL-1 β mRNA expression was measured over 0-72h. LPS stimulation of MIO-M1 cells did not induce any change in IL-1 β mRNA expression at any time-point (3-72h) when compared with t=0 control (graph 4.5). IL-1 β control (t=0) C_t value was 31.7 ± 0.5 (n=3; mean \pm S.E.M).



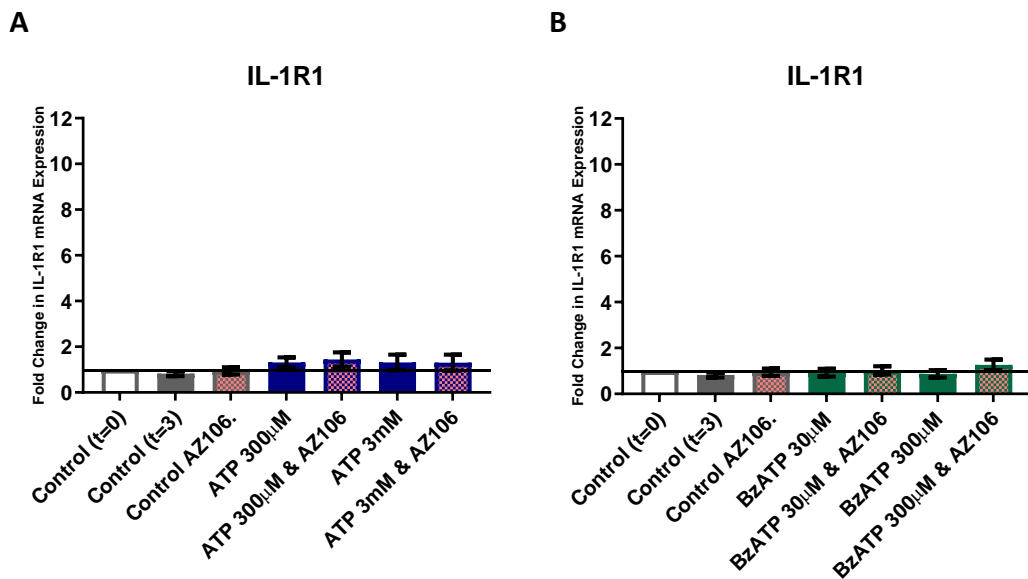
Graph 4.5: Fold change in IL-1β mRNA expression in MIO-M1 cells stimulated with LPS 0.5μg/mL (t=3h, 6h, 12h, 24h, 48h and 72h; n=3)

LPS 0.5μg/mL (dark orange) was applied to MIO-M1 and any IL-1β mRNA release was measured over time. Data is illustrated as a fold-change compared to the t=0 hour control. LPS stimulation of MIO-M1 cells did not induce any change in IL-1β mRNA expression when compared to t=0 control. IL-1β control (t=0) Ct value was 31.7 ± 0.5 . Data is mean \pm SEM, statistical significance ($P < 0.05$) calculated by a one-way ANOVA with Dunnett's post-hoc test (*).

4.2.3.3 P2X7R-mediated IL-1R1 mRNA expression in MIO-M1 cells

P2X7R-mediated IL-1R1 mRNA expression was determined using the experimental conditions described in *section 4.2.3* above.

ATP and BzATP stimulation of MIO-M1 cells did not induce any change in IL-1R1 mRNA expression compared with t=0 or t=3 controls (graph 4.6). IL-1R1 control (t=0) Ct value was 28.4 ± 0.4 (n=4; mean \pm S.E.M).



KEY:



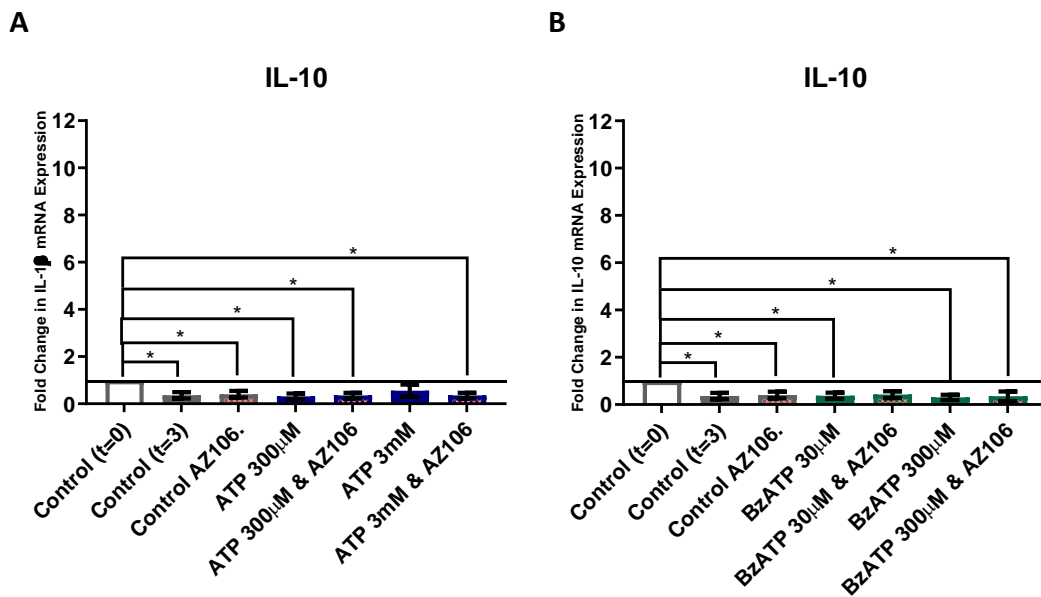
Graph 4.6: Fold change in IL-1R1 mRNA expression in MIO-M1 cells stimulated with P2X7R agonists and antagonists (t=3h; n=4)

Purinergic agonists (A) ATP (300 μ M and 3000 μ M; blue) and (B) BzATP (30 μ M and 300 μ M; green) were applied to MIO-M1 cells that were either untreated or pre-treated with P2X7R antagonist AZ10606120 (10 μ M; pink). Data is illustrated as a fold-change compared to the t=0 hour control. ATP and BzATP stimulation of MIO-M1 cells did not induce any change in IL-1R1 mRNA expression compared with t=0 or t=3 controls. IL-1R1 control (t=0) C_t value was 28.4 ± 0.4 . Data is mean \pm SEM, statistical significance ($P < 0.05$) calculated by a one-way ANOVA with Dunnett's post-hoc test (*).

4.2.3.4 P2X7R-mediated IL-10 mRNA expression in MIO-M1 cells

P2X7R-mediated IL-10 mRNA expression was determined using the experimental conditions described in *section 4.2.3* above.

ATP and BzATP stimulation of MIO-M1 cells did not induce any change in IL-10 mRNA expression compared with t=0 or t=3 controls. IL-10 mRNA expression decreased over time, with nearly all t=3 conditions significantly reduced compared to t=0 control (graph 4.7). IL-10 control (t=0) C_t value was 37.4 ± 1.1 (n=4; mean \pm S.E.M).



KEY:

ATP BzATP AZ10606120

Graph 4.7: Fold change in IL-10 mRNA expression in MIO-M1 cells stimulated with P2X7R agonists and antagonists (t=3h; n=4)

Purinergic agonists (A) ATP (300µM and 3000µM; blue) and (B) BzATP (30µM and 300µM; green) were applied to MIO-M1 cells that were either untreated or pre-treated with P2X7R antagonist AZ10606120 (10µM; pink). Data is illustrated as a fold-change compared to the t=0 hour control. ATP and BzATP stimulation of MIO-M1 cells did not induce any change in IL-10 mRNA expression compared with t=0 or t=3 controls. IL-10 mRNA expression decreased over time, with nearly all t=3 conditions significantly reduced compared to t=0 control. IL-10 control (t=0) Ct value was 37.4 ± 1.1 . Data is mean \pm SEM, statistical significance ($P < 0.05$) calculated by a one-way ANOVA with Dunnett's post-hoc test (*).

4.3 Discussion

4.3.1 Prolonged stimulation of the P2X7R does not cause cell death in human Müller cells.

BzATP is a potent and selective agonist of the P2X7R in human Müller cells (3.3.8 *The synthetic agonist BzATP induced calcium responses selectively via the P2X7R in human Müller cells*). Endogenously high concentrations of ATP are known to activate the P2X7R (Ferrari *et al.*, 2006), this has also been demonstrated above in human Müller cells (graph 3.3 and 3.3.4 *ATP activates P2Y₁Rs, with higher concentrations also activating P2X7Rs in human Müller cells*). ATP and BzATP were therefore used to investigate P2X7R-mediated cell death.

There was no evidence of P2X7R-mediated cell death of human Müller cells (graph 4.1). P2X7R-mediated cell death may not have occurred because: (i) prolonged activation of the P2X7R in human Müller cells does cause pore-formation and cell death or (ii) the immortalised cell line model used (MIO-M1) expresses a polymorphism of the P2X7R effecting receptor function (Tao *et al.*, 2017; Jiang *et al.*, 2013; Gartland *et al.*, 2012).

Pannicke *et al.*, in 2000 investigated BzATP stimulation of the P2X7R on primary human Müller cells: their dye-filling experiments showed no opening of membrane pores to allow fluorescent dyes to enter the cells faster than under control conditions. However, it is important to note that their evidence was equivocal as many of their control cells exhibited uptake of dye. It is known that some cell types expressing P2X7R are non-pore forming, possibly because they lack the intracellular machinery for this (Donnelly-Roberts and Jarvis 2007; North, 2002; Pelegrin and Surprenant, 2006).

Prolonged stimulation of the P2X7R does not cause Müller cell death, however it may contribute to the P2X7R associated RGC death previously described in our groups proposed pathogenesis of glaucoma (Niyadurupola *et al.*, 2013). Stimulation of the P2X7R in Müller cells may result in downstream processes which could contribute to the pathogenesis of glaucoma, these will be investigated further in the next two chapters.

4.3.2 Stimulation of the P2X7R in human Müller cells does not induce IL-1 α , IL-1 β or IL-10 mRNA expression

Previous work by our group showed that stimulation of the P2X7R in a human retinal model was associated with upregulation in IL-1 β and IL-10 mRNA expression with IL-1 β protein release. IL-10 protein release was not investigated (Niyadurupola *et al.*, 2009). The retinal cell type(s) involved in interleukin release were not identified, therefore Müller cell contribution to P2X7R-mediated interleukin release was investigated in the current research.

ATP 3000 μ M or BzATP 300 μ M were used to stimulate the P2X7R in human Müller cells, there was no subsequent upregulation of IL-1 α , IL-1 β or IL-10 mRNA expression. Furthermore, RT-qPCR Ct values obtained for these interleukins were high (Ct > 35.0), which is not considered reliable evidence of mRNA expression. At these levels it is difficult to reliably distinguish a real amplification signal from background signals so Ct values above 35 are commonly disregarded (ThermoFisher, 2015). However, any increase above this background as a result of treatment would be expected to be detected.

4.3.2 Human Müller cells may be a contributing source of IL-1 β in the retina via pathway(s) independent of the P2X7R

IL-1 β is implicated in several mechanisms of glaucoma pathogenesis (1.5.2 *Interleukins and glaucoma*). It is not produced in healthy physiological states as it is a potent pro-inflammatory cytokine (Madej *et al.*, 2017): similarly, table 4.1 shows it is not produced by human Müller cells in healthy physiological states.

Several PAMPs and DAMPs stimulate NLRP3 inflammasome assembly, this converts pro IL-1 β to mature IL-1 β (1.5.3.3 *IL-1 β* and figure 1.23). High millimolar concentrations of ATP act as a DAMP signal and activate the P2X7R; in some cell-types this initiates the process of mature IL-1 β synthesis and release (Giuliani *et al.*, 2017; Choi *et al.*, 2014; Sanz *et al.*, 2009; Di Virgilio *et al.*, 1998 and Pelegrin *et al.*, 2008). Results (graph 4.3) show that millimolar ATP stimulation of the P2X7R does not induce IL-1 β expression in human Müller cells. Similarly BzATP, a selective P2X7R agonist, did not induce IL-1 β expression in human Müller cells as it had in intact human retina (Niyadurupola 2009). If human Müller cells produce IL-1 β , translation and transcription appear to involve pathways independent of the P2X7R.

Interestingly, micromolar concentrations of ATP did induce a significant 8.2-fold increase in IL-1 β mRNA expression in the MIO-M1 cells (graph 4.3 A). At micromolar concentrations ATP is sub-threshold for P2X7R stimulation, so upregulation of mRNA is probably via a pathway independent of the P2X7R. The corresponding Ct value was

high (C_t 34.4 ± 0.3), but below the cut-off value ($C_t > 35.0$): therefore, although there was a significant up-regulation of IL-1 β mRNA there was low concentration of this in the sample. The same micromolar ATP stimulation of human Müller cells did not cause corresponding IL-1 β protein release. Considering this, it seems likely that human Müller cells are not the main contributor to the IL-1 β mRNA and protein expression seen in experimental models of glaucomatous eyes. Alternatively, it may be that certain additional stimuli are required to potentiate the upregulation of IL-1 β mRNA and protein release in the Muller cells.

It would have been interesting to determine whether there was P2X7R-mediated IL-1 β release in MIO-M1 cells. LPS is the most common PAMP used to upregulate IL-1 β mRNA (referred to as LPS-priming) ahead of P2X7R mediated release. However, LPS did not induce IL-1 β mRNA expression in MIO-M1 cells (graph 4.5) so release could not be investigated. LPS is a gram-negative bacterial cell wall component, a potent PAMP it activates TLR-4 inducing pro-IL-1 β in some cell-types (1.5.3.3 *IL-1 β* : Yao *et al.*, 2005 and Janeway, 2001). Functional TLR-4 has been characterised in human and murine Müller cells (Lin *et al.*, 2013; Kumar and Shamsuddin., 2012). Kumar and Shamsuddin demonstrated LPS stimulation of TLR-4 in human Müller cells (MIO/M1 model) induced IL-1 β mRNA upregulation (4h) and subsequent protein release (8h). However, Lin *et al.* found LPS stimulation of TLR-4 in murine Müller cells did not induce significant change in IL-1 β mRNA expression. A notable difference in experimental design was the concentration of LPS used; this research and Lin *et al.* stimulated cells at lower LPS concentrations (0.5 μ g/mL and 0.1 μ g/mL respectively) than Kumar and Shamsuddin (10 μ g/mL). Other research has shown that TLR-4 is activated by LPS at picomolar concentrations (Marshall, 2005) and is cytotoxic at doses ranging between 1 μ g/mL-200 μ g/mL depending on the cell-type (Sharifi *et al.*, 2010 and Vogel *et al.*, 1979). Considering this the induction of IL-1 β observed by Kumar and Shamsuddin may be related to LPS induced cytotoxicity rather than LPS activation of TLR-4.

4.3.2 Human Müller cells express IL-1R1

IL-1R1 mRNA was expressed by human Müller cells in resting conditions (table 4.1). IL-1R1 mRNA expression was unchanged by purinergic agonist stimulation of human Müller cells (graph 4.6). Our group has previously performed immunohistochemistry for IL-1R1 in human retinal tissue: the pattern of fluorescence was suggestive that these receptors are on the human Müller cell, although it was important to note that work to co-localise these with Müller cell markers was not performed.

Results in this chapter show that direct stimulation of the P2X7R in human Müller cells does not cause upregulation of IL-1 β and IL-10 mRNA expression or IL-1 β protein release. Our group previously demonstrated upregulation of these cytokines with stimulation of the P2X7R in human retinal tissue (Niyadurupola *et al.*, 2009) so it would appear that these observed changes are not simply due to actions on the Müller cells. However, there may be indirect pathways involving the Müller cells and these may involve the IL-1R1 receptors identified here on the Müller cells. The next chapter will specifically investigate IL-1 β -mediated IL-10 mRNA expression and protein release in human Müller cells.

Chapter 5: IL-1 β -mediated IL-10 mRNA expression and protein release in a human Müller cell model

5.1 Introduction

The purpose of the research presented in this chapter was to investigate the effect of IL-1 β on IL-10 expression in a human Müller cell model.

IL-1 β (1.5.3.3 *IL-1 β*) is a potent pro-inflammatory cytokine and as such it is not expressed by cells in healthy physiological conditions. Furthermore, IL-1 β synthesis and release are tightly regulated during pathological conditions (Dinarello, 1997). Of all the interleukins, IL-1 β is most frequently associated with glaucoma, with both neurodegenerative and neuroprotective effects (1.5.2 *Interleukins and glaucoma*).

IL-1 β is a ligand at two receptors from the IL-1R family: IL-1R1 and IL-1R2 (table 1.7; Dinarello *et al.*, 2018). IL-1R1 is an “activating receptor” containing a Toll/interleukin-1 receptor (TIR) homology domain in both of its subunits which are necessary for downstream signalling (Dinarello *et al.*, 1996). IL-1R2 is a “decoy receptor” lacking TIR-domains (Dinarello *et al.*, 1996). IL-1R1 contains TIR domains and IL-1 β -IL-1R1 binding initiates a downstream signalling cascade (*figure 5.1*). IL-1R2 does not contain TIR domains, subsequently IL-1 β -IL-1R2 binding does not initiate a downstream signalling cascade (*figure 5.1*; Yazdi and Ghoreschi, 2016; Boraschi and Tagliabue, 2013 and Dinarello, 1996). IL-1 β binding at IL-1R1 recruits the accessory chain IL-1R3: IL-1 β -IL-1R1-IL-1R3 signal transduction complex recruits MyD88 and IL-1 receptor-associated kinases (IRAK). MyD88 activates IRAK leading in turn to the recruitment and oligomerisation of tumour necrosis factor-associated factor 6 (TRAF6). TRAF6 and IRAKs form complexes with TGF- β -activated kinase 1 (TAK1) and TAK1-binding proteins (TAB1 and TAB2) initiating further stages of protein modifications. From here the intracellular signal can propagate via the: (i) MAPK pathway or the (ii) NF- κ B pathway. In the ‘MAPK pathway’ TAK1 activates the MAP

kinases: p38, JNK and extracellular signal-related kinases (ERK). Downstream from this pathway are transcription factors that modify mRNA production in the nucleus (Ozbabacan *et al.*, 2014 and Wojdasiewicz *et al.*, 2014). In the 'NF- κ B pathway' TAK1 activates the IKK kinase complex which comprises NF- κ B essential modulator (NEMO)-IKK1 (or IKK α)-IKK2 (or IKK β). The IKK kinase complex inactivates I κ B. The I κ B family are a group of inhibitory proteins that keep the NF- κ B family of transcription factors inactive and sequestered in the cell's cytoplasm. I κ B inactivation allows NF- κ B transcription factors p50, p52, p65, RelB and RelC to migrate to the nucleus where they can modify mRNA production (Liu *et al.*, 2017; Ozbabacan *et al.*, 2014; Wojdasiewicz *et al.*, 2014 and Israel, 2010).

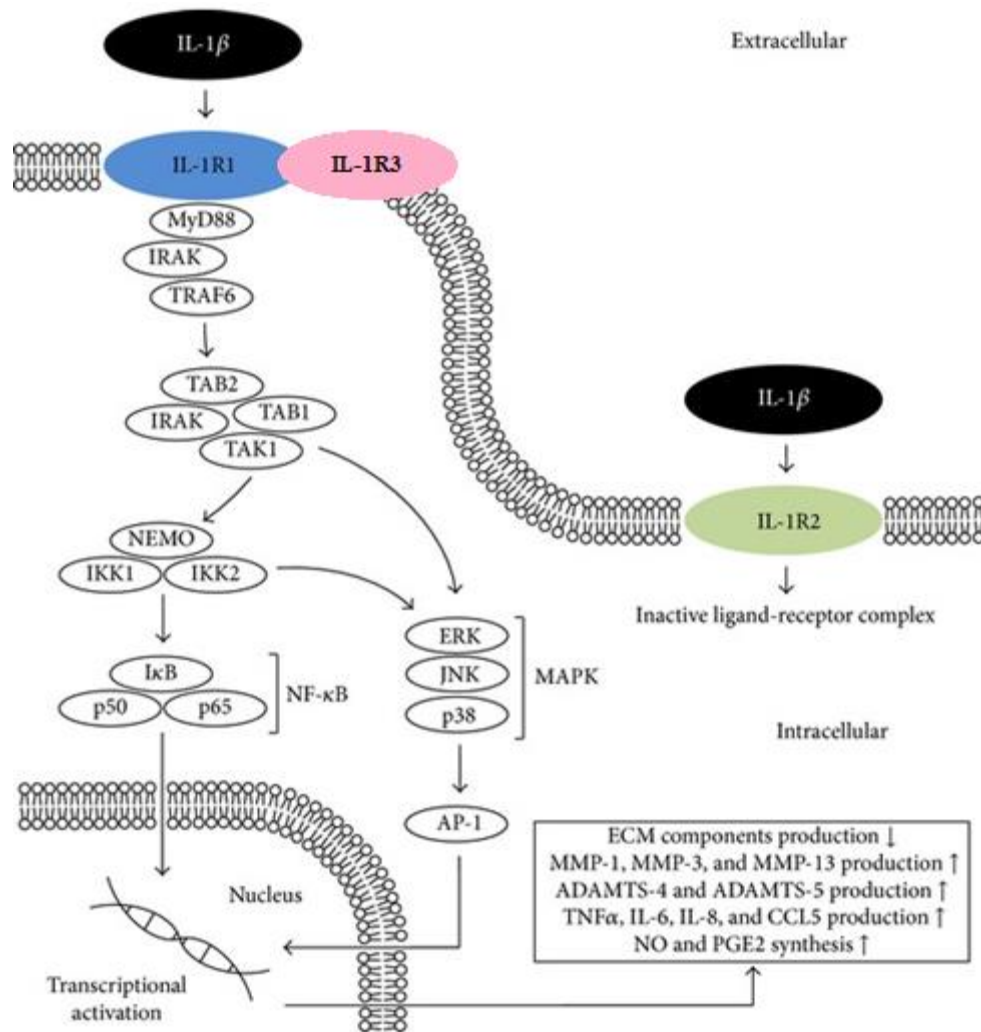


Figure 5.1: IL-1 β binding to IL-1R1 and IL-1R2 and subsequent downstream signalling (adapted from Wojdasiewicz *et al.*, 2014).

IL-1 β -IL-1R1 binding initiates a downstream signalling cascade. IL-1R2 acts as a 'decoy receptor' and IL-1 β -IL-1R2 binding does not initiate a downstream signalling cascade. IL-1 β -IL-1R1 binding recruits accessory protein IL-1R3 to form a signal transduction complex, the intracellular signal propagates through a series of molecule recruitment and modification stages involving MyD88, IRAK, TRAF6, TAB1 and TAB 2. The intracellular signal can then propagate via the NF- κ B pathway or the MAPK pathway. Downstream from both pathways are a family of transcription factors which become available to migrate to the nucleus to modify mRNA production.

One of the downstream signalling effects of IL-1 β -IL-1R1 binding is the production of other inflammatory mediators including fellow cytokines. IL-1 β -IL-1R1 binding and down-stream MAPK and NF- κ B transcription factors are known to induce IL-6 production in leucocytes (Panzer *et al.*, 1993) neuronal cells (Tsakiri *et al.*, 2008) and

Müller cells (Yoshida *et al.*, 2001). Similarly, IL-1 β -1L-1R1 binding and down-stream MAPK transcription factors are known to induce IL-8 production in some cell-types (Hwang *et al.*, 2004). IL-1 β induces IL-12 in dendritic cells (Wesa and Galy, 2001).

IL-10 is a predominantly anti-inflammatory cytokine (1.5.4 IL-10) inhibiting certain pro-inflammatory functions of leucocytes (table 1.7). Research into the relationship between IL-10 and IL-1 β shows: (i) they are both produced in inflammatory or pathological conditions (Wang *et al.*, 1997); (ii) both interleukins can be produced by microglia, another type of glial cell (Jenkins *et al.*, 1994) and (iii) IL-10 inhibits IL-1 β expression (Jenkins *et al.*, 1994 and Vieira *et al.*, 1991). Previous research using an LPS model of neuroinflammation demonstrated IL-1 β and IL-10 localisation in the brain, however the stimulus for IL-10 production was not identified (Wang *et al.*, 1997). Our research group looked at a glaucomatous neuroinflammation in the retina and demonstrated P2X7R-mediated increase IL-1 β and IL-10 expression (Niyadurupola *et al.*, 2009). The following chapter research will explore the relationship between IL-1 β and IL-10 cytokines in a human Müller retinal cell.

In the previous chapter (*Chapter 4: P2X7R-mediated Interleukin mRNA Expression in Human Müller Cells*) human Müller cells were shown to express mRNA for IL-1R1. When stimulated with LPS or purinergic agonists human Müller cells were not shown to produce IL-1 β protein. Similarly, when stimulated with purinergic agonists human Müller cells were not shown to induce IL-10 mRNA expression. In this chapter IL-1 β will be used to simulate the IL-1R1 on human Müller cells to see if this induces IL-10 mRNA and or protein expression.

5.2 Results

IL-1 β mediated IL-10 mRNA and protein expression in MIO-M1 cells was investigated using RT-qPCR (2.4 *Reverse transcription quantitative polymerase chain reaction*) and ELISA (2.8 *Enzyme-linked immunosorbent assay*) respectively.

To determine if any induced changes in IL-10 expression occurred due to IL-1 β binding to the IL-1R1 in MIO-M1 cells, inhibitors of downstream signalling (*figure 5.2*) LY294002 (PI3K inhibitor), bardoxolone methyl (NF- κ B pathway inhibitor) and SB 203580 (MAPK pathway p38 inhibitor) were used.

A.

IL-1R1 downstream Signalling Inhibitor	Description	IC ₅₀	Typical concentration for cellular experiments
LY294002	Selective competitive inhibitor of PI3K	PI3K α = 0.73 μ M PI3K β = 0.31 μ M PI3K δ = 1.06 μ M PI3K γ = 6.60 μ M	10-50 μ M
Bardoxolone methyl	Activation of nuclear factor erythroid 2-related factor 2 (Nrf2) which stabilises NF- κ B	0.1nM – 0.27 μ M	5 μ M
SB 203580	Selective competitive inhibitor of p38 MAPK	SAPK2a/p38 = 50nM SAPK2b/p38 β 2 = 500nM	1-10 μ M

B.

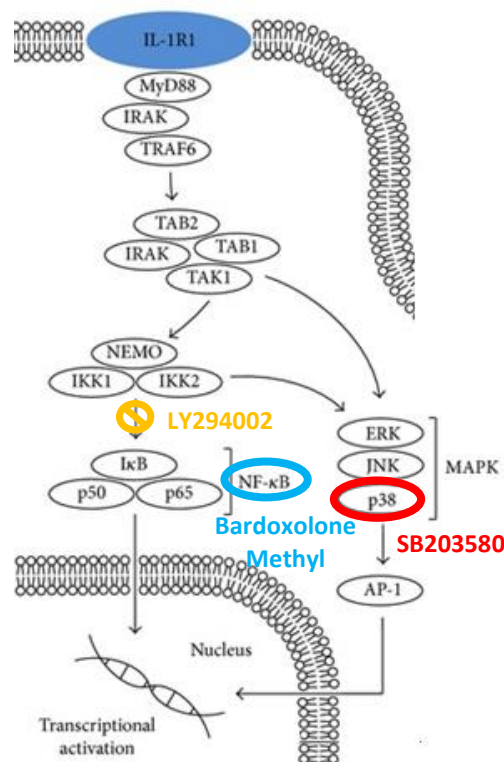


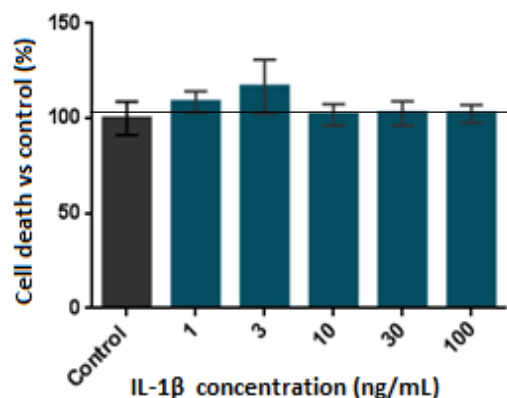
Figure 5.2: IL-1R1 downstream signalling inhibitors: (A) characteristics and (B) site of action.

LY294002 (**orange**) is a PI3K inhibitor: PI3K plays a role in transducing the signal from IL-1R1 to NF- κ B. PI3K acts by liberating NF- κ B transcription factors. The mechanism by which this occurs has not been fully elucidated, perhaps by liberating NF- κ B from I κ B (Reddy *et al.*, 1997) or by a pathway separate from I κ B degradation that results in phosphorylation of NF- κ B (Sizemore *et al.*, 1999). Bardoxolone methyl (**blue**) causes activation of Nrf2 which stabilises NF- κ B (Pei *et al.*, 2019; Wang *et al.*, 2017 and de Zeeuw *et al.*, 2013). SB203580 (**red**) is a specific p38 MAPK inhibitor (Zer *et al.*, 2007).

5.2.1 MIO-M1 evoked cell death in response to IL-1 β and IL-1R1 downstream signalling inhibitors

MIO-M1 cell death when stimulated with IL-1 β and IL-1R1 downstream signalling inhibitors was determined with LDH assays (2.6 LDH assay).

MIO-M1 cells were incubated in a range of IL-1 β (1-100ng/mL) concentrations for 24 hours. As discussed previously IL-1 β is a potent pro-inflammatory cytokine and can be cytotoxic at high concentrations in some cell types (Osborn *et al.*, 2008; Rosenwasser, 1998 and Shimabukuro *et al.*, 1997). Prolonged stimulation with IL-1 β at all concentrations showed no significant change in MIO-M1 cell death when compared with control (n=4; graph 5.1). Therefore, for the next series of experiments concentrations of IL-1 β up to 100ng/mL could be used to stimulate the IL-1R1 in MIO-M1 cells and any subsequent change in IL-10 mRNA or protein expression would not be attributable to lytic cell-death associated cytokine release (Place and Kanneganti *et al.*, 2019).

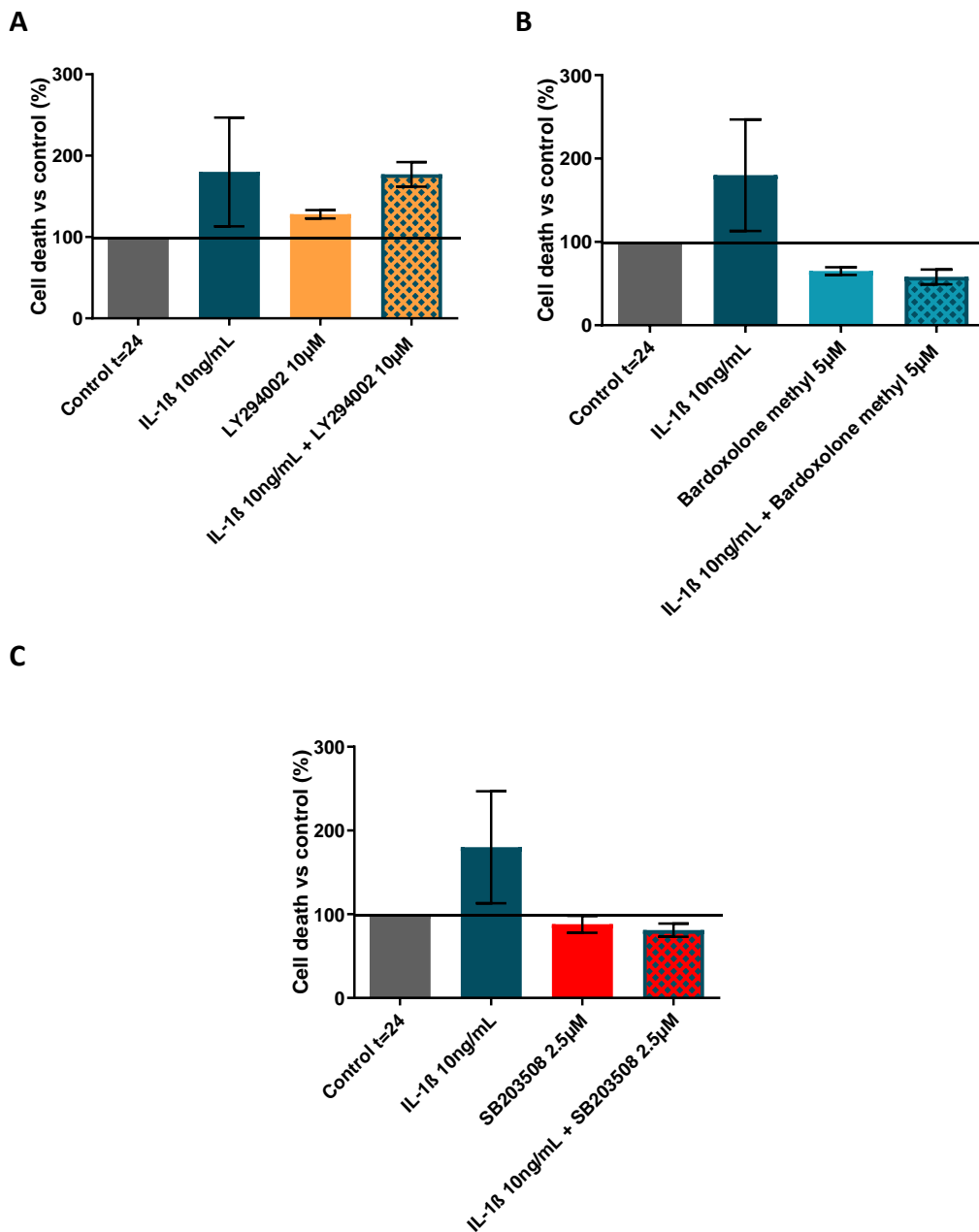


Graph 5.1: Evoked cell death of MIO-M1 cells after exposure to IL-1 β (1-100ng/mL) for 24h (n=4)

Stimulation with IL-1 β at concentrations 1-100ng/mL for 24 hours did not cause cell-death compared to control. Cell death was determined by LDH assay. Data is mean \pm SEM.

MIO-M1 cells were incubated in IL-1 β 10ng/mL with each of the IL-1R1 downstream signalling inhibitors LY294002 10 μ M (PI3K inhibitor; graph 5.2A), bardoxolone methyl

5 μ M (NF- κ B pathway inhibitor; *graph 5.2B*) and SB 203580 2.5 μ M (MAPK pathway p38 inhibitor; *graph 5.4C*) for 24h. The IL-1R1 antagonists did not appear to be cytotoxic at any of the concentrations used as they did not induce any significant MIO-M1 cell death when compared with control either in the presence or absence of IL-1 β (*graph 5.2 A-C*; n=4).



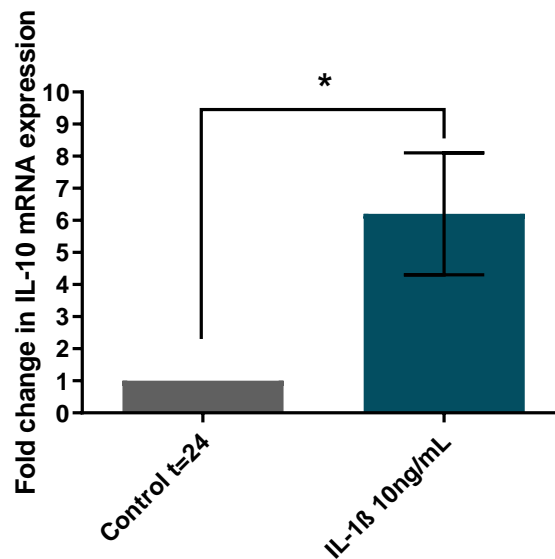
Graph 5.2: Evoked cell death of MIO-M1 cells after exposure to IL-1 β 10ng/mL and IL-1R1 downstream signalling inhibitors (A) LY294002 10 μ M, (B) bardoxylone methyl 5 μ M and (C) SB203508 2.5 μ M for 24h (n=4)

Stimulation with IL-1 β 10ng/mL and IL-1R1 downstream signalling inhibitors for 24 hours did not cause cell-death compared to control. Cell death was determined by LDH assay. Data is mean \pm SEM.

5.2.2 IL-1 β induced IL-10 mRNA and protein expression in MIO-M1 cells

MIO-M1 cells were incubated in IL-1 β 10ng/mL for 24 hours, subsequent change in IL-10 mRNA expression was evaluated using RT-qPCR (2.4 Reverse transcription

quantitative polymerase chain reaction). IL-1 β stimulation of MIO-M1 cells produced a significant 6.2-fold rise in IL-10 mRNA expression at 24 hours (n=4; graph 5.3).



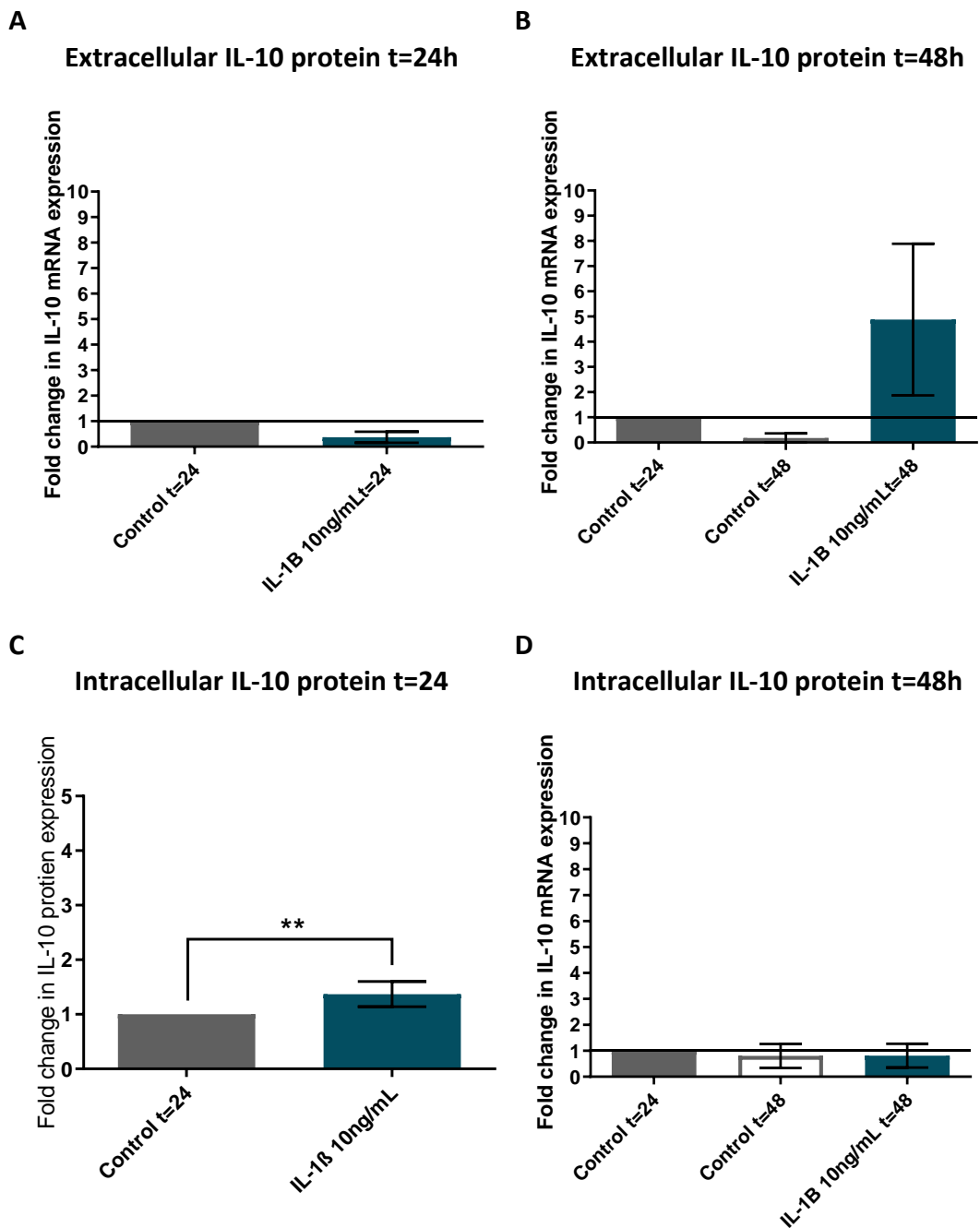
Graph 5.3: IL-10 mRNA expression in MIO-M1 cells in response to IL-1 β 10ng/mL stimulation (t=24h; n=4).

IL-1 β 10ng/mL stimulation of MIO-M1 cells produced a significant 6.2-fold rise in IL-10 mRNA expression at 24 hours ($P = 0.0339$). IL-10 mRNA expression was determined by RT-qPCR. Data is expressed as mean fold change \pm SEM, statistical significance ($P < 0.05$) calculated by t-test (*).

Given that IL-1 β 10ng/mL stimulation of MIO-M1 cells induced an upregulation of IL-10mRNA at 24 hours, IL-10 protein expression and release at 24 hours and 48 hours was evaluated using ELISA (2.8 Enzyme-linked immunosorbent assay).

IL-1 β stimulation of MIO-M1 cells did not cause any IL-10 protein to be released into the extracellular medium, as measured at 24 hours. In most of the experimental runs there was an increase in IL-10 release at 48 hours, however this increase was variable and therefore on analysis this was not statistically significant (n=4; graph 5.4 A-B). MIO-M1 cells were lysed to detect any intracellular IL-10 protein. IL-1 β stimulation of MIO-M1 cells produced a small but significant 1.37-fold rise in intracellular IL-10

protein at 24 hours (n=4; graph 5.4 C). No subsequent significant IL-10 protein rise at 48 hours was detected (n=4; graph 5.4 D).



Graph 5.4: Extracellular (A-B) and intracellular (C-D) IL-10 protein expression in MIO-M1 cells in response to IL-1 β 10ng/mL stimulation (t=24h and 48h; n=4)

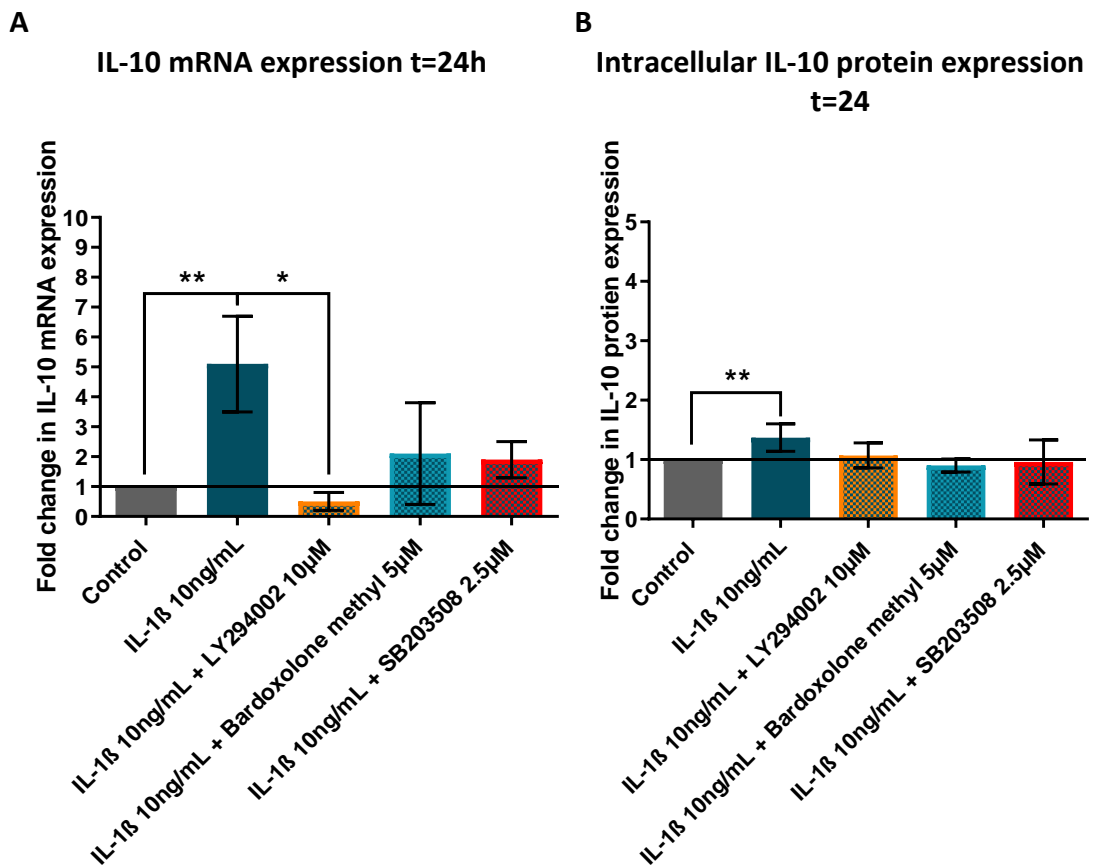
IL-1 β 10ng/mL stimulation of MIO-M1 cells did not cause any extracellular IL-10 protein release at 24 hours. IL-10 protein release at 48 hours was not statistically significant. MIO-M1 cells were lysed to detect any intracellular IL-10 protein. IL-1 β 10ng/mL stimulation of MIO-M1 cells produced a small but significant 1.37-fold rise in intracellular IL-10 protein at 24 hours $P < 0.0001$, there was no subsequent significant protein rise at 48 hours. IL-10 protein was determined by ELISA. Data is expressed as mean fold change \pm SEM, statistical significance ($P < 0.05$) calculated by t-test (*).

5.2.3 IL-1 β induced IL-10 in MIO-M1 cells treated with IL-1R1 downstream signalling inhibitors

The previous section demonstrated IL-1 β induced IL-10 mRNA and protein expression in MIO-M1 cells. This section investigates if the increase in IL-1 β induced IL-10 mRNA and protein was affected by inhibitors of the pathways downstream of binding of IL-1 β to IL-1R1.

MIO-M1 cells were pre-incubated for 30min in IL-1R1 downstream signalling inhibitors LY294002 10 μ M (PI3K inhibitor), bardoxolone methyl 5 μ M (NF- κ B pathway inhibitor) and SB 203580 2.5 μ M (MAPK pathway p38 inhibitor; figure 5.2). IL-1 β 10ng/mL was used to stimulate cells in the presence of the downstream signalling inhibitors. Subsequent IL-10 mRNA and intracellular protein expression was evaluated using RT-qPCR (2.4 *Reverse transcription quantitative polymerase chain reaction*) and ELISA (2.8 *Enzyme-linked immunosorbent assay*) respectively.

The IL-1 β induced IL-10 mRNA expression demonstrated previously (graph 5.3) was confirmed, with IL-1 β stimulation producing a significant 5.1-fold rise in IL-10 mRNA expression at 24 hours (graph 5.5 A). Each of the IL-1R1 downstream signalling inhibitors appeared to cause inhibition of IL-10 mRNA expression, although this was only significant with LY294002 (PI3K inhibitor). IL-1 β induced IL-10 protein was not inhibited by any of the IL-1R1 downstream signalling inhibitors, although again, they were back to baseline levels (graph 5.5 B).



Graph 5.5 IL-1 β 10ng/mL mediated IL-10 (A) mRNA and (B) intracellular protein expression in MIO-M1 cells pre-treated with IL-1R1 downstream signalling antagonists (t=24h; n=4)

MIO-M1 cells were pre-treated for 30 min with IL-1R1 signalling inhibitors LY294002 10 μ M, bardoxolone methyl 5 μ M and SB 203580 2.5 μ M. MIO-M1 cells were then stimulated with IL-1 β 10ng/mL and subsequent IL-10 mRNA (A) and intracellular protein (B) were measured at 24 hours with PCR and ELISA respectively. (A) IL-1 β induced IL-10 mRNA expression which was statistically significant: IL-10 mRNA appeared to be reduced by all IL-1R1 downstream signalling antagonists however only LY294002 produced a statistically significant reduction P = 0.0091. (B) IL-1 β induced IL-10 intracellular protein was not significantly reduced by any IL-1R1 downstream signalling antagonist. Data is expressed as mean fold change \pm SEM, statistical significance (P<0.05) calculated by t-test (*).

5.3 Discussion

5.3.1 IL-1 β stimulation of human Müller cells induces IL-10 mRNA expression and intracellular protein

One of the aims of this thesis was to explore any role(s) the human Müller cell has in relation to the IL-1 β and IL-10 release in the glaucomatous human retina.

The previous chapter (*Chapter 4: P2X7R-mediated Interleukin mRNA Expression in Human Müller Cells*) showed that ATP stimulation, such as that found in neuroinflammatory conditions including glaucoma, produce a small upregulation in IL-1 β mRNA but no mature protein release. It is known that neuroinflammatory conditions are associated with an increase in IL-1 β protein in the retina. Therefore, it is likely that human Müller cells are either not the main contributing source of IL-1 β in the retina or require additional signals to produce and potentiate IL-1 β mature protein release.

The aim of this chapter was to investigate any effect of retinal IL-1 β on IL-10 expression in human Müller cells. IL-1 β stimulation of human Müller cells produced a significant increase in IL-10 mRNA expression at 24 hours. The increase in IL-10 mRNA was significantly inhibited by the IL-1R1 downstream signalling inhibitor LY294002 (PI3K inhibitor). The other IL-1R1 downstream signalling inhibitors bardoxolone methyl (NF- κ B inhibitor) and SB 203580 (p38 inhibitor) also appeared to reduce IL-10 mRNA expression, however this was not statistically significant. Considering these results, it is likely that IL-1 β binds at the IL-1R1 on human Müller cells and transcription factors downstream of PI3K signalling upregulate IL-10 mRNA expression. NF- κ B and MAPK (p38) IL-1R1 downstream signalling pathways may also contribute to IL-10 mRNA expression but these have not been clearly implicated in the results obtained. It may be that bardoxolone methyl (NF- κ B inhibitor) and SB 203580 (p38 inhibitor) IL-1R1 downstream signalling inhibitors did not produce a statistically significant reduction in IL-10 mRNA due to: (i) variability in the results (*graph 5.5 A, see IL-1 β + bardoxolone methyl*); (ii) they were not used at an effective concentration or (iii) that other timepoints might have been more appropriate. It is important to note that as part of these experiments signalling inhibitors were used at their 'typical use' concentrations (*figure 5.2*) and that these might not have been the most appropriate for these experimental conditions.

IL-1 β stimulation of human Müller cells caused significant intracellular IL-10 protein expression without any extracellular IL-10 protein release at 24 hours. IL-1 β stimulation caused a rise in extracellular IL-10 protein release at 48 hours, however

this was not statistically significant due to variability in the results but does suggest that the IL-10 synthesized was subsequently released (*graph 5.4 B*). The IL-1 β mediated intracellular IL-10 protein expression was not significantly inhibited by any IL-1R1 downstream signalling inhibitors, but the trends were that inhibition had been achieved. Putting together the results obtained in this chapter, it is likely that IL-1 β binds at the IL-1R1 on human Müller cells initiating downstream signalling. Predominantly PI3K downstream signalling upregulates IL-10 mRNA expression which is translated into intracellular IL-10 protein within 24 hours. There may be some subsequent IL-10 protein release at 48 hours. Certainly, the intracellular level of IL-10 was back to baseline by this timepoint. The proposed mechanism of IL-1 β induced IL-10 mRNA and protein expression in human Müller cells is illustrated in the diagram below (figure 5.3).

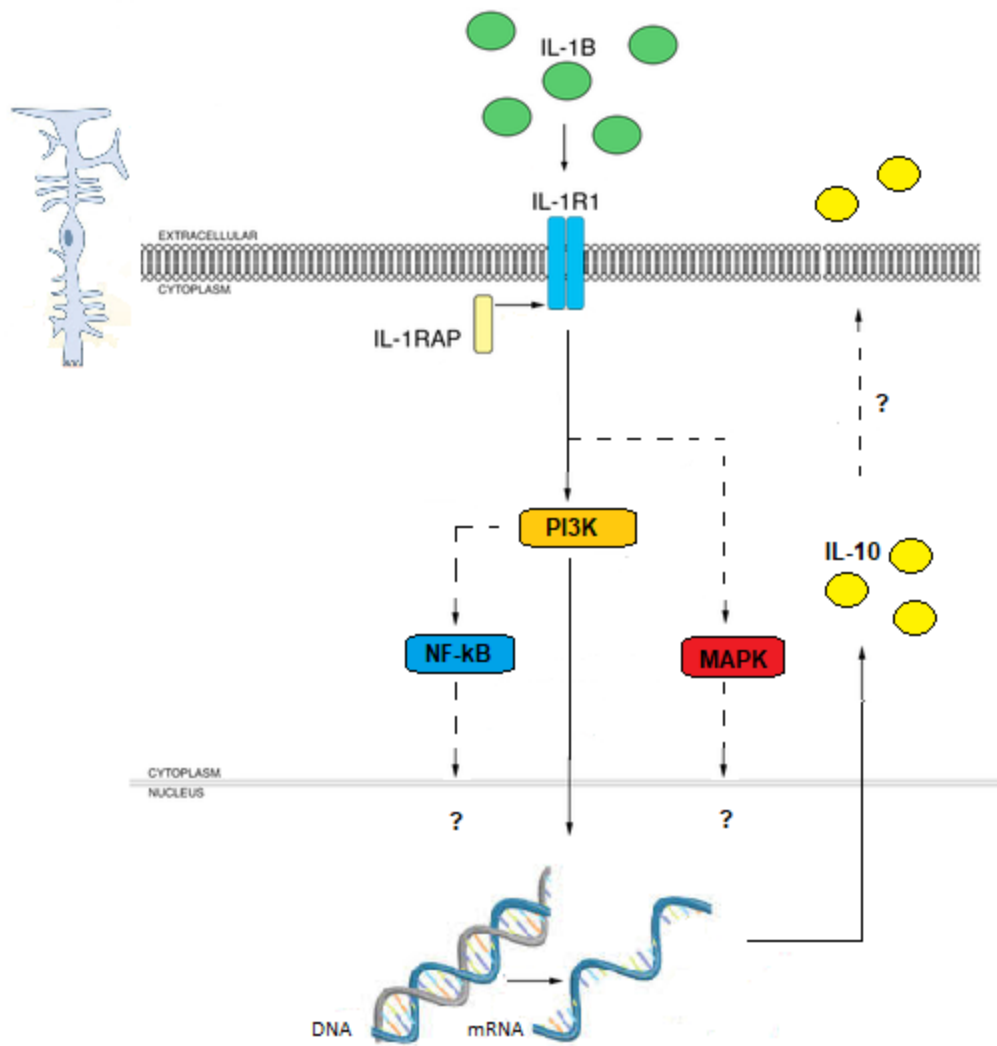


Figure 5.3 IL-1 β induced IL-10 mRNA and protein expression in human Müller cells

IL-1 β binds at the IL-1R1 on human Müller cells initiating downstream signalling. Predominantly PI3K signalling upregulates IL-10 mRNA expression with likely contribution via the NF- κ B and MAPK pathways. IL-10 mRNA expression is translated into intracellular IL-10 protein within 24 hours. This may lead to IL-10 protein release.

Chapter 6: Discussion

6.1 Summary discussion

Glaucoma is the leading cause of irreversible blindness worldwide (Flaxman *et al.*, 2017). Glaucoma describes a group of progressive optic neuropathies characterised by a pattern of RGC death that leads to blindness if untreated (Quigley, 1998). The pathophysiology behind RGC death has yet to be fully defined and mechanisms are likely to be multifactorial including mechanical stress, ischemia, excitotoxicity and inflammation. Our group focuses on understanding the role(s) purinergic signalling may have in the pathogenesis of RGC death in glaucoma. Relating to this our research group has previously shown that stimulation of the purinergic receptor subtype P2X7 in human retinal tissue is associated with RGC death and an increase in the expression of cytokines IL-1 β and IL-10 which are proposed to play a role in the neurodegenerative process. The retinal cell-types involved in P2X7-mediated RGC death and cytokine release have yet to be identified. The aims of this thesis research were to:

- (i) Identify the purinergic (P2) receptors in the human Müller cell**
- (ii) Determine if stimulation of the P2X7R in human Müller cells mediated their cell-death**
- (iii) Determine if stimulation of the P2X7R in human Müller cells mediate pro-inflammatory IL-1 β and anti-inflammatory IL-10 cytokine mRNA expression and protein release.**

6.1.1 P2X7, P2Y₁, P2Y₄, P2Y₁₂ and P2Y₁₄ were identified as functioning receptors in the MIO-M1 cell model of human Müller cells.

As part of this thesis the full set of P2 receptors were investigated in human Müller cells (MIO-M1 model) for the first time. mRNA and functional (Ca²⁺ imaging) evidence was demonstrated for P2X7, P2Y₁, P2Y₄, P2Y₁₂ and P2Y₁₄ receptors. P2X7 and P2Y₄ receptors were shown to be significantly enriched in human Müller cells (MIO-M1 model) when compared to human retinal tissue, perhaps suggesting that they may have a more prominent role in determining the cellular functions. Furthermore, at the time of writing, research presented in this thesis demonstrates the first time

P2Y₁₂ and P2Y₁₄ receptors have been identified in human Müller cells (MIO-M1 model) and the first time the P2Y₁₄ receptor has been identified in the human retina: the role of these receptors in the human Müller cell has yet to be identified. P2Y₁₂R has neuroprotective (Gao *et al.*, 2010) and pro-inflammatory roles (Tozaki-Saitoh *et al.*, 2017 and Cattaneo, 2015). Similarly, the P2Y₁₄R also causes pro-inflammatory cytokine release (Curet and Watters, 2018; Gao *et al.*, 2013; Kinoshita *et al.*, 2013 and Sesma *et al.*, 2012).

It was of particular importance to identify the P2X7R in MIO-M1 cells. Furthermore, it was important to demonstrate agonist activation and Ca²⁺ responses in MIO-M1 cells consistent to that which has already been published in human Müller cells. Establishing these constancies formed the basis for proceeding with MIO-M1 cells as a model for researching down-stream signalling functions of the P2X7R in human Müller cells.

6.1.2 Stimulation of P2X7R in the MIO-M1 cell model of human Müller cells does not appear to cause cell-death.

As part of this thesis research it was established there was a functioning P2X7R in the MIO-M1 model of human Müller cells. The P2X7R was activated with high concentrations of ATP and with the selective agonist BzATP and it was antagonised with the selective antagonists AZ10606120 and A438079. P2X7R pharmacology in the MIO-M1 cell model of human Müller cells is consistent with what has been published in the literature (Jacobson *et al.*, 2020; Jacobson 2018; Sluyter, 2017) validating this cell-line as a tool to study P2X7R electrophysiological responses. Prolonged stimulation (>24h) of the P2X7R with ATP and BzATP cells did not cause MIO-M1 cell-death as evaluated by cell viability and cell death assays. It appears, therefore, that stimulation of the P2X7R in human Müller cells does not cause their cell death as it does in other cell-types, perhaps because the receptor does not form a cytolytic pore. P2X7R that do not form cytolytic pores have previously been demonstrated in other immunocompetent cell types (table 1.5) including human Müller cells (Pannicke *et al.*, 2000). However, it is important to consider alternative explanations. MIO-M1 cells are an immortalised cell line, as such they may have a

higher viability than human Müller cells *in vivo* or primary cultures *in vitro* (Pereiro *et al.*, 2020). Additionally, MIO-M1 cells may express a polymorphism of the P2X7R that alters native receptor function (Tao *et al.*, 2017; Jiang *et al.*, 2013; Gartland *et al.*, 2012). Several P2X7R polymorphisms (table 6.2) such as *G150R* (Stokes *et al.*, 2010 and Denlinger *et al.*, 2006) *E496A* (Bradley *et al.*, 2011 Sluyter *et al.*, 2004) and *I568N* (Oyanguren-Desez *et al.*, 2011) have shown no cytolytic pore formation, but further research would be needed to investigate if one of these are expressed in the MIO-M1 cell line.

Stimulation of the P2X7R in human Müller cells may play a role in P2X7R associated RGC death in our groups proposed pathogenesis of glaucoma (Niyadurupola *et al.*, 2013). Whilst it is possible that stimulation of the P2X7R in human Müller cells causes the release of pro-inflammatory cytokines contributing to glaucomatous neurodegeneration, the thesis research discussed in the next sections suggest that the P2X7R in this supportive glial cell contributes to more of a neuroprotective role in the pathophysiology of glaucoma (6.2 Possibility of an IL-10-IL-1 β axis in the human retina).

6.1.3 Stimulation of the P2X7R in the MIO-M1 cell model of human Müller cells did not cause pro-inflammatory IL-1 β or anti-inflammatory IL-10 cytokine mRNA expression or protein release.

During resting conditions, the MIO-M1 model of human Müller cells did not express IL-1 α , IL-1 β or IL-10. IL-1 α and IL-1 β are not usually expressed by cells until they are in pathological conditions due to their potent pro-inflammatory responses (Dinarello, 1997).

Stimulation of the P2X7R in the MIO-M1 model of human Müller cells did not cause subsequent IL-1 (IL-1 α and IL-1 β) or IL-10 expression. Stimulation of the P2X7R is a well-established potent trigger of IL-1 β release in some cell types (figure 1.23; Giuliani *et al.*, 2017). In the human retina microglial cells are the main source of IL-1 β (Todd *et al.*, 2019). IL-1 β is secreted in pathological states such as: glaucoma (Niyadurupola *et al.*, 2013); ARMD (Zhao *et al.*, 2015); photo-oxidative damage (Hu *et al.*, 2015);

retinitis pigmentosa (Zhao *et al.*, 2015) and retinal detachment (Kataoka *et al.*, 2015). In the human retina RPE cells (Bian *et al.*, 2018) and microglial (Leclaire *et al.*, 2019) cells secrete IL-1 α in response to inflammatory (Liu *et al.*, 2015) and infectious conditions (Mora Scarpetta *et al.*, 2021). Recently increased levels of IL-1 α have been associated with ocular hypertension (Sterling *et al.*, 2020). Raised IL-10 is associated with ocular toxoplasmosis (Raouf-Rahmati *et al.*, 2021 and Rudzinski, *et al.*, 2020) and vitreoretinal lymphoma (Pochat-Cotilloux *et al.*, 2018; Touitou *et al.*, 2015); in the former it is postulated to play an anti-inflammatory role. Human Müller cells have not yet been linked to the release of these interleukins.

6.2 Possibility of an IL-10-IL-1 β axis in the human retina

ATP is released by all retinal cell types (Ward *et al.*, 2010). High concentrations of ATP in the retina are found in pro-inflammatory states, including glaucoma (Li *et al.*, 2011; Zhang *et al.*, 2007). Inflammation leads to responses including glial cell activation and production of interleukins. ATP activates the P2X7R, documented as the most important trigger of IL-1 β release in certain cell types (Di Virgilio *et al.*, 1998; Pelegrin *et al.*, 2008; Sanz *et al.*, 2009). IL-1 β is predominantly produced in pathological states and is one of the most pro-inflammatory agents (Giuliani *et al.*, 2017; Dinarello, 2011 and Gabay *et al.*, 2010). Microglial cells are the predominant source of retinal IL-1 β (Todd *et al.*, 2019). ATP stimulation of the P2X7R in the MIO-M1 cell model of human Müller cells did not cause an increase in IL-1 β mRNA expression or protein release. However, stimulation of an unidentified purinergic P2-receptor(s) with ATP caused a significant increase in IL-1 β mRNA expression, although there was no subsequent (0-72h) protein release. It may be that with additional stimulation human Müller cells contribute to IL-1 β in the human retina in inflammatory states, this is likely to be via a P2X7R-independent pathway. Human Müller cells are unlikely to be a significant contributor to retinal IL-1 β .

IL-1R1 is the interleukin receptor for IL-1 α , IL-1 β and IL-1R1A. IL-1 α and IL-1 β are agonists at the IL-1R1 and their binding causes subsequent downstream signalling. Research presented (*chapter 4: P2X7R-mediated IL-1R1 mRNA expression in MIO-M1*

cells) shows the MIO-M1 model of human Müller cells express mRNA for *IL-1R1*. IL-1 β stimulation of the IL-1R1 in the MIO-M1 cell model of human Müller cells resulted in significant IL-10 mRNA expression and intracellular protein production. Further research is required to identify stimuli that may cause a release of IL-10 protein into the retina. IL-10 is a predominantly anti-inflammatory cytokine, it modulates responses to infection or inflammation so that there is minimal resultant tissue damage (Ding and Shevach, 1992; de Waal Malefyt *et al.*, 1991 and Fiorentino *et al.*, 1991). Other groups have shown that IL-1 β stimulation of the IL-1R1 in the MIO-M1 cell model of human Müller cells significantly increases expression of the protein Galectin 1 (Hirose *et al.*, 2019) and the chemokines: C–C motif chemokine ligand 2 (CCL2); C-X-C motif chemokine 1 (CXCL1) and C-X-C motif chemokine ligand 10 (CXCL10) (Natoli *et al.*, 2017). Galectin 1, CCL2 and CXCL10 all have immunoregulatory roles.

Thereby, high concentrations of ATP trigger release of pro-inflammatory (IL- β) and anti-inflammatory cytokines (IL-10) in the retina, concurring with previous research from our group in the HORC model (Niyadurupola *et al.*, 2009). Cytokines released may have neurodegenerative and neuroprotective effects on RGCs (Angel *et al.*, 2019). Since high concentrations of ATP do not cause P2X7R mediated Müller cell death, these cells are able to survive and mediate this IL-10-IL-1 β axis in the human retina (figure 6.1).

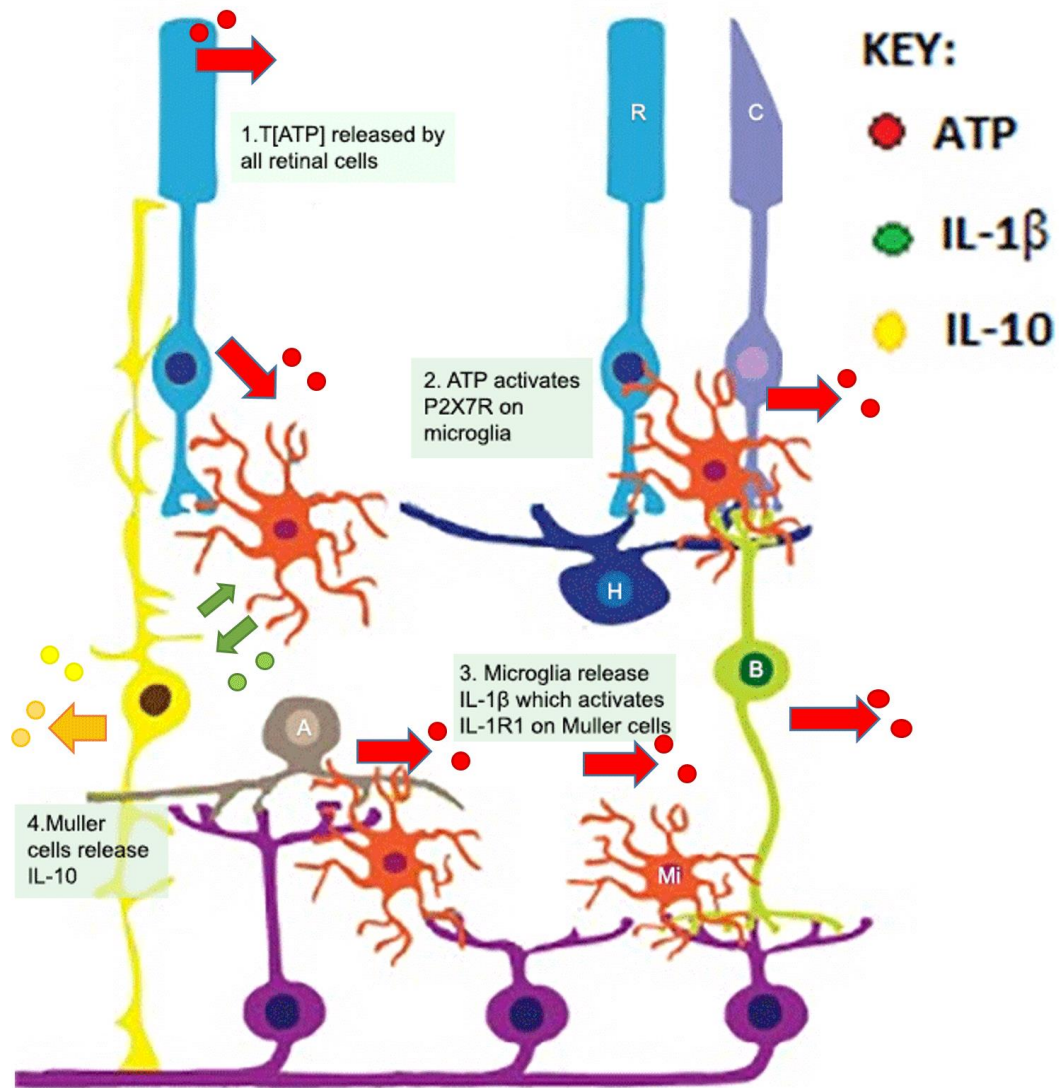


Figure 6.1 Proposed IL-10-IL-1 β axis in the human retina

High concentrations of retinal ATP are found in pro-inflammatory states including glaucoma. High concentrations of ATP activate the P2X7R which mediates IL-1 β release in the retina. P2X7R mediated IL-1 β release is predominantly from retinal microglial cells (red, Mi). ATP stimulation of a currently unidentified P2-receptor increases *IL-1 β* mRNA expression in Müller cells (yellow, M). Perhaps with additional stimuli Müller cells may contribute a small amount to IL-1 β released in the human retina. IL-1 β in a paracrine, and potentially an autocrine, manner activates IL-1R1 in Müller cells. Activation of IL-1R1 causes IL-10 mRNA upregulation and intracellular protein production. Subsequent unidentified stimuli may cause a release of IL-10 protein into the retina. Thereby high concentrations of ATP are triggering release of pro-inflammatory (IL- β) and anti-inflammatory cytokines (IL-10) in the retina, concurring with previous research from our group in the HORC model (Niyadurupola *et al.*, 2009). Cytokines released may have neurodegenerative and neuroprotective effects on RGCs. Since high concentrations of ATP do not cause P2X7R mediated Müller cell death, these cells are able to survive and mediate this IL-10-IL-1 β axis in the human retina.

6.3 Limitations

6.3.1 The MIO-M1 cell line as a research model for studying human Müller cells

Research models for studying human Müller cells (human or animal) include retinal tissue, primary Müller cell culture and immortalised Müller cell lines. At the time of conducting this thesis research human eyes for research purposes were not easily accessible. Porcine eyes were used to produce a primary Müller cell culture (*Appendix 1*): the intention was to develop a Müller cell isolation protocol using porcine retina so that an optimised protocol could be used on human retina if accessible in future (*6.4 future work*). The research presented as part of this thesis has been focused on human Müller cells and therefore the MIO-M1 immortalised human Müller cell line was used as a research tool.

MIO-M1 cells were the first immortalised human Müller cell line (Lawrence *et al.*, 2013). MIO-M1 cells have now been utilised by numerous research groups as a model for studying human Müller cells. MIO-M1 cells are a useful tool for studying human Müller cells since they are:

- (i) relatively easily available
- (ii) a human cell line, thereby eliminating the issue of interspecies variation
- (iii) easy to culture
- (iv) display good longevity when compared with long-term primary cultures.

When compared with human Müller cells they displayed consistent morphology, glial cell markers and electrical responses to glutamate (Limb *et al.*, 2002). By contrast, primary cultures of human Muller cells:

- (i) are limited in availability
- (ii) may be contaminated with other cell types which could lead to inconsistent experimental results

- (iii) display heterogeneity across different batches since they are from different donors – again this could lead to inconsistent experimental results
- (iv) display phenotypic instability across passages (Augustine et al., 2018; Sarthy et al., 1998)

However, if available, primary cultures are considered the preferred model for research purposes since long-term immortalised cell-lines display abnormalities. Karyotypic analysis of MIO-M1 cells demonstrated characteristic chromosomal abnormalities typical of cell-lines, for example triploidy and satellite chromosomes (Limb *et al.*, 2002). Karyotypic differences may alter the way the MIO-M1 cell line functions when compared to *in vivo* physiological functions. Additionally, they are a homogenous population and do not display heterogeneity in receptor expression that may otherwise be found in primary cultures or *in vivo*.

Alternate immortalised Müller cell lines are primarily derived from rodent species including:

- (i) Rat: **rMC-1** (Sarthy *et al.*, 1998); **TR-MUL** (Tomi et al., 2003; Hosoya and Tomi, 2005) and **SIRMu-1** (Kittipassorn *et al.*, 2019)
- (ii) Murine: **ImM10** (Otteson and Phillips *et al.*, 2010) and **QMMuC-1** (Augustine *et al.*, 2018).

Each Müller cell line expressed its own characteristics and on the basis of these characteristics are used by researchers to study different cell functions.

Müller cell line	Animal	Characteristics	Research advantages
MIO-M1 cells	Human	Express: sex determining region Y-box 2 (SOX 2); paired box 6 (PAX 6) and Notch 1. Form neurospheres in ECM with fibroblast growth factor 2.	Useful for studying glial reprogramming and progenitor behaviors
rMC-1	Rat	Express: high levels of GFAP and alanine, serine, cysteine transporter 2 (ASCT-2)	Useful for studying NMDA regulation
ImM10	Mouse	Form neurospheres	Useful for studying progenitor behaviors
QMMuC-1	Mouse	Maintain electrophysiological characteristics	Useful for studying electrophysiological responses

Table 6.1: Characteristics of Müller cell lines (Text contained adapted from information presented in Augustine *et al.*, 2018).

6.3.1 P2X7R gene polymorphisms and post-transcriptional regulation

The *P2X7R* gene is highly polymorphic. Variation in the *P2X7R* gene DNA sequence can occur because of single nucleotide polymorphisms (SNPs), sequence repeats, recombination and point insertions or deletions. SNPs are widespread in the human *P2X7R* genes, with over 13,000 identified (Roger *et al.*, 2010; Sperlagh and Illes, 2014; Di Virgilio *et al.*, 2017; Sluyter, 2017). *P2X7R* polymorphisms are associated with different health conditions and altered receptor functions (Caseley *et al.*, 2014): receptor functions examined include effects on Ca²⁺ influx, ATP evoked currents, dye-uptake and pore formation (table 6.2). Some *P2X7R* variants express altered IL-1 β expression and release when compared to the wild-type: the *E496A* variant has increased ATP induced IL-1 β release when compared with the wild-type (Wesselius *et al.*, 2012). MIO-M1 cells are a homogenous cell line population and may express *P2X7R* polymorphism(s) that alters these receptor functions when compared to the wild-type.

Polymorphic variant Change in nucleotide sequence	Change(s) in P2X7R function
A76V From alanine to valine at position 76	Increase Ca ²⁺ influx Increase ATP evoked currents Increased dye-uptake when stimulated with ATP Reduced functional activity ¹
V76A From valine to alanine at position 76	Reduced Ca ²⁺ influx Reduced ATP evoked currents Reduced dye-uptake when stimulated with ATP No change in ATP sensitivity Increased functional activity ^{2&3}
G150R From glycine to arginine at position 150	No ATP evoked currents Reduced dye-uptake when stimulated with ATP Reduced to no pore formation ^{3&4}
H155Y From histidine to tyrosine at position 155	Increased Ca ²⁺ influx Increases ATP evoked currents Increased dye-uptake when stimulated with ATP No change in ATP sensitivity ^{5 & 6} Increased P2X7R expression on the cell surface ^{7,8}
R270H From arginine to histidine at position 270	Increased dye-uptake when stimulated with ATP Reduced functional activity to no functional activity ^{3,9}
A348T From alanine to threonine at position 348	Increase ATP evoked currents Increased dye uptake No effect on ATP sensitivity Increased P2X7R expression ^{8,10}
Q460R From glutamine to arginine at position 460	No change in ATP evoked currents Equivocal evidence on changes in dye uptake Equivocal evidence on changes in pore formation No significant effect on receptor function ^{2,3,4,6}
E496A From glutamic acid to alanine at position 496	Equivocal evidence on changes in ATP evoked currents ^{2,11} Reduced dye-uptake Reduced pore-formation No functional activity at low density expression, unchanged functional activity at high density expression ^{7,12}
I568N From isoleucine to asparagine at position 568	Reduced to no ATP evoked currents ^{2,13} No dye uptake ²

Table 6.2: Common P2X7R gene polymorphisms and associated changes in receptor function (Text contained adapted from information presented in Caseley *et al.*, 2014).

Post-transcriptional regulation of *P2X7R* occurs by two main mechanisms splicing and microRNAs (miRNAs). *P2X7R* has multiple splice variants, *P2X7A-J* and *P2X7-V3* (Feng *et al.*, 2006 and Cheewatrakoolpong *et al.*, 2005). *P2X7R* splice isoforms are generated by the inclusion or exclusion of exons or genetic regions. *P2X7RA* is the 'full-length' mRNA code for the complete protein (Benzaquen *et al.*, 2019). *P2X7RB*, *E*, *G*, *I* and *J* code for a truncated protein (Feng *et al.*, 2006 and Cheewatrakoolpong *et al.*, 2005). *P2X7RB* is the only variant to function as a small ion channel and exerts a dominant positive influence at the wild-type receptor (Adinolfi *et al.*, 2010; Giuliani *et al.*, 2014). *P2X7RJ* and *P2X7R-V3* code non-functional proteins (Feng *et al.*, 2006 and Cheewatrakoolpong *et al.*, 2005). MIO-M1 cells are an immortalised cell-line and single-cell lines tend to express a predominant splice variant rather than a range of variants.

6.3.2 Purinergic signalling is a promiscuous system

Nearly all human retinal cells: (i) release nucleotides and nucleosides; (ii) contain nucleotide and nucleoside metabolising enzymes; (iii) express nucleotide or nucleoside transporters and (iv) express multiple types of purinergic receptor (Sanderson *et al.*, 2014). In this way, one nucleotide or nucleoside released in the retina can activate directly, or by its enzymatic degradation products, a multitude of purinergic receptors in an autocrine and paracrine manner. Complexity of retinal cell purinomes is not fully appreciated in this thesis research which focuses on a single retinal cell type and isolates a specific P2-receptor by using a combination of synthetic agonists or antagonists. *In vivo* endogenous purinergic agonists will act in an autocrine and paracrine manner on Müller cells activating several purinergic receptors on the cell and surrounding retinal cells causing several downstream effects, some of which will be neuroprotective and others which will be neurodegenerative.

6.4 Future Work

Research presented in the earlier part of this thesis focused on identification of the P2 receptor profile (P2X7, P2Y₁, P2Y₄, P2Y₁₂ and P2Y₁₄ receptors) and IL-1R1 in the

MIO-M1 cell model of human Müller cells. Further Immunohistochemistry experiments would localise the P2 receptors and IL-1R1 in the MIO-M1 cell. It would also be important to use immunohistochemistry to determine whether expression is seen in Muller cells in the human retina.

It is the first time that P2Y₁₄R has been identified in the MIO-M1 or any retinal cell type. The presence of P2Y₄R is also indicated for the first time in Muller cells, although confirmation of functional expression of this receptor is difficult due to the lack of selective pharmacological tools. P2Y₁₄R expression is limited to certain tissues; it has previously been identified in other neuronal tissues (Wang and Duan, 2021), where it has roles in inflammation, such as recruitment of immune cells (Fosters *et al.*, 2021; Sesma *et al.*, 2016 and Gao *et al.*, 2013). Other groups have found that P2Y₄R also has roles in neuroinflammation and suppression of inflammatory cytokines (Zhou *et al.*, 2019). It would be interesting to see if P2Y₄R and P2Y₁₄R are involved in the regulation of inflammatory cytokines in the human retina.

Presented as part of this thesis research is a pro-inflammatory IL-1 β and anti-inflammatory IL-10 axis (figure 6.1). There may be other pro- or anti-inflammatory cytokines within this axis. In cardiac and renal tissue there is a pro-inflammatory TNF- α and anti-inflammatory IL-10 axis (Stenvinkal *et al.*, 2005). IL-10 down regulates TNF- α production (Stenvinkal *et al.*, 2005). To explore this further immunohistochemistry of HORC tissue and/or retinal cells would identify which retinal cell types express the IL-10R and where in the cell(s) it is localised. Similarly, the effect of TNF- α stimulation of human Müller cell IL-10 production could be investigated with PCR and ELISA. IL-1 β binds to IL-1R1 and through predominantly PI3K downstream signalling pathways increases IL-10 expression. IL-1 α binds to IL-1R1 also and initiates the same downstream signalling pathways: leading to the research question '*does IL-1 α stimulation of human Müller cells upregulate IL-10 production?*'.

ATP increased *IL-1 β* mRNA expression in the MIO-M1 model of human Müller cells. No subsequent protein release was detected under these experimental conditions. ATP induced *IL-1 β* mRNA expression occurred in a pathway independent of the

P2X7R. Further research is needed to identify the P2-receptor(s) which mediate this observed upregulation of *IL-1 β* mRNA, this may show that ATP could both prime the cells by upregulating mRNA and cause protein release.

MIO-M1 cells were used as a cell-model for human Müller cells. As discussed previously, MIO-M1 cells may have a *P2X7R* polymorphism and flow cytometry could help identify any common variant. Results obtained in this thesis indicate the *P2X7R* in the MIO-M1 cell model of human Müller cells functions as a small cation channel and is not capable of pore-formation.

It would be of interest to compare some of the results obtained in MIO-M1 cells with primary human Müller cells. Whilst completing this thesis, a protocol was developed for extracting primary Müller cells from retinal tissue (*appendix 1*), which was successful with porcine retina, however the human retinal tissue available at that time was too many hours post-mortem to obtain a viable culture of primary Müller cells.

Appendix 1: Isolation of Primary Müller Cells from Porcine Retina

Appendix 1.1 Introduction

Müller cells are the predominant glial cell in the retina and account for approximately 5% of all retinal cells (Strettoi and Masland, 1995; Jeon *et al.*, 1998). Thesis research is focussed on purinergic signalling in Müller cells any role(s) they may have in glaucomatous neuroinflammation and neurodegeneration. Throughout this thesis MIO-M1 cells (2.1 *MIO-M1 cells*) have been used as a model for human Müller cells, their advantages and limitations have been discussed previously (6.3.1 *The MIO-M1 cell line as a research model for studying human Müller cells*). Primary Müller cells are generally the preferred model for research purposes. The following protocol has been developed to isolate Müller cells from porcine retinal tissue. Müller cells have previously been isolated from rabbit retina using Percoll gradient (Trachtenberg and Packey, 1983). The Trachtenberg and Packey 1983 methodology has been modified and incorporated in the protocol below.

Appendix 1.2 Materials and Methods

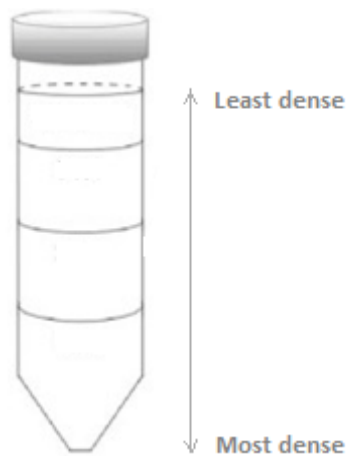
Appendix 1.2.1 Preparation of a Percoll stock solution and Percoll density gradients

Stock isotonic Percoll (SIP) and Percoll gradients were prepared in advance. Percoll (Sigma Aldrich) does not diffuse over time. The SIP was prepared by mixing 1-part Percoll (undiluted) to 9-parts DPBS (10 x concentration; Invitrogen). The SIP was diluted to lower densities by adding DPBS (1 x concentration; Invitrogen) as described in appendix table 1.1 below. Osmolality of the SIP and Percoll densities were checked regularly with an osmometer (ELITechGroup, Berkhamsted, UK) to ensure reproducibility between experimental repetitions. Cell density is dependent on osmolality (Sigma Aldrich, 2022).

Percoll density	100%	90%	80%	70%	60%	50%	40%	30%	20%	10%
SIP (mL)	10	9	8	7	6	5	4	3	2	1
DPBS (mL)	0	1	2	3	4	5	6	7	8	9

Appendix table 1.1: Dilution of stock isotonic Percoll to lower densities

Percoll gradients were assembled in a 5mL tube (Sigma Aldrich). Percoll was slowly pipetted down the side of the tube to assemble discrete layers. Percoll was layered from most dense to least dense (appendix figure 1.1).



Appendix figure 1.1: Discontinuous Percoll gradient

Schematic diagram representing a discontinuous or 'step' Percoll gradient. The SIP is diluted to different densities (appendix table 1.1). Percoll is layered from most dense to least dense. Percoll gradients may be assembled with a single step or many steps.

Appendix 1.2.2 Porcine retinal dissection

Porcine eyes were obtained from an abattoir (HG Blake Limited, Norwich) within an hour of slaughter. Porcine eyes were transported in cold DPBS with 10% antibiotic antimycotic solution (penicillin, streptomycin and amphotericin B; Sigma Aldrich) contained within a 50mL falcon tube (Corning). Porcine retinal tissue was dissected from the remainder of the globe. To gain access to the retina a circumferential ring of sclera was removed at the ora serrata and the vitreous body removed. The retina was mechanically detached from the underlying RPE and choroid using gentle

traction with Calibri straight forceps, the attachment of the retina at the optic nerve was cut using Westcott curved tenotomy scissors. Retinal tissue was washed with 1.5mL DPBS to remove any remaining adherent RPE cells.

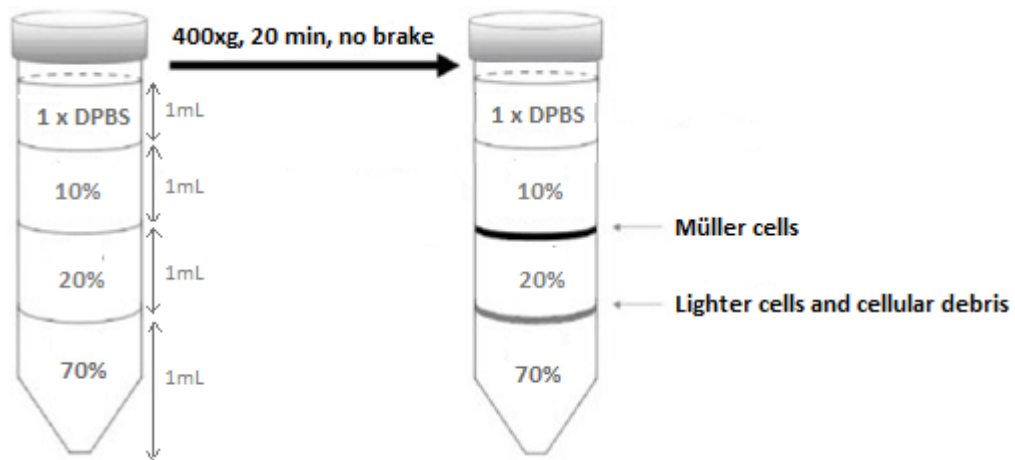
Appendix 1.2.3 Mechanical and enzymatic digestion of retinal tissue

Retinal tissue was disassociated into a mixed cell suspension through a series of mechanical and enzymatic digestion steps. Retinal tissue was placed in a 35mm dish (Corning) containing preheated 0.25% Trypsin-EDTA (Life technologies) and mechanically chopped with scissors into at least 10 fragments. Retinal fragments in trypsin were left to enzymatically digest in a humidified incubator at 35°C for 30 minutes. Mechanical trituration of retinal tissue was performed by repeat pipetting with a P1000 pipette. The cell suspension was centrifuged at 300 x G for 5 min to form a cell pellet. Supernatant was removed and two washing steps were performed by re-suspending the cell pellet in DPBS and centrifuging again. The cell suspension was passed through a 100µm cell strainer (Sigma-Aldrich, Merck, Dorset, UK) ready for experimental use.

Appendix 1.2.4 Loading cell suspension onto Percoll gradient

A volume of 250µL cell suspension was loaded onto a 5mL Percoll gradient. Preliminary experiments were performed using several Percoll gradient iterations (data not included) and it was determined a Percoll gradient of 70%: 20%: 10%: DPBS (appendix figure 1.2) was optimal for isolation of Müller cells from porcine retinal tissue. The sample was centrifuged at 400 x G for 20 minutes to cause isopycnic banding of Müller cells at the 20%:10% Percoll interface. The centrifuge was stopped with no break to avoid interrupting the Percoll interfaces. Percoll solution above the cell band was gently removed and the cell band was collected. The cells were added to 5mL of DPBS and were washed twice by centrifuging 200 x G for 10minutes. The cell pellet was resuspended in 1mL of DMEM with FBS. The cell suspension was placed in the centre of a T25 flask (Nunc™) for 1 hour in a humidified incubator at 35°C in

95% air, 5% CO₂. The T25 flask was subsequently flooded with 3mL of DMEM with FBS and left to expand in the incubator until 80-90% confluent.



Appendix figure 1.2: Isopycnic banding of retinal cells at percoll interfaces

A Percoll gradient of determined a gradient of 70%: 20%: 10%: DPBS (1mL each density) was assembled. The retinal cell suspension was applied. Isopycnic banding of cells were located primarily at the 20%: 10% interface and a lighter band at the 70%: 20% interface. Subsequent light microscopy showed that the 'heavy band' predominantly contained Müller cells and the 'lighter band' contained lighter cells and cellular debris.

Appendix 1.2.5 Cell counting

Once the Müller cells reached confluence, culture medium was aspirated and cells washed with DPBS. For cellular detachment 0.25% Trypsin was applied for 5 min whilst incubating. Trypsin was neutralised by the addition of DMEM with FBS. The cell suspension was transferred to a 15mL universal tube and centrifuged at 50 x G for 5 minutes to cause formation of a cell pellet. After removal of the supernatant the cell pellet was re-suspended in culture medium. Cells were counted with haemocytometer (Assistant, Sondheim-Rhön, Germany). Concentration of cells determined by:

$$\text{Cell concentration (cells/mL)} = \frac{\text{Total number of cells in the four large grids}}{4} \times 10,000$$

Appendix 1.2.6 Optical microscopy and immunohistochemistry

Phase contrast microscopy (Leica optical microscope, Leica Microsystems, Germany) images were taken of the porcine Müller cells at subconfluence and confluence allowing for morphological assessment.

Porcine Müller cells were cultured on coverslips (Marienfeld, Germany) for immunostaining. Coverslips were placed in 35mm dish and sterilised in UV light for 20 minutes. Subsequently, 200µL of the cell suspension was placed on the coverslip and left to expand in a humidified incubator until confluent. Cells were washed with phosphate buffered saline (PBS) and then fixed with 4% paraformaldehyde (ThermoFisher) at room temperature for 10 min. Cells were washed a further three times with PBS. Cell membranes were permeabilised with 1mL of 0.5% NP-40 (ThermoFisher) in PBS for 3 minutes at room temperature and then blocked with 3% bovine serum albumin (BSA, ThermoFischer) in PBS for 1 hour at room temperature. The blocking solution was discarded. Cells were incubated with 100µM primary antibody glutamine synthetase (GS; mouse monoclonal; Millipore, Watford, UK) at a dilution of 1: 200 in 3% BSA in PBS. Cells were incubated at 4°C overnight. After 3 washes with PBS cells were incubated with the corresponding secondary antibody Alexa Flour 488 anti-mouse (Invitrogen) at a dilution of 1: 1000 in 3% BSA in PBS. Cells were incubated at room temperature for 1 hour. After 3 washes with PBS the coverslips were mounted with Histomount (Invitrogen) onto glass slides and stored in the dark. Fluorescent images were obtained with Zeiss Axiovert (Carl Zeiss Microscopy).

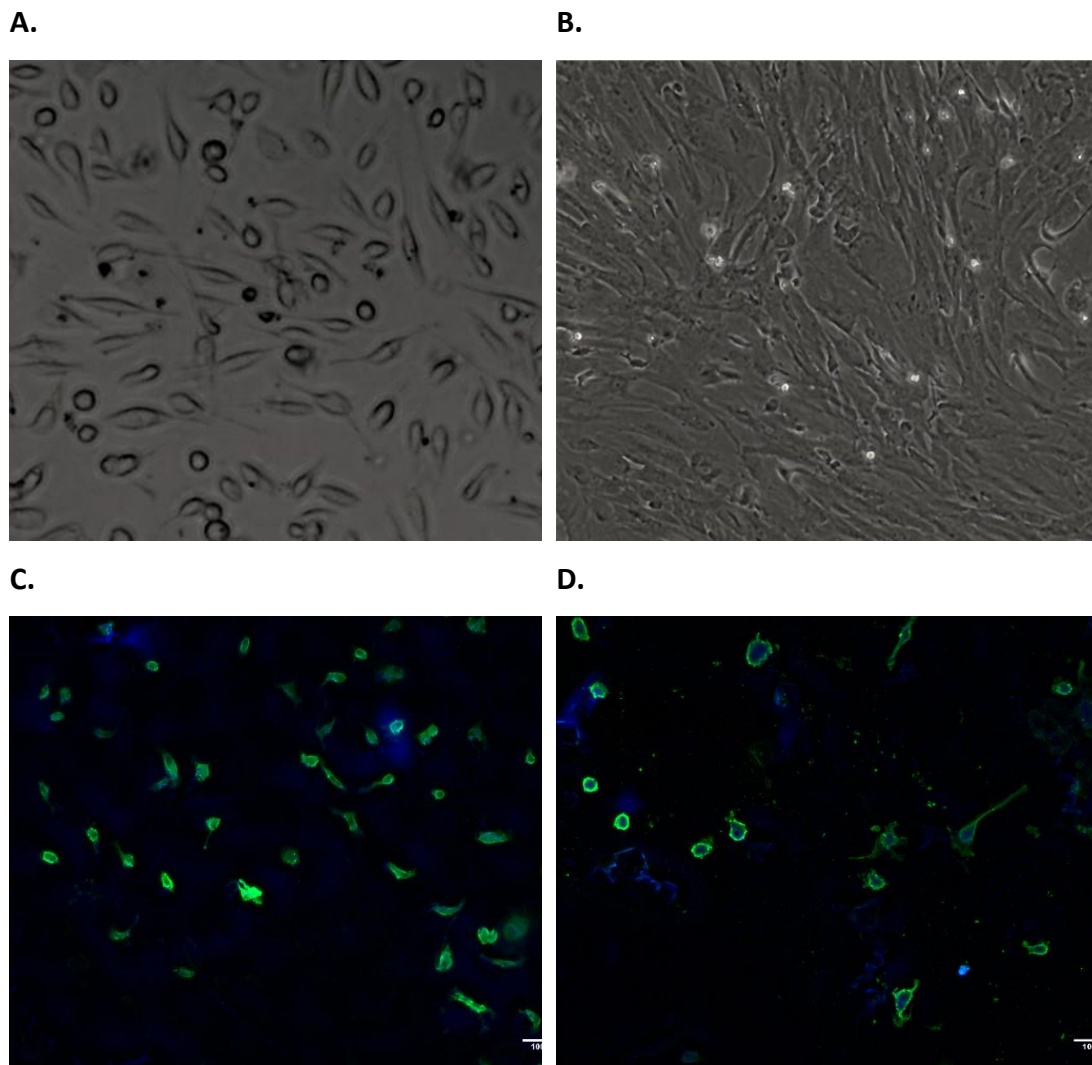
Appendix 1.3 Results

Appendix 1.3.1 Cell yield

One porcine retina yielded a primary culture containing 730,000 Müller cells at the first passage, as assessed with the haemocytometer (182, 500 cells/mL, n=1).

Appendix 1.3.2 Identification of isolated Müller cells with optical microscopy and immunofluorescence

Phase contrast microscopy (PCM) images of subconfluent and confluent porcine Müller cells (appendix figure 1.3 A & B) showed what macroscopically appear to be a homogenous population of spindle-like cells similar in appearances to subconfluent and confluent MIO-M1 cells (figure 2.1). Immunofluorescence images (appendix figure 1.3 C & D) show co-staining with Hoechst (blue, nuclear DNA) and GS (green, Müller glial cell marker) identifying isolated cells as Müller cells.



Appendix figure 1.3: Optical microscopy (A & B) and immunofluorescence (C & D) images of primary porcine Müller cell culture

PCM images of a subconfluent (A) and confluent (B) monolayer of primary porcine Müller cells showing spindle morphology, similar in appearances to MIO-M1 cells in culture. Immunofluorescent images (C & D) showing co-staining with the nuclear stain Hoechst (blue) and the Müller cell marker GS (green). Scale illustrates 100μM.

Appendix 1.4 Discussion

Presented is a protocol for isolating Müller cells from porcine retinal tissue using a Percoll gradient. Percoll is a silica-based colloid ideal for the separation of cells:

- (i) It is non-toxic and sterile (Sigma Aldrich, 2022)
- (ii) It has a low osmolality (<25 mOsm/kg H₂O) and can form a density gradient without forming an osmolality gradient (Sigma Aldrich, 2022)
- (iii) It is more economical than other methods of cell separation such as fluorescence activated cell sorting (FACS; Zhong *et al.*, 2021).

Whilst developing the presented protocol, several iterations of percoll gradients were assembled and trialled (research not presented). A percoll density step of 20%:10% consistently produced a “heavy band”, optical microscopy showed a population of predominantly Müller cells. Interestingly a density step of 20%: 10% was more effective at isolating Müller cells than a 25%: 20% step and a 20%: DPBS step. A minimum volume of 1mL of each percoll density was required for effective isolation of Müller cells. A percoll gradient of three interfaces (70%: 20%: 10%: DPBS) was more effective at isolating Müller cells than one with two (70%: 20%: 10% or 20%: 10%: DPBS) or one (20%: 10%) interface. Future work would involve quantification of these observations.

Similarly, 40µM, 70µM and 100µM cell strainers were trialled (research not presented). The 100µM cell strainer was more effective at producing a population of Müller cells, as these are approximately 100µM in the mammalian retina, larger than other retinal cell types (Labin *et al.*, 2014). Pereiro *et al.*, showed a significant increase in the number of porcine Müller cells isolated when papain was used for enzymatic digestion of retinal tissue compared with trypsin (Pereiro *et al.*, 2020), although this was not trialled when developing the protocol presented above.

The presented protocol demonstrated a relatively high yield of cells at 182, 500 cells/mL, compared to another published porcine Müller cell isolation protocol yielding $14,083.59 \pm 2,635.36$ cells/cm² (Pereiro *et al.*, 2020).

Optical microscopy and immunofluorescence showed a homogenous population of a retinal cell type, macroscopically resembling Müller cells and staining with the Müller cell marker GS. Other glial cells such as astrocytes and microglia also express GS so ideally immunohistochemistry should be performed for an additional Müller cell marker such as GFAP, Vimentin and CRALBP. A preliminary experiment to identify isolated cells as Müller cells using flow cytometry was also performed (data not shown) which if repeated in future would further demonstrate the effectiveness of this protocol.

References

Abbas, Z., Latif, M. L., Dovlatova, N., Fox, S. C., Heptinstall, S., Dunn, W. R., & Ralevic, V. (2018). UDP-sugars activate P2Y₁₄ receptors to mediate vasoconstriction of the porcine coronary artery. *Vascular Pharmacology*, *103-105*, 36–46.

Abbracchio, M. P., & Burnstock, G. (1998). Purinergic signalling: pathophysiological roles. *Japanese Journal of Pharmacology*, *78(2)*, 113–145.

Abbracchio, M. P., & Burnstock, G. (1994). Purinoceptors: are there families of P2X and P2Y purinoceptors?. *Pharmacology & Therapeutics*, *64(3)*, 445–475.

Abbracchio, M. P., Burnstock, G., Boeynaems, J. M., Barnard, E. A., Boyer, J. L., Kennedy, C., Knight, G. E., Fumagalli, M., Gachet, C., Jacobson, K. A., & Weisman, G. A. (2006). International Union of Pharmacology LVIII: update on the P2Y G protein-coupled nucleotide receptors: from molecular mechanisms and pathophysiology to therapy. *Pharmacological Reviews*, *58(3)*, 281–341.

Abe, R. Y., Gracitelli, C. P., Diniz-Filho, A., Tatham, A. J., & Medeiros, F. A. (2015). Lamina Cribrosa in Glaucoma: Diagnosis and Monitoring. *Current Ophthalmology Reports*, *3(2)*, 74–84.

Abraham, E. H., Prat, A. G., Gerweck, L., Seneveratne, T., Arceci, R. J., Kramer, R., Guidotti, G., & Cantiello, H. F. (1993). The multidrug resistance (mdr1) gene product functions as an ATP channel. *Proceedings of the National Academy of Sciences of the United States of America*, *90(1)*, 312–316.

Adefule-Ositelu, A. O., Adegbehingbe, B. O., Adefule, A. K., Adegbehingbe, O. O., Samaila, E., & Oladigbolu, K. (2010). Efficacy of Garcinia kola 0.5% Aqueous Eye Drops in Patients with Primary Open-Angle Glaucoma or Ocular Hypertension. *Middle East African journal of ophthalmology*, *17(1)*, 88–93.

Aden, N., Nuttall, A., Shiwen, X., de Winter, P., Leask, A., Black, C. M., Denton, C. P., Abraham, D. J., & Stratton, R. J. (2010). Epithelial cells promote fibroblast activation via IL-1alpha in systemic sclerosis. *The Journal of Investigative Dermatology*, *130*(9), 2191–2200.

Adinolfi, E., Cirillo, M., Woltersdorf, R., Falzoni, S., Chiozzi, P., Pellegatti, P., Callegari, M. G., Sandonà, D., Markwardt, F., Schmalzing, G., & Di Virgilio, F. (2010). Trophic activity of a naturally occurring truncated isoform of the P2X7 receptor. *The Federation of American Societies for Experimental Biology Journal*, *24*(9), 3393–3404.

Agarwal, R., Gupta, S. K., Agarwal, P., Saxena, R., & Agrawal, S. S. (2009). Current concepts in the pathophysiology of glaucoma. *Indian Journal of Ophthalmology*, *57*(4), 257–266.

Agrawal, P., Dulku, S., Nolan, W., & Sung, V. (2011). The UK National Cyclodiode Laser Survey. *Eye (London, England)*, *25*(2), 168–173.

Ahmad, S., Fatteh, N., El-Sherbiny, N. M., Naime, M., Ibrahim, A. S., El-Sherbini, A. M., El-Shafey, S. A., Khan, S., Fulzele, S., Gonzales, J., & Liou, G. I. (2013). Potential role of A2A adenosine receptor in traumatic optic neuropathy. *Journal of Neuroimmunology*, *264*(1-2), 54–64.

Ahmed, I., Fea, A., Au, L., Ang, R. E., Harasymowycz, P., Jampel, H. D., Samuelson, T. W., Chang, D. F., Rhee, D. J., & COMPARE Investigators (2020). A Prospective Randomized Trial Comparing Hydrus and iStent Microinvasive Glaucoma Surgery Implants for Standalone Treatment of Open-Angle Glaucoma: The COMPARE Study. *Ophthalmology*, *127*(1), 52–61.

Ahmed, I., Rhee, D. J., Jones, J., Singh, I. P., Radcliffe, N., Gazzard, G., Samuelson, T. W., Ong, J., Singh, K., & HORIZON Investigators (2021). Three-Year Findings of the

HORIZON Trial: A Schlemm Canal Microstent for Pressure Reduction in Primary Open-Angle Glaucoma and Cataract. *Ophthalmology*, 128(6), 857–865.

Aihara, M., Kuwayama, Y., Miyata, K., Ohtani, S., Ideta, R., Hashimoto, Y., Sasaki, N., & Shirato, S. (2019). Twelve-month efficacy and safety of glaucoma filtration device for surgery in patients with normal-tension glaucoma. *Japanese Journal of Ophthalmology*, 63(5), 402–409.

Aires, I. D., Boia, R., Rodrigues-Neves, A. C., Madeira, M. H., Marques, C., Ambrósio, A. F., & Santiago, A. R. (2019). Blockade of microglial adenosine A2A receptor suppresses elevated pressure-induced inflammation, oxidative stress, and cell death in retinal cells. *Glia*, 67(5), 896–914.

Alabduladhem, T.O., Bordoni, B.. Physiology, Krebs Cycle. [Updated 2021 Nov 21]. In: StatPearls [Internet]. Treasure Island (FL): *StatPearls Publishing*; 2022 Jan-. Available from: <https://www.ncbi.nlm.nih.gov/books/NBK556032/>

Albalawi, F., Lu, W., Beckel, J. M., Lim, J. C., McCaughey, S. A., & Mitchell, C. H. (2017). The P2X7 Receptor Primes IL-1 β and the NLRP3 Inflammasome in Astrocytes Exposed to Mechanical Strain. *Frontiers in Cellular Neuroscience*, 11, 227.

Albizu, L., Moreno, J. L., González-Maeso, J., & Sealfon, S. C. (2010). Heteromerization of G protein-coupled receptors: relevance to neurological disorders and neurotherapeutics. *CNS & Neurological Disorders - Drug Targets*, 9(5), 636–650.

Alkayed, F., Kashimata, M., Koyama, N., Hayashi, T., Tamura, Y., & Azuma, Y. (2012). P2Y₁₁ purinoceptor mediates the ATP-enhanced chemotactic response of rat neutrophils. *Journal of Pharmacological Sciences*, 120(4), 288–295.

Alm, A., & Nilsson, S. F. (2009). Uveoscleral outflow--a review. *Experimental Eye Research*, 88(4), 760–768.

Anderson, C. M., & Parkinson, F. E. (1997). Potential signalling roles for UTP and UDP: sources, regulation and release of uracil nucleotides. *Trends in Pharmacological Sciences*, *18*(10), 387–392.

Anderson, D. R., & Normal Tension Glaucoma Study (2003). Collaborative Normal Tension Glaucoma Study. *Current Opinion in Ophthalmology*, *14*(2), 86–90.

Anderson, D. R., Drance, S. M., Schulzer, M., & Collaborative Normal-Tension Glaucoma Study Group (2001). Natural history of normal-tension glaucoma. *Ophthalmology*, *108*(2), 247–253.

Anderson D. R. (1969). Ultrastructure of human and monkey lamina cribrosa and optic nerve head. *Archives of Ophthalmology*, *82*(6), 800–814.

Andrade, J. C. F., Kanadani, F. N., Furlanetto, R. L., Lopes, F. S., Ritch, R., & Prata, T. S. (2022). Elucidation of the role of the lamina cribrosa in glaucoma using optical coherence tomography. *Survey of ophthalmology*, *67*(1), 197–216.

Arimura, S., Miyake, S., Iwasaki, K., Gozawa, M., Matsumura, T., Takamura, Y., & Inatani, M. (2018). Randomised Clinical Trial for Postoperative Complications after Ex-PRESS Implantation versus Trabeculectomy with 2-Year Follow-Up. *Scientific Reports*, *8*(1), 16168.

Augustine, J., Pavlou, S., O'Hare, M., Harkin, K., Stitt, A., Curtis, T., Xu, H., & Chen, M. (2018). Characterization of a Spontaneously Immortalized Murine Müller Glial Cell Line QMMuC-1. *Investigative Ophthalmology & Visual Science*, *59*(3), 1666–1674.

Ayata, C. K., Ganal, S. C., Hockenjos, B., Willim, K., Vieira, R. P., Grimm, M., Robaye, B., Boeynaems, J. M., Di Virgilio, F., Pellegatti, P., Diefenbach, A., Idzko, M., & Hasselblatt, P. (2012). Purinergic P2Y₂ receptors promote neutrophil infiltration and hepatocyte death in mice with acute liver injury. *Gastroenterology*, *143*(6), 1620–1629.

Azuara-Blanco, A., Burr, J. M., Cochran, C., Ramsay, C., Vale, L., Foster, P., Friedman, D., Quayyum, Z., Lai, J., Nolan, W., Aung, T., Chew, P., McPherson, G., McDonald, A., Norrie, J., & Effectiveness in Angle-closure Glaucoma of Lens Extraction (EAGLE) Study Group (2011). The effectiveness of early lens extraction with intraocular lens implantation for the treatment of primary angle-closure glaucoma (EAGLE): study protocol for a randomized controlled trial. *Trials*, *12*, 133.

Bagur, R., & Hajnóczky, G. (2017). Intracellular Ca²⁺ Sensing: Its Role in Calcium Homeostasis and Signaling. *Molecular Cell*, *66*(6), 780–788.

Baker, N. D., Barnebey, H. S., Moster, M. R., Stiles, M. C., Vold, S. D., Khatana, A. K., Flowers, B. E., Grover, D. S., Strouthidis, N. G., Panarelli, J. F., & INN005 Study Group (2021). Ab-Externo MicroShunt versus Trabeculectomy in Primary Open-Angle Glaucoma: One-Year Results from a 2-Year Randomized, Multicenter Study. *Ophthalmology*, *128*(12), 1710–1721.

Bao, L., Locovei, S., & Dahl, G. (2004). Pannexin membrane channels are mechanosensitive conduits for ATP. *FEBS Letters*, *572*(1-3), 65–68.

Bar-David, L., & Blumenthal, E. Z. (2018). Evolution of Glaucoma Surgery in the Last 25 Years. *Rambam Maimonides Medical Journal*, *9*(3).

Barlow, H. B., Hill, R. M., & Levick, W. R. (1964). Retinal ganglion cells responding selectively to direction and speed of image motion in the rabbit. *The Journal of Physiology*, *173*(3), 377–407.

Barlow, H. B., & Levick, W. R. (1965). The mechanism of directionally selective units in rabbit's retina. *The Journal of Physiology*, *178*(3), 477–504.

Barragán-Iglesias, P., Pineda-Farias, J. B., Cervantes-Durán, C., Bravo-Hernández, M., Rocha-González, H. I., Murbartián, J., & Granados-Soto, V. (2014). Role of spinal P2Y₆

and P2Y₁₁ receptors in neuropathic pain in rats: possible involvement of glial cells. *Molecular Pain*, *10*, 29.

Baurand, A., & Gachet, C. (2003). The P2Y(1) receptor as a target for new antithrombotic drugs: a review of the P2Y(1) antagonist MRS-2179. *Cardiovascular Drug Reviews*, *21*(1), 67–76.

Bazargani, N., & Attwell, D. (2016). Astrocyte calcium signaling: the third wave. *Nature Neuroscience*, *19*(2), 182–189.

Bean B. P. (1990). ATP-activated channels in rat and bullfrog sensory neurons: concentration dependence and kinetics. *The Journal of Neuroscience*, *10*(1), 1–10.

Beckel, J. M., Argall, A. J., Lim, J. C., Xia, J., Lu, W., Coffey, E. E., Macarak, E. J., Shahidullah, M., Delamere, N. A., Zode, G. S., Sheffield, V. C., Shestopalov, V. I., Laties, A. M., & Mitchell, C. H. (2014). Mechanosensitive release of adenosine 5'-triphosphate through pannexin channels and mechanosensitive upregulation of pannexin channels in optic nerve head astrocytes: a mechanism for purinergic involvement in chronic strain. *Glia*, *62*(9), 1486–1501.

Bekő, K., Koványi, B., Göllöncsér, F., Horváth, G., Dénes, Á., Környei, Z., Botz, B., Helyes, Z., Müller, C. E., & Sperlág, B. (2017). Contribution of platelet P2Y₁₂ receptors to chronic Complete Freund's adjuvant-induced inflammatory pain. *Journal of Thrombosis and Haemostasis*, *15*(6), 1223–1235.

Bengtsson, B., Leske, M. C., Hyman, L., Heijl, A., & Early Manifest Glaucoma Trial Group (2007). Fluctuation of intraocular pressure and glaucoma progression in the early manifest glaucoma trial. *Ophthalmology*, *114*(2), 205–209.

Bengtsson, B., Leske, M. C., Yang, Z., Heijl, A., & EMGT Group (2008). Disc hemorrhages and treatment in the early manifest glaucoma trial. *Ophthalmology*, *115*(11), 2044–2048.

Benzaquen, J., Heeke, S., Janho Dit Hreich, S., Douguet, L., Marquette, C. H., Hofman, P., & Vouret-Craviari, V. (2019). Alternative splicing of P2RX7 pre-messenger RNA in health and diseases: Myth or reality?. *Biomedical Journal*, *42*(3), 141–154.

Berdahl, J. P., Allingham, R. R., & Johnson, D. H. (2008). Cerebrospinal fluid pressure is decreased in primary open-angle glaucoma. *Ophthalmology*, *115*(5), 763–768.

Berdahl, J. P., Fautsch, M. P., Stinnett, S. S., & Allingham, R. R. (2008). Intracranial pressure in primary open angle glaucoma, normal tension glaucoma, and ocular hypertension: a case-control study. *Investigative Ophthalmology & Visual Science*, *49*(12), 5412–5418.

Bernier, L. P., Ase, A. R., Boué-Grabot, E., & Séguéla, P. (2012). P2X4 receptor channels form large noncytolytic pores in resting and activated microglia. *Glia*, *60*(5), 728–737.

Berridge, M. J., Lipp, P., & Bootman, M. D. (2000). The versatility and universality of calcium signalling. *Nature Reviews Molecular Cell Biology*, *1*(1), 11–21.

Bersudsky, M., Luski, L., Fishman, D., White, R. M., Ziv-Sokolovskaya, N., Dotan, S., Rider, P., Kaplanov, I., Aychek, T., Dinarello, C. A., Apte, R. N., & Voronov, E. (2014). Non-redundant properties of IL-1 α and IL-1 β during acute colon inflammation in mice. *Gut*, *63*(4), 598–609.

Beynon, S. B., & Walker, F. R. (2012). Microglial activation in the injured and healthy brain: what are we really talking about? Practical and theoretical issues associated with the measurement of changes in microglial morphology. *Neuroscience*, *225*, 162–171.

Bhartiya, S., & Ichhpujani, P. (2014). Complementary and Alternate Management of Glaucoma: The Verdict so Far. *Journal of Current Glaucoma Practice*, *8*(2), 54–57.

Bianchi, G., Vuerich, M., Pellegatti, P., Marimpietri, D., Emionite, L., Marigo, I., Bronte, V., Di Virgilio, F., Pistoia, V., & Raffaghello, L. (2014). ATP/P2X7 axis modulates myeloid-derived suppressor cell functions in neuroblastoma microenvironment. *Cell Death & Disease*, 5(3).

Biber, K., Tsuda, M., Tozaki-Saitoh, H., Tsukamoto, K., Toyomitsu, E., Masuda, T., Boddeke, H., & Inoue, K. (2011). Neuronal CCL21 up-regulates microglia P2X4 expression and initiates neuropathic pain development. *The EMBO Journal*, 30, 1864–1873.

Bill A. (2003). Some thoughts on the pressure dependence of uveoscleral flow. *Journal of Glaucoma*, 12(1), 88–94.

Bill, A., & Hellsing, K. (1965). Production and Drainage of Aqueous Humor in the Cynomolgus Monkey (*Macaca irus*). *Investigative Ophthalmology & Visual Science*, 4(5), 920–926.

Bodin, P., & Burnstock, G. (2001). Purinergic signalling: ATP release. *Neurochemical Research*, 26(8-9), 959–969.

Boia, R., Salinas-Navarro, M., Gallego-Ortega, A., Galindo-Romero, C., Aires, I. D., Agudo-Barriuso, M., Ambrósio, A. F., Vidal-Sanz, M., & Santiago, A. R. (2020). Activation of adenosine A3 receptor protects retinal ganglion cells from degeneration induced by ocular hypertension. *Cell Death & Disease*, 11(5), 401.

Boldt, W., Klapperstück, M., Büttner, C., Sadtler, S., Schmalzing, G., & Markwardt, F. (2003). Glu496Ala polymorphism of human P2X7 receptor does not affect its electrophysiological phenotype. *American Journal of Physiology - Cell Physiology*, 284(3), 749–756.

Bonora, M., Patergnani, S., Rimessi, A., De Marchi, E., Suski, J. M., Bononi, A., Giorgi, C., Marchi, S., Missiroli, S., Poletti, F., Wieckowski, M. R., & Pinton, P. (2012). ATP synthesis and storage. *Purinergic Signalling*, 8(3), 343–357.

Boraschi, D., & Tagliabue, A. (2013). The interleukin-1 receptor family. *Seminars in Immunology*, 25(6), 394–407.

Bourne R. R. (2012). The optic nerve head in glaucoma. *Community Eye Health*, 25(79-80), 55–57.

Braddock, M., & Quinn, A. (2004). Targeting IL-1 in inflammatory disease: new opportunities for therapeutic intervention. *Nature reviews. Drug Discovery*, 3(4), 330–339.

Bradley, H. J., Baldwin, J. M., Goli, G. R., Johnson, B., Zou, J., Sivaprasadarao, A., Baldwin, S. A., & Jiang, L. H. (2011). Residues 155 and 348 contribute to the determination of P2X7 receptor function via distinct mechanisms revealed by single-nucleotide polymorphisms. *The Journal of Biological Chemistry*, 286(10), 8176–8187.

Brake, A. J., Wagenbach, M. J., & Julius, D. (1994). New structural motif for ligand-gated ion channels defined by an ionotropic ATP receptor. *Nature*, 371(6497), 519–523.

Brightbill, H. D., Plevy, S. E., Modlin, R. L., & Smale, S. T. (2000). A prominent role for Sp1 during lipopolysaccharide-mediated induction of the IL-10 promoter in macrophages. *Journal of Immunology*, 164(4), 1940–1951.

Bringmann, A., Pannicke, T., Grosche, J., Francke, M., Wiedemann, P., Skatchkov, S. N., Osborne, N. N., & Reichenbach, A. (2006). Müller cells in the healthy and diseased retina. *Progress in Retinal and Eye Research*, 25(4), 397–424.

Bringmann, A., Iandiev, I., Pannicke, T., Wurm, A., Hollborn, M., Wiedemann, P., Osborne, N. N., & Reichenbach, A. (2009). Cellular signaling and factors involved in Müller cell gliosis: neuroprotective and detrimental effects. *Progress in Retinal and Eye Research*, 28(6), 423–451.

Bringmann, A., Pannicke, T., Moll, V., Milenkovic, I., Faude, F., Enzmann, V., Wolf, S., & Reichenbach, A. (2001). Upregulation of P2X(7) receptor currents in Müller glial cells during proliferative vitreoretinopathy. *Investigative Ophthalmology & Visual Science*, 42(3), 860–867.

Bringmann, A., Pannicke, T., Weick, M., Biedermann, B., Uhlmann, S., Kohlen, L., Wiedemann, P., & Reichenbach, A. (2002). Activation of P2Y receptors stimulates potassium and cation currents in acutely isolated human Müller (glial) cells. *Glia*, 37(2), 139–152.

Browne, L. E., Compan, V., Bragg, L., & North, R. A. (2013). P2X7 receptor channels allow direct permeation of nanometer-sized dyes. *The Journal of Neuroscience*, 33(8), 3557–3566.

Brubaker R. F. (2001). Measurement of uveoscleral outflow in humans. *Journal of Glaucoma*, 10(5 Suppl 1), S45–S48.

Budenz, D. L., Anderson, D. R., Feuer, W. J., Beiser, J. A., Schiffman, J., Parrish, R. K., 2nd, Piltz-Seymour, J. R., Gordon, M. O., Kass, M. A., & Ocular Hypertension Treatment Study Group (2006). Detection and prognostic significance of optic disc hemorrhages during the Ocular Hypertension Treatment Study. *Ophthalmology*, 113(12), 2137–2143.

Burnstock, G., Campbell, G., Satchell, D., & Smythe, A. (1970). Evidence that adenosine triphosphate or a related nucleotide is the transmitter substance released by non-adrenergic inhibitory nerves in the gut. *British Journal of Pharmacology*, 40(4), 668–688.

Burnstock, G., & Verkhratsky, A. (2010). Long-term (trophic) purinergic signalling: purinoceptors control cell proliferation, differentiation and death. *Cell Death & Disease*, 1(1).

Burnstock G. (2012). Purinergic signalling: Its unpopular beginning, its acceptance and its exciting future. *BioEssays*, 34(3), 218–225.

Burnstock G. (2006). Pathophysiology and therapeutic potential of purinergic signaling. *Pharmacological Reviews*, 58(1), 58–86.

Burnstock G. (1978). A basis for distinguishing two types of purinergic receptor. *Chemistry*.

Burnstock, G., & Kennedy, C. (1985). Is there a basis for distinguishing two types of P2-purinoceptor?. *General Pharmacology*, 16(5), 433–440.

Burnstock, G., Nistri, A., Khakh, B. S., & Giniatullin, R. (2014). ATP-gated P2X receptors in health and disease. *Frontiers in Cellular Neuroscience*, 8, 204.

Burnstock, G., & Kennedy, C. (2011). P2X receptors in health and disease. *Advances in Pharmacology*, 61, 333–372.

Burnstock G. (2014). Purinergic signalling: from discovery to current developments. *Experimental Physiology*, 99(1), 16–34.

Burnstock, G., & Knight, G. E. (2004). Cellular distribution and functions of P2 receptor subtypes in different systems. *International Review of Cytology*, 240, 31–304.

Burnstock G. (2007). Purine and pyrimidine receptors. *Cellular and Molecular Life Sciences*, 64(12), 1471–1483.

Cabrini, G., Falzoni, S., Forchap, S. L., Pellegatti, P., Balboni, A., Agostini, P., Cuneo, A., Castoldi, G., Baricordi, O. R., & Di Virgilio, F. (2005). A His-155 to Tyr polymorphism confers gain-of-function to the human P2X7 receptor of human leukemic lymphocytes. *Journal of Immunology*, *175*(1), 82–89.

Cairns J. E. (1970). Trabeculectomy for chronic simple open-angle glaucoma. *Transactions of the Ophthalmological Societies of the United Kingdom*, *89*, 481–490.

Cairns J. E. (1969). Trabeculectomy. Sub-title: "a surgical method of reducing intra-ocular pressure in chronic simple glaucoma without sub-conjunctival drainage of aqueous humour". *Transactions of the Ophthalmological Societies of the United Kingdom*, *88*, 231–233.

Cairns J. E. (1968). Trabeculectomy. Preliminary report of a new method. *American Journal of Ophthalmology*, *66*(4), 673–679.

Calovi, S., Mut-Arbona, P., & Sperlágh, B. (2019). Microglia and the Purinergic Signaling System. *Neuroscience*, *405*, 137–147.

Canadananović, V., Latinović, S., Barišić, S., Babić, N., & Jovanović, S. (2015). Age-related changes of vitamin C levels in aqueous humour. *Vojnosanitetski pregled*, *72*(9), 823–826.

Carson, M. J., Doose, J. M., Melchior, B., Schmid, C. D., & Ploix, C. C. (2006). CNS immune privilege: hiding in plain sight. *Immunological Reviews*, *213*, 48–65.

Carter, M. and Shieh, J., 2014. Guide to Research Techniques in Neuroscience. *Journal of Undergraduate Neuroscience Education*, *13*(1).

Carter, R. L., Fricks, I. P., Barrett, M. O., Burianek, L. E., Zhou, Y., Ko, H., Das, A., Jacobson, K. A., Lazarowski, E. R., & Harden, T. K. (2009). Quantification of Gi-

mediated inhibition of adenylyl cyclase activity reveals that UDP is a potent agonist of the human P2Y₁₄ receptor. *Molecular Pharmacology*, 76(6), 1341–1348.

Caseley, E. A., Muench, S. P., Roger, S., Mao, H. J., Baldwin, S. A., & Jiang, L. H. (2014). Non-synonymous single nucleotide polymorphisms in the P2X receptor genes: association with diseases, impact on receptor functions and potential use as diagnosis biomarkers. *International Journal of Molecular Sciences*, 15(8), 13344–13371.

Caspi, R. R., & Roberge, F. G. (1989). Glial cells as suppressor cells: characterization of the inhibitory function. *Journal of Autoimmunity*, 2(5), 709–722.

Cattaneo M. (2011). The platelet P2Y₁₂ receptor for adenosine diphosphate: congenital and drug-induced defects. *Blood*, 117(7), 2102–2112.

Cellini, M., Possati, G. L., Profazio, V., Sbrocca, M., Caramazza, N., & Caramazza, R. (1997). Color Doppler imaging and plasma levels of endothelin-1 in low-tension glaucoma. *Acta Ophthalmologica Scandinavica. Supplement*, (224), 11–13.

Chadet, S., Ivanes, F., Benoist, L., Salmon-Gandonnière, C., Guibon, R., Velge-Roussel, F., Babuty, D., Baron, C., Roger, S., & Angoulvant, D. (2015). Hypoxia/Reoxygenation Inhibits P2Y₁₁ Receptor Expression and Its Immunosuppressive Activity in Human Dendritic Cells. *Journal of Immunology*, 195(2), 651–660.

Chambers, J. K., Macdonald, L. E., Sarau, H. M., Ames, R. S., Freeman, K., Foley, J. J., Zhu, Y., McLaughlin, M. M., Murdock, P., McMillan, L., Trill, J., Swift, A., Aiyar, N., Taylor, P., Vawter, L., Naheed, S., Szekeres, P., Hervieu, G., Scott, C., Watson, J. M., ... Livi, G. P. (2000). A G protein-coupled receptor for UDP-glucose. *The Journal of Biological Chemistry*, 275(15), 10767–10771.

Chan, M., Broadway, D. C., Khawaja, A. P., Yip, J., Garway-Heath, D. F., Burr, J. M., Luben, R., Hayat, S., Dalzell, N., Khaw, K. T., & Foster, P. J. (2017). Glaucoma and

intraocular pressure in EPIC-Norfolk Eye Study: cross sectional study. *BMJ (Clinical research ed.)*, 358.

Chandra, D. B., Varma, R., Ahmad, S., & Varma, S. D. (1986). Vitamin C in the human aqueous humor and cataracts. *International journal for vitamin and nutrition research. Internationale Zeitschrift für Vitamin- und Ernährungsforschung*, 56(2), 165–168.

Chaudhry, R., Varacallo, M., Biochemistry, Glycolysis. [Updated 2021 Aug 17]. In: StatPearls [Internet]. Treasure Island (FL): *StatPearls Publishing*; 2022 Jan-. Available from: <https://www.ncbi.nlm.nih.gov/books/NBK482303/>

Cheewatrakoolpong, B., Gilchrest, H., Anthes, J. C., & Greenfeder, S. (2005). Identification and characterization of splice variants of the human P2X7 ATP channel. *Biochemical and Biophysical Research Communications*, 332(1), 17–27.

Chen, Z., Jalabi, W., Hu, W., Park, H. J., Gale, J. T., Kidd, G. J., Bernatowicz, R., Gossman, Z. C., Chen, J. T., Dutta, R., & Trapp, B. D. (2014). Microglial displacement of inhibitory synapses provides neuroprotection in the adult brain. *Nature Communications*, 5, 4486.

Chen, T. C., Bhatia, L. S., Halpern, E. F., & Walton, D. S. (2006). Risk factors for the development of aphakic glaucoma after congenital cataract surgery. *Journal of Pediatric Ophthalmology and Strabismus*, 43(5), 274–307.

Chen, T. C., Walton, D. S., & Bhatia, L. S. (2004). Aphakic glaucoma after congenital cataract surgery. *Archives of Ophthalmology*, 122(12), 1819–1825.

Chikanza, I. C., Kingsley, G., & Panayi, G. S. (1995). Peripheral blood and synovial fluid monocyte expression of interleukin 1 alpha and 1 beta during active rheumatoid arthritis. *The Journal of Rheumatology*, 22(4), 600–606.

- Chițu, I., Voinea, L. M., Istrate, S., Vrapciu, A., Ciuluvică, R. C., & Tudosescu, R. (2019). The neuroprotective role of citicoline treatment in glaucoma - 6 months results of a prospective therapeutic trial. *Romanian Journal of Ophthalmology*, *63*(3), 222–230.
- Choi, A. J., & Ryter, S. W. (2014). Inflammasomes: molecular regulation and implications for metabolic and cognitive diseases. *Molecules and Cells*, *37*(6), 441–448.
- Choi, D. W., Maulucci-Gedde, M., & Kriegstein, A. R. (1987). Glutamate neurotoxicity in cortical cell culture. *The Journal of Neuroscience*, *7*(2), 357–368.
- Choi, R. C., Simon, J., Tsim, K. W., & Barnard, E. A. (2008). Constitutive and agonist-induced dimerizations of the P2Y₁ receptor: relationship to internalization and scaffolding. *The Journal of Biological Chemistry*, *283*(16), 11050–11063.
- Choquet, H., Thai, K. K., Yin, J., Hoffmann, T. J., Kvale, M. N., Banda, Y., Schaefer, C., Risch, N., Nair, K. S., Melles, R., & Jorgenson, E. (2017). A large multi-ethnic genome-wide association study identifies novel genetic loci for intraocular pressure. *Nature Communications*, *8*(1), 2108.
- Chow, J., Hutnik, C., Solo, K., & Malvankar-Mehta, M. S. (2017). When Is Evidence Enough Evidence? A Systematic Review and Meta-Analysis of the Trabectome as a Solo Procedure in Patients with Primary Open-Angle Glaucoma. *Journal of Ophthalmology*, *2017*, 2965725.
- Chowdhury, U. R., Madden, B. J., Charlesworth, M. C., & Fautsch, M. P. (2010). Proteome analysis of human aqueous humor. *Investigative Ophthalmology & Visual Science*, *51*(10), 4921–4931.
- Chua, J., Vania, M., Cheung, C. M., Ang, M., Chee, S. P., Yang, H., Li, J., & Wong, T. T. (2012). Expression profile of inflammatory cytokines in aqueous from glaucomatous eyes. *Molecular Vision*, *18*, 431–438.

Cieślak, M., Wojtczak, A., & Komoszyński, M. (2017). Role of the purinergic signaling in epilepsy. *Pharmacological Reports*, 69(1), 130–138.

Cleland, B. G., Dubin, M. W., & Levick, W. R. (1971). Sustained and transient neurones in the cat's retina and lateral geniculate nucleus. *The Journal of Physiology*, 217(2), 473–496.

Coca-Prados M. (2014). The blood-aqueous barrier in health and disease. *Journal of Glaucoma*, 23(8 Suppl 1), S36–S38.

Cohen, I., Rider, P., Carmi, Y., Braiman, A., Dotan, S., White, M. R., Voronov, E., Martin, M. U., Dinarello, C. A., & Apte, R. N. (2010). Differential release of chromatin-bound IL-1 α discriminates between necrotic and apoptotic cell death by the ability to induce sterile inflammation. *Proceedings of the National Academy of Sciences of the United States of America*, 107(6), 2574–2579.

Cohen, R., Shainberg, A., Hochhauser, E., Cheporko, Y., Tobar, A., Birk, E., Pinhas, L., Leipziger, J., Don, J., & Porat, E. (2011). UTP reduces infarct size and improves mice heart function after myocardial infarct via P2Y₂ receptor. *Biochemical Pharmacology*, 82(9), 1126–1133.

Coleman A. L. (2012). Advances in Glaucoma Treatment and Management: Surgery. *Investigative Ophthalmology & Visual Science*, 53(5), 2491–2494.

Collaborative Normal-Tension Glaucoma Study Group. (1998). The effectiveness of intraocular pressure reduction in the treatment of normal-tension glaucoma. *American Journal of Ophthalmology*, 126(4), 498–505.

Collison, D. J., Tovell, V. E., Coombes, L. J., Duncan, G., & Sanderson, J. (2005). Potentiation of ATP-induced Ca²⁺ mobilisation in human retinal pigment epithelial cells. *Experimental Eye Research*, 80(4), 465–475.

Colton C. A. (2009). Heterogeneity of microglial activation in the innate immune response in the brain. *Journal of Neuroimmune Pharmacology*, 4(4), 399–418.

Communi, D., Gonzalez, N. S., Detheux, M., Brézillon, S., Lannoy, V., Parmentier, M., & Boeynaems, J. M. (2001). Identification of a novel human ADP receptor coupled to G(i). *The Journal of Biological Chemistry*, 276(44), 41479–41485.

Corraliza I. (2014). Recruiting specialized macrophages across the borders to restore brain functions. *Frontiers in Cellular Neuroscience*, 8, 262.

Corriden, R., & Insel, P. A. (2010). Basal release of ATP: an autocrine-paracrine mechanism for cell regulation. *Science Signaling*, 3(104).

Costagliola, C., dell'Omo, R., Agnifili, L., Bartollino, S., Fea, A. M., Uva, M. G., Zeppa, L., & Mastropasqua, L. (2020). How many aqueous humor outflow pathways are there?. *Survey of Ophthalmology*, 65(2), 144–170.

Cousins, S. W., McCabe, M. M., Danielpour, D., & Streilein, J. W. (1991). Identification of transforming growth factor-beta as an immunosuppressive factor in aqueous humor. *Investigative Ophthalmology & Visual Science*, 32(8), 2201–2211.

Cressman, V. L., Lazarowski, E., Homolya, L., Boucher, R. C., Koller, B. H., & Grubb, B. R. (1999). Effect of loss of P2Y(2) receptor gene expression on nucleotide regulation of murine epithelial Cl(-) transport. *The Journal of Biological Chemistry*, 274(37), 26461–26468.

Cristóvão-Ferreira, S., Navarro, G., Brugarolas, M., Pérez-Capote, K., Vaz, S. H., Fattorini, G., Conti, F., Lluís, C., Ribeiro, J. A., McCormick, P. J., Casadó, V., Franco, R., & Sebastião, A. M. (2013). A1R-A2AR heteromers coupled to Gs and G i/o proteins modulate GABA transport into astrocytes. *Purinergic Signalling*, 9(3), 433–449.

Cuenca, N., Fernández-Sánchez, L., Campello, L., Maneu, V., De la Villa, P., Lax, P., & Pinilla, I. (2014). Cellular responses following retinal injuries and therapeutic approaches for neurodegenerative diseases. *Progress in Retinal and Eye Research, 43*, 17–75.

Cunha-Vaz, J., Bernardes, R., & Lobo, C. (2011). Blood-retinal barrier. *European Journal of Ophthalmology, 21 Suppl 6*, S3–S9.

Cunha-Vaz, J. G., Shakib, M., & Ashton, N. (1966). Studies on the permeability of the blood-retinal barrier. I. On the existence, development, and site of a blood-retinal barrier. *The British Journal of Ophthalmology, 50*(8), 441–453.

Cunha-Vaz, J. G., & Maurice, D. M. (1967). The active transport of fluorescein by the retinal vessels and the retina. *The Journal of Physiology, 191*(3), 467–486.

Curet, M. A., & Watters, J. J. (2018). P2Y₁₄ receptor activation decreases interleukin-6 production and glioma GL261 cell proliferation in microglial transwell cultures. *Journal of Neuro-oncology, 137*(1), 23–31.

Dahan, E., Ben Simon, G. J., & Lafuma, A. (2012). Comparison of trabeculectomy and Ex-PRESS implantation in fellow eyes of the same patient: a prospective, randomised study. *Eye (London, England), 26*(5), 703–710.

Daly, J.W., 1985. Adenosine receptors. *Adv Cyclic Nucleotide Protein Phosphorylation Res, 19*, pp.29-46.

de Diego García, L., Sebastián-Serrano, Á., Hernández, I. H., Pintor, J., Lucas, J. J., & Díaz-Hernández, M. (2018). The regulation of proteostasis in glial cells by nucleotide receptors is key in acute neuroinflammation. *FASEB Journal, 32*(6), 3020–3032.

de Jong L. A. (2009). The Ex-PRESS glaucoma shunt versus trabeculectomy in open-angle glaucoma: a prospective randomized study. *Advances in Therapy*, 26(3), 336–345.

de Waal Malefyt, R., Haanen, J., Spits, H., Roncarolo, M. G., te Velde, A., Figdor, C., Johnson, K., Kastelein, R., Yssel, H., & de Vries, J. E. (1991). Interleukin 10 (IL-10) and viral IL-10 strongly reduce antigen-specific human T cell proliferation by diminishing the antigen-presenting capacity of monocytes via downregulation of class II major histocompatibility complex expression. *The Journal of Experimental Medicine*, 174(4), 915–924.

de Zeeuw, D., Akizawa, T., Agarwal, R., Audhya, P., Bakris, G. L., Chin, M., Krauth, M., Lambers Heerspink, H. J., Meyer, C. J., McMurray, J. J., Parving, H. H., Pergola, P. E., Remuzzi, G., Toto, R. D., Vaziri, N. D., Wanner, C., Warnock, D. G., Wittes, J., & Chertow, G. M. (2013). Rationale and trial design of Bardoxolone Methyl Evaluation in Patients with Chronic Kidney Disease and Type 2 Diabetes: the Occurrence of Renal Events (BEACON). *American Journal of Nephrology*, 37(3), 212–222.

Deleuran, B. W., Chu, C. Q., Field, M., Brennan, F. M., Katsikis, P., Feldmann, M., & Maini, R. N. (1992). Localization of interleukin-1 alpha, type 1 interleukin-1 receptor and interleukin-1 receptor antagonist in the synovial membrane and cartilage/pannus junction in rheumatoid arthritis. *British Journal of Rheumatology*, 31(12), 801–809.

Deng, Z., Li, C., Liu, C., Du, E., & Xu, C. (2018). Catestatin is involved in neuropathic pain mediated by purinergic receptor P2X₄ in the spinal microglia of rats. *Brain research bulletin*, 142, 138–146.

Denniston, A. and Murray, P., 2018. *Oxford handbook of Ophthalmology*. 4th ed. United Kingdom: Oxford University Press.

Denlinger, L. C., Coursin, D. B., Schell, K., Angelini, G., Green, D. N., Guadarrama, A. G., Halsey, J., Prabhu, U., Hogan, K. J., & Bertics, P. J. (2006). Human P2X7 pore function predicts allele linkage disequilibrium. *Clinical Chemistry*, 52(6), 995–1004.

Department of Health., 1998. *Free NHS sight tests for close relatives of people who have glaucoma*. DoH: London

Deshpande, O.A., Mohiuddin, S.S. Biochemistry, Oxidative Phosphorylation. [Updated 2021 Aug 3]. In: StatPearls [Internet]. Treasure Island (FL): StatPearls Publishing; 2022 Jan-. Available from: <https://www.ncbi.nlm.nih.gov/books/NBK553192/>

Dhyani, V., Gare, S., Gupta, R. K., Swain, S., Venkatesh, K. V., & Giri, L. (2020). GPCR mediated control of calcium dynamics: A systems perspective. *Cellular Signalling*, 74, 109717.

Di Paolo, N. C., & Shayakhmetov, D. M. (2016). Interleukin 1 α and the inflammatory process. *Nature Immunology*, 17(8), 906–913.

Di Virgilio F. (1998). ATP as a death factor. *BioFactors (Oxford, England)*, 8(3-4), 301–303.

Díaz-Coránguez, M., Ramos, C., & Antonetti, D. A. (2017). The inner blood-retinal barrier: Cellular basis and development. *Vision Research*, 139, 123–137.

Dickinson, J. C., Durham, D. G., & Hamilton, P. B. (1968). Ion exchange chromatography of free amino acids in aqueous fluid and lens of the human eye. *Investigative Ophthalmology*, 7(5), 551–563.

Dielemans, I., Vingerling, J. R., Wolfs, R. C., Hofman, A., Grobbee, D. E., & de Jong, P. T. (1994). The prevalence of primary open-angle glaucoma in a population-based

study in The Netherlands. The Rotterdam Study. *Ophthalmology*, 101(11), 1851–1855.

Dinarello C. A. (1996). Biologic basis for interleukin-1 in disease. *Blood*, 87(6), 2095–2147.

Dinarello C. A. (1997). Induction of interleukin-1 and interleukin-1 receptor antagonist. *Seminars in Oncology*, 24(3 Suppl 9), 9–93.

Dinarello C. A. (2004). Therapeutic strategies to reduce IL-1 activity in treating local and systemic inflammation. *Current Opinion in Pharmacology*, 4(4), 378–385.

Dinarello C. A. (2007). Interleukin-18 and the pathogenesis of inflammatory diseases. *Seminars in Nephrology*, 27(1), 98–114.

Dinarello C. A. (2009). Immunological and inflammatory functions of the interleukin-1 family. *Annual Review of Immunology*, 27, 519–550.

Dinarello C. A. (2011). A clinical perspective of IL-1 β as the gatekeeper of inflammation. *European Journal of Immunology*, 41(5), 1203–1217.

Dinarello C. A. (2018). Overview of the IL-1 family in innate inflammation and acquired immunity. *Immunological Reviews*, 281(1), 8–27.

Dinarello, C. A., Simon, A., & van der Meer, J. W. (2012). Treating inflammation by blocking interleukin-1 in a broad spectrum of diseases. *Nature Reviews. Drug Discovery*, 11(8), 633–652.

Ding, L., & Shevach, E. M. (1992). IL-10 inhibits mitogen-induced T cell proliferation by selectively inhibiting macrophage costimulatory function. *Journal of Immunology*, 148(10), 3133–3139.

Dong, Z., Saikumar, P., Weinberg, J. M., & Venkatachalam, M. A. (2006). Calcium in cell injury and death. *Annual Review of Pathology, 1*, 405–434.

Donnelly-Roberts, D. L., & Jarvis, M. F. (2007). Discovery of P2X7 receptor-selective antagonists offers new insights into P2X7 receptor function and indicates a role in chronic pain states. *British Journal of Pharmacology, 151*(5), 571–579.

Donnelly-Roberts, D. L., Namovic, M. T., Han, P., & Jarvis, M. F. (2009). Mammalian P2X7 receptor pharmacology: comparison of recombinant mouse, rat and human P2X7 receptors. *British Journal of Pharmacology, 157*(7), 1203–1214.

Downs, J. C., & Girkin, C. A. (2017). Lamina cribrosa in glaucoma. *Current Opinion in Ophthalmology, 28*(2), 113–119.

Drance, S., Anderson, D. R., Schulzer, M., & Collaborative Normal-Tension Glaucoma Study Group (2001). Risk factors for progression of visual field abnormalities in normal-tension glaucoma. *American Journal of Ophthalmology, 131*(6), 699–708.

Drance S. M. (1999). The Collaborative Normal-Tension Glaucoma Study and some of its lessons. *Canadian Journal of Ophthalmology. Journal Canadien d'Ophthalmologie, 34*(1), 1–6.

Drance S. M. (2004). Some clinical implications of the collaborative normal tension glaucoma study. *Klinika Oczna, 106*(4-5), 588–592.

Drance, S. M., Sweeney, V. P., Morgan, R. W., & Feldman, F. (1973). Studies of factors involved in the production of low tension glaucoma. *Archives of Ophthalmology, 89*(6), 457–465.

Drescher, K. M., & Whittum-Hudson, J. A. (1996). Modulation of immune-associated surface markers and cytokine production by murine retinal glial cells. *Journal of Neuroimmunology, 64*(1), 71–81.

Dubyak G. R. (2007). Go it alone no more--P2X7 joins the society of heteromeric ATP-gated receptor channels. *Molecular Pharmacology*, 72(6), 1402–1405.

Dvorianchikova, G., Ivanov, D., Panchin, Y., & Shestopalov, V. I. (2006). Expression of pannexin family of proteins in the retina. *FEBS Letters*, 580(9), 2178–2182.

Egan, T. M., & Khakh, B. S. (2004). Contribution of calcium ions to P2X channel responses. *The Journal of Neuroscience*, 24(13), 3413–3420.

Ekşioğlu, Ü., Yakın, M., Balta, Ö., Şingar-Özdemir, E., Hüsniye Telek, H., Örnek, F., & Yalvaç, I. (2018). The Profile and Management of Glaucoma in Adult Aphakic Patients Following Complicated Cataract Surgery. *Turkish Journal of Ophthalmology*, 48(1), 19–22.

Eltzschig, H. K., Eckle, T., Mager, A., Küper, N., Karcher, C., Weissmüller, T., Boengler, K., Schulz, R., Robson, S. C., & Colgan, S. P. (2006). ATP release from activated neutrophils occurs via connexin 43 and modulates adenosine-dependent endothelial cell function. *Circulation Research*, 99(10), 1100–1108.

Emery, J. M., Landis, D., Paton, D., Boniuk, M., & Craig, J. M. (1974). The lamina cribrosa in normal and glaucomatous human eyes. *Transactions - American Academy of Ophthalmology and Otolaryngology. American Academy of Ophthalmology and Otolaryngology*, 78(2), 290–297.

Encyclopædia Britannica. 2021. *Cross section of the human eye*. [online] Available at: <<https://kids.britannica.com/students/assembly/view/100415>> [Accessed 30 December 2021].

Eskdale, J., Wordsworth, P., Bowman, S., Field, M., & Gallagher, G. (1997). Association between polymorphisms at the human IL-10 locus and systemic lupus erythematosus. *Tissue antigens*, 49(6), 635–639. European Glaucoma Society

Terminology and Guidelines for Glaucoma, 4th Edition. (2017). *The British Journal of Ophthalmology*, 101(5), 73–127.

Evans, R. J., Lewis, C., Virginio, C., Lundstrom, K., Buell, G., Surprenant, A., & North, R. A. (1996). Ionic permeability of, and divalent cation effects on, two ATP-gated cation channels (P2X receptors) expressed in mammalian cells. *The Journal of Physiology*, 497(Pt 2), 413–422.

Fakhraie, G., Parvini, F., Ghanavi, J., Saif, S., & Farnia, P. (2020). Association of IL-10 gene promoter polymorphisms with susceptibility to pseudoexfoliation syndrome, pseudoexfoliative and primary open-angle glaucoma. *BMC Medical Genetics*, 21(1), 32.

Fea A. M. (2010). Phacoemulsification versus phacoemulsification with micro-bypass stent implantation in primary open-angle glaucoma: randomized double-masked clinical trial. *Journal of Cataract and Refractive Surgery*, 36(3), 407–412.

Fea, A. M., Consolandi, G., Zola, M., Pignata, G., Cannizzo, P., Lavia, C., Rolle, T., & Grignolo, F. M. (2015). Micro-Bypass Implantation for Primary Open-Angle Glaucoma Combined with Phacoemulsification: 4-Year Follow-Up. *Journal of Ophthalmology*, 2015, 795357.

Feng, Y. H., Li, X., Zeng, R., & Gorodeski, G. I. (2006). Endogenously expressed truncated P2X7 receptor lacking the C-terminus is preferentially upregulated in epithelial cancer cells and fails to mediate ligand-induced pore formation and apoptosis. *Nucleosides, Nucleotides & Nucleic Acids*, 25(9-11), 1271–1276.

Ferrari, D., Pizzirani, C., Adinolfi, E., Lemoli, R. M., Curti, A., Idzko, M., Panther, E., & Di Virgilio, F. (2006). The P2X7 receptor: a key player in IL-1 processing and release. *Journal of Immunology*, 176(7), 3877–3883.

Ferrari, D., La Sala, A., Chiozzi, P., Morelli, A., Falzoni, S., Girolomoni, G., Idzko, M., Dichmann, S., Norgauer, J., & Di Virgilio, F. (2000). The P2 purinergic receptors of human dendritic cells: identification and coupling to cytokine release. *FASEB Journal*, *14*(15), 2466–2476.

Fields, R. D., & Burnstock, G. (2006). Purinergic signalling in neuron-glia interactions. *Nature Reviews. Neuroscience*, *7*(6), 423–436.

Fiorentino, D. F., Zlotnik, A., Vieira, P., Mosmann, T. R., Howard, M., Moore, K. W., & O'Garra, A. (1991). IL-10 acts on the antigen-presenting cell to inhibit cytokine production by Th1 cells. *Journal of Immunology*, *146*(10), 3444–3451.

Fitz J. G. (2007). Regulation of cellular ATP release. *Transactions of the American Clinical and Climatological Association*, *118*, 199–208.

Flaxman, S. R., Bourne, R., Resnikoff, S., Ackland, P., Braithwaite, T., Cicinelli, M. V., Das, A., Jonas, J. B., Keeffe, J., Kempen, J. H., Leasher, J., Limburg, H., Naidoo, K., Pesudovs, K., Silvester, A., Stevens, G. A., Tahhan, N., Wong, T. Y., Taylor, H. R., & Vision Loss Expert Group of the Global Burden of Disease Study (2017). Global causes of blindness and distance vision impairment 1990-2020: a systematic review and meta-analysis. *The Lancet. Global Health*, *5*(12), e1221–e1234.

Fleming, S. B., McCaughan, C. A., Andrews, A. E., Nash, A. D., & Mercer, A. A. (1997). A homolog of interleukin-10 is encoded by the poxvirus orf virus. *Journal of Virology*, *71*(6), 4857–4861.

Fontana, L., Bhandari, A., Fitzke, F. W., & Hitchings, R. A. (1998). In vivo morphometry of the lamina cribrosa and its relation to visual field loss in glaucoma. *Current Eye Research*, *17*(4), 363–369.

Ford, A. P., Gever, J. R., Nunn, P. A., Zhong, Y., Cefalu, J. S., Dillon, M. P., & Cockayne, D. A. (2006). Purinoceptors as therapeutic targets for lower urinary tract dysfunction. *British Journal of Pharmacology*, *147 Suppl 2*(Suppl 2), 132–143.

Foster, P. S., Tay, H. L., & Hogan, S. P. (2021). Uridine diphosphate-glucose/P2Y₁₄R axis is a nonchemokine pathway that selectively promotes eosinophil accumulation. *The Journal of Clinical Investigation*, *131*(7), e147735.

Francke, M., Makarov, F., Kacza, J., Seeger, J., Wendt, S., Gärtner, U., Faude, F., Wiedemann, P., & Reichenbach, A. (2001). Retinal pigment epithelium melanin granules are phagocytosed by Müller glial cells in experimental retinal detachment. *Journal of Neurocytology*, *30*(2), 131–136.

Franke, H., & Illes, P. (2014). Nucleotide signaling in astrogliosis. *Neuroscience Letters*, *565*, 14–22.

Franke, H., & Illes, P. (2006). Involvement of P2 receptors in the growth and survival of neurons in the CNS. *Pharmacology & Therapeutics*, *109*(3), 297–324.

Franze, K., Grosche, J., Skatchkov, S. N., Schinkinger, S., Foja, C., Schild, D., Uckermann, O., Travis, K., Reichenbach, A., & Guck, J. (2007). Muller cells are living optical fibers in the vertebrate retina. *Proceedings of the National Academy of Sciences of the United States of America*, *104*(20), 8287–8292.

Fredholm, B. B., IJzerman, A. P., Jacobson, K. A., Klotz, K. N., & Linden, J. (2001). International Union of Pharmacology. XXV. Nomenclature and classification of adenosine receptors. *Pharmacological Reviews*, *53*(4), 527–552.

Freedman, J., & Iserovich, P. (2013). Pro-inflammatory cytokines in glaucomatous aqueous and encysted Molteno implant blebs and their relationship to pressure. *Investigative Ophthalmology & Visual Science*, *54*(7), 4851–4855.

- Frey, T., & Antonetti, D. A. (2011). Alterations to the blood-retinal barrier in diabetes: cytokines and reactive oxygen species. *Antioxidants & Redox Signaling*, *15*(5), 1271–1284.
- Fries, J. E., Goczalik, I. M., Wheeler-Schilling, T. H., Kohler, K., Guenther, E., Wolf, S., Wiedemann, P., Bringmann, A., Reichenbach, A., Francke, M., & Pannicke, T. (2005). Identification of P2Y receptor subtypes in human muller glial cells by physiology, single cell RT-PCR, and immunohistochemistry. *Investigative Ophthalmology & Visual Science*, *46*(8), 3000–3007.
- Fries, J. E., Wheeler-Schilling, T. H., Kohler, K., & Guenther, E. (2004). Distribution of metabotropic P2Y receptors in the rat retina: a single-cell RT-PCR study. *Brain Research. Molecular Brain Research*, *130*(1-2), 1–6.
- Fujita, R., Ma, Y., & Ueda, H. (2008). Lysophosphatidic acid-induced membrane ruffling and brain-derived neurotrophic factor gene expression are mediated by ATP release in primary microglia. *Journal of Neurochemistry*, *107*(1), 152–160.
- Gaasterland, D. E., Pederson, J. E., MacLellan, H. M., & Reddy, V. N. (1979). Rhesus monkey aqueous humor composition and a primate ocular perfusate. *Investigative Ophthalmology & Visual Science*, *18*(11), 1139–1150.
- Gabay, C., Lamacchia, C., & Palmer, G. (2010). IL-1 pathways in inflammation and human diseases. *Nature Reviews. Rheumatology*, *6*(4), 232–241.
- Galvao, J., Elvas, F., Martins, T., Cordeiro, M. F., Ambrósio, A. F., & Santiago, A. R. (2015). Adenosine A3 receptor activation is neuroprotective against retinal neurodegeneration. *Experimental Eye Research*, *140*, 65–74.
- Gao, Z. G., Ding, Y., & Jacobson, K. A. (2010). P2Y₁₃ receptor is responsible for ADP-mediated degranulation in RBL-2H3 rat mast cells. *Pharmacological Research*, *62*(6), 500–505.

Gao, Z. G., Wei, Q., Jayasekara, M. P., & Jacobson, K. A. (2013). The role of P2Y(14) and other P2Y receptors in degranulation of human LAD2 mast cells. *Purinergic Signalling*, *9*(1), 31–40.

Garcia, R. A., Yan, M., Search, D., Zhang, R., Carson, N. L., Ryan, C. S., Smith-Monroy, C., Zheng, J., Chen, J., Kong, Y., Tang, H., Hellings, S. E., Wardwell-Swanson, J., Dinchuk, J. E., Psaltis, G. C., Gordon, D. A., Glunz, P. W., & Gargalovic, P. S. (2014). P2Y₆ receptor potentiates pro-inflammatory responses in macrophages and exhibits differential roles in atherosclerotic lesion development. *PLOS ONE*, *9*(10), 111385.

Garcia-Valenzuela, E., Sharma, S. C., & Piña, A. L. (2005). Multilayered retinal microglial response to optic nerve transection in rats. *Molecular Vision*, *11*, 225–231.

Garlanda, C., Dinarello, C. A., & Mantovani, A. (2013). The interleukin-1 family: back to the future. *Immunity*, *39*(6), 1003–1018.

Gartland, A., Skarratt, K. K., Hocking, L. J., Parsons, C., Stokes, L., Jørgensen, N. R., Fraser, W. D., Reid, D. M., Gallagher, J. A., & Wiley, J. S. (2012). Polymorphisms in the P2X7 receptor gene are associated with low lumbar spine bone mineral density and accelerated bone loss in post-menopausal women. *European Journal of Human Genetics*, *20*(5), 559–564.

Garway-Heath, D. F., Crabb, D. P., Bunce, C., Lascaratos, G., Amalfitano, F., Anand, N., Azuara-Blanco, A., Bourne, R. R., Broadway, D. C., Cunliffe, I. A., Diamond, J. P., Fraser, S. G., Ho, T. A., Martin, K. R., McNaught, A. I., Negi, A., Patel, K., Russell, R. A., Shah, A., Spry, P. G., Suzuki, K., White, E. T., Wormald, R. P., Xing, W., & Zeyen, T. G. (2015). Latanoprost for open-angle glaucoma (UKGTS): a randomised, multicentre, placebo-controlled trial. *Lancet*, *385*(9975), 1295–1304.

Gasser, P., Flammer, J., Guthauser, U., & Mahler, F. (1990). Do vasospasms provoke ocular diseases?. *Angiology*, *41*(3), 213–220.

Gazzard, G., Konstantakopoulou, E., Garway-Heath, D., Garg, A., Vickerstaff, V., Hunter, R., Ambler, G., Bunce, C., Wormald, R., Nathwani, N., Barton, K., Rubin, G., Buszewicz, M., & LiGHT Trial Study Group (2019). Selective laser trabeculoplasty versus eye drops for first-line treatment of ocular hypertension and glaucoma (LiGHT): a multicentre randomised controlled trial. *Lancet*, 393(10180), 1505–1516.

Gazzard, G. (2016). Minimally Invasive Glaucoma Surgery: MIGS. *Eye*: London

Gedde, S. J., Feuer, W. J., Lim, K. S., Barton, K., Goyal, S., Ahmed, I., Brandt, J. D., & Primary Tube Versus Trabeculectomy Study Group (2020). Treatment Outcomes in the Primary Tube Versus Trabeculectomy Study after 3 Years of Follow-up. *Ophthalmology*, 127(3), 333–345.

Gedde, S. J., Schiffman, J. C., Feuer, W. J., Herndon, L. W., Brandt, J. D., Budenz, D. L., & Tube versus Trabeculectomy Study Group (2012). Treatment outcomes in the Tube Versus Trabeculectomy (TVT) study after five years of follow-up. *American Journal of Ophthalmology*, 153(5), 789–803

Gharahkhani, P., Jorgenson, E., Hysi, P., Khawaja, A. P., Pendergrass, S., Han, X., Ong, J. S., Hewitt, A. W., Segre, A. V., Rouhana, J. M., Hamel, A. R., Igo, R. P., Jr, Choquet, H., Qassim, A., Josyula, N. S., Cooke Bailey, J. N., Bonnemaier, P., Iglesias, A., Siggs, O. M., Young, T. L., Vitart, V., Thiadens, A. A. H. J., Karjalainen, J., Uebe, S., Melles, R. B., Nair, K. S., Luben, R., Simcoe, M., Amersinghe, N., Cree, A. J., Hohn, R., Poplawski, A., Chen, L. J., Rong, S., Aung, T., Vithana, E. N., NEIGHBORHOOD consortium; ANZRAG consortium; Biobank Japan project; FinnGen study; UK Biobank Eye and Vision Consortium; GIGA study group; 23 and Me Research Team; Tamiya, G., Shiga, Y., Yamamoto, M., Nakazawa, T., Currant, H., Birney, E., Wang, X., Auton, A., Lupton, M. K., Martin, N. G., Ashaye, A., Olowoya, O., Williams, S. E., Akafo, S., Ramsay, M., Hashimoto, K., Kamatani, Y., Akiyama, M., Momozawa, Y., Foster, P. J., Khaw, P. T., Morgan, J. E., Strouthidis, N. G., Kraft, P., Kang, J. H., Pang, C. P., Pasutto, F., Mitchell, P., Lotery, A. J., Palotie, A., Van Duijn, C., Haines, J. L., Hammond, C., Pasquale, L. R.,

Klaver, C. C. W., Hauser, M., Khor, C. C., Mackey, D. A., Kubo, M., Cheng, C., Craig, J. E., MacGregor, S., Wiggs, J. L. (2021). Genome-wide meta-analysis identifies 127 open-angle glaucoma loci with consistent effect across ancestries. *Nature Communications*, 12(1), 1258.

Gillmann, K., Bravetti, G. E., Mermoud, A., Rao, H. L., & Mansouri, K. (2019). XEN Gel Stent in Pseudoexfoliative Glaucoma: 2-Year Results of a Prospective Evaluation. *Journal of Glaucoma*, 28(8), 676–684.

Ginsburg-Shmuel, T., Haas, M., Grbic, D., Arguin, G., Nadel, Y., Gendron, F. P., Reiser, G., & Fischer, B. (2012). UDP made a highly promising stable, potent, and selective P2Y₆-receptor agonist upon introduction of a boranophosphate moiety. *Bioorganic & Medicinal Chemistry*, 20(18), 5483–5495.

Giuliani, A. L., Sarti, A. C., & Di Virgilio, F. (2019). Extracellular nucleotides and nucleosides as signalling molecules. *Immunology Letters*, 205, 16–24.

Giuliani, A. L., Sarti, A. C., Falzoni, S., & Di Virgilio, F. (2017). The P2X7 Receptor-Interleukin-1 Liaison. *Frontiers in Pharmacology*, 8, 123.

Goel, M., Picciani, R. G., Lee, R. K., & Bhattacharya, S. K. (2010). Aqueous humor dynamics: a review. *The Open Ophthalmology Journal*, 4, 52–59.

Goetz, J., Jessen, Z. F., Jacobi, A., Mani, A., Cooler, S., Greer, D., Kadri, S., Segal, J., Shekhar, K., Sanes, J. R., & Schwartz, G. W. (2022). Unified classification of mouse retinal ganglion cells using function, morphology, and gene expression. *Cell reports*, 40(2), 111040.

Gong, Q. J., Li, Y. Y., Xin, W. J., Zang, Y., Ren, W. J., Wei, X. H., Li, Y. Y., Zhang, T., & Liu, X. G. (2009). ATP induces long-term potentiation of C-fiber-evoked field potentials in spinal dorsal horn: the roles of P2X4 receptors and p38 MAPK in microglia. *Glia*, 57(6), 583–591.

González-Amaro, R., Portales-Pérez, D., Baranda, L., Abud-Mendoza, C., Llorente, L., Richaud-Patin, Y., Alcocer-Varela, J., & Alarcón-Segovia, D. (1998). Role of IL-10 in the abnormalities of early cell activation events of lymphocytes from patients with systemic lupus erythematosus. *Journal of Autoimmunity*, *11*(5), 395–402.

Gonzalez-Rodriguez, J. M., Trope, G. E., Drori-Wagschal, L., Jinapriya, D., & Buys, Y. M. (2016). Comparison of trabeculectomy versus Ex-PRESS: 3-year follow-up. *The British Journal of Ophthalmology*, *100*(9), 1269–1273.

Gordon, M. O., & Kass, M. A. (1999). The Ocular Hypertension Treatment Study: design and baseline description of the participants. *Archives of Ophthalmology*, *117*(5), 573–583.

Gordon, M. O., Beiser, J. A., Brandt, J. D., Heuer, D. K., Higginbotham, E. J., Johnson, C. A., Keltner, J. L., Miller, J. P., Parrish, R. K., 2nd, Wilson, M. R., & Kass, M. A. (2002). The Ocular Hypertension Treatment Study: baseline factors that predict the onset of primary open-angle glaucoma. *Archives of Ophthalmology*, *120*(6), 714–830.

Graham, S. L., Drance, S. M., Wijsman, K., Douglas, G. R., & Mikelberg, F. S. (1995). Ambulatory blood pressure monitoring in glaucoma. The nocturnal dip. *Ophthalmology*, *102*(1), 61–69.

Greco, N. J., Tonon, G., Chen, W., Luo, X., Dalal, R., & Jamieson, G. A. (2001). Novel structurally altered P(2X1) receptor is preferentially activated by adenosine diphosphate in platelets and megakaryocytic cells. *Blood*, *98*(1), 100–107.

Green, C. M., Kearns, L. S., Wu, J., Barbour, J. M., Wilkinson, R. M., Ring, M. A., Craig, J. E., Wong, T. L., Hewitt, A. W., & Mackey, D. A. (2007). How significant is a family history of glaucoma? Experience from the Glaucoma Inheritance Study in Tasmania. *Clinical & Experimental Ophthalmology*, *35*(9), 793–799.

Griffin, W. S., Sheng, J. G., Roberts, G. W., & Mrak, R. E. (1995). Interleukin-1 expression in different plaque types in Alzheimer's disease: significance in plaque evolution. *Journal of Neuropathology and Experimental Neurology*, *54*(2), 276–281.

Griffin, W. S., Stanley, L. C., Ling, C., White, L., MacLeod, V., Perrot, L. J., White, C. L., 3rd, & Araoz, C. (1989). Brain interleukin 1 and S-100 immunoreactivity are elevated in Down syndrome and Alzheimer disease. *Proceedings of the National Academy of Sciences of the United States of America*, *86*(19), 7611–7615.

Gröndal, G., Kristjansdottir, H., Gunnlaugsdottir, B., Arnason, A., Lundberg, I., Klareskog, L., & Steinsson, K. (1999). Increased number of interleukin-10-producing cells in systemic lupus erythematosus patients and their first-degree relatives and spouses in Icelandic multicase families. *Arthritis and Rheumatism*, *42*(8), 1649–1654.

Grosche, A., Pannicke, T., Chen, J., Wiedemann, P., Reichenbach, A., & Bringmann, A. (2013). Disruption of endogenous purinergic signaling inhibits vascular endothelial growth factor- and glutamate-induced osmotic volume regulation of Müller glial cells in knockout mice. *Ophthalmic Research*, *50*(4), 209–214.

Gudipaty, L., Munetz, J., Verhoef, P. A., & Dubyak, G. R. (2003). Essential role for Ca²⁺ in regulation of IL-1 β secretion by P2X7 nucleotide receptor in monocytes, macrophages, and HEK-293 cells. *American Journal of Physiology. Cell Physiology*, *285*(2), 286–299.

Guha, S., Baltazar, G. C., Coffey, E. E., Tu, L. A., Lim, J. C., Beckel, J. M., Patel, S., Eysteinson, T., Lu, W., O'Brien-Jenkins, A., Laties, A. M., & Mitchell, C. H. (2013). Lysosomal alkalinization, lipid oxidation, and reduced phagosome clearance triggered by activation of the P2X7 receptor. *FASEB Journal*, *27*(11), 4500–4509.

Guha, S., Coffey, E. E., Lu, W., Lim, J. C., Beckel, J. M., Laties, A. M., Boesze-Battaglia, K., & Mitchell, C. H. (2014). Approaches for detecting lysosomal alkalinization and

impaired degradation in fresh and cultured RPE cells: evidence for a role in retinal degenerations. *Experimental Eye Research*, 126, 68–76.

Guo, C., Masin, M., Qureshi, O. S., & Murrell-Lagnado, R. D. (2007). Evidence for functional P2X4/P2X7 heteromeric receptors. *Molecular Pharmacology*, 72(6), 1447–1456.

Haargaard, B., Ritz, C., Oudin, A., Wohlfahrt, J., Thygesen, J., Olsen, T., & Melbye, M. (2008). Risk of glaucoma after pediatric cataract surgery. *Investigative Ophthalmology & Visual Science*, 49(5), 1791–1796.

Haines, W. R., Torres, G. E., Voigt, M. M., & Egan, T. M. (1999). Properties of the novel ATP-gated ionotropic receptor composed of the P2X(1) and P2X(5) isoforms. *Molecular Pharmacology*, 56(4), 720–727.

Hangai, M., Yoshimura, N., Yoshida, M., Yabuuchi, K., & Honda, Y. (1995). Interleukin-1 gene expression in transient retinal ischemia in the rat. *Investigative Ophthalmology & Visual Science*, 36(3), 571–578.

Harkat, M., Peverini, L., Cerdan, A. H., Dunning, K., Beudez, J., Martz, A., Calimet, N., Specht, A., Cecchini, M., Chataigneau, T., & Grutter, T. (2017). On the permeation of large organic cations through the pore of ATP-gated P2X receptors. *Proceedings of the National Academy of Sciences of the United States of America*, 114(19), 3786–3795.

Hattori, M., & Gouaux, E. (2012). Molecular mechanism of ATP binding and ion channel activation in P2X receptors. *Nature*, 485(7397), 207–212.

Hayasaka, S., Yamada, T., Nitta, K., Kaji, Y., Hiraki, S., Tachinami, K., Matsumoto, M., Yamamoto, S., & Yamamoto, S. (1997). Ascorbic acid and amino acid values in the aqueous humor of a patient with Lowe's syndrome. *Graefe's Archive for Clinical and*

Experimental Ophthalmology = Albrecht von Graefes Archiv fur Klinische und Experimentelle Ophthalmologie, 235(4), 217–221.

Hayreh S. S. (1995). The 1994 Von Sallman Lecture. The optic nerve head circulation in health and disease. *Experimental Eye Research*, 61(3), 259–272.

He, Y., Taylor, N., Fourgeaud, L., & Bhattacharya, A. (2017). The role of microglial P2X7: modulation of cell death and cytokine release. *Journal of Neuroinflammation*, 14(1), 135.

Heijl, A., Leske, M. C., Hyman, L., Yang, Z., Bengtsson, B., & EMGT Group (2011). Intraocular pressure reduction with a fixed treatment protocol in the Early Manifest Glaucoma Trial. *Acta Ophthalmologica*, 89(8), 749–754.

Heijl, A., Bengtsson, B., Hyman, L., Leske, M. C., & Early Manifest Glaucoma Trial Group (2009). Natural history of open-angle glaucoma. *Ophthalmology*, 116(12), 2271–2276.

Heijl, A., Leske, M. C., Bengtsson, B., Bengtsson, B., Hussein, M., & Early Manifest Glaucoma Trial Group (2003). Measuring visual field progression in the Early Manifest Glaucoma Trial. *Acta Ophthalmologica Scandinavica*, 81(3), 286–293.

Heijl, A., Leske, M. C., Bengtsson, B., Hyman, L., Bengtsson, B., Hussein, M., & Early Manifest Glaucoma Trial Group (2002). Reduction of intraocular pressure and glaucoma progression: results from the Early Manifest Glaucoma Trial. *Archives of Ophthalmology*, 120(10), 1268–1279.

Herman, D. C., Gordon, M. O., Beiser, J. A., Chylack, L. T., Jr, Lamping, K. A., Schein, O. D., Soltau, J. B., Kass, M. A., & Ocular Hypertension Treatment Study (OHTS) Group (2006). Topical ocular hypotensive medication and lens opacification: evidence from the ocular hypertension treatment study. *American Journal of Ophthalmology*, 142(5), 800–810.

Heys, J. J., & Barocas, V. H. (2002). A boussinesq model of natural convection in the human eye and the formation of Krukenberg's spindle. *Annals of Biomedical Engineering*, 30(3), 392–401.

Higginbotham, E., Yue, B. Y., Crean, E., & Peace, J. (1988). Effects of ascorbic acid on trabecular meshwork cells in culture. *Experimental Eye Research*, 46(4), 507–516.

Ho, T., Jobling, A. I., Greferath, U., Chuang, T., Ramesh, A., Fletcher, E. L., & Vessey, K. A. (2015). Vesicular expression and release of ATP from dopaminergic neurons of the mouse retina and midbrain. *Frontiers in Cellular Neuroscience*, 9, 389.

Ho, T., Vessey, K. A., & Fletcher, E. L. (2014). Immunolocalization of the P2X4 receptor on neurons and glia in the mammalian retina. *Neuroscience*, 277, 55–71.

Holländer, H., Makarov, F., Stefani, F. H., & Stone, J. (1995). Evidence of constriction of optic nerve axons at the lamina cribrosa in the normotensive eye in humans and other mammals. *Ophthalmic Research*, 27(5), 296–309.

Horckmans, M., León-Gómez, E., Robaye, B., Balligand, J. L., Boeynaems, J. M., Dessy, C., & Communi, D. (2012). Gene deletion of P2Y₄ receptor lowers exercise capacity and reduces myocardial hypertrophy with swimming exercise. *American Journal of Physiology. Heart and Circulatory Physiology*, 303(7), 835–843.

Horckmans, M., Esfahani, H., Beauloye, C., Clouet, S., di Pietrantonio, L., Robaye, B., Balligand, J. L., Boeynaems, J. M., Dessy, C., & Communi, D. (2015). Loss of mouse P2Y₄ nucleotide receptor protects against myocardial infarction through endothelin-1 downregulation. *Journal of Immunology*, 194(4), 1874–1881.

Horváth, G., Göllöncsér, F., Csölle, C., Király, K., Andó, R. D., Baranyi, M., Koványi, B., Máté, Z., Hoffmann, K., Algaier, I., Baqi, Y., Müller, C. E., Von Kügelgen, I., & Sperlágh, B. (2014). Central P2Y₁₂ receptor blockade alleviates inflammatory and neuropathic pain and cytokine production in rodents. *Neurobiology of Disease*, 70, 162–178.

Hosoda, M., Yamabayashi, S., Furuta, M., & Tsukahara, S. (1995). Do glaucoma patients use eye drops correctly?. *Journal of Glaucoma*, 4(3), 202–206.

Hosoya, K., & Tomi, M. (2005). Advances in the cell biology of transport via the inner blood-retinal barrier: establishment of cell lines and transport functions. *Biological & Pharmaceutical Bulletin*, 28(1), 1–8.

How, A. C., Aung, T., Chew, X., Yong, V. H., Lim, M. C., Lee, K. Y., Toh, J. Y., Li, Y., Liu, J., & Vithana, E. N. (2007). Lack of association between interleukin-1 gene cluster polymorphisms and glaucoma in Chinese subjects. *Investigative Ophthalmology & Visual Science*, 48(5), 2123–2126.

Hosoya, K., & Tachikawa, M. (2012). The inner blood-retinal barrier: molecular structure and transport biology. *Advances in Experimental Medicine and Biology*, 763, 85–104.

Hu, B., Senkler, C., Yang, A., Soto, F., & Liang, B. T. (2002). P2X4 receptor is a glycosylated cardiac receptor mediating a positive inotropic response to ATP. *The Journal of Biological Chemistry*, 277, 15752–15757.

Hu, H., Lu, W., Zhang, M., Zhang, X., Argall, A. J., Patel, S., Lee, G. E., Kim, Y. C., Jacobson, K. A., Laties, A. M., & Mitchell, C. H. (2010). Stimulation of the P2X7 receptor kills rat retinal ganglion cells in vivo. *Experimental Eye Research*, 91(3), 425–432.

Hu, S. J., Calippe, B., Lavalette, S., Roubéix, C., Montassar, F., Housset, M., Levy, O., Delarasse, C., Paques, M., Sahel, J. A., Sennlaub, F., & Guillonéau, X. (2015). Upregulation of P2X7R in Cx3cr1-Deficient Mononuclear Phagocytes Leads to Increased Interleukin-1 β Secretion and Photoreceptor Neurodegeneration. *The Journal of Neuroscience*, 35(18), 6987–6996.

Haung, W., Koralewska-Makár, A., Bauer, B., & Akesson, B. (1997). Extracellular glutathione peroxidase and ascorbic acid in aqueous humor and serum of patients operated on for cataract. *Clinica Chimica Acta*, 261(2), 117–130.

Huang, Z., Xie, N., Illes, P., Di Virgilio, F., Ulrich, H., Semyanov, A., Verkhatsky, A., Sperlagh, B., Yu, S. G., Huang, C., & Tang, Y. (2021). From purines to purinergic signalling: molecular functions and human diseases. *Signal Transduction and Targeted Therapy*, 6(1), 162.

Hubens, W. H. G., Mohren, R. J. C., Liesenborghs, I., Eijssen, L. M. T., Ramdas, W. D., Webers, C. A. B., & Gorgels, T. G. M. F. (2020). The aqueous humor proteome of primary open angle glaucoma: An extensive review. *Experimental Eye Research*, 197, 108077.

Hwang, Y. S., Jeong, M., Park, J. S., Kim, M. H., Lee, D. B., Shin, B. A., Mukaida, N., Ellis, L. M., Kim, H. R., Ahn, B. W., & Jung, Y. D. (2004). Interleukin-1beta stimulates IL-8 expression through MAP kinase and ROS signaling in human gastric carcinoma cells. *Oncogene*, 23(39), 6603–6611.

Hyman, L., Heijl, A., Leske, M. C., Bengtsson, B., Yang, Z., & Early Manifest Glaucoma Trial Group (2010). Natural history of intraocular pressure in the early manifest glaucoma trial: A 6-year follow-up. *Archives of Ophthalmology*, 128(5), 601–607.

Hyman, L. G., Komaroff, E., Heijl, A., Bengtsson, B., Leske, M. C., & Early Manifest Glaucoma Trial Group (2005). Treatment and vision-related quality of life in the early manifest glaucoma trial. *Ophthalmology*, 112(9), 1505–1513.

Hysi, P. G., Cheng, C. Y., Springelkamp, H., Macgregor, S., Bailey, J., Wojciechowski, R., Vitart, V., Nag, A., Hewitt, A. W., Höhn, R., Venturini, C., Mirshahi, A., Ramdas, W. D., Thorleifsson, G., Vithana, E., Khor, C. C., Stefansson, A. B., Liao, J., Haines, J. L., Amin, N., Wang, Y.X., Wild, P.S., Ozel, A.B., Li, J.Z., Fleck, B.W., Zeller, T., Staffieri, S.E., Teo, Y.Y., Cuellar-Partida, G., Luo, X., Allingham, R.R., Richards, J.E., Senft, A., Karssen,

L.C., Zheng, Y., Bellenguez, C., Xu, L., Iglesias, A.I., Wilson, J.F., Kang, J.H., van Leeuwen, E.M., Jonsson, V., Thorsteinsdottir, U., Despret, D.D.G., Ennis, S., Moroi, S.E., Martin, N.G., Jansonius, N.M., Yazar, S., Tai, E.S., Amouyel, P., Kirwan, J., van Koolwijk, L.M.E., Hauser, M.A., Jonasson, F., Leo, P., Loomis, S.J., Fogarty, R., Rivadeneira, F., Kearns, L., Lackner, K.J., de Jong, P.T.V.M., Simpson, C.L., Pennell, C.E., Oostra, B.A., Uitterlinden, A.G., Saw, S.M., Lotery, A.J., Bailey-Wilson, J.E., Hofman, A., Vingerling, J.R., Maubaret, C., Pfeiffer, N., Wolfs, R.C.W., Lemij, H.G., Young, T.L., Pasquale, L.R., Delcourt, C., Spector, T.D., Klaver, C.C.W., Small, K.S., Burdon, K.P., Stefansson, K., Wong, T.Y., BMES GWAS Group., NEIGHBORHOOD Consortium., Wellcome Trust Case Control Consortium 2., Viswanathan, A., Mackey, D.A., Craig, J.E., Wiggs, J.L., van Duijn, C.M., Hammond, C.J., and Aung, T (2014). Genome-wide analysis of multi-ancestry cohorts identifies new loci influencing intraocular pressure and susceptibility to glaucoma. *Nature Genetics*, 46(10), 1126–1130.

Iglesias, R., Locovei, S., Roque, A., Alberto, A. P., Dahl, G., Spray, D. C., & Scemes, E. (2008). P2X7 receptor-Pannexin1 complex: pharmacology and signaling. *American Journal of Physiology. Cell Physiology*, 295(3), C752–C760.

Illes, P., Müller, C. E., Jacobson, K. A., Grutter, T., Nicke, A., Fountain, S. J., Kennedy, C., Schmalzing, G., Jarvis, M. F., Stojilkovic, S. S., King, B. F., & Di Virgilio, F. (2021). Update of P2X receptor properties and their pharmacology: IUPHAR Review 30. *British Journal of Pharmacology*, 178(3), 489–514.

Ito, S., Sairenchi, T., Machida, T., Takino, Y., Kondo, Y., Mukai, K., Kobashi, G., Ishigami, A., & Senoo, T. (2019). Reduced aqueous humour ascorbic-acid concentration in women with smaller anterior chamber depth. *Scientific Reports*, 9(1), 372.

Inoue, K., & Tsuda, M. (2012). P2X4 receptors of microglia in neuropathic pain. *CNS & neurological disorders drug targets*, 11(6), 699–704.

Jabs, R., Guenther, E., Marquardt, K., & Wheeler-Schilling, T. H. (2000). Evidence for P2X(3), P2X(4), P2X(5) but not for P2X(7) containing purinergic receptors in Müller cells of the rat retina. *Brain Research. Molecular Brain Research*, 76(2), 205–210.

Jacobson, K. A. (2018). P2X and P2Y Receptors. *Tocris Scientific Review Series*.

Jacobson, K. A., Delicado, E. G., Gachet, C., Kennedy, C., von Kügelgen, I., Li, B., Miras-Portugal, M. T., Novak, I., Schöneberg, T., Perez-Sen, R., Thor, D., Wu, B., Yang, Z., & Müller, C. E. (2020). Update of P2Y receptor pharmacology: IUPHAR Review 27. *British Journal of Pharmacology*, 177(11), 2413–2433.

Jacobson, K. A., & Civan, M. M. (2016). Ocular Purine Receptors as Drug Targets in the Eye. *Journal of Ocular Pharmacology and Therapeutics*, 32(8), 534–547.

Jacobson, K. A., & Müller, C. E. (2016). Medicinal chemistry of adenosine, P2Y and P2X receptors. *Neuropharmacology*, 104, 31–49.

Jacobson, K. A., Ivanov, A. A., de Castro, S., Harden, T. K., & Ko, H. (2009). Development of selective agonists and antagonists of P2Y receptors. *Purinergic Signalling*, 5(1), 75–89.

Janeway, C., Travers, P., Walport, M. and Shlomchik, M. (2001). *Immunobiology: The Immune System in Health and Disease*. 5th ed. New York: Garland Science.

Jenkins, J. K., Malyak, M., & Arend, W. P. (1994). The effects of interleukin-10 on interleukin-1 receptor antagonist and interleukin-1 beta production in human monocytes and neutrophils. *Lymphokine and Cytokine Research*, 13(1), 47–54.

Jeon, C. J., Strettoi, E., & Masland, R. H. (1998). The major cell populations of the mouse retina. *The Journal of Neuroscience*, 18(21), 8936–8946.

Jiang, L. H., Baldwin, J. M., Roger, S., & Baldwin, S. A. (2013). Insights into the Molecular Mechanisms Underlying Mammalian P2X7 Receptor Functions and

Contributions in Diseases, Revealed by Structural Modeling and Single Nucleotide Polymorphisms. *Frontiers in Pharmacology*, 4, 55.

Jørgensen, N. R., Grove, E. L., Schwarz, P., & Vestergaard, P. (2012). Clopidogrel and the risk of osteoporotic fractures: a nationwide cohort study. *Journal of Internal Medicine*, 272(4), 385–393.

Josephson, K., DiGiacomo, R., Indelicato, S. R., Iyo, A. H., Nagabhushan, T. L., Parker, M. H., & Walter, M. R. (2000). Design and analysis of an engineered human interleukin-10 monomer. *The Journal of Biological Chemistry*, 275(18), 13552–13557.

Jung, K. Y., Moon, H. D., Lee, G. E., Lim, H. H., Park, C. S., & Kim, Y. C. (2007). Structure-activity relationship studies of spinorphin as a potent and selective human P2X(3) receptor antagonist. *Journal of Medicinal Chemistry*, 50(18), 4543–4547.

Justiz Vaillant, A. A., & Qurie, A. (2021). Interleukin. In StatPearls. *StatPearls Publishing*

Kakurai, K., Sugiyama, T., Kurimoto, T., Oku, H., & Ikeda, T. (2013). Involvement of P2X(7) receptors in retinal ganglion cell death after optic nerve crush injury in rats. *Neuroscience Letters*, 534, 237–241.

Kamoto, D., Thach, L., Bernard, R., Chan, V., Zheng, W., Kaur, H., Brimble, M., Osman, N., & Little, P. J. (2015). Structure, Function, Pharmacology, and Therapeutic Potential of the G Protein, G α /q,11. *Frontiers in Cardiovascular Medicine*, 2, 14.

Kaneda, M., Ishii, K., Morishima, Y., Akagi, T., Yamazaki, Y., Nakanishi, S., & Hashikawa, T. (2004). OFF-cholinergic-pathway-selective localization of P2X2 purinoceptors in the mouse retina. *The Journal of Comparative Neurology*, 476(1), 103–111.

Kang, J. M., & Lin, S. (2018). Ginkgo biloba and its potential role in glaucoma. *Current Opinion in Ophthalmology*, 29(2), 116–120.

Karperien, A., Ahammer, H., & Jelinek, H. F. (2013). Quantitating the subtleties of microglial morphology with fractal analysis. *Frontiers in Cellular Neuroscience*, 7, 3.

Kass, M. A., Heuer, D. K., Higginbotham, E. J., Johnson, C. A., Keltner, J. L., Miller, J. P., Parrish, R. K., 2nd, Wilson, M. R., & Gordon, M. O. (2002). The Ocular Hypertension Treatment Study: a randomized trial determines that topical ocular hypotensive medication delays or prevents the onset of primary open-angle glaucoma. *Archives of Ophthalmology*, 120(6), 701–830.

Kass, M. A., Gordon, M. O., Gao, F., Heuer, D. K., Higginbotham, E. J., Johnson, C. A., Keltner, J. K., Miller, J. P., Parrish, R. K., Wilson, M. R., & Ocular Hypertension Treatment Study Group (2010). Delaying treatment of ocular hypertension: the ocular hypertension treatment study. *Archives of Ophthalmology*, 128(3), 276–287.

Kassack, M. U., Braun, K., Ganso, M., Ullmann, H., Nickel, P., Böing, B., Müller, G., & Lambrecht, G. (2004). Structure-activity relationships of analogues of NF449 confirm NF449 as the most potent and selective known P2X1 receptor antagonist. *European Journal of Medicinal Chemistry*, 39(4), 345–357.

Kataoka, K., Matsumoto, H., Kaneko, H., Notomi, S., Takeuchi, K., Sweigard, J. H., Atik, A., Murakami, Y., Connor, K. M., Terasaki, H., Miller, J. W., & Vavvas, D. G. (2015). Macrophage- and RIP3-dependent inflammasome activation exacerbates retinal detachment-induced photoreceptor cell death. *Cell Death & Disease*, 6(4), e1731.

Kaufman P. L. (2020). Deconstructing aqueous humor outflow - The last 50 years. *Experimental Eye Research*, 197, 108105.

Kawaguchi, Y., Hara, M., & Wright, T. M. (1999). Endogenous IL-1 α from systemic sclerosis fibroblasts induces IL-6 and PDGF-A. *The Journal of Clinical Investigation*, 103(9), 1253–1260.

Keech, R. V., Tongue, A. C., & Scott, W. E. (1989). Complications after surgery for congenital and infantile cataracts. *American Journal of Ophthalmology*, 108(2), 136–141.

Keller, M., Rüegg, A., Werner, S., & Beer, H. D. (2008). Active caspase-1 is a regulator of unconventional protein secretion. *Cell*, 132(5), 818–831.

Keltner, J. L., Johnson, C. A., Anderson, D. R., Levine, R. A., Fan, J., Cello, K. E., Quigley, H. A., Budenz, D. L., Parrish, R. K., Kass, M. A., Gordon, M. O., & Ocular Hypertension Treatment Study Group (2006). The association between glaucomatous visual fields and optic nerve head features in the Ocular Hypertension Treatment Study. *Ophthalmology*, 113(9), 1603–1612.

Kennedy, C., Tasker, P. N., Gallacher, G., & Westfall, T. D. (2007). Identification of atropine- and P2X1 receptor antagonist-resistant, neurogenic contractions of the urinary bladder. *The Journal of Neuroscience*, 27(4), 845–851.

Kennedy, C., Assis, T. S., Currie, A. J., & Rowan, E. G. (2003). Crossing the pain barrier: P2 receptors as targets for novel analgesics. *The Journal of Physiology*, 553(Pt 3), 683–694.

Kersey, J. P., & Broadway, D. C. (2006). Corticosteroid-induced glaucoma: a review of the literature. *Eye (London, England)*, 20(4), 407–416.

Khakh, B. S., Bao, X. R., Labarca, C., & Lester, H. A. (1999). Neuronal P2X transmitter-gated cation channels change their ion selectivity in seconds. *Nature Neuroscience*, 2(4), 322–330.

Khaw, P. T., Chiang, M., Shah, P., Sii, F., Lockwood, A., & Khalili, A. (2017). Enhanced Trabeculectomy: The Moorfields Safer Surgery System. *Developments in Ophthalmology*, 59, 15–35.

Khaw, P. T., Chiang, M., Shah, P., Sii, F., Lockwood, A., & Khalili, A. (2012). Enhanced trabeculectomy: the Moorfields Safer Surgery System. *Developments in ophthalmology*, 50, 1–28.

Khawaja, A. P., Cooke Bailey, J. N., Wareham, N. J., Scott, R. A., Simcoe, M., Igo, R. P., Jr, Song, Y. E., Wojciechowski, R., Cheng, C. Y., Khaw, P. T., Pasquale, L. R., Haines, J. L., Foster, P. J., Wiggs, J. L., Hammond, C. J., Hysi, P. G., UK Biobank Eye and Vision Consortium, & NEIGHBORHOOD Consortium (2018). Genome-wide analyses identify 68 new loci associated with intraocular pressure and improve risk prediction for primary open-angle glaucoma. *Nature Genetics*, 50(6), 778–782.

Killer H. E. (2020). Is stagnant cerebrospinal fluid involved in the pathophysiology of normal tension glaucoma. *Progress in Brain Research*, 256(1), 209–220.

Kim, B., Lee, Y., Kim, E., Kwak, A., Ryoo, S., Bae, S. H., Azam, T., Kim, S., & Dinarello, C. A. (2013). The Interleukin-1 α Precursor is Biologically Active and is Likely a Key Alarmin in the IL-1 Family of Cytokines. *Frontiers in Immunology*, 4, 391.

Kim, H. J., Ajit, D., Peterson, T. S., Wang, Y., Camden, J. M., Gibson Wood, W., Sun, G. Y., Erb, L., Petris, M., & Weisman, G. A. (2012). Nucleotides released from A β_{1-42} - treated microglial cells increase cell migration and A β_{1-42} uptake through P2Y₂ receptor activation. *Journal of Neurochemistry*, 121(2), 228–238.

Kim, J. M., Brannan, C. I., Copeland, N. G., Jenkins, N. A., Khan, T. A., & Moore, K. W. (1992). Structure of the mouse IL-10 gene and chromosomal localization of the mouse and human genes. *Journal of Immunology*, 148(11), 3618–3623.

Kim, T. W., Kang, K. B., Choung, H. K., Park, K. H., & Kim, D. M. (2000). Elevated glutamate levels in the vitreous body of an in vivo model of optic nerve ischemia. *Archives of Ophthalmology*, 118(4), 533–536.

Kinoshita, M., Nasu-Tada, K., Fujishita, K., Sato, K., & Koizumi, S. (2013). Secretion of matrix metalloproteinase-9 from astrocytes by inhibition of tonic P2Y₁₄-receptor-mediated signal(s). *Cellular and Molecular Neurobiology*, 33(1), 47–58.

Kinsey V. E. (1953). Comparative chemistry of aqueous humor in posterior and anterior chambers of rabbit eye, its physiologic significance. *A.M.A. Archives of Ophthalmology*, 50(4), 401–417.

Kinsey V. E. (1951). The chemical composition and the osmotic pressure of the aqueous humor and plasma of the rabbit. *The Journal of General Physiology*, 34(3), 389–402.

Kirsch, R. E., Levine, O., & Singer, J. A. (1976). Ridge at internal edge of cataract incision. *Archives of Ophthalmology*, 94(12), 2098–2104.

Kitaoka, Y., Munemasa, Y., Nakazawa, T., & Ueno, S. (2007). NMDA-induced interleukin-1beta expression is mediated by nuclear factor-kappa B p65 in the retina. *Brain Research*, 1142, 247–255.

Ko, H., Fricks, I., Ivanov, A. A., Harden, T. K., & Jacobson, K. A. (2007). Structure-activity relationship of uridine 5'-diphosphoglucose analogues as agonists of the human P2Y₁₄ receptor. *Journal of Medicinal Chemistry*, 50(9), 2030–2039.

Kobayashi, Y., Yamamoto, K., Saido, T., Kawasaki, H., Oppenheim, J. J., & Matsushima, K. (1990). Identification of calcium-activated neutral protease as a processing enzyme of human interleukin 1 alpha. *Proceedings of the National Academy of Sciences of the United States of America*, 87(14), 5548–5552.

Koizumi, S., Shigemoto-Mogami, Y., Nasu-Tada, K., Shinozaki, Y., Ohsawa, K., Tsuda, M., Joshi, B. V., Jacobson, K. A., Kohsaka, S., & Inoue, K. (2007). UDP acting at P2Y₆ receptors is a mediator of microglial phagocytosis. *Nature*, *446*(7139), 1091–1095.

Koliakos, G. G., Konstas, A. G., Schlötzer-Schrehardt, U., Bufidis, T., Georgiadis, N., & Ringvold, A. (2002). Ascorbic acid concentration is reduced in the aqueous humor of patients with exfoliation syndrome. *American Journal of Ophthalmology*, *134*(6), 879–883.

Kotenko, S. V., Saccani, S., Izotova, L. S., Mirochnitchenko, O. V., & Pestka, S. (2000). Human cytomegalovirus harbors its own unique IL-10 homolog (cmvIL-10). *Proceedings of the National Academy of Sciences of the United States of America*, *97*(4), 1695–1700.

Kotnis, S., Bingham, B., Vasilyev, D. V., Miller, S. W., Bai, Y., Yeola, S., Chanda, P. K., Bowlby, M. R., Kaftan, E. J., Samad, T. A., & Whiteside, G. T. (2010). Genetic and functional analysis of human P2X₅ reveals a distinct pattern of exon 10 polymorphism with predominant expression of the nonfunctional receptor isoform. *Molecular Pharmacology*, *77*(6), 953–960.

Kozera, M., Konopińska, J., Mariak, Z., & Rękas, M. (2021). Effectiveness of iStent Trabecular Microbypass System Combined with Phacoemulsification versus Phacoemulsification Alone in Patients with Glaucoma and Cataract Depending on the Initial Intraocular Pressure. *Ophthalmic Research*, *64*(2), 327–336.

Kristensen, M., Deleuran, B., Eedy, D. J., Feldmann, M., Breathnach, S. M., & Brennan, F. M. (1992). Distribution of interleukin 1 receptor antagonist protein (IRAP), interleukin 1 receptor, and interleukin 1 alpha in normal and psoriatic skin. Decreased expression of IRAP in psoriatic lesional epidermis. *The British Journal of Dermatology*, *127*(4), 305–311.

Kubo, Y., Akanuma, S. I., & Hosoya, K. I. (2018). Recent advances in drug and nutrient transport across the blood-retinal barrier. *Expert opinion on drug metabolism & toxicology*, 14(5), 513–531.

Küchle, M., Ho, T. S., Nguyen, N. X., Hannappel, E., & Naumann, G. O. (1994). Protein quantification and electrophoresis in aqueous humor of pseudoexfoliation eyes. *Investigative Ophthalmology & Visual Science*, 35(2), 748–752.

Kuchtey, J., Rezaei, K. A., Jaru-Ampornpan, P., Sternberg, P., Jr, & Kuchtey, R. W. (2010). Multiplex cytokine analysis reveals elevated concentration of interleukin-8 in glaucomatous aqueous humor. *Investigative Ophthalmology & Visual Science*, 51(12), 6441–6447.

Kukulski, F., Lévesque, S. A., & Sévigny, J. (2011). Impact of ectoenzymes on p2 and p1 receptor signaling. *Advances in Pharmacology*, 61, 263–299.

Kumar, A., & Shamsuddin, N. (2012). Retinal Muller glia initiate innate response to infectious stimuli via toll-like receptor signaling. *PLOS ONE*, 7(1), 29830.

Kurt-Jones, E. A., Beller, D. I., Mizel, S. B., & Unanue, E. R. (1985). Identification of a membrane-associated interleukin 1 in macrophages. *Proceedings of the National Academy of Sciences of the United States of America*, 82(4), 1204–1208.

Kurt-Jones, E. A., Virgin, H. W., 4th, & Unanue, E. R. (1986). In vivo and in vitro expression of macrophage membrane interleukin 1 in response to soluble and particulate stimuli. *Journal of Immunology*, 137(1), 10–14.

Kurt-Jones, E. A., Fiers, W., & Pober, J. S. (1987). Membrane interleukin 1 induction on human endothelial cells and dermal fibroblasts. *Journal of Immunology*, 139(7), 2317–2324.

La Morgia, C., Di Vito, L., Carelli, V., & Carbonelli, M. (2017). Patterns of Retinal Ganglion Cell Damage in Neurodegenerative Disorders: Parvocellular vs Magnocellular Degeneration in Optical Coherence Tomography Studies. *Frontiers in Neurology, 8*, 710.

Labin, A. M., Safuri, S. K., Ribak, E. N., & Perlman, I. (2014). Müller cells separate between wavelengths to improve day vision with minimal effect upon night vision. *Nature Communications, 5*, 4319.

Lacey, J., Cate, H., & Broadway, D. C. (2009). Barriers to adherence with glaucoma medications: a qualitative research study. *Eye (London, England), 23*(4), 924–932.

Lalo, U., Pankratov, Y., Wichert, S. P., Rossner, M. J., North, R. A., Kirchhoff, F., & Verkhratsky, A. (2008). P2X1 and P2X5 subunits form the functional P2X receptor in mouse cortical astrocytes. *The Journal of Neuroscience, 28*(21), 5473–5480.

Lalo, U., Allsopp, R. C., Mahaut-Smith, M. P., & Evans, R. J. (2010). P2X1 receptor mobility and trafficking; regulation by receptor insertion and activation. *Journal of Neurochemistry, 113*(5), 1177–1187.

Lamacchia, C., Rodriguez, E., Palmer, G., & Gabay, C. (2013). Endogenous IL-1 α is a chromatin-associated protein in mouse macrophages. *Cytokine, 63*(2), 135–144.

Larrosa, J. M., Moreno-Montañés, J., Martínez-de-la-Casa, J. M., Polo, V., Velázquez-Villoria, Á., Berrozpe, C., & García-Granero, M. (2015). A Diagnostic Calculator for Detecting Glaucoma on the Basis of Retinal Nerve Fiber Layer, Optic Disc, and Retinal Ganglion Cell Analysis by Optical Coherence Tomography. *Investigative Ophthalmology & Visual Science, 56*(11), 6788–6795.

Lavin-Dapena, C., Cordero-Ros, R., D'Anna, O., & Mogollón, I. (2021). XEN 63 gel stent device in glaucoma surgery: A 5-years follow-up prospective study. *European Journal of Ophthalmology, 31*(4), 1829–1835.

Layhadi, J. A., & Fountain, S. J. (2019). ATP-evoked intracellular Ca(2+) responses in M-CSF differentiated human monocyte-derived macrophage are mediated by P2X4 and P2Y11 receptor activation. *International Journal of Molecular Sciences*, 20, 5113.

Layhadi, J. A., Turner, J., Crossman, D., & Fountain, S. J. (2018). ATP evokes Ca(2+) responses and CXCL5 secretion via P2X4 receptor activation in human monocyte-derived macrophages. *Journal of Immunology*, 200, 1159–1168.

Lazarowski E. R. (2012). Vesicular and conductive mechanisms of nucleotide release. *Purinergic Signalling*, 8(3), 359–373.

Lazarowski, E. R., Sesma, J. I., Seminario-Vidal, L., & Kreda, S. M. (2011). Molecular mechanisms of purine and pyrimidine nucleotide release. *Advances in Pharmacology*, 61, 221–261.

Lazarus, M., Hajeer, A. H., Turner, D., Sinnott, P., Worthington, J., Ollier, W. E., & Hutchinson, I. V. (1997). Genetic variation in the interleukin 10 gene promoter and systemic lupus erythematosus. *The Journal of Rheumatology*, 24(12), 2314–2317.

Le, A., Mukesh, B. N., McCarty, C. A., & Taylor, H. R. (2003). Risk factors associated with the incidence of open-angle glaucoma: the visual impairment project. *Investigative Ophthalmology & Visual Science*, 44(9), 3783–3789.

Le Feuvre, R., Brough, D., & Rothwell, N. (2002). Extracellular ATP and P2X7 receptors in neurodegeneration. *European Journal of Pharmacology*, 447(2-3), 261–269.

Lê, K. T., Boué-Grabot, E., Archambault, V., & Séguéla, P. (1999). Functional and biochemical evidence for heteromeric ATP-gated channels composed of P2X1 and P2X5 subunits. *The Journal of Biological Chemistry*, 274(22), 15415–15419.

Lecut, C., Frederix, K., Johnson, D. M., Deroanne, C., Thiry, M., Faccinnetto, C., Marée, R., Evans, R. J., Volders, P. G., Bours, V., & Oury, C. (2009). P2X1 ion channels promote neutrophil chemotaxis through Rho kinase activation. *Journal of Immunology*, *183*(4), 2801–2809.

Ledderose, C., Bao, Y., Kondo, Y., Fakhari, M., Slubowski, C., Zhang, J., & Junger, W. G. (2016). Purinergic Signaling and the Immune Response in Sepsis: A Review. *Clinical Therapeutics*, *38*(5), 1054–1065.

Lee, J., & Pelis, R. M. (2016). Drug Transport by the Blood-Aqueous Humor Barrier of the Eye. *Drug metabolism and Disposition: The Biological Fate of Chemicals*, *44*(10), 1675–1681.

Leitman, M., 2016. *Manual for eye examination and diagnosis*. 9th ed. United Kingdom: Wiley-Blackwell.

Leske, M. C., Heijl, A., Hyman, L., Bengtsson, B., Dong, L., Yang, Z., & EMGT Group (2007). Predictors of long-term progression in the early manifest glaucoma trial. *Ophthalmology*, *114*(11), 1965–1972.

Leske, M. C., Heijl, A., Hussein, M., Bengtsson, B., Hyman, L., Komaroff, E., & Early Manifest Glaucoma Trial Group (2003). Factors for glaucoma progression and the effect of treatment: the early manifest glaucoma trial. *Archives of Ophthalmology*, *121*(1), 48–56.

Leske, M. C., Heijl, A., Hyman, L., & Bengtsson, B. (1999). Early Manifest Glaucoma Trial: design and baseline data. *Ophthalmology*, *106*(11), 2144–2153.

Levin A. V. (2007). Aphakic glaucoma: a never-ending story?. *The British Journal of Ophthalmology*, *91*(12), 1574–1575.

Levin, L. A., Nilsson, S. F., Ver Hoeve, J., Wu, S. M., 2011. *Adler's Physiology of the Eye*. Elsevier, Oxford

Li, H., Ambade, A., & Re, F. (2009). Cutting edge: Necrosis activates the NLRP3 inflammasome. *Journal of Immunology*, *183*(3), 1528–1532.

Li, M., Kawate, T., Silberberg, S. D., & Swartz, K. J. (2010). Pore-opening mechanism in trimeric P2X receptor channels. *Nature Communications*, *1*(4), 44.

Li, M., Toombes, G. E., Silberberg, S. D., & Swartz, K. J. (2015). Physical basis of apparent pore dilation of ATP-activated P2X receptor channels. *Nature Neuroscience*, *18*(11), 1577–1583.

Li, S., Li, J., Wang, N., Hao, G., & Sun, J. (2018). Characterization of UDP-Activated Purinergic Receptor P2Y₆ Involved in Japanese Flounder *Paralichthys olivaceus* Innate Immunity. *International Journal of Molecular Sciences*, *19*(7), 2095.

Lichter, P. R., Musch, D. C., Gillespie, B. W., Guire, K. E., Janz, N. K., Wren, P. A., Mills, R. P., & CIGTS Study Group (2001). Interim clinical outcomes in the Collaborative Initial Glaucoma Treatment Study comparing initial treatment randomized to medications or surgery. *Ophthalmology*, *108*(11), 1943–1953.

Lim, S. Y., Yuzhalin, A. E., Gordon-Weeks, A. N., & Muschel, R. J. (2016). Targeting the CCL2-CCR2 signaling axis in cancer metastasis. *Oncotarget*, *7*(19), 28697–28710.

Limb, G. A., Salt, T. E., Munro, P. M., Moss, S. E., & Khaw, P. T. (2002). In vitro characterization of a spontaneously immortalized human Müller cell line (MIO-M1). *Investigative Ophthalmology & Visual Science*, *43*(3), 864–869.

Lin, H. J., Tsai, S. C., Tsai, F. J., Chen, W. C., Tsai, J. J., & Hsu, C. D. (2003). Association of interleukin 1beta and receptor antagonist gene polymorphisms with primary open-angle glaucoma. *Ophthalmologica. Journal International d'Ophthalmologie*.

International Journal of Ophthalmology. Zeitschrift fur Augenheilkunde, 217(5), 358–364.

Lin, S. S., Tang, Y., Illes, P., & Verkhatsky, A. (2021). The Safeguarding Microglia: Central Role for P2Y₁₂ Receptors. *Frontiers in Pharmacology*, 11, 627760.

Lin, X., Fang, D., Zhou, H., & Su, S. B. (2013). The expression of Toll-like receptors in murine Müller cells, the glial cells in retina. *Neurological Sciences*, 34(8), 1339–1346.

Lipp, S., Wurm, A., Pannicke, T., Wiedemann, P., Reichenbach, A., Chen, J., & Bringmann, A. (2009). Calcium responses mediated by type 2 IP₃-receptors are required for osmotic volume regulation of retinal glial cells in mice. *Neuroscience Letters*, 457(2), 85–88.

Liu, T., Zhang, L., Joo, D., & Sun, S. C. (2017). NF-κB signaling in inflammation. *Signal Transduction and Targeted Therapy*, 2, 17023

Liu, X., Huang, P., Wang, J., Yang, Z., Huang, S., Luo, X., Qi, J., Shen, X., & Zhong, Y. (2016). The Effect of A2A Receptor Antagonist on Microglial Activation in Experimental Glaucoma. *Investigative Ophthalmology & Visual Science*, 57(3), 776–786.

Liu, X., Surprenant, A., Mao, H. J., Roger, S., Xia, R., Bradley, H., & Jiang, L. H. (2008). Identification of key residues coordinating functional inhibition of P2X₇ receptors by zinc and copper. *Molecular Pharmacology*, 73(1), 252–259.

Liu, Y., Wei, S. H., Ho, A. S., de Waal Malefyt, R., & Moore, K. W. (1994). Expression cloning and characterization of a human IL-10 receptor. *Journal of Immunology*, 152(4), 1821–1829.

Liverani, E., Kilpatrick, L. E., Tsygankov, A. Y., & Kunapuli, S. P. (2014). The role of P2Y₁₂ receptor and activated platelets during inflammation. *Current Drug Targets*, *15*(7), 720–728.

Llorente, L., Richaud-Patin, Y., Couderc, J., Alarcon-Segovia, D., Ruiz-Soto, R., Alcocer-Castillejos, N., Alcocer-Varela, J., Granados, J., Bahena, S., Galanaud, P., & Emilie, D. (1997). Dysregulation of interleukin-10 production in relatives of patients with systemic lupus erythematosus. *Arthritis and Rheumatism*, *40*(8), 1429–1435.

Llorente, L., Zou, W., Levy, Y., Richaud-Patin, Y., Wijdenes, J., Alcocer-Varela, J., Morel-Fourrier, B., Brouet, J. C., Alarcon-Segovia, D., Galanaud, P., & Emilie, D. (1995). Role of interleukin 10 in the B lymphocyte hyperactivity and autoantibody production of human systemic lupus erythematosus. *The Journal of Experimental Medicine*, *181*(3), 839–844.

Locovei, S., Wang, J., & Dahl, G. (2006). Activation of pannexin 1 channels by ATP through P2Y receptors and by cytoplasmic calcium. *FEBS Letters*, *580*(1), 239–244.

Lomedico, P. T., Gubler, U., Hellmann, C. P., Dukovich, M., Giri, J. G., Pan, Y. C., Collier, K., Semionow, R., Chua, A. O., & Mizel, S. B. (1984). Cloning and expression of murine interleukin-1 cDNA in *Escherichia coli*. *Nature*, *312*(5993), 458–462.

Lu, L. J., Tsai, J. C., & Liu, J. (2017). Novel Pharmacologic Candidates for Treatment of Primary Open-Angle Glaucoma. *The Yale Journal of Biology and Medicine*, *90*(1), 111–118.

Lustig, K. D., Shiau, A. K., Brake, A. J., & Julius, D. (1993). Expression cloning of an ATP receptor from mouse neuroblastoma cells. *Proceedings of the National Academy of Sciences of the United States of America*, *90*(11), 5113–5117.

Lutfalla, G., Gardiner, K., & Uzé, G. (1993). A new member of the cytokine receptor gene family maps on chromosome 21 at less than 35 kb from IFNAR. *Genomics*, *16*(2), 366–373.

Lütjen-Drecoll E. (1973). Structural factors influencing outflow facility and its changeability under drugs. A study in *Macaca arctoides*. *Investigative Ophthalmology*, *12*(4), 280–294.

Madeira, M. H., Boia, R., Elvas, F., Martins, T., Cunha, R. A., Ambrósio, A. F., & Santiago, A. R. (2016). Selective A2A receptor antagonist prevents microglia-mediated neuroinflammation and protects retinal ganglion cells from high intraocular pressure-induced transient ischemic injury. *Translational Research: The Journal of Laboratory and Clinical Medicine*, *169*, 112–128.

Madeira, M. H., Elvas, F., Boia, R., Gonçalves, F. Q., Cunha, R. A., Ambrósio, A. F., & Santiago, A. R. (2015). Adenosine A2AR blockade prevents neuroinflammation-induced death of retinal ganglion cells caused by elevated pressure. *Journal of Neuroinflammation*, *12*, 115.

Madej, M. P., Töpfer, E., Boraschi, D., & Italiani, P. (2017). Different Regulation of Interleukin-1 Production and Activity in Monocytes and Macrophages: Innate Memory as an Endogenous Mechanism of IL-1 Inhibition. *Frontiers in Pharmacology*, *8*, 335.

Magnusson, G., Abrahamsson, M., & Sjöstrand, J. (2000). Glaucoma following congenital cataract surgery: an 18-year longitudinal follow-up. *Acta ophthalmologica Scandinavica*, *78*(1), 65–70.

Maier, P. C., Funk, J., Schwarzer, G., Antes, G., & Falck-Ytter, Y. T. (2005). Treatment of ocular hypertension and open angle glaucoma: meta-analysis of randomised controlled trials. *BMJ*, *331*(7509), 134.

Maier, R., Glatz, A., Mosbacher, J., & Bilbe, G. (1997). Cloning of P2Y₆ cDNAs and identification of a pseudogene: comparison of P2Y receptor subtype expression in bone and brain tissues. *Biochemical and Biophysical Research Communications*, 240(2), 298–302.

Majeed, M., Nagabhushanam, K., Natarajan, S., Vaidyanathan, P., Karri, S. K., & Jose, J. A. (2015). Efficacy and safety of 1% forskolin eye drops in open angle glaucoma - An open label study. *Saudi Journal of Ophthalmology*, 29(3), 197–200.

Malin, S. A., & Molliver, D. C. (2010). Gi- and Gq-coupled ADP (P2Y) receptors act in opposition to modulate nociceptive signaling and inflammatory pain behavior. *Molecular Pain*, 6, 21.

Malmsjö, M., Hou, M., Pendergast, W., Erlinge, D., & Edvinsson, L. (2003). Potent P2Y₆ receptor mediated contractions in human cerebral arteries. *BMC Pharmacology*, 3, 4.

Maminishkis, A., Jalickee, S., Blaug, S. A., Rymer, J., Yerxa, B. R., Peterson, W. M., & Miller, S. S. (2002). The P2Y(2) receptor agonist INS37217 stimulates RPE fluid transport in vitro and retinal reattachment in rat. *Investigative Ophthalmology & Visual Science*, 43(11), 3555–3566.

Mano, T., & Puro, D. G. (1990). Phagocytosis by human retinal glial cells in culture. *Investigative Ophthalmology & Visual Science*, 31(6), 1047–1055.

Mariathasan, S., Newton, K., Monack, D. M., Vucic, D., French, D. M., Lee, W. P., Roose-Girma, M., Erickson, S., & Dixit, V. M. (2004). Differential activation of the inflammasome by caspase-1 adaptors ASC and Ipaf. *Nature*, 430(6996), 213–218.

Mariathasan, S., Weiss, D. S., Newton, K., McBride, J., O'Rourke, K., Roose-Girma, M., Lee, W. P., Weinrauch, Y., Monack, D. M., & Dixit, V. M. (2006). Cryopyrin activates the inflammasome in response to toxins and ATP. *Nature*, 440(7081), 228–232.

Markiewicz, L., Majsterek, I., Przybyłowska, K., Dżiki, L., Waszczyk, M., Gacek, M., Kamińska, A., Szaflik, J., & Szaflik, J. P. (2013). Gene polymorphisms of the MMP1, MMP9, MMP12, IL-1 β and TIMP1 and the risk of primary open-angle glaucoma. *Acta Ophthalmologica*, 91(7), 516–523.

Markovskaya, A., Crooke, A., Guzmán-Aranguez, A. I., Peral, A., Ziganshin, A. U., & Pintor, J. (2008). Hypotensive effect of UDP on intraocular pressure in rabbits. *European Journal of Pharmacology*, 579(1-3), 93–97.

Marshall J. C. (2005). Lipopolysaccharide: an endotoxin or an exogenous hormone?. *Clinical Infectious Diseases*, 41 Suppl 7, 470–480.

Martínez, M., Martínez, N. A., & Silva, W. I. (2017). Measurement of the Intracellular Calcium Concentration with Fura-2 AM Using a Fluorescence Plate Reader. *Bio-protocol*, 7(14), e2411.

Masis, M., Mineault, P. J., Phan, E., & Lin, S. C. (2018). The role of phacoemulsification in glaucoma therapy: A systematic review and meta-analysis. *Survey of Ophthalmology*, 63(5), 700–710.

Matikainen, N., Pekkarinen, T., Ryhänen, E. M., & Schalin-Jääntti, C. (2021). Physiology of Calcium Homeostasis: An Overview. *Endocrinology and Metabolism Clinics of North America*, 50(4), 575–590.

Mawrin, C., Pap, T., Pallas, M., Dietzmann, K., Behrens-Baumann, W., & Vorwerk, C. K. (2003). Changes of retinal glutamate transporter GLT-1 mRNA levels following optic nerve damage. *Molecular Vision*, 9, 10–13.

McClellan, B. H., Whitney, C. R., Newman, L. P., & Allansmith, M. R. (1973). Immunoglobulins in tears. *American journal of ophthalmology*, 76(1), 89–101

Meister, J., Le Duc, D., Ricken, A., Burkhardt, R., Thiery, J., Pfannkuche, H., Polte, T., Grosse, J., Schöneberg, T., & Schulz, A. (2014). The G protein-coupled receptor P2Y₁₄ influences insulin release and smooth muscle function in mice. *The Journal of Biological Chemistry*, 289(34), 23353–23366.

Merz, J., Albrecht, P., von Garlen, S., Ahmed, I., Dimanski, D., Wolf, D., Hilgendorf, I., Härdtner, C., Grotius, K., Willecke, F., Heidt, T., Bugger, H., Hoppe, N., Kintscher, U., von Zur Mühlen, C., Idzko, M., Bode, C., Zirlik, A., & Stachon, P. (2018). Purinergic receptor Y₂ (P2Y₂)-dependent VCAM-1 expression promotes immune cell infiltration in metabolic syndrome. *Basic Research in Cardiology*, 113(6), 45.

Miklavc, P., Mair, N., Wittekindt, O. H., Haller, T., Dietl, P., Felder, E., Timmler, M., & Frick, M. (2011). Fusion-activated Ca²⁺ entry via vesicular P2X₄ receptors promotes fusion pore opening and exocytotic content release in pneumocytes. *Proceedings of the National Academy of Sciences of the United States of America*, 108, 14503–14508.

Milligan G. (2009). G protein-coupled receptor hetero-dimerization: contribution to pharmacology and function. *British Journal of Pharmacology*, 158(1), 5–14.

Mills, M. D., & Robb, R. M. (1994). Glaucoma following childhood cataract surgery. *Journal of Pediatric Ophthalmology and Strabismus*, 31(6), 355–361.

Minckler, D. S., Bunt, A. H., & Johanson, G. W. (1977). Orthograde and retrograde axoplasmic transport during acute ocular hypertension in the monkey. *Investigative Ophthalmology & Visual Science*, 16(5), 426–441.

Miras-Portugal, M. T., Queipo, M. J., Gil-Redondo, J. C., Ortega, F., Gómez-Villafuertes, R., Gualix, J., Delicado, E. G., & Pérez-Sen, R. (2019). P2 receptor interaction and signalling cascades in neuroprotection. *Brain Research Bulletin*, 151, 74–83.

Mitchell, P., Smith, W., Attebo, K., & Healey, P. R. (1996). Prevalence of open-angle glaucoma in Australia. The Blue Mountains Eye Study. *Ophthalmology*, *103*(10), 1661–1669.

Modi, W. S., Masuda, A., Yamada, M., Oppenheim, J. J., Matsushima, K., & O'Brien, S. J. (1988). Chromosomal localization of the human interleukin 1 alpha (IL-1 alpha) gene. *Genomics*, *2*(4), 310–314.

Mookherjee, S., Banerjee, D., Chakraborty, S., Banerjee, A., Mukhopadhyay, I., Sen, A., & Ray, K. (2010). Association of IL1A and IL1B loci with primary open angle glaucoma. *BMC Medical Genetics*, *11*, 99.

Moore, K. W., de Waal Malefyt, R., Coffman, R. L., & O'Garra, A. (2001). Interleukin-10 and the interleukin-10 receptor. *Annual Review of Immunology*, *19*, 683–765.

Moore, K. W., O'Garra, A., de Waal Malefyt, R., Vieira, P., & Mosmann, T. R. (1993). Interleukin-10. *Annual Review of Immunology*, *11*, 165–190.

Moore, K. W., Vieira, P., Fiorentino, D. F., Trounstein, M. L., Khan, T. A., & Mosmann, T. R. (1990). Homology of cytokine synthesis inhibitory factor (IL-10) to the Epstein-Barr virus gene BCRF1. *Science*, *248*(4960), 1230–1234.

Moriyama, S., & Hiasa, M. (2016). Expression of Vesicular Nucleotide Transporter in the Mouse Retina. *Biological & Pharmaceutical Bulletin*, *39*(4), 564–569.

Moriyama, Y., Hiasa, M., Sakamoto, S., Omote, H., & Nomura, M. (2017). Vesicular nucleotide transporter (VNUT): appearance of an actress on the stage of purinergic signaling. *Purinergic Signalling*, *13*(3), 387–404.

Müller, T., Robaye, B., Vieira, R. P., Ferrari, D., Grimm, M., Jakob, T., Martin, S. F., Di Virgilio, F., Boeynaems, J. M., Virchow, J. C., & Idzko, M. (2010). The purinergic

receptor P2Y₂ receptor mediates chemotaxis of dendritic cells and eosinophils in allergic lung inflammation. *Allergy*, 65(12), 1545–1553.

Muñoz-Planillo, R., Kuffa, P., Martínez-Colón, G., Smith, B. L., Rajendiran, T. M., & Núñez, G. (2013). K⁺ efflux is the common trigger of NLRP3 inflammasome activation by bacterial toxins and particulate matter. *Immunity*, 38(6), 1142–1153.

Murakami, T., Ockinger, J., Yu, J., Byles, V., McColl, A., Hofer, A. M., & Horng, T. (2012). Critical role for calcium mobilization in activation of the NLRP3 inflammasome. *Proceedings of the National Academy of Sciences of the United States of America*, 109(28), 11282–11287.

Musch, D. C., Gillespie, B. W., Niziol, L. M., Lichter, P. R., Varma, R., & CIGTS Study Group (2011). Intraocular pressure control and long-term visual field loss in the Collaborative Initial Glaucoma Treatment Study. *Ophthalmology*, 118(9), 1766–1773.

Musch, D. C., Gillespie, B. W., Lichter, P. R., Niziol, L. M., Janz, N. K., & CIGTS Study Investigators (2009). Visual field progression in the Collaborative Initial Glaucoma Treatment Study the impact of treatment and other baseline factors. *Ophthalmology*, 116(2), 200–207.

Musch, D. C., Gillespie, B. W., Niziol, L. M., Cashwell, L. F., Lichter, P. R., & Collaborative Initial Glaucoma Treatment Study Group (2008). Factors associated with intraocular pressure before and during 9 years of treatment in the Collaborative Initial Glaucoma Treatment Study. *Ophthalmology*, 115(6), 927–933.

Musch, D. C., Gillespie, B. W., Niziol, L. M., Janz, N. K., Wren, P. A., Rockwood, E. J., Lichter, P. R., & Collaborative Initial Glaucoma Treatment Study Group (2006). Cataract extraction in the collaborative initial glaucoma treatment study: incidence, risk factors, and the effect of cataract progression and extraction on clinical and quality-of-life outcomes. *Archives of Ophthalmology*, 124(12), 1694–1700.

Musch, D. C., Lichter, P. R., Guire, K. E., & Standardi, C. L. (1999). The Collaborative Initial Glaucoma Treatment Study: study design, methods, and baseline characteristics of enrolled patients. *Ophthalmology*, *106*(4), 653–662.

Mwanza, J. C., Warren, J. L., Budenz, D. L., & Ganglion Cell Analysis Study Group (2013). Combining spectral domain optical coherence tomography structural parameters for the diagnosis of glaucoma with early visual field loss. *Investigative Ophthalmology & Visual Science*, *54*(13), 8393–8400.

Mwanza, J. C., Oakley, J. D., Budenz, D. L., Anderson, D. R., & Cirrus Optical Coherence Tomography Normative Database Study Group (2011). Ability of cirrus HD-OCT optic nerve head parameters to discriminate normal from glaucomatous eyes. *Ophthalmology*, *118*(2), 241–8.

Nadzirin, I. B., Fortuny-Gomez, A., Ngum, N., Richards, D., Ali, S., Searcey, M., & Fountain, S. J. (2021). Taspine is a natural product that suppresses P2X4 receptor activity via phosphoinositide 3-kinase inhibition. *British Journal of Pharmacology*, *178*(24), 4859–4872.

Nakahira, K., Haspel, J. A., Rathinam, V. A., Lee, S. J., Dolinay, T., Lam, H. C., Englert, J. A., Rabinovitch, M., Cernadas, M., Kim, H. P., Fitzgerald, K. A., Ryter, S. W., & Choi, A. M. (2011). Autophagy proteins regulate innate immune responses by inhibiting the release of mitochondrial DNA mediated by the NALP3 inflammasome. *Nature Immunology*, *12*(3), 222–230.

Namekata, K., Harada, C., Kohyama, K., Matsumoto, Y., & Harada, T. (2008). Interleukin-1 stimulates glutamate uptake in glial cells by accelerating membrane trafficking of Na⁺/K⁺-ATPase via actin depolymerization. *Molecular and Cellular Biology*, *28*(10), 3273–3280.

Nash, M. S., Young, K. W., Challiss, R. A., & Nahorski, S. R. (2001). Intracellular signalling. Receptor-specific messenger oscillations. *Nature*, *413*(6854), 381–382.

Naskar, R., Vorwerk, C. K., & Dreyer, E. B. (2000). Concurrent downregulation of a glutamate transporter and receptor in glaucoma. *Investigative Ophthalmology & Visual Science*, 41(7), 1940–1944.

National Health Service (NHS). (2022). *Glaucoma - Diagnosis*. [online] nhs.uk. Available at: <https://www.nhs.uk/conditions/glaucoma/diagnosis/> [Accessed 6 June 2022].

Nemet, A. Y., Assia, E. I., Meyerstein, D., Meyerstein, N., Gedanken, A., & Topaz, M. (2007). Protective effect of free-radical scavengers on corneal endothelial damage in phacoemulsification. *Journal of Cataract and Refractive Surgery*, 33(2), 310–315.

Netland, P. A., Sarkisian, S. R., Jr, Moster, M. R., Ahmed, I. I., Condon, G., Salim, S., Sherwood, M. B., & Siegfried, C. J. (2014). Randomized, prospective, comparative trial of EX-PRESS glaucoma filtration device versus trabeculectomy (XVT study). *American Journal of Ophthalmology*, 157(2), 433–440.

Newman E. A. (2003). Glial cell inhibition of neurons by release of ATP. *The Journal of Neuroscience*, 23(5), 1659–1666.

Newman E. A. (2001). Propagation of intercellular calcium waves in retinal astrocytes and Müller cells. *The Journal of Neuroscience*, 21(7), 2215–2223.

Newman E. A. (2005). Calcium increases in retinal glial cells evoked by light-induced neuronal activity. *The Journal of Neuroscience*, 25(23), 5502–5510.

NICE. (2022). *Glaucoma: diagnosis and management*. [online] Available at: <https://www.nice.org.uk/guidance/NG81> [Accessed 6 June 2022].

Nicke A. (2008). Homotrimeric complexes are the dominant assembly state of native P2X7 subunits. *Biochemical and Biophysical Research Communications*, 377(3), 803–808.

Nie, J., Huang, G. L., Deng, S. Z., Bao, Y., Liu, Y. W., Feng, Z. P., Wang, C. H., Chen, M., Qi, S. T., & Pan, J. (2017). The purine receptor P2X7R regulates the release of pro-inflammatory cytokines in human craniopharyngioma. *Endocrine-Related Cancer*, 24(6), 287–296.

Niyadurupola, N., Sidaway, P., Ma, N., Rhodes, J. D., Broadway, D. C., & Sanderson, J. (2013). P2X7 receptor activation mediates retinal ganglion cell death in a human retina model of ischemic neurodegeneration. *Investigative Ophthalmology & Visual Science*, 54(3), 2163–2170.

Niyadurupola, N., Sidaway, P., Osborne, A., Broadway, D. C., & Sanderson, J. (2011). The development of human organotypic retinal cultures (HORCs) to study retinal neurodegeneration. *The British Journal of Ophthalmology*, 95(5), 720–726.

Niyadurupola, N. (2009). The Development of Human Organotypic Retinal Cultures for Glaucoma Research: P2X7 receptor stimulation and interleukin 1B regulation in relation to retinal ganglion cell death [MD]. University of East Anglia.

Noailles, A., Fernández-Sánchez, L., Lax, P., & Cuenca, N. (2014). Microglia activation in a model of retinal degeneration and TUDCA neuroprotective effects. *Journal of Neuroinflammation*, 11, 186.

Norsworthy, M. W., Bei, F., Kawaguchi, R., Wang, Q., Tran, N. M., Li, Y., Brommer, B., Zhang, Y., Wang, C., Sanes, J. R., Coppola, G., & He, Z. (2017). Sox11 Expression Promotes Regeneration of Some Retinal Ganglion Cell Types but Kills Others. *Neuron*, 94(6), 1112–1120.

North R. A. (1996). P2X receptors: a third major class of ligand-gated ion channels. *Ciba Foundation Symposium*, 198, 91–109.

North R. A. (2002). Molecular physiology of P2X receptors. *Physiological Reviews*, 82(4), 1013–1067.

North R. A. (2016). P2X receptors. *Philosophical Transactions of the Royal Society of London. Series B, Biological Sciences*, 371(1700), 20150427.

Noske, W., Hensen, J., & Wiederholt, M. (1997). Endothelin-like immunoreactivity in aqueous humor of patients with primary open-angle glaucoma and cataract. *Graefe's Archive for Clinical and Experimental Ophthalmology = Albrecht von Graefes Archiv fur Klinische und Experimentelle Ophthalmologie*, 235(9), 551–552.

Oakes, S. G., Martin, W. J., 2nd, Lisek, C. A., & Powis, G. (1988). Incomplete hydrolysis of the calcium indicator precursor fura-2 pentaacetoxymethyl ester (fura-2 AM) by cells. *Analytical Biochemistry*, 169(1), 159–166.

Ohkubo, S., Kimura, J., Nakanishi, H., & Matsuoka, I. (2000). Effects of P(1) and P2 receptor antagonists on beta, gamma-methyleneATP- and CGS21680-induced cyclic AMP formation in NG108-15 cells. *British Journal of Pharmacology*, 129(2), 291–298.

Ohkubo, T., Yamazaki, J., Nakashima, Y., & Kitamura, K. (2000). Presence and possible role of the spliced isoform of the P2X1 receptor in rat vascular smooth muscle cells. *Pflugers Archiv: European Journal of Physiology*, 441(1), 57–64.

Olsen, I., & Yilmaz, Ö. (2016). Modulation of inflammasome activity by *Porphyromonas gingivalis* in periodontitis and associated systemic diseases. *Journal of Oral Microbiology*, 8, 30385.

Ong, K., Farinelli, A., Billson, F., Houang, M., & Stern, M. (1995). Comparative study of brain magnetic resonance imaging findings in patients with low-tension glaucoma and control subjects. *Ophthalmology*, *102*(11), 1632–1638.

Orriss, I., Syberg, S., Wang, N., Robaye, B., Gartland, A., Jorgensen, N., Arnett, T., & Boeynaems, J. M. (2011). Bone phenotypes of P2 receptor knockout mice. *Frontiers in Bioscience*, *3*(3), 1038–1046.

Orriss, I. R., Wang, N., Burnstock, G., Arnett, T. R., Gartland, A., Robaye, B., & Boeynaems, J. M. (2011). The P2Y(6) receptor stimulates bone resorption by osteoclasts. *Endocrinology*, *152*(10), 3706–3716.

Osborn, O., Brownell, S. E., Sanchez-Alavez, M., Salomon, D., Gram, H., & Bartfai, T. (2008). Treatment with an Interleukin 1 beta antibody improves glycemic control in diet-induced obesity. *Cytokine*, *44*(1), 141–148.

Otteson, D. C., & Phillips, M. J. (2010). A conditional immortalized mouse muller glial cell line expressing glial and retinal stem cell genes. *Investigative Ophthalmology & Visual Science*, *51*(11), 5991–6000.

Oyanguren-Desez, O., Rodríguez-Antigüedad, A., Villoslada, P., Domercq, M., Alberdi, E., & Matute, C. (2011). Gain-of-function of P2X7 receptor gene variants in multiple sclerosis. *Cell Calcium*, *50*(5), 468–472.

Palm, E. (1947). On the occurrence in the retina of conditions corresponding to the blood-brain barrier. *Acta Ophthalmologica*, *25*(1), 29–35.

Palomino, D. C., & Marti, L. C. (2015). Chemokines and immunity. *Einstein*, *13*(3), 469–473.

Pannicke, T., Fischer, W., Biedermann, B., Schädlich, H., Grosche, J., Faude, F., Wiedemann, P., Allgaier, C., Illes, P., Burnstock, G., & Reichenbach, A. (2000). P2X7

receptors in Müller glial cells from the human retina. *The Journal of Neuroscience*, 20(16), 5965–5972.

Panzer, S., Madden, M., & Matsuki, K. (1993). Interaction of IL-1 beta, IL-6 and tumour necrosis factor-alpha (TNF-alpha) in human T cells activated by murine antigens. *Clinical and Experimental Immunology*, 93(3), 471–478.

Parisi, V., Centofanti, M., Ziccardi, L., Tanga, L., Michelessi, M., Roberti, G., & Manni, G. (2015). Treatment with citicoline eye drops enhances retinal function and neural conduction along the visual pathways in open angle glaucoma. *Graefe's Archive for Clinical and Experimental Ophthalmology = Albrecht von Graefes Archiv fur Klinische und Experimentelle Ophthalmologie*, 253(8), 1327–1340.

Parisi, V., Oddone, F., Roberti, G., Tanga, L., Carnevale, C., Ziccardi, L., & Manni, G. (2019). Enhancement of Retinal Function and of Neural Conduction Along the Visual Pathway Induced by Treatment with Citicoline Eye Drops in Liposomal Formulation in Open Angle Glaucoma: A Pilot Electrofunctional Study. *Advances in Therapy*, 36(4), 987–996.

Park, J. H., Nam, K. T., Yoo, C., & Kim, Y. Y. (2016). Head Elevation and Intraocular Pressure in Glaucoma. *Optometry and Vision Science*, 93(9), 1163–1170.

Parri H. R. (2013). Star spangled manner: astrocytes and neurons contribute to adenosine release in the hippocampus. *The Journal of Physiology*, 591(16), 3805–3806.

Pasmatzi, E., Papadionysiou, C., Monastirli, A., Badavanis, G., & Tsambaos, D. (2019). Galectin 1 in dermatology: current knowledge and perspectives. *Acta Dermatovenerologica Alpina, Pannonica, et Adriatica*, 28(1), 27–31.

Pearson, R. A., Dale, N., Llaudet, E., & Mobbs, P. (2005). ATP released via gap junction hemichannels from the pigment epithelium regulates neural retinal progenitor proliferation. *Neuron*, *46*(5), 731–744.

Pei, X., Zhang, X. J., & Chen, H. M. (2019). Bardoxolone treatment alleviates lipopolysaccharide (LPS)-induced acute lung injury through suppressing inflammation and oxidative stress regulated by Nrf2 signaling. *Biochemical and Biophysical Research Communications*, *516*(1), 270–277.

Pekny, M., Wilhelmsson, U., & Pekna, M. (2014). The dual role of astrocyte activation and reactive gliosis. *Neuroscience Letters*, *565*, 30–38.

Pelegrin, P., & Surprenant, A. (2006). Pannexin-1 mediates large pore formation and interleukin-1beta release by the ATP-gated P2X7 receptor. *The EMBO Journal*, *25*(21), 5071–5082.

Pelegrin, P., Barroso-Gutierrez, C., & Surprenant, A. (2008). P2X7 receptor differentially couples to distinct release pathways for IL-1beta in mouse macrophage. *Journal of Immunology*, *180*(11), 7147–7157.

Pereiro, X., Ruzafa, N., Acera, A., Urcola, A., & Vecino, E. (2020). Optimization of a Method to Isolate and Culture Adult Porcine, Rats and Mice Müller Glia in Order to Study Retinal Diseases. *Frontiers in Cellular Neuroscience*, *14*, 7.

Perera, S. A., Wong, T. Y., Tay, W. T., Foster, P. J., Saw, S. M., & Aung, T. (2010). Refractive error, axial dimensions, and primary open-angle glaucoma: the Singapore Malay Eye Study. *Archives of Ophthalmology*, *128*(7), 900–905.

Perez, M., & Hirschberg, C. B. (1986). Transport of sugar nucleotides and adenosine 3'-phosphate 5'-phosphosulfate into vesicles derived from the Golgi apparatus. *Biochimica et Biophysica Acta*, *864*(2), 213–222.

Petrou, S., Ugur, M., Drummond, R. M., Singer, J. J., & Walsh, J. V., Jr (1997). P2X7 purinoceptor expression in *Xenopus* oocytes is not sufficient to produce a pore-forming P2Z-like phenotype. *FEBS Letters*, *411*(2-3), 339–345.

Pfeiffer, N., Garcia-Feijoo, J., Martinez-de-la-Casa, J. M., Larrosa, J. M., Fea, A., Lemij, H., Gandolfi, S., Schwenn, O., Lorenz, K., & Samuelson, T. W. (2015). A Randomized Trial of a Schlemm's Canal Microstent with Phacoemulsification for Reducing Intraocular Pressure in Open-Angle Glaucoma. *Ophthalmology*, *122*(7), 1283–1293.

Pfeiffer, R. L., Marc, R. E., Kondo, M., Terasaki, H., & Jones, B. W. (2016). Müller cell metabolic chaos during retinal degeneration. *Experimental Eye Research*, *150*, 62–70.

Pietrowska, K., Dmuchowska, D. A., Krasnicki, P., Mariak, Z., Kretowski, A., & Ciborowski, M. (2018). Analysis of pharmaceuticals and small molecules in aqueous humor. *Journal of Pharmaceutical and Biomedical Analysis*, *159*, 23–36.

Pietrowski, M. J., Gabr, A. A., Kozlov, S., Blum, D., Halle, A., & Carvalho, K. (2021). Glial Purinergic Signaling in Neurodegeneration. *Frontiers in Neurology*, *12*, 654850.

Place, D. E., & Kanneganti, T. D. (2019). Cell death-mediated cytokine release and its therapeutic implications. *The Journal of Experimental Medicine*, *216*(7), 1474–1486.

Portales-Cervantes, L., Niño-Moreno, P., Salgado-Bustamante, M., García-Hernández, M. H., Baranda-Candido, L., Reynaga-Hernández, E., Barajas-López, C., González-Amaro, R., & Portales-Pérez, D. P. (2012). The His155Tyr (489C>T) single nucleotide polymorphism of P2RX7 gene confers an enhanced function of P2X7 receptor in immune cells from patients with rheumatoid arthritis. *Cellular Immunology*, *276*(1-2), 168–175.

Prinz, M., & Priller, J. (2014). Microglia and brain macrophages in the molecular age: from origin to neuropsychiatric disease. *Nature Reviews. Neuroscience*, *15*(5), 300–312.

Próchnicki, T., Mangan, M. S., & Latz, E. (2016). Recent insights into the molecular mechanisms of the NLRP3 inflammasome activation. *F1000Research*, 5, F1000 Faculty Rev-1469.

Prokai-Tatrai, K., Xin, H., Nguyen, V., Szarka, S., Blazics, B., Prokai, L., & Koulen, P. (2013). 17 β -estradiol eye drops protect the retinal ganglion cell layer and preserve visual function in an in vivo model of glaucoma. *Molecular Pharmaceutics*, 10(8), 3253–3261.

Promega. (2018). *CellTiter 96 Aqueous Non-Radioactive Cell Proliferation Assay (MTS)*. [online] Promega UK. Available at: https://www.promega.co.uk/products/cell-health-assays/cell-viability-and-cytotoxicity-assays/celltiter-96-aqueous-non_radioactive-cell-proliferation-assay-_mts_/?catNum=G5421 [Accessed 6 June 2022].

Puthussery, T., & Fletcher, E. (2009). Extracellular ATP induces retinal photoreceptor apoptosis through activation of purinoceptors in rodents. *The Journal of Comparative Neurology*, 513(4), 430–440.

Puthussery, T., & Fletcher, E. L. (2006). P2X2 receptors on ganglion and amacrine cells in cone pathways of the rat retina. *The Journal of Comparative Neurology*, 496(5), 595–609.

Puthussery, T., & Fletcher, E. L. (2004). Synaptic localization of P2X7 receptors in the rat retina. *The Journal of Comparative Neurology*, 472(1), 13–23.

Qiu, M., Wang, S. Y., Singh, K., & Lin, S. C. (2013). Association between myopia and glaucoma in the United States population. *Investigative Ophthalmology & Visual Science*, 54(1), 830–835.

Quaranta, L., Riva, I., & Floriani, I. (2014). Ginkgo biloba extract improves visual field damage in some patients affected by normal-tension glaucoma. *Investigative Ophthalmology & Visual Science*, 55(4), 2417.

Quigley H. A. (1999). Neuronal death in glaucoma. *Progress in Retinal and Eye Research*, 18(1), 39–57.

Quigley, H. A., & Addicks, E. M. (1981). Regional differences in the structure of the lamina cribrosa and their relation to glaucomatous optic nerve damage. *Archives of Ophthalmology*, 99(1), 137–143.

Quigley, H. A., Addicks, E. M., Green, W. R., & Maumenee, A. E. (1981). Optic nerve damage in human glaucoma. II. The site of injury and susceptibility to damage. *Archives of Ophthalmology*, 99(4), 635–649.

Quigley, H. A., & Addicks, E. M. (1980). Chronic experimental glaucoma in primates. II. Effect of extended intraocular pressure elevation on optic nerve head and axonal transport. *Investigative Ophthalmology & Visual Science*, 19(2), 137–152.

Quigley, H., & Anderson, D. R. (1976). The dynamics and location of axonal transport blockade by acute intraocular pressure elevation in primate optic nerve. *Investigative Ophthalmology*, 15(8), 606–616.

Quintas, C., Pinho, D., Pereira, C., Saraiva, L., Gonçalves, J., & Queiroz, G. (2014). Microglia P2Y₆ receptors mediate nitric oxide release and astrocyte apoptosis. *Journal of Neuroinflammation*, 11, 141.

Ralevic, V., & Dunn, W. R. (2015). Purinergic transmission in blood vessels. *Autonomic Neuroscience: Basic & Clinical*, 191, 48–66.

Rangel-Yescas, G. E., Vazquez-Cuevas, F. G., Garay, E., & Arellano, R. O. (2012). Cloning and functional analysis of P2X1b, a new variant in rat optic nerve that

regulates the P2X1 receptor in a use-dependent manner. *Acta Neurobiologiae Experimentalis*, 72(1), 18–32.

Ransohoff, R. M., & Brown, M. A. (2012). Innate immunity in the central nervous system. *The Journal of Clinical Investigation*, 122(4), 1164–1171.

Razeghinejad, M. R., & Katz, L. J. (2012). Steroid-induced iatrogenic glaucoma. *Ophthalmic Research*, 47(2), 66–80.

Reardon, G., Kotak, S., & Schwartz, G. F. (2011). Objective assessment of compliance and persistence among patients treated for glaucoma and ocular hypertension: a systematic review. *Patient Preference and Adherence*, 5, 441–463.

Reddish, F. N., Miller, C. L., Gorkhali, R., & Yang, J. J. (2017). Monitoring ER/SR Calcium Release with the Targeted Ca²⁺ Sensor CatchER. *Journal of Visualized Experiments*, (123), 55822.

Reddy, S. A., Huang, J. H., & Liao, W. S. (1997). Phosphatidylinositol 3-kinase in interleukin 1 signaling. Physical interaction with the interleukin 1 receptor and requirement in NFκB and AP-1 activation. *The Journal of Biological Chemistry*, 272(46), 29167–29173.

Reddy, V. N., Giblin, F. J., Lin, L. R., & Chakrapani, B. (1998). The effect of aqueous humor ascorbate on ultraviolet-B-induced DNA damage in lens epithelium. *Investigative Ophthalmology & Visual Science*, 39(2), 344–350.

Reichenbach, A., & Bringmann, A. (2020). Glia of the human retina. *Glia*, 68(4), 768–796.

Reichenbach, A., & Bringmann, A. (2016). Purinergic signaling in retinal degeneration and regeneration. *Neuropharmacology*, 104, 194–211.

Reichenbach, A., & Bringmann, A. (2013). New functions of Müller cells. *Glia*, *61*(5), 651–678.

Reichenbach, A., Siegel, A., Rickmann, M., Wolff, J. R., Noone, D., & Robinson, S. R. (1995). Distribution of Bergmann glial somata and processes: implications for function. *Journal fur Hirnforschung*, *36*(4), 509–517.

Reigada, D., Lu, W., Zhang, M., & Mitchell, C. H. (2008). Elevated pressure triggers a physiological release of ATP from the retina: Possible role for pannexin hemichannels. *Neuroscience*, *157*(2), 396–404.

Reiss, G. R., Werness, P. G., Zollman, P. E., & Brubaker, R. F. (1986). Ascorbic acid levels in the aqueous humor of nocturnal and diurnal mammals. *Archives of Ophthalmology*, *104*(5), 753–755.

Relvas, L. J., Makhoul, M., Dewispelaere, R., Caspers, L., Communi, D., Boeynaems, J. M., Robaye, B., Bruyns, C., & Willermain, F. (2015). P2Y₂R deficiency attenuates experimental autoimmune uveitis development. *PLOS ONE*, *10*(2).

Ren, K., & Torres, R. (2009). Role of interleukin-1beta during pain and inflammation. *Brain Research Reviews*, *60*(1), 57–64.

Resta, V., Novelli, E., Vozzi, G., Scarpa, C., Caleo, M., Ahluwalia, A., Solini, A., Santini, E., Parisi, V., Di Virgilio, F., & Galli-Resta, L. (2007). Acute retinal ganglion cell injury caused by intraocular pressure spikes is mediated by endogenous extracellular ATP. *The European Journal of Neuroscience*, *25*(9), 2741–2754.

Retamal M. A. (2014). Connexin and Pannexin hemichannels are regulated by redox potential. *Frontiers in Physiology*, *5*, 80.

Ribelayga, C., & Mangel, S. C. (2005). A circadian clock and light/dark adaptation differentially regulate adenosine in the mammalian retina. *The Journal of Neuroscience*, 25(1), 215–222.

Rider, P., Kaplanov, I., Romzova, M., Bernardis, L., Braiman, A., Voronov, E., & Apte, R. N. (2012). The transcription of the alarmin cytokine interleukin-1 alpha is controlled by hypoxia inducible factors 1 and 2 alpha in hypoxic cells. *Frontiers in Immunology*, 3, 290.

Rider, P., Carmi, Y., Voronov, E., & Apte, R. N. (2013). Interleukin-1 α . *Seminars in Immunology*, 25(6), 430–438.

Riedel, T., Schmalzing, G., & Markwardt, F. (2007). Influence of extracellular monovalent cations on pore and gating properties of P2X7 receptor-operated single-channel currents. *Biophysical Journal*, 93(3), 846–858.

Rieg, T., Gerasimova, M., Boyer, J. L., Insel, P. A., & Vallon, V. (2011). P2Y₂ receptor activation decreases blood pressure and increases renal Na⁺ excretion. *American Journal of Physiology. Regulatory, Integrative and Comparative Physiology*, 301(2), 510–518.

Ringvold A. (1996). The significance of ascorbate in the aqueous humour protection against UV-A and UV-B. *Experimental Eye Research*, 62(3), 261–264.

Robaye, B., Ghanem, E., Wilkin, F., Fokan, D., Van Driessche, W., Schurmans, S., Boeynaems, J. M., & Beauwens, R. (2003). Loss of nucleotide regulation of epithelial chloride transport in the jejunum of P2Y₄-null mice. *Molecular Pharmacology*, 63(4), 777–783.

Roberge, F. G., Caspi, R. R., Chan, C. C., & Nussenblatt, R. B. (1991). Inhibition of T lymphocyte proliferation by retinal glial Müller cells: reversal of inhibition by glucocorticoids. *Journal of Autoimmunity*, 4(2), 307–314.

Robson, S. C., Sévigny, J., & Zimmermann, H. (2006). The E-NTPDase family of ectonucleotidases: Structure function relationships and pathophysiological significance. *Purinergic Signalling*, 2(2), 409–430.

Roger, S., Mei, Z. Z., Baldwin, J. M., Dong, L., Bradley, H., Baldwin, S. A., Surprenant, A., & Jiang, L. H. (2010). Single nucleotide polymorphisms that were identified in affective mood disorders affect ATP-activated P2X7 receptor functions. *Journal of Psychiatric Research*, 44(6), 347–355.

Roger, S., Pelegrin, P., & Surprenant, A. (2008). Facilitation of P2X7 receptor currents and membrane blebbing via constitutive and dynamic calmodulin binding. *The Journal of Neuroscience*, 28(25), 6393–6401.

Rood, M. J., Keijsers, V., van der Linden, M. W., Tong, T. Q., Borggreve, S. E., Verweij, C. L., Breedveld, F. C., & Huizinga, T. W. (1999). Neuropsychiatric systemic lupus erythematosus is associated with imbalance in interleukin 10 promoter haplotypes. *Annals of the Rheumatic Diseases*, 58(2), 85–89.

Rose, R. C., & Bode, A. M. (1991). Ocular ascorbate transport and metabolism. *Comparative Biochemistry and Physiology. A, Comparative Physiology*, 100(2), 273–285.

Rosenfeld, C., Price, M. O., Lai, X., Witzmann, F. A., & Price, F. W., Jr (2015). Distinctive and pervasive alterations in aqueous humor protein composition following different types of glaucoma surgery. *Molecular Vision*, 21, 911–918.

Rosenwasser L. J. (1998). Biologic activities of IL-1 and its role in human disease. *The Journal of Allergy and Clinical Immunology*, 102(3), 344–350.

Rubartelli, A., Cozzolino, F., Talio, M., & Sitia, R. (1990). A novel secretory pathway for interleukin-1 beta, a protein lacking a signal sequence. *The EMBO Journal*, *9*(5), 1503–1510.

Rubowitz, A., Assia, E. I., Rosner, M., & Topaz, M. (2003). Antioxidant protection against corneal damage by free radicals during phacoemulsification. *Investigative Ophthalmology & Visual Science*, *44*(5), 1866–1870.

Rudnicka, A. R., Mt-Isa, S., Owen, C. G., Cook, D. G., & Ashby, D. (2006). Variations in primary open-angle glaucoma prevalence by age, gender, and race: a Bayesian meta-analysis. *Investigative Ophthalmology & Visual Science*, *47*(10), 4254–4261.

Saheb, H., Donnenfeld, E. D., Solomon, K. D., Voskanyan, L., Chang, D. F., Samuelson, T. W., Ahmed, I., & Katz, L. J. (2021). Five-Year Outcomes Prospective Study of Two First-Generation Trabecular Micro-Bypass Stents (iStent®) in Open-Angle Glaucoma. *Current Eye Research*, *46*(2), 224–231.

Samuelson, T. W., Katz, L. J., Wells, J. M., Duh, Y. J., Giamporcaro, J. E., & US iStent Study Group (2011). Randomized evaluation of the trabecular micro-bypass stent with phacoemulsification in patients with glaucoma and cataract. *Ophthalmology*, *118*(3), 459–467.

Samuelson, T. W., Chang, D. F., Marquis, R., Flowers, B., Lim, K. S., Ahmed, I., Jampel, H. D., Aung, T., Crandall, A. S., Singh, K., & HORIZON Investigators (2019). A Schlemm Canal Microstent for Intraocular Pressure Reduction in Primary Open-Angle Glaucoma and Cataract: The HORIZON Study. *Ophthalmology*, *126*(1), 29–37.

Sanderson, J., Dartt, D. A., Trinkaus-Randall, V., Pintor, J., Civan, M. M., Delamere, N. A., Fletcher, E. L., Salt, T. E., Grosche, A., & Mitchell, C. H. (2014). Purines in the eye: recent evidence for the physiological and pathological role of purines in the RPE, retinal neurons, astrocytes, Müller cells, lens, trabecular meshwork, cornea and lacrimal gland. *Experimental Eye Research*, *127*, 270–279.

Sanes, J. R., & Masland, R. H. (2015). The types of retinal ganglion cells: current status and implications for neuronal classification. *Annual Review of Neuroscience*, *38*, 221–246.

Santiago, A. R., Baptista, F. I., Santos, P. F., Cristóvão, G., Ambrósio, A. F., Cunha, R. A., & Gomes, C. A. (2014). Role of microglia adenosine A(2A) receptors in retinal and brain neurodegenerative diseases. *Mediators of Inflammation*, *2014*, 465694.

Santos, P. F., Caramelo, O. L., Carvalho, A. P., & Duarte, C. B. (1999). Characterization of ATP release from cultures enriched in cholinergic amacrine-like neurons. *Journal of Neurobiology*, *41*(3), 340–348.

Sanz, J. M., & Di Virgilio, F. (2000). Kinetics and mechanism of ATP-dependent IL-1 beta release from microglial cells. *Journal of Immunology*, *164*(9), 4893–4898.

Sanz, J. M., Chiozzi, P., Ferrari, D., Colaianna, M., Idzko, M., Falzoni, S., Fellin, R., Trabace, L., & Di Virgilio, F. (2009). Activation of microglia by amyloid {beta} requires P2X7 receptor expression. *Journal of Immunology*, *182*(7), 4378–4385.

Sarafoff, N., Byrne, R. A., & Sibbing, D. (2012). Clinical use of clopidogrel. *Current Pharmaceutical Design*, *18*(33), 5224–5239.

Sarthy, V. P., Brodjian, S. J., Dutt, K., Kennedy, B. N., French, R. P., & Crabb, J. W. (1998). Establishment and characterization of a retinal Müller cell line. *Investigative Ophthalmology & Visual Science*, *39*(1), 212–216.

Saunders, N. R., Dreifuss, J. J., Dziegielewska, K. M., Johansson, P. A., Habgood, M. D., Møllgård, K., & Bauer, H. C. (2014). The rights and wrongs of blood-brain barrier permeability studies: a walk through 100 years of history. *Frontiers in Neuroscience*, *8*, 404.

Savio, L., de Andrade Mello, P., da Silva, C. G., & Coutinho-Silva, R. (2018). The P2X7 Receptor in Inflammatory Diseases: Angel or Demon?. *Frontiers in Pharmacology*, *9*, 52.

Schmid, R., & Evans, R. J. (2019). ATP-Gated P2X Receptor Channels: Molecular Insights into Functional Roles. *Annual Review of Physiology*, *81*, 43–62.

Schwartz Lab. (2023). *Retinal Types and Circuits*. [online] Schwartz Lab. Available at: <http://schwartzlab.feinberg.northwestern.edu/research/retinal-types-and-circuits/>. [Accessed 10 April 2023].

Senthilkumari, S., Talwar, B., Dharmalingam, K., Ravindran, R. D., Jayanthi, R., Sundaresan, P., Saravanan, C., Young, I. S., Dangour, A. D., & Fletcher, A. E. (2014). Polymorphisms in sodium-dependent vitamin C transporter genes and plasma, aqueous humor and lens nucleus ascorbate concentrations in an ascorbate depleted setting. *Experimental Eye Research*, *124*, 24–30.

Sesma, J. I., Kreda, S. M., Steinckwich-Besancon, N., Dang, H., García-Mata, R., Harden, T. K., & Lazarowski, E. R. (2012). The UDP-sugar-sensing P2Y(14) receptor promotes Rho-mediated signaling and chemotaxis in human neutrophils. *American Journal of Physiology. Cell Physiology*, *303*(5), 490–498.

Sesma, J. I., Weitzer, C. D., Livraghi-Butrico, A., Dang, H., Donaldson, S., Alexis, N. E., Jacobson, K. A., Harden, T. K., & Lazarowski, E. R. (2016). UDP-glucose promotes neutrophil recruitment in the lung. *Purinergic Signalling*, *12*(4), 627–635. <https://doi.org/10.1007/s11302-016-9524-5>

Sharifi, A. M., Hoda, F. E., & Noor, A. M. (2010). Studying the effect of LPS on cytotoxicity and apoptosis in PC12 neuronal cells: role of Bax, Bcl-2, and Caspase-3 protein expression. *Toxicology Mechanisms and Methods*, *20*(6), 316–320.

Sheybani, A., Lenzhofer, M., Hohensinn, M., Reitsamer, H., & Ahmed, I. I. (2015). Phacoemulsification combined with a new ab interno gel stent to treat open-angle glaucoma: Pilot study. *Journal of Cataract and Refractive Surgery*, *41*(9), 1905–1909.

Shigetomi, E., Hirayama, Y. J., Ikenaka, K., Tanaka, K. F., & Koizumi, S. (2018). Role of Purinergic Receptor P2Y₁ in Spatiotemporal Ca²⁺ Dynamics in Astrocytes. *The Journal of Neuroscience*, *38*(6), 1383–1395.

Shimabukuro, M., Koyama, K., Lee, Y., & Unger, R. H. (1997). Leptin- or troglitazone-induced lipopenia protects islets from interleukin 1beta cytotoxicity. *The Journal of Clinical Investigation*, *100*(7), 1750–1754.

Shimada, K., Crother, T. R., Karlin, J., Dagvadorj, J., Chiba, N., Chen, S., Ramanujan, V. K., Wolf, A. J., Vergnes, L., Ojcius, D. M., Rentsendorj, A., Vargas, M., Guerrero, C., Wang, Y., Fitzgerald, K. A., Underhill, D. M., Town, T., & Arditi, M. (2012). Oxidized mitochondrial DNA activates the NLRP3 inflammasome during apoptosis. *Immunity*, *36*(3), 401–414.

Shinozaki, Y., Kashiwagi, K., Namekata, K., Takeda, A., Ohno, N., Robaye, B., Harada, T., Iwata, T., & Koizumi, S. (2017). Purinergic dysregulation causes hypertensive glaucoma-like optic neuropathy. *Journal of Clinical Investigation - Insight*, *2*(19), 93456.

Shinozaki, Y., Shibata, K., Yoshida, K., Shigetomi, E., Gachet, C., Ikenaka, K., Tanaka, K. F., & Koizumi, S. (2017). Transformation of Astrocytes to a Neuroprotective Phenotype by Microglia via P2Y₁ Receptor Downregulation. *Cell Reports*, *19*(6), 1151–1164.

Sigmaaldrich.com. 2022. How to Make and Use Percoll Gradients. [online] Available at: <https://www.sigmaaldrich.com/GB/en/technical-documents/protocol/cell-culture-and-cell-culture-analysis/mammalian-cell-culture/how-to-make-and-use-gradients-of-percoll> [Accessed 1 June 2022].

Silver, I. A., Deas, J., & Erecińska, M. (1997). Ion homeostasis in brain cells: differences in intracellular ion responses to energy limitation between cultured neurons and glial cells. *Neuroscience*, 78(2), 589–601.

Sizemore, N., Leung, S., & Stark, G. R. (1999). Activation of phosphatidylinositol 3-kinase in response to interleukin-1 leads to phosphorylation and activation of the NF- κ B p65/RelA subunit. *Molecular and Cellular Biology*, 19(7), 4798–4805.

Sluyter R. (2017). The P2X7 Receptor. *Advances in Experimental Medicine and Biology*, 1051, 17–53

Sluyter, R., Dalitz, J. G., & Wiley, J. S. (2004). P2X7 receptor polymorphism impairs extracellular adenosine 5'-triphosphate-induced interleukin-18 release from human monocytes. *Genes and Immunity*, 5(7), 588–591.

Snell, R. S., & Lemp, M. A. (2016). *Clinical Anatomy of the Eye*. 2nd ed. India: Wiley.

Solle, M., Labasi, J., Perregaux, D. G., Stam, E., Petrushova, N., Koller, B. H., Griffiths, R. J., & Gabel, C. A. (2001). Altered cytokine production in mice lacking P2X(7) receptors. *The Journal of Biological Chemistry*, 276(1), 125–132.

Sommer, A., Tielsch, J. M., Katz, J., Quigley, H. A., Gottsch, J. D., Javitt, J., & Singh, K. (1991). Relationship between intraocular pressure and primary open angle glaucoma among white and black Americans. The Baltimore Eye Survey. *Archives of Ophthalmology*, 109(8), 1090–1095.

Song, X., Guo, W., Yu, Q., Liu, X., Xiang, Z., He, C., & Burnstock, G. (2011). Regional expression of P2Y(4) receptors in the rat central nervous system. *Purinergic Signalling*, 7(4), 469–488.

Song, Y., Song, Q., Li, L., Xu, J., & Liu, X. (2018). Effect of ranibizumab on levels of IL-6 and VEGF in peripheral blood and aqueous humor of glaucoma rat model and association of IL-6 and VEGF with optic nerve damage. *Experimental and Therapeutic Medicine*, *16*(3), 2506–2510.

Sperlágh, B., & Illes, P. (2014). P2X7 receptor: an emerging target in central nervous system diseases. *Trends in Pharmacological Sciences*, *35*(10), 537–547.

Spildrejorde, M., Bartlett, R., Stokes, L., Jalilian, I., Peranec, M., Sluyter, V., Curtis, B. L., Skarratt, K. K., Skora, A., Bakhsh, T., Seavers, A., McArthur, J. D., Downton, M., & Sluyter, R. (2014). R270C polymorphism leads to loss of function of the canine P2X7 receptor. *Physiological Genomics*, *46*(14), 512–522.

Springelkamp, H., Iglesias, A. I., Mishra, A., Höhn, R., Wojciechowski, R., Khawaja, A. P., Nag, A., Wang, Y. X., Wang, J. J., Cuellar-Partida, G., Gibson, J., Bailey, J. N., Vithana, E. N., Gharahkhani, P., Boutin, T., Ramdas, W. D., Zeller, T., Luben, R. N., Yonova-Doing, E., Viswanathan, A. C., Yazar, S., Cree, A.J., Haines, J.L., Koh, J.Y., Souzeau, E., Wilson, J.F., Amin, N., Müller, C., Venturini, C., Kearns, L.S., Kang, J.H., NEIGHBORHOOD Consortium., Tham, Y.C., Zhou, T., van Leeuwen, E.M., Nickels, S., Sanfilippo, P., Liao, J., van der Linde, H., Zhao, W., Ivan Koolwijk, L.M., Zheng, L., Rivadeneira, F., Baskaran, M., van der Lee, S.J., Perera, S., de Jong, P.T., Oostra, B.A., Uitterlinden, A.G., Fan, Q., Hofman, A., Tai, E.S., Vingerling, J.R., Sim, X., Wolfs, R.C., Teo, Y.Y., Lemij, H.G., Khor, C.C., Willemsen, R., Lackner, K.J., Aung, T., Jansonius, N.M., Montgomery, G., Wild, P.S., Young, T.L., Burdon, K.P., Hysi, P.G., Pasquale, L.R., Wong, T.Y., Klaver, C.C., Hewitt, A.W., Jonas, J.B., Mitchell, P., Lotery, A.J., Foster, P.J., Vitart, V., Pfeiffer, N., Craig, J.E., Mackey, D.A., Hammond, C.J., Wiggs, J.L., Cheng, C.Y., van Duijn, C.M., MacGregor, S. (2017). New insights into the genetics of primary open-angle glaucoma based on meta-analyses of intraocular pressure and optic disc characteristics. *Human Molecular Genetics*, *26*(2), 438–453.

Stech, M., Grundel, B., Daniel, M., Böhringer, D., Joachimsen, L., Gross, N., Wolf, C., Link, H., Gilles, U., & Lagrèze, W. A. (2019). Risk of aphakic glaucoma after pars plana-

lensectomy with and without removal of the peripheral lens capsule. *Eye*, 33(9), 1472–1477.

Stenvinkel, P., Ketteler, M., Johnson, R. J., Lindholm, B., Pecoits-Filho, R., Riella, M., Heimbürger, O., Cederholm, T., & Girndt, M. (2005). IL-10, IL-6, and TNF-alpha: central factors in the altered cytokine network of uremia--the good, the bad, and the ugly. *Kidney International*, 67(4), 1216–1233.

Stokes, L., Fuller, S. J., Sluyter, R., Skarratt, K. K., Gu, B. J., & Wiley, J. S. (2010). Two haplotypes of the P2X(7) receptor containing the Ala-348 to Thr polymorphism exhibit a gain-of-function effect and enhanced interleukin-1beta secretion. *FASEB Journal*, 24(8), 2916–2927.

Stolzenburg, J. U., Haas, J., Härtig, W., Paulke, B. R., Wolburg, H., Reichelt, W., Chao, T. I., Wolff, J. R., & Reichenbach, A. (1992). Phagocytosis of latex beads by rabbit retinal Müller (glial) cells in vitro. *Journal für Hirnforschung*, 33(4-5), 557–564.

Stone, J., Makarov, F., & Holländer, H. (1995). The glial ensheathment of the soma and axon hillock of retinal ganglion cells. *Visual Neuroscience*, 12(2), 273–279.

Strettoi, E., & Masland, R. H. (1995). The organization of the inner nuclear layer of the rabbit retina. *The Journal of Neuroscience*, 15(1 Pt 2), 875–888.

Stroman, G. A., Stewart, W. C., Golnik, K. C., Curé, J. K., & Olinger, R. E. (1995). Magnetic resonance imaging in patients with low-tension glaucoma. *Archives of Ophthalmology*, 113(2), 168–172.

Su, X., Floyd, D. H., Hughes, A., Xiang, J., Schneider, J. G., Uluckan, O., Heller, E., Deng, H., Zou, W., Craft, C. S., Wu, K., Hirbe, A. C., Grabowska, D., Eagleton, M. C., Townsley, S., Collins, L., Piwnica-Worms, D., Steinberg, T. H., Novack, D. V., Conley, P. B., Hurchla, M.A., Rogers, M., Weilbaecher, K. N. (2012). The ADP receptor P2RY₁₂

regulates osteoclast function and pathologic bone remodeling. *The Journal of Clinical Investigation*, 122(10), 3579–3592.

Südhof, T. C., & Rothman, J. E. (2009). Membrane fusion: grappling with SNARE and SM proteins. *Science*, 323(5913), 474–477.

Sullivan, R. K., Woldemussie, E., Macnab, L., Ruiz, G., & Pow, D. V. (2006). Evoked expression of the glutamate transporter GLT-1c in retinal ganglion cells in human glaucoma and in a rat model. *Investigative Ophthalmology & Visual Science*, 47(9), 3853–3859.

Surprenant, A., & North, R. A. (2009). Signaling at purinergic P2X receptors. *Annual Review of Physiology*, 71, 333–359.

Surprenant, A., Rassendren, F., Kawashima, E., North, R. A., & Buell, G. (1996). The cytolytic P2Z receptor for extracellular ATP identified as a P2X receptor (P2X7). *Science*, 272(5262), 735–738.

Syberg, S., Brandao-Burch, A., Patel, J. J., Hajjawi, M., Arnett, T. R., Schwarz, P., Jorgensen, N. R., & Orriss, I. R. (2012). Clopidogrel (Plavix), a P2Y₁₂ receptor antagonist, inhibits bone cell function in vitro and decreases trabecular bone in vivo. *Journal of Bone and Mineral Research*, 27(11), 2373–2386

Syed, N., & Kennedy, C., (2011). Pharmacology of P2X receptors. *Wiley Interdisciplinary Reviews: Membrane Transport and Signaling*, 1(1), 16–30.

Takai, Y., Tanito, M., & Ohira, A. (2012). Multiplex cytokine analysis of aqueous humor in eyes with primary open-angle glaucoma, exfoliation glaucoma, and cataract. *Investigative Ophthalmology & Visual Science*, 53(1), 241–247

Tan, J. C., Indelicato, S. R., Narula, S. K., Zavodny, P. J., & Chou, C. C. (1993). Characterization of interleukin-10 receptors on human and mouse cells. *The Journal of Biological Chemistry*, 268(28), 21053–21059.

Tan, N. Y., Koh, V., Girard, M. J., & Cheng, C. Y. (2018). Imaging of the lamina cribrosa and its role in glaucoma: a review. *Clinical & Experimental Ophthalmology*, 46(2), 177–188.

Tanna, A. P., & Johnson, M. (2018). Rho Kinase Inhibitors as a Novel Treatment for Glaucoma and Ocular Hypertension. *Ophthalmology*, 125(11), 1741–1756.

Tao, J. H., Cheng, M., Tang, J. P., Dai, X. J., Zhang, Y., Li, X. P., Liu, Q., & Wang, Y. L. (2017). Single nucleotide polymorphisms associated with P2X7R function regulate the onset of gouty arthritis. *PLOS ONE*, 12(8), 0181685.

Taruno A. (2018). ATP Release Channels. *International Journal of Molecular Sciences*, 19(3), 808.

Taruno, A., Vingtdeux, V., Ohmoto, M., Ma, Z., Dvoryanchikov, G., Li, A., Adrien, L., Zhao, H., Leung, S., Abernethy, M., Koppel, J., Davies, P., Civan, M. M., Chaudhari, N., Matsumoto, I., Hellekant, G., Tordoff, M. G., Marambaud, P., & Foskett, J. K. (2013). CALHM1 ion channel mediates purinergic neurotransmission of sweet, bitter and umami tastes. *Nature*, 495(7440), 223–226.

Taylor, A., Jacques, P. F., Nowell, T., Perrone, G., Blumberg, J., Handelman, G., Jozwiak, B., & Nadler, D. (1997). Vitamin C in human and guinea pig aqueous, lens and plasma in relation to intake. *Current Eye Research*, 16(9), 857–864.

Taylor, R. H., Ainsworth, J. R., Evans, A. R., & Levin, A. V. (1999). The epidemiology of pediatric glaucoma: the Toronto experience. *Journal of American Association for Pediatric Ophthalmology and Strabismus*, 3(5), 308–315.

Teixeira, J. M., Dos Santos, G. G., Neves, A. F., Athie, M. C. P., Bonet, I. J. M., Nishijima, C. M., Farias, F. H., Figueiredo, J. G., Hernandez-Olmos, V., Alshaibani, S., Tambeli, C. H., Müller, C. E., & Parada, C. A. (2019). Diabetes-induced Neuropathic Mechanical Hyperalgesia Depends on P2X4 Receptor Activation in Dorsal Root Ganglia. *Neuroscience*, *398*, 158–170.

Tham, Y. C., Li, X., Wong, T. Y., Quigley, H. A., Aung, T., & Cheng, C. Y. (2014). Global prevalence of glaucoma and projections of glaucoma burden through 2040: a systematic review and meta-analysis. *Ophthalmology*, *121*(11), 2081–2090.

Thermo Fisher Scientific. (2017). *Fura-2 Calcium Indicator*. [online] Thermo Fisher. Available at: <https://www.thermofisher.com/uk/en/home/industrial/pharma-biopharma/drug-discovery-development/target-and-lead-identification-and-validation/g-protein-coupled/cell-based-second-messenger-assays/fura-2-calcium-indicator.html> [Accessed 6 June 2022].

Thermo Fisher Scientific. (2018). *Reverse Transcription — Most Common Applications*. [online] Thermo Fisher. Available at: <https://www.thermofisher.com/uk/en/home/life-science/cloning/cloning-learning-center/invitrogen-school-of-molecular-biology/rt-education/reverse-transcription-applications.html> [Accessed 6 June 2022].

The AGIS Investigators. (2000). The Advanced Glaucoma Intervention Study (AGIS): 7. The relationship between control of intraocular pressure and visual field deterioration. *American Journal of Ophthalmology*, *130*(4), 429–440.

Tien, N. W., Pearson, J. T., Heller, C. R., Demas, J., & Kerschensteiner, D. (2015). Genetically Identified Suppressed-by-Contrast Retinal Ganglion Cells Reliably Signal Self-Generated Visual Stimuli. *The Journal of Neuroscience*, *35*(30), 10815–10820.

Ting, J., Rudnisky, C. J., & Damji, K. F. (2018). Prospective randomized controlled trial of phaco-trabectome versus phaco-trabeculectomy in patients with open angle glaucoma. *Canadian Journal of Ophthalmology*, 53(6), 588–594.

Todd, L., Palazzo, I., Suarez, L., Liu, X., Volkov, L., Hoang, T. V., Campbell, W. A., Blackshaw, S., Quan, N., & Fischer, A. J. (2019). Reactive microglia and IL1 β /IL-1R1-signaling mediate neuroprotection in excitotoxin-damaged mouse retina. *Journal of Neuroinflammation*, 16(1), 118.

Tone, M., Powell, M. J., Tone, Y., Thompson, S. A., & Waldmann, H. (2000). IL-10 gene expression is controlled by the transcription factors Sp1 and Sp3. *Journal of Immunology*, 165(1), 286–291.

Topouzis, F., Wilson, M. R., Harris, A., Anastasopoulos, E., Yu, F., Mavroudis, L., Pappas, T., Koskosas, A., & Coleman, A. L. (2007). Prevalence of open-angle glaucoma in Greece: the Thessaloniki Eye Study. *American Journal of Ophthalmology*, 144(4), 511–519.

Toris, C. B., Gleason, M. L., Camras, C. B., & Yablonski, M. E. (1995). Effects of brimonidine on aqueous humor dynamics in human eyes. *Archives of Ophthalmology*, 113(12), 1514–1517.

Torres, G. E., Haines, W. R., Egan, T. M., & Voigt, M. M. (1998). Co-expression of P2X1 and P2X5 receptor subunits reveals a novel ATP-gated ion channel. *Molecular Pharmacology*, 54(6), 989–993.

Tovell, V. E., & Sanderson, J. (2008). Distinct P2Y receptor subtypes regulate calcium signaling in human retinal pigment epithelial cells. *Investigative Ophthalmology & Visual Science*, 49(1), 350–357.

Tozaki-Saitoh, H., Tsuda, M., Miyata, H., Ueda, K., Kohsaka, S., & Inoue, K. (2008). P2Y₁₂ receptors in spinal microglia are required for neuropathic pain after peripheral nerve injury. *The Journal of Neuroscience*, 28(19), 4949–4956.

Tozaki-Saitoh, H., Miyata, H., Yamashita, T., Matsushita, K., Tsuda, M., & Inoue, K. (2017). P2Y₁₂ receptors in primary microglia activate nuclear factor of activated T-cell signaling to induce C-C chemokine 3 expression. *Journal of Neurochemistry*, 141(1), 100–110.

Trachtenberg, M. C., & Packey, D. J. (1983). Rapid isolation of mammalian Müller cells. *Brain Research*, 261(1), 43–52.

Trautmann, A. (2009). Extracellular ATP in the immune system: more than just a "danger signal". *Science Signaling*, 2(56), 6.

Tripathi, R. C., Millard, C. B., & Tripathi, B. J. (1989). Protein composition of human aqueous humor: SDS-PAGE analysis of surgical and post-mortem samples. *Experimental Eye Research*, 48(1), 117–130.

Troutman, M. (2015). *The Significance of Early Ct's – Ask TaqMan #35*. [online] Thermo Fisher. Available at: <https://www.thermofisher.com/blog/behindthebench/the-significance-of-early-cts-ask-taqman-35/> [Accessed 6 June 2022].

Tsakiri, N., Kimber, I., Rothwell, N. J., & Pinteaux, E. (2008). Interleukin-1-induced interleukin-6 synthesis is mediated by the neutral sphingomyelinase/Src kinase pathway in neurones. *British Journal of Pharmacology*, 153(4), 775–783.

Tseng, V. L., Coleman, A. L., Chang, M. Y., & Caprioli, J. (2017). Aqueous shunts for glaucoma. *The Cochrane Database of Systematic Reviews*, 7(7).

Tsakaguchi, H., Tokui, T., Mackenzie, B., Berger, U. V., Chen, X. Z., Wang, Y., Brubaker, R. F., & Hediger, M. A. (1999). A family of mammalian Na⁺-dependent L-ascorbic acid transporters. *Nature*, *399*(6731), 70–75.

Uckermann, O., Wolf, A., Kutzera, F., Kalisch, F., Beck-Sickinger, A. G., Wiedemann, P., Reichenbach, A., & Bringmann, A. (2006). Glutamate release by neurons evokes a purinergic inhibitory mechanism of osmotic glial cell swelling in the rat retina: activation by neuropeptide Y. *Journal of Neuroscience Research*, *83*(4), 538–550.

Uckermann, O., Grosche, J., Reichenbach, A., & Bringmann, A. (2002). ATP-evoked calcium responses of radial glial (Müller) cells in the postnatal rabbit retina. *Journal of Neuroscience Research*, *70*(2), 209–218.

Uhlmann, S., Bringmann, A., Uckermann, O., Pannicke, T., Weick, M., Ulbricht, E., Goczalik, I., Reichenbach, A., Wiedemann, P., & Francke, M. (2003). Early glial cell reactivity in experimental retinal detachment: effect of suramin. *Investigative Ophthalmology & Visual Science*, *44*(9), 4114–4122.

Ulmann, L., Hatcher, J. P., Hughes, J. P., Chaumont, S., Green, P. J., Conquet, F., Buell, G. N., Reeve, A. J., Chessell, I. P., & Rassendren, F. (2008). Up-regulation of P2X4 receptors in spinal microglia after peripheral nerve injury mediates BDNF release and neuropathic pain. *The Journal of Neuroscience*, *28*, 11263–11268.

United Kingdom National Screening Committee (UK NSC). (2019). *The UK NSC recommendation on Glaucoma screening in adults*. [online] UK NSC. Available at: <https://legacyscreening.phe.org.uk/glaucoma>. [Accessed 22 January 2020].

Ursu, D., Ebert, P., Langron, E., Ruble, C., Munsie, L., Zou, W., Fijal, B., Qian, Y. W., McNearney, T. A., Mogg, A., Grubisha, O., Merchant, K., & Sher, E. (2014). Gain and loss of function of P2X7 receptors: mechanisms, pharmacology and relevance to diabetic neuropathic pain. *Molecular Pain*, *10*, 37.

Valera, S., Hussy, N., Evans, R. J., Adami, N., North, R. A., Surprenant, A., & Buell, G. (1994). A new class of ligand-gated ion channel defined by P2X receptor for extracellular ATP. *Nature*, *371*(6497), 516–519.

Vaure, C., & Liu, Y. (2014). A comparative review of toll-like receptor 4 expression and functionality in different animal species. *Frontiers in Immunology*, *5*, 316.

Vecino, E., Rodriguez, F. D., Ruzafa, N., Pereiro, X., & Sharma, S. C. (2016). Glia-neuron interactions in the mammalian retina. *Progress in Retinal and Eye Research*, *51*, 1–40.

Ventura, A., Dos Santos-Rodrigues, A., Mitchell, C. H., & Faillace, M. P. (2019). Purinergic signaling in the retina: From development to disease. *Brain Research Bulletin*, *151*, 92–108.

Vessey, K. A., & Fletcher, E. L. (2012). Rod and cone pathway signalling is altered in the P2X7 receptor knock out mouse. *PLOS ONE*, *7*(1), e29990.

Vohra, R., Tsai, J. C., & Kolko, M. (2013). The role of inflammation in the pathogenesis of glaucoma. *Survey of Ophthalmology*, *58*(4), 311–320.

Vieira, P., de Waal-Malefyt, R., Dang, M. N., Johnson, K. E., Kastelein, R., Fiorentino, D. F., deVries, J. E., Roncarolo, M. G., Mosmann, T. R., & Moore, K. W. (1991). Isolation and expression of human cytokine synthesis inhibitory factor cDNA clones: homology to Epstein-Barr virus open reading frame BCRF1. *Proceedings of the National Academy of Sciences of the United States of America*, *88*(4), 1172–1176.

Vinore S. A. (1995). Assessment of blood-retinal barrier integrity. *Histology and Histopathology*, *10*(1), 141–154.

Virginio, C., MacKenzie, A., Rassendren, F. A., North, R. A., & Surprenant, A. (1999). Pore dilation of neuronal P2X receptor channels. *Nature Neuroscience*, *2*(4), 315–321.

Vogel, S. N., Marshall, S. T., & Rosenstreich, D. L. (1979). Analysis of the effects of lipopolysaccharide on macrophages: differential phagocytic responses of C3H/HeN and C3H/HeJ macrophages in vitro. *Infection and Immunity*, 25(1), 328–336.

Volonté, C., Amadio, S., Cavaliere, F., D'Ambrosi, N., Vacca, F., & Bernardi, G. (2003). Extracellular ATP and neurodegeneration. *Current drug targets. CNS and Neurological Disorders*, 2(6), 403–412.

von Kügelgen, I., & Wetter, A. (2000). Molecular pharmacology of P2Y-receptors. *Naunyn-Schmiedeberg's Archives of Pharmacology*, 362(4-5), 310–323.

von Kügelgen I. (2019). Pharmacology of P2Y receptors. *Brain Research Bulletin*, 151, 12–24.

Vrabec F. (1976). Glaucomatous cupping of the human optic disk: a neuro-histologic study. *Albrecht von Graefes Archiv für Klinische und Experimentelle Ophthalmologie*, 198(3), 223–234.

Vroman, R., Klaassen, L. J., Howlett, M. H., Cenedese, V., Klooster, J., Sjoerdsma, T., & Kamermans, M. (2014). Extracellular ATP hydrolysis inhibits synaptic transmission by increasing pH buffering in the synaptic cleft. *PLOS Biology*, 12(5), e1001864.

Wagschal, L. D., Trope, G. E., Jinapriya, D., Jin, Y. P., & Buys, Y. M. (2015). Prospective Randomized Study Comparing Ex-PRESS to Trabeculectomy: 1-Year Results. *Journal of Glaucoma*, 24(8), 624–629.

Wagschal, L. D., Trope, G. E., Jinapriya, D., Jin, Y. P., & Buys, Y. M. (2015). Prospective Randomized Study Comparing Ex-PRESS to Trabeculectomy: 1-Year Results. *Journal of Glaucoma*, 24(8), 624–629.

Wajda, B. (2016). *The Wills Eye Manual: Office and Emergency Room Diagnosis and Treatment of Eye Disease*. 7th ed. USA: Lippincott Williams and Wilkins.

Waldo, G. L., & Harden, T. K. (2004). Agonist binding and Gq-stimulating activities of the purified human P2Y₁ receptor. *Molecular Pharmacology*, 65(2), 426–436.

Walter, M. R., & Nagabhushan, T. L. (1995). Crystal structure of interleukin 10 reveals an interferon gamma-like fold. *Biochemistry*, 34(38), 12118–12125.

Wang, B., Jaffe, D. B., & Brenner, R. (2014). Current understanding of iberiotoxin-resistant BK channels in the nervous system. *Frontiers in Physiology*, 5, 382.

Wang, C. Y., Liang, C. Y., Feng, S. C., Lin, K. H., Lee, H. N., Shen, Y. C., Wei, L. C., Chang, C. J., Hsu, M. Y., Yang, Y. Y., Chiu, C. H., & Wang, C. Y. (2017). Analysis of the Interleukin-6 (-174) Locus Polymorphism and Serum IL-6 Levels with the Severity of Normal Tension Glaucoma. *Ophthalmic Research*, 57(4), 224–229

Wang, C. Y., Shen, Y. C., Lo, F. Y., Su, C. H., Lee, S. H., Lin, K. H., Tsai, H. Y., Kuo, N. W., & Fan, S. S. (2006). Polymorphism in the IL-1 α (-889) locus associated with elevated risk of primary open angle glaucoma. *Molecular Vision*, 12, 1380–1385.

Wang, N., De Bock, M., Decrock, E., Bol, M., Gadicherla, A., Vinken, M., Rogiers, V., Bukauskas, F. F., Bultynck, G., & Leybaert, L. (2013). Paracrine signaling through plasma membrane hemichannels. *Biochimica et Biophysica Acta*, 1828(1), 35–50.

Wang, N., Robaye, B., Gossiel, F., Boeynaems, J. M., & Gartland, A. (2014). The P2Y₁₃ receptor regulates phosphate metabolism and FGF-23 secretion with effects on skeletal development. *FASEB journal*, 28(5), 2249–2259.

Wang, X., Qin, W., Xu, X., Xiong, Y., Zhang, Y., Zhang, H., & Sun, B. (2017). Endotoxin-induced autocrine ATP signaling inhibits neutrophil chemotaxis through enhancing

myosin light chain phosphorylation. *Proceedings of the National Academy of Sciences of the United States of America*, 114(17), 4483–4488.

Wang, Y., & Duan, Y. (2021). P2Y₁₄R for inflammation therapy: is it a promising target?. *Future Medicinal Chemistry*, 13(18), 1493–1495.

Wang, Y. Y., Yang, Y. X., Zhe, H., He, Z. X., & Zhou, S. F. (2014). Bardoxolone methyl (CDDO-Me) as a therapeutic agent: an update on its pharmacokinetic and pharmacodynamic properties. *Drug design, development and therapy*, 8, 2075–2088.

Ward, M. M., Puthussery, T., Vessey, K. A., & Fletcher, E. L. (2010). The role of purinergic receptors in retinal function and disease. *Advances in Experimental Medicine and Biology*, 664, 385–391.

Ward, M. M., & Fletcher, E. L. (2009). Subsets of retinal neurons and glia express P2Y₁ receptors. *Neuroscience*, 160(2), 555–566.

Ward, M. M., Puthussery, T., & Fletcher, E. L. (2008). Localization and possible function of P2Y(4) receptors in the rodent retina. *Neuroscience*, 155(4), 1262–1274.

Wareham, K., Vial, C., Wykes, R. C., Bradding, P., & Seward, E. P. (2009). Functional evidence for the expression of P2X₁, P2X₄ and P2X₇ receptors in human lung mast cells. *British Journal of Pharmacology*, 157, 1215– 1224.

Wässle, H., Peichl, L., & Boycott, B. B. (1981). Dendritic territories of cat retinal ganglion cells. *Nature*, 292(5821), 344–345.

Watson, P. G., & Barnett, F. (1975). Effectiveness of trabeculectomy in glaucoma. *American Journal of Ophthalmology*, 79(5), 831–845.

Webb, T. E., Simon, J., Krishek, B. J., Bateson, A. N., Smart, T. G., King, B. F., Burnstock, G., & Barnard, E. A. (1993). Cloning and functional expression of a brain G-protein-coupled ATP receptor. *FEBS letters*, 324(2), 219–225.

Weber, A., Wasiliew, P., & Kracht, M. (2010). Interleukin-1 (IL-1) pathway. *Science Signaling*, 3(105).

Wei, L., Liang, G., Cai, C., & Lv, J. (2016). Association of vitamin C with the risk of age-related cataract: a meta-analysis. *Acta Ophthalmologica*, 94(3), 170–176.

Weick, M., Wiedemann, P., Reichenbach, A., & Bringmann, A. (2005). Resensitization of P2Y receptors by growth factor-mediated activation of the phosphatidylinositol-3 kinase in retinal glial cells. *Investigative Ophthalmology & Visual Science*, 46(4), 1525–1532.

Wesa, A. K., & Galy, A. (2001). IL-1 beta induces dendritic cells to produce IL-12. *International Immunology*, 13(8), 1053–1061.

Wesselius, A., Bours, M. J., Arts, I. C., Theunisz, E. H., Geusens, P., & Dagnelie, P. C. (2012). The P2X(7) loss-of-function Glu496Ala polymorphism affects ex vivo cytokine release and protects against the cytotoxic effects of high ATP-levels. *BMC Immunology*, 13, 64.

Wienbar, S., & Schwartz, G. W. (2018). The dynamic receptive fields of retinal ganglion cells. *Progress in Retinal and Eye Research*, 67, 102–117.

Wihlborg, A. K., Wang, L., Braun, O. O., Eyjolfsson, A., Gustafsson, R., Gudbjartsson, T., & Erlinge, D. (2004). ADP receptor P2Y₁₂ is expressed in vascular smooth muscle cells and stimulates contraction in human blood vessels. *Arteriosclerosis, Thrombosis, and Vascular Biology*, 24(10), 1810–1815.

Wilczek M. (1947). The lamina cribrosa and its nature. *The British journal of Ophthalmology*, 31(9), 551–565.

Wiley, J. S., Dao-Ung, L. P., Li, C., Shemon, A. N., Gu, B. J., Smart, M. L., Fuller, S. J., Barden, J. A., Petrou, S., & Sluyter, R. (2003). An Ile-568 to Asn polymorphism prevents normal trafficking and function of the human P2X7 receptor. *The Journal of Biological Chemistry*, 278(19), 17108–17113.

Wilkin, F., Duhant, X., Bruyns, C., Suarez-Huerta, N., Boeynaems, J. M., & Robaye, B. (2001). The P2Y₁₁ receptor mediates the ATP-induced maturation of human monocyte-derived dendritic cells. *Journal of immunology*, 166(12), 7172–7177.

Wirtz, M. K., & Keller, K. E. (2016). The Role of the IL-20 Subfamily in Glaucoma. *Mediators of Inflammation*, 2016, 4083735.

Wojdasiewicz, P., Poniatowski, Ł. A., & Szukiewicz, D. (2014). The role of inflammatory and anti-inflammatory cytokines in the pathogenesis of osteoarthritis. *Mediators of Inflammation*, 2014, 561459.

Wolfs, R. C., Klaver, C. C., Ramrattan, R. S., van Duijn, C. M., Hofman, A., & de Jong, P. T. (1998). Genetic risk of primary open-angle glaucoma. Population-based familial aggregation study. *Archives of Ophthalmology*, 116(12), 1640–1645.

Wu, H., de Boer, J. F., & Chen, T. C. (2012). Diagnostic capability of spectral-domain optical coherence tomography for glaucoma. *American Journal of Ophthalmology*, 153(5), 815–826.

Wu, H., de Boer, J. F., & Chen, T. C. (2012). Diagnostic capability of spectral-domain optical coherence tomography for glaucoma. *American Journal of Ophthalmology*, 153(5), 815–826.

Wurm, A., Lipp, S., Pannicke, T., Linnertz, R., Krügel, U., Schulz, A., Färber, K., Zahn, D., Grosse, J., Wiedemann, P., Chen, J., Schöneberg, T., Illes, P., Reichenbach, A., & Bringmann, A. (2010). Endogenous purinergic signaling is required for osmotic

volume regulation of retinal glial cells. *Journal of Neurochemistry*, 112(5), 1261–1272.

Wurm, A., Pannicke, T., Iandiev, I., Francke, M., Hollborn, M., Wiedemann, P., Reichenbach, A., Osborne, N. N., & Bringmann, A. (2011). Purinergic signaling involved in Müller cell function in the mammalian retina. *Progress in Retinal and Eye Research*, 30(5), 324–342.

Wurm, A., Pannicke, T., Wiedemann, P., Reichenbach, A., & Bringmann, A. (2008). Glial cell-derived glutamate mediates autocrine cell volume regulation in the retina: activation by VEGF. *Journal of Neurochemistry*, 104(2), 386–399.

Wurm, A., Erdmann, I., Bringmann, A., Reichenbach, A., & Pannicke, T. (2009). Expression and function of P2Y receptors on Müller cells of the postnatal rat retina. *Glia*, 57(15), 1680–1690.

Xia, J., Lim, J. C., Lu, W., Beckel, J. M., Macarak, E. J., Laties, A. M., & Mitchell, C. H. (2012). Neurons respond directly to mechanical deformation with pannexin-mediated ATP release and autostimulation of P2X7 receptors. *The Journal of Physiology*, 590(10), 2285–2304.

Xu, L., Wang, Y., Wang, S., Wang, Y., & Jonas, J. B. (2007). High myopia and glaucoma susceptibility the Beijing Eye Study. *Ophthalmology*, 114(2), 216–220.

Xu, X. J., Boumechache, M., Robinson, L. E., Marschall, V., Gorecki, D. C., Masin, M., & Murrell-Lagnado, R. D. (2012). Splice variants of the P2X7 receptor reveal differential agonist dependence and functional coupling with pannexin-1. *Journal of Cell Science*, 125(Pt 16), 3776–3789.

Xu, Y., Hu, W., Liu, Y., Xu, P., Li, Z., Wu, R., Shi, X., & Tang, Y. (2016). P2Y₆ Receptor-Mediated Microglial Phagocytosis in Radiation-Induced Brain Injury. *Molecular Neurobiology*, 53(6), 3552–3564.

Xue, Y., Xie, Y., Xue, B., Hu, N., Zhang, G., Guan, H., & Ji, M. (2016). Activated Müller Cells Involved in ATP-Induced Upregulation of P2X7 Receptor Expression and Retinal Ganglion Cell Death. *BioMed Research International*, 2016, 9020715.

Yang, T., Shen, J. B., Yang, R., Redden, J., Dodge-Kafka, K., Grady, J., Jacobson, K. A., & Liang, B. T. (2014). Novel protective role of endogenous cardiac myocyte P2X4 receptors in heart failure. *Circulation. Heart Failure*, 7, 510– 518.

Yang, Y., Wang, H., Kouadir, M., Song, H., & Shi, F. (2019). Recent advances in the mechanisms of NLRP3 inflammasome activation and its inhibitors. *Cell Death & Disease*, 10(2), 128.

Yanoff, M. & Duker, J.S. (2018). *Ophthalmology*. 5th ed. USA: Elsevier.

Yazdi, A. S., & Ghoreschi, K. (2016). The Interleukin-1 Family. *Advances in Experimental Medicine and Biology*, 941, 21–29.

Ye, S. S., Tang, Y., & Song, J. T. (2021). ATP and Adenosine in the Retina and Retinal Diseases. *Frontiers in Pharmacology*, 12, 654445.

Yegutkin G. G. (2008). Nucleotide- and nucleoside-converting ectoenzymes: Important modulators of purinergic signalling cascade. *Biochimica et Biophysica Acta*, 1783(5), 673–694.

Yeon, D. Y., Yoo, C., Lee, T. E., Park, J. H., & Kim, Y. Y. (2014). Effects of head elevation on intraocular pressure in healthy subjects: raising bed head vs using multiple pillows. *Eye (London, England)*, 28(11), 1328–1333.

Yoneda, S., Tanihara, H., Kido, N., Honda, Y., Goto, W., Hara, H., & Miyawaki, N. (2001). Interleukin-1beta mediates ischemic injury in the rat retina. *Experimental Eye Research*, 73(5), 661–667.

Yoshida, S., Sotozono, C., Ikeda, T., & Kinoshita, S. (2001). Interleukin-6 (IL-6) production by cytokine-stimulated human Müller cells. *Current Eye Research*, 22(5), 341–347.

Yue, B. Y., Higginbotham, E. J., & Chang, I. L. (1990). Ascorbic acid modulates the production of fibronectin and laminin by cells from an eye tissue-trabecular meshwork. *Experimental cell research*, 187(1), 65–68.

Zdanov, A., Schalk-Hihi, C., & Wlodawer, A. (1996). Crystal structure of human interleukin-10 at 1.6 Å resolution and a model of a complex with its soluble receptor. *Protein Science*, 5(10), 1955–1962.

Zdanov, A., Schalk-Hihi, C., Gustchina, A., Tsang, M., Weatherbee, J., & Wlodawer, A. (1995). Crystal structure of interleukin-10 reveals the functional dimer with an unexpected topological similarity to interferon gamma. *Structure*, 3(6), 591–601.

Zer, C., Sachs, G., & Shin, J. M. (2007). Identification of genomic targets downstream of p38 mitogen-activated protein kinase pathway mediating tumor necrosis factor- α signaling. *Physiological Genomics*, 31(2), 343–351.

Zhang, C. L., Wilson, J. A., Williams, J., & Chiu, S. Y. (2006). Action potentials induce uniform calcium influx in mammalian myelinated optic nerves. *Journal of Neurophysiology*, 96(2), 695–709.

Zhang, P. P., Yang, X. L., & Zhong, Y. M. (2012). Cellular localization of P2Y₆ receptor in rat retina. *Neuroscience*, 220, 62–69.

Zhang, J. L., Song, X. Y., Chen, Y. Y., Nguyen, T., Zhang, J. Y., Bao, S. S., & Zhang, Y. Y. (2019). Novel inflammatory cytokines (IL-36, 37, 38) in the aqueous humor from patients with chronic primary angle closure glaucoma. *International Immunopharmacology*, 71, 164–168.

Zhang, X., Zhang, M., Laties, A. M., & Mitchell, C. H. (2005). Stimulation of P2X7 receptors elevates Ca²⁺ and kills retinal ganglion cells. *Investigative Ophthalmology & Visual Science*, *46*(6), 2183–2191.

Zhang, X., & Chintala, S. K. (2004). Influence of interleukin-1 beta induction and mitogen-activated protein kinase phosphorylation on optic nerve ligation-induced matrix metalloproteinase-9 activation in the retina. *Experimental Eye Research*, *78*(4), 849–860.

Zhang, Y., Peti-Peterdi, J., Müller, C. E., Carlson, N. G., Baqi, Y., Strasburg, D. L., Heiney, K. M., Villanueva, K., Kohan, D. E., & Kishore, B. K. (2015). P2Y₁₂ Receptor Localizes in the Renal Collecting Duct and Its Blockade Augments Arginine Vasopressin Action and Alleviates Nephrogenic Diabetes Insipidus. *Journal of the American Society of Nephrology*, *26*(12), 2978–2987.

Zhou, F., Liu, X., Gao, L., Zhou, X., Cao, Q., Niu, L., Wang, J., Zuo, D., Li, X., Yang, Y., Hu, M., Yu, Y., Tang, R., Lee, B. H., Choi, B. W., Wang, Y., Izumiya, Y., Xue, M., Zheng, K., & Gao, D. (2019). HIV-1 Tat enhances purinergic P2Y₄ receptor signaling to mediate inflammatory cytokine production and neuronal damage via PI3K/Akt and ERK MAPK pathways. *Journal of Neuroinflammation*, *16*(1), 71.

Zhao, L., Zabel, M. K., Wang, X., Ma, W., Shah, P., Fariss, R. N., Qian, H., Parkhurst, C. N., Gan, W. B., & Wong, W. T. (2015). Microglial phagocytosis of living photoreceptors contributes to inherited retinal degeneration. *EMBO Molecular Medicine*, *7*(9), 1179–1197.

Zhao, M., Bai, Y., Xie, W., Shi, X., Li, F., Yang, F., Sun, Y., Huang, L., & Li, X. (2015). Interleukin-1 β Level Is Increased in Vitreous of Patients with Neovascular Age-Related Macular Degeneration (nAMD) and Polypoidal Choroidal Vasculopathy (PCV). *PLOS ONE*, *10*(5), e0125150.

Zhao, X., Reifler, A. N., Schroeder, M. M., Jaeckel, E. R., Chervenak, A. P., & Wong, K. Y. (2017). Mechanisms creating transient and sustained photoresponses in mammalian retinal ganglion cells. *The Journal of general physiology*, *149*(3), 335–353.

Zhong, H., Yu, H., Sun, J., Chen, J., Huang, S., Huang, P., Liu, X., & Zhong, Y. (2021). Isolation of microglia from retinas of chronic ocular hypertensive rats. *Open Life Sciences*, *16*(1), 992–1001.

Zhong, Y., Dunn, P. M., Xiang, Z., Bo, X., & Burnstock, G. (1998). Pharmacological and molecular characterization of P2X receptors in rat pelvic ganglion neurons. *British Journal of Pharmacology*, *125*(4), 771–781.